UNIVERSITÀ
DEGLI STUDI
DI PADOVA

Sede Amministrativa: Università degli Studi di Padova

Dipartimento di Ingegneria Industriale

SCUOLA DI DOTTORATO DI RICERCA IN : INGEGNERIA INDUSTRIALE

INDIRIZZO: FISICA TECNICA

CICLO XXV

MATHEMATICAL MODELS FOR THE USE OF LOW AND MEDIUM TEMPERATURE GEOTHERMAL ENERGY

Direttore della Scuola :	Ch.mo Prof.	Paolo Colombo
Coordinatore d'indirizzo:	Ch.mo Prof.ssa	Luisa Rossetto
Supervisore :	Ch.mo Prof.	Michele De Carli
Correlatori :	Ch.mo Prof.	Guðni A. Jóhannesson
	Ch.mo Prof. ssa	Guðrún A. Sævarsdóttir

Dottorando : Mirco Donà

N. di matricola 967471 – DR

UNIVERSITÀ DEGLI STUDI DI PADOVA

Sede Amministrativa: Università degli Studi di Padova

Dipartimento di Ingegneria Industriale

SCUOLA DI DOTTORATO DI RICERCA IN : INGEGNERIA INDUSTRIALE
INDIRIZZO: FISICA TECNICA
CICLO XXV

MATHEMATICAL MODELS FOR THE USE OF LOW AND MEDIUM TEMPERATURE GEOTHERMAL ENERGY

Direttore della Scuola : Ch.mo Prof. Paolo Colombo
Coordinatore d'indirizzo: Ch.ma Prof.ssa Luisa Rossetto
Supervisore :Ch.mo Prof. Michele De Carli

Dottorando : Marco Donà
firma

Summary

Alla mia famiglia,

e a tutti coloro che mi hanno voluto bene

e che mi hanno sostenuto in questi anni

ABSTRACT

This thesis looks at the geothermal energy, that is, energy emitted continuously in the form of heat from our planet, that from the deepest areas propagates towards the surface. The research activities have been carried out for evaluating different aspects related to geothermal energy and more specifically the way in which this energy can be extracted. The present work has tried to deal with all the different levels of temperature in which the geothermal energy is classified, i.e. low temperature, medium temperature and high temperature, as hereafter described more in detail.

Geothermal Energy low temperature: this energy is transferred by means of ground heat exchangers coupled with a heat pump. In this case usually the heat transfer fluid can be water or a mixture containing water and an antifreeze fluid. In the frame of this technology first the characteristics of a GRT (ground response test) has been tested, in order to check the accuracy of the method to evaluate the average temperature of the ground, as well as to determine the thermal conductivity of the soil and the overall coefficient of linear heat exchange between the transfer fluid and the soil. The accuracy of the GRT has been evaluated for different sizes of the grout (an usual ground heat exchanger and a pile) as well as for different velocities of the aquifer. The simulations have been carried out by means of a Finite Element Method (FEM) software. Then the FEM has been used for evaluating the energy and structural analysis on piles foundations when they are used as ground heat exchangers. The work has shown the combined effect of structural loads in heating and cooling periods. The results are in agreement to the theory as well as to results carried out by measurements which have been found in literature. Finally a study for comparing different heat pumps and different fluids in the ground heat exchangers has been carried out in mild climates. The work shows the benefits of using pure water as heat transfer fluid in almost all conditions, since in mild climates the temperature of the ground is around 14°C and usually heat pumps are used for both heating and cooling, thus allowing the ground to be regenerated over one year. The use of flooded evaporators in the heat pumps will allow the ground heat pumps to be more attractive in the next future.

Geothermal Energy medium temperature: in this case the ATES (Aquifer Thermal Energy Storage) has been investigated. ATES is a particular type of thermal storage which uses water from the subsoil where the groundwater can vary between 15 °C and 130 °C. The extraction and reinjection wells should be sufficiently distant in order to avoid short-circuits. This technology could be used also for low temperature aquifers; in this case the water of the aquifer is used for cooling the condenser during summertime, while it is cooled down in winter time to transfer heat to the evaporator. The wells are used alternatively in order to accumulate a cold storage during winter time and a warm storage during summer time. The work of the present thesis has focused on the thermal influence of the reinjection well on the

undisturbed temperature conditions along the aquifer, depending on the thickness of the aquifer. Results of a FEM model have been compared to the analytical solution of various authors (Carslaw and Jaeger, Lauwerier, Ghassemi). The goal is to evaluate the distance between the two wells in order to prevent thermal interference, as a function of the thickness of the aquifer.

Geothermal Energy high temperature: it allows to extract dry and superheated steam without liquid phase (in this case they are called "dominant steam systems") or liquid water mixed with steam (in this case they are called "water-dominated systems"). The usual depth of these systems is between 3 km and 15 km in correspondence of magmatic intrusions. For these systems the thesis has the aim to study the heat exchange between the rock and hot water, considering the variation of the outlet temperature of the water as a function of time. These studies were developed at first considering a single fracture in the rock, then we moving to a more realistic model consisting in a multi rock-fracture. The model proposed in literature based on analytical methods have been compared with a FEM mathematical model. The models have been then applied to a site in the Philippines where experimental data were available.

RIASSUNTO

La presente tesi si basa sullo studio di ricerca dell'energia geotermica, energia continuamente emessa sottoforma di calore dal nostro pianeta, che si propaga dalle zone più profonde della Terra verso la superficie. Le attività di ricerca sono state svolte per valutare differenti aspetti legati all'energia geotermica e più specificamente i modi con cui questa energia può essere estratta. Il presente lavoro è stato effettuato considerando i diversi livelli di temperatura per i quali viene classificata l'energia geotermica: bassa temperatura, media temperatura e alta temperatura, come di seguito descritto in dettaglio.

Geotermia a bassa temperatura: questa energia è trasferita dal terreno mediante una pompa di calore utilizzando un fluido termovettore che può essere acqua o una miscela contenente acqua e fluido anticongelante. Per tale tecnologia sono stati analizzati i risultati derivanti dalla prova denominata GRT (Ground Response Test), che permette di valutare la temperatura media del terreno e determina la conduttività termica del terreno stesso ed il coefficiente globale di scambio termico lineare tra il fluido termovettore ed il sottosuolo. L'accuratezza del GRT è stata analizzata per differenti dimensioni cementizia del diametro dello scambiatore di calore al terreno e per differenti velocità dell'acquifero. Le simulazioni sono state eseguite mediante un software che applica il Metodo agli Elementi Finiti (FEM). Successivamente il metodo FEM è stato applicato anche per valutare l'energia e l'analisi strutturale sui pali di fondazione utilizzati come scambiatori di calore a terreno. A tal fine è stato analizzato l'effetto combinato di carichi strutturali con quelli derivanti da sollecitazioni termiche nei periodi di riscaldamento e raffrescamento. I risultati ottenuti sono in accordo sia con le teorie presenti in letteratura che con i dati sperimentali raccolti in bibliografia. Gli studi svolti sulla geotermia a bassa temperatura si concludono con uno studio di confronto in Pianura Padana tra diverse pompe di calore e differenti fluidi termovettori all'interno di un campo di sonde geotermiche. Tale studio ha dimostrato i possibili benefici usando acqua pura come fluido termovettore in quasi tutte le condizioni, visto l'utilizzo delle pompe di calore sia per il riscaldamento che per il raffrescamento, permettendo in tal modo che il terreno si rigeneri tra una stagione e l'altra. L'uso dell'evaporatore allagato in una pompa di calore geotermica permette maggiore attrattiva nei confronti degli impianti geotermici nel prossimo futuro.

Geotermia a media temperatura: in questo caso sono stati studiati i sistemi ATES (stoccaggio energetico in acquiferi termali). I sistemi ATES sono un particolare tipo di stoccaggio termico nel quale si usa acqua del sottosuolo con temperature variabili tra 15°C 130°C. I pozzi di estrazione e di reiniezione dovranno essere sufficientemente distanti per evitare il cortocircuito. Questa tecnologia può essere usata anche per acquiferi a bassa temperatura; in questo caso l'acqua dell'acquifero è usata come raffreddamento al condensatore durante il periodo estivo, mentre è raffreddato in inverno per trasferire calore all'evaporatore. I pozzi sono usati alternativamente al fine di accumulare uno stoccaggio di

energia frigorifera durante il periodo invernale e uno stoccaggio di energia termica durante il periodo estivo. Il lavoro della tesi è stato focalizzato sull'interferenza termica del pozzo di reiniezione sulle condizioni di temperatura indisturbata lungo l'acquifero, in funzione dello spessore dell'acquifero. I risultati del modello FEM sono stati poi confrontati con la soluzione analitica proposta da vari autori (Carslaw-Jaeger, Lauwerier, Ghassemi). L'obiettivo è valutare la distanza tra i due pozzi così da prevenire l'interferenza termica in funzione dello spessore dell'acquifero.

Geotermia ad alta temperatura: consente l'estrazione di vapore secco surriscaldato in assenza di fase liquida (in questo caso è definito "sistema di vapore dominante") o acqua in fase liquida miscelata a vapore (in questo caso è definito "sistema ad acqua dominante). Generalmente la profondità di questi sistemi è tra 3 km e 15 km in corrispondenza di intrusioni magmatici. Per questi sistemi la ricerca si è concentrata sullo scambio termico tra roccia e acqua, considerandola variazione della temperatura di uscita dell'acqua in funzione del tempo. Inizialmente lo studio si è concentrato sullo scambio di calore all'interno di una singola frattura; l'analisi si è poi estesa al caso di roccia con multiple fratture. Il modello proposto è stato descritto in letteratura mediante metodi analitici, per poi essere confrontato con metodi FEM. I modelli sono stati applicati ad un sito nelle Filippine dove erano disponibili alcuni dati sperimentali.

1. GEOTHERMAL ENERGY

The increase in well-being and human activities have in recent years led to an intensification of the greenhouse effect, with possible climate change, linked to the increase in global mean temperature. With the subscription of the Kyoto Protocol, it would have been required for each signatory country, to lower their greenhouse gas emissions in the period 2008 - 2012 of at least 5% below 1990 levels, which is considered as the base year.

In December 2008, the European Council approved the plan that is necessary, by 2020, to 20% reduction in CO2 emissions, and increase by the same percentage energy savings, and the portion of renewable energy in the energy mix, despite some concessions given by some countries.

To comply with these standards, it is important both to improve the energy efficiency of systems, including through the development of new technologies to diversify as much as possible energy sources.

In this argument fits very well the energy extracted from the earth, that is, the geothermal energy.

Hence, for geothermal energy represents the heat contained within the Earth, due to the presence of geological phenomena on a planetary scale, which can be extracted from the ground and exploited by man; in the nature of our planet, therefore are the origins of this energy.

1.1 Structure of the Earth

Our planet has the shape of an ellipsoid of rotation, slightly flattened at the poles, due to the movement of the earth's rotation. The average equatorial radius (about 6378.2 km) is greater than the average polar radius (approximately 6356.7 km). Such depths have made it impossible so far the direct study of the Earth, since the well deeper, as yet perforated (Kola, Russia) reached only a depth of about 12 km.

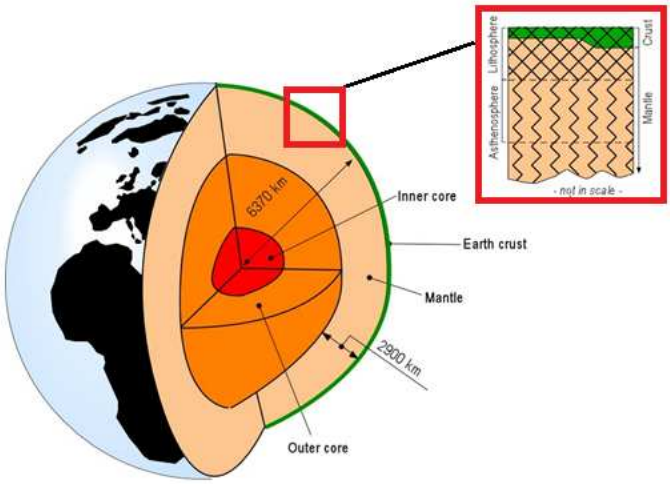

Fig. 1.1- The Earth's crust, mantle, and core. Top right: a section through the crust and the uppermost mantle.

The information available to date, therefore derive from indirect methods of observation, such as geophysical tests, such as studies of propagation of seismic waves due to earthquakes and artificial atomic explosions.

Thanks to these studies it was possible to divide the internal structure of the planet into three parts, determined by the discontinuity of composition and mineralogical structure:

- Nucleus;

- Cloak;

- Crust.

The nucleus, the inner shell of the Earth, occupies a total volume equal to 16% of the Earth and has a mass equal to 31% of it. The nucleus is composed primarily of iron and nickel, extending from the centre of the Earth, up to 2900 km depth, and it is divided into Internal nucleus and External nucleus. In the zone of separation the estimated temperature is about 5000-5500 [K]. The density of the matter of the outer nucleus is 10 g/cm^3, and the state is liquid. The convective motions of the iron in this physical state are the likely cause of the Earth's magnetic field.

The mantle occupies 84% of the Earth's volume and contributed, the 68% of the mass. The density of this layer is between 3.3 and 6 g/cm3, as derived from the analysis of the velocity of propagation of seismic waves in this stratum. The pressure at the base of the mantle is about 130 GPa. The magma is erupted by volcanoes, the material is in the solid state, semi-plastic mantle, which melts, rising through the earth's crust due to the decrease in pressure. In the upper part of the mantle there is a part, called Low Velocity Zone (LVZ), where a slowdown of 3-6%, of the velocity of seismic waves has been studied probably caused by the presence of molten material between the solid granules of metallic material.

Above the surface of the LVZ, according to the theory of tectonics plates, there would be the movement of the masses outer envelope of the planet, the so-called Lithosphere. This casing present cold and rigid behaviour, floats on Asthenosphere, very hot and plastic, which consists of that portion of the mantle, that goes from LVZ up to 700 km depth.

Inside the mantle a convective circulation of material is present, due to the temperature difference between coast and nucleus. Here, cool material sinks and warms up towards the earth's crust. The so-called subduction process is precisely caused by the descent of the portions of colder mantle.

Finally, the Crust is the most superficial shell of our planet, with a mass equal to 0.4% of the total of the planet. The thickness varies from 30 to 70 km; the continents present a density between 2.2 and 2.5 g/cm^3, while between 5 and 15 km the oceans have higher specific weight (density 3 g/cm^3).

Below are shown the figures that highlight: the major tectonic plates of the world Figure 1.2, areas of the world with potential for producing electricity using geothermal energy Figure 1.3 (Renner 2002), and Geothermoelectric installed capacity worldwide in early 2005 Figure 1.4 (Bertani 2005).

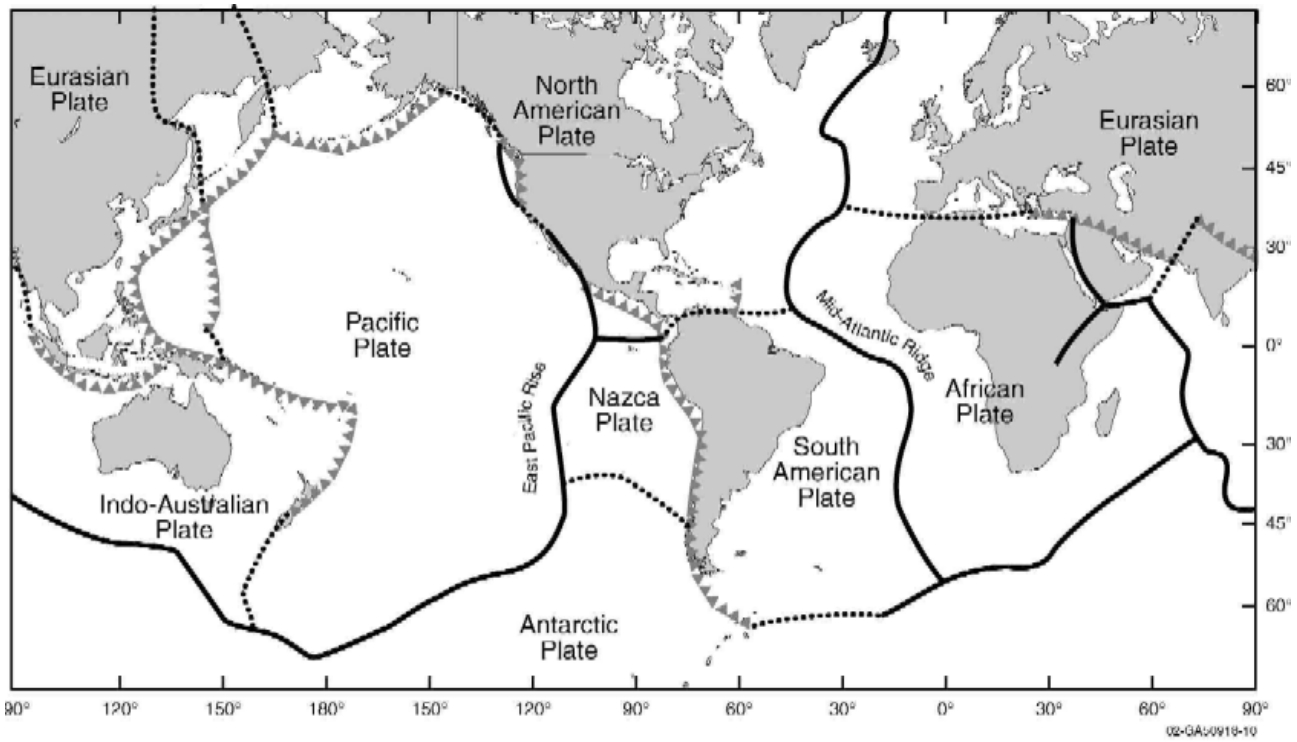

Figure 1.2 - Major tectonic plates of the world, (Renner 2002).

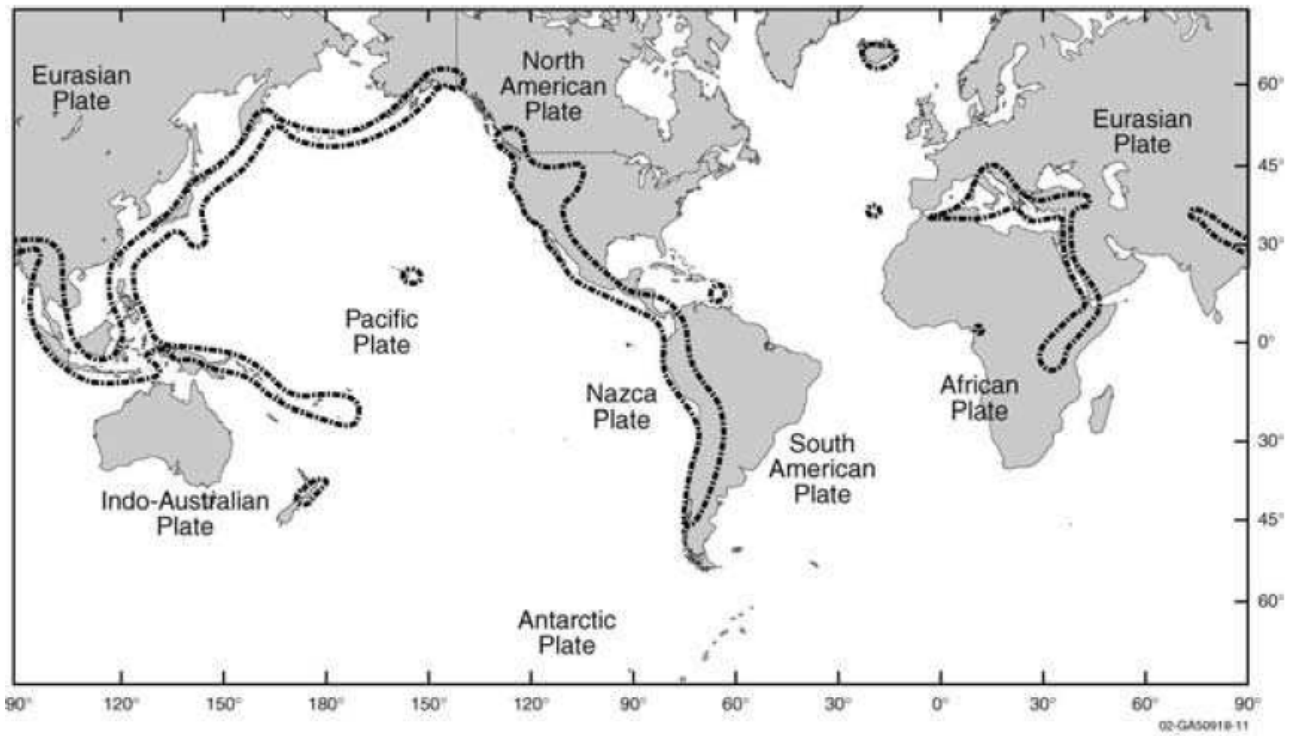

Figure 1.3 - Areas of the world with potential for producing electricity using geothermal energy (Renner 2002).

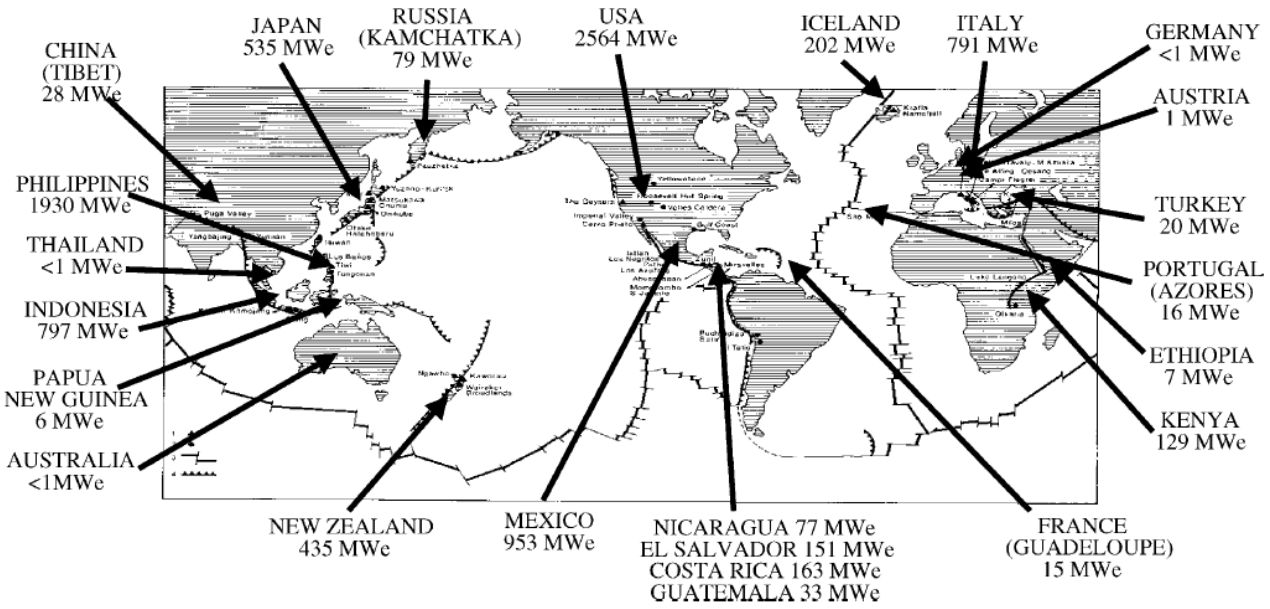

Figure 1.4 – Geothermoelectric installed capacity worldwide in early 2005.(Bertani 2005)

1.2 Geothermal flux

The temperature increases with increasing depth within the earth, and this corresponds to a flow of heat directed towards the outside. The geothermal flux is estimated to be between 59 and 81 mW/m^2, which means, given the entire surface of our planet (510 x 106 km^2), a thermal power of between 30 and 42 TW (average 315 PWH / year) .

It is interesting to note that the thermal power at stake, is enormous compared to the total world energy demand to 2007, about 130 PWh[1] If one compares this energy with the value of thermal power that the sun irradiates, about 200 W/m^2 at mid-latitudes, the power supplied by the geothermal flux is very small.

The geothermal heat flow is still very variable as it is very high the oceanic ridges, rather low within continents, less than the subsurface thermal anomalies.

The origins of geothermal heat are due to different causes, such as:

- Heat emission from radioactive isotopes decay;
- Crystallization processes of the nucleus;
- Solidification of magma.

[1] Source ENEA, Rapporto Energia Ambiente 2010.

The heat emission by radioactive isotopes is the 20-80% of the total heat flow. These isotopes are more present in the granitic rocks in the continental crust in amounts greater than the oceanic crust.

The heat source is constituted by the processes of phase change and chemical reaction, such as the passage of material from the liquid state to a solid state with crystal structure or the heat transfer of heat due to the solidification of the magma in the liquid state.

The result of such geothermal flux is the geothermal gradient, defined as the variation of temperature T as a function of depth z:

$$\text{Geothermal gradient} = \frac{dT}{dz} \qquad (1.1)$$

The reference value for the thermal gradient is approximately 3 ° C per 100 m for lithosphere, however, this value varies greatly depending on the presence of heat sources and aquifers. There, the thermal gradient is much greater than the average values, hence heat sources in the subsoil are potentially exploitable.

1.3 Geothermal systems

A geothermal system is a portion of the subsoil, consisting of porous and permeable rocks, in which are present simultaneously an aquifer and a heat source.

As defined by Hochstein, 1990, the geothermal reservoir is "a vapour convective system, which, in a confined space of the upper part of the earth's crust, transports the heat from a heat source to the place, generally the surface, where the heat same, is absorbed (dispersed or used) ", see Figure 1.5.

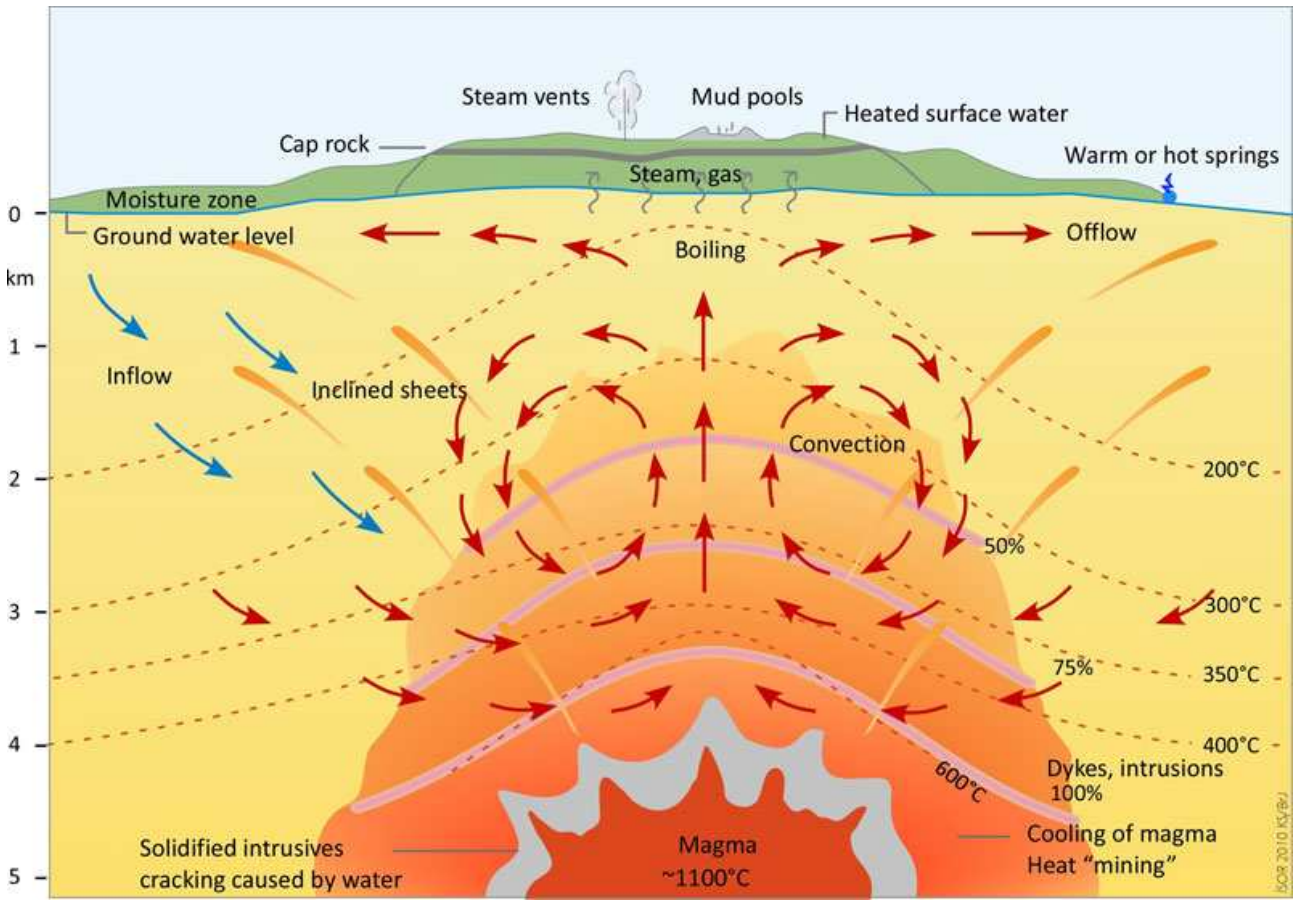

Figure 1.5 – Simplified model of a geothermal reservoir by Kristjan Saemundsson, ISOR.

The boundaries of geothermal reservoirs over the millennia were waterproofed for effect of movements, which trigger phenomena of deposition of minerals in the discontinuity, and pores of the rocks of the reservoir (self-sealing). It is possible that the heat of geothermal fluids has not been cooled the surrounding cold water. Sometimes, the geothermal system can come up on the surface in the form of geysers, fumaroles or shower heads.

There are different types of geothermal reservoirs:

- *Hydrothermal geothermal systems;*
- *In hot dry rock geothermal systems;*
- *Magmatic geothermal systems;*
- *Geopressured geothermal systems.*

Hydrothermal geothermal systems:

They are the most exploited systems, for the production of energy. They include the presence of an aquifer in contact with a heat source. The geological structure of the aquifer present an impermeable cover, which prevents the hot fluids to rise to the surface, keeping them under pressure.

Such systems are in turn divided into dry steam, humid steam, hot water systems, as shown hereafter:

- Dry steam system: these systems have high temperature, and are rather rare. They are present when particular geological conditions and thermodynamic properties allow the geothermal fluid to appear at the wellhead, such as dry saturated steam accompanied by other gases such as CO_2, H_2S, CH_4, B, NH_3 (in low amounts). Normally co-exist in the reservoir liquid water and steam. The most famous are the sites of Larderello (Tuscany, Italy), The Geysers (California, USA), Matsukawa (Japan) and Kawah Kamojang (Indonesia).

- Humid steam or water-dominated system: the fluid present in the subsurface occurs at high temperature and pressure, which vaporizes when reducing the pressure in the tank or during the ascent in the well: they can produce, as a function of their temperature and pressure, hot water, a mixture of water and steam, wet steam and, in some cases, dry steam. These geothermal systems, where the temperature can range from 125 ° to 225 ° C, are the most prevalent in the world. Reservoirs of this type are present in New Zealand (Wairakei), Cerro Prieto (Mexico) and Campi Flegrei (Campania, Italy). For the production of electricity it is required the separation of the vapor from the liquid, often being only used the steam for the expansion in the turbine.

- Hot water systems: The temperatures are lower than the other types of tank, the temperatures are in fact below 100 ° C (50 - 82 ° C). This is due to the absence of a waterproof roof which usually maintains the isolation. In these cases the fluid, generally liquid water, is rarely used for the production of electricity, but it can be exploited for direct uses such as heating buildings, and greenhouses, agriculture, spas.

Hot Dry Rock systems (HDR)

"Hot Dry Rocks" (HDR) are areas of subsoil where the temperature is higher than the average, but the rocks are poorly permeable, and thus do not have the presence of water.

In HDR Project, launched in the U.S. in the early 70s, both the fluid and the reservoir are artificial. Through an artificial well, high pressure water is pumped into a hot compact rock formation, causing its hydraulic fracturing. The water enters and circulates in artificial fractures, extracting heat from the surrounding rock, which acts as a natural reservoir. Thanks to these processes (hydro - fracturing and fracturing thermoplastic) the heat allows to vaporize the injected water.

This system, therefore, is well used for hydraulic fracturing, through which cold water is injected into the artificial reservoir, and into the well for the extraction of the hot water (Fig. 1.6). The entire system, comprising also the utilization plant on the surface, forms a closed circuit, avoiding any contact between the fluid and the external environment (Garnish, 1987).

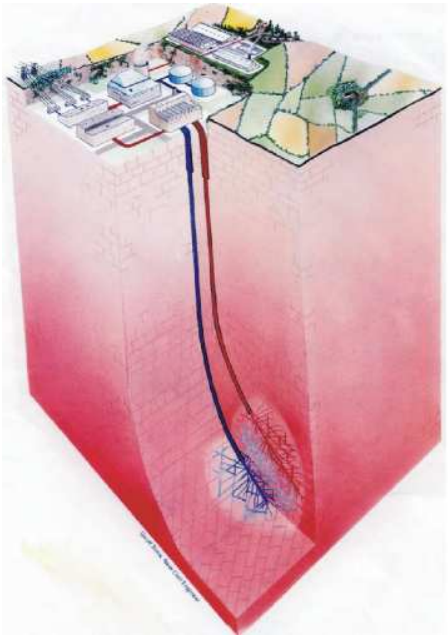

Figure 1.6 – Schematic of a commercial – scale Hot Dry Rock HDR.

These systems are still in the testing phase: an example can be seen in Los Alamos (New Mexico, USA), where the edge of a volcanic caldera at 4000 meters depth reach heat fluxes over 250 mW/m^2.

The project HDR Los Alamos has been followed by other projects based on similar concepts, which were developed in France, Australia, Japan, Germany and Great Britain. To date, advanced research has been carried out in Japan and in Alsace (France). The various projects began in Japan in the 80s (at Hijiori, Ogachi and Yunomori) gave very interesting results, both from a scientific, and industrial point of view. The European HDR project, has been developed in several stages, including the drilling of two wells, one of which has reached the depth of 5060 meters. From geophysical exploration and hydraulic tests very encouraging results were obtained and the European project seems to be more promising.

Magmatic geothermal systems:

These systems allow to exploit the molten rocks of magmatic origin, with temperatures from 600 to 1400 ° C at a depth of 5-7 km, through heating and vaporization of cold water of an artificial well. These systems are still in the experimental stage due to the technological limitations of the materials, which must withstand corrosive magma, and high temperatures, and uncertainties related to the thermal behaviour of magma cooling around the well.

Geopressured geothermal systems:

Geopressured systems may be formed in large sedimentary basins (e. g. Gulf of Mexico) at depths of 3-7 km. The geopressured reservoirs are formed by permeable sedimentary rocks, included within impermeable low conductivity layers, containing hot water at a pressure higher than the hydrostatic pressure, which is trapped at the time of deposition of sediments. The hot water pressure is close to the lithostatic pressure, greatly exceeding the hydrostatic pressure. The water temperature is approximately between 120 °C and 170 °C. The geopressured can also contain significant amounts of methane. Geopressured systems could produce thermal energy, hydraulic (pressurized hot water) and methane gas. This resource has been studied extensively, but, so far, it is not industrial exploitation.

1.4 Low and medium enthalpy geothermal energy

The enthalpy is a thermodynamic defined as

$$E = U + pV \tag{1.2}$$

where E = enthalpy (J), U = internal energy (J), p = pressure (Pa), V = volume (m^3).

Enthalpy is used as a parameter to define a range of temperatures and pressures above which the fluid extracted may be used for the production of electricity. Based on this distinction, the fluids originating from low-temperature geothermal reservoirs are better exploited for direct uses, such as heating of buildings, greenhouses and fish farming.

According to different criteria, resources are divided into resources of low, medium and high enthalpy. Table 1.1 reports the classifications proposed by some researchers. When talking about geothermal fluids is better, however, to indicate their temperature, or at least a temperature range, because terms such as low, medium or high can have different meanings, and frequently misleading.

Table 1.1- Classification of geothermal resources based on the Temperature (°C).

	(a)	(b)	(c)	(d)	(e)
Low enthalpy resources	< 90	< 125	< 100	≤ 150	≤ 190
Media enthalpy resources	90 - 150	125 – 225	100 - 200	-	-
High enthalpy resources	>150	>225	>200	>150	>190

(a) Muffler and Cataldi (1978);

(b) Hochstein (1990);

(c) Benderitter and Cormy (1990);

(d) Nicholson (1993);

(e) Axelsson and Gunnlaugsson (2000).

Figure 1.7 represents the three main systems of geothermal energy:

- low temperature (with a maximum depth of 100m) coupling and closed-loop geothermal heat pump and a temperature of about 10 ° C;
- hydrothermal geothermal systems, wells with open circuit depth water extraction up to 3 km and variable temperatures around 100 ° C;
- high temperature and geothermal HDR, with deep wells up to 6 km and the water extracted temperatures greater than 220 ° C.

In Figure 1.8 shows the Lindal diagram (1973), as modified by ISOR: it shows the possible uses of geothermal fluids at different temperatures.

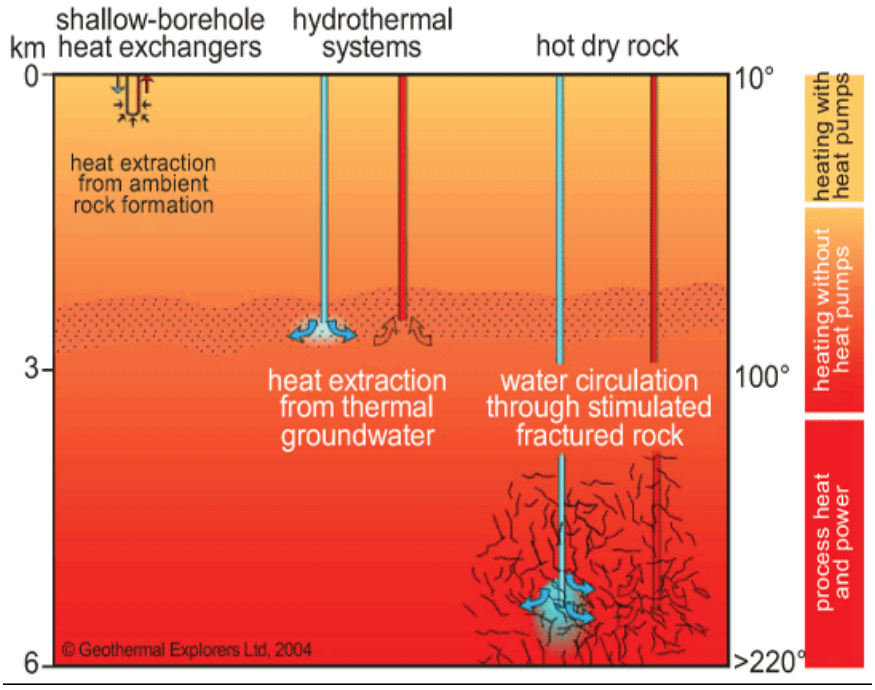

Figure 1.7– Difference between geothermal systems.
http://www.geothermal.uwa.edu.au/home/energy

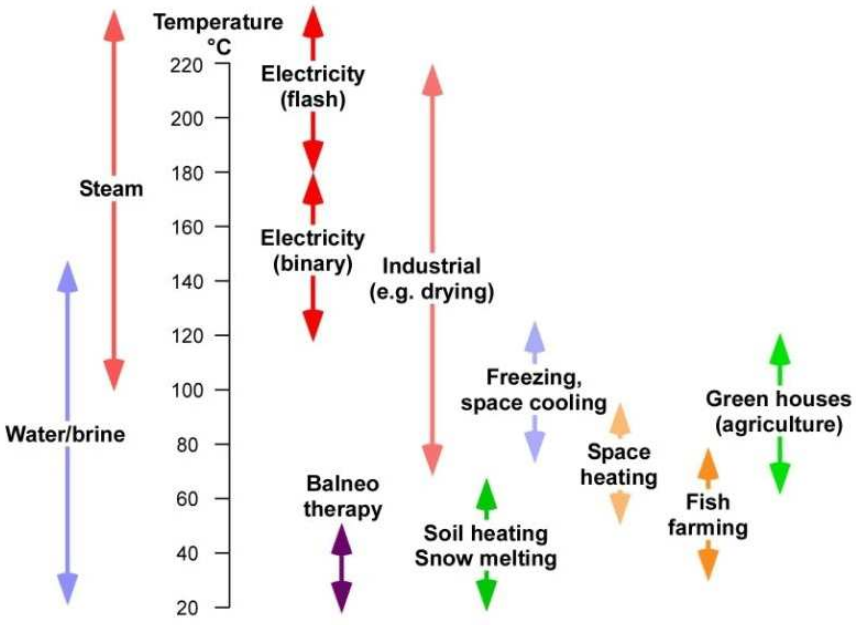

Figure 1.8- Geothermal utilization at different Temperatures – Lindal 1973, modified by ISOR.

1.5 Geothermal Energy use

1.5.1 Geothermal plants

The generation of electricity by geothermal sources presents the advantage of avoiding the use of fossil fuel use, a clear environmental advantage. The heat of the Earth is always available and does not depend on the climate, nor the seasons. It is also not necessary to store the geothermal energy: the earth itself acts as a reservoir.

Geothermal plants are modular, meaning they can grow with increasing needs, flexible in their use, operating 24 hours a day and with a long service life. The plants can be simultaneously used both to generate electricity and for direct applications of geothermal fluid, if its temperature is sufficiently high. The geothermal power plants produce electricity with the energy of geothermal fluid from underground. The steam or hot water of geothermal origin set in motion the turbines connected to generators. The waste water, is then reinjected into the depth, through appropriate wells. In this way it keeps the pressure of the tank and prevents pollution of watercourses in surface or groundwater.

The type of installations varies according to the type of hydrothermal system provided ,according to the above mentioned classification: dominant steam, dominant water, hot water. Therefore, geothermal plants can be divided into the following categories:

Dry-steam plants: in these plants, the steam can be sent directly to the turbine plant. After passing through the turbine, the steam can be condensed and then re-injected in the form of liquid into the ground, (condensing power plants), or it can be released to the atmosphere (central free discharge).

Single or double flash: it exploits the water-dominated reservoirs, at temperatures above 170 ° C. The water, with temperatures between 180 °C and 370 ° C, reaches the surface along the wells and, for the rapid variation of pressure from the tank to the environment is separated (flash) in a part of steam. The steam is used in central, and the liquid part is reinjected into the ground. If the temperatures of the geothermal fluid at the surface are particularly high, then it can be subject to a double flash process at high pressure (160 ° C) and low pressure (120 ° C). The flows of steam obtained are sent to separate turbines. Most of the geothermal power plants in the world are based this type.

Binary Cycle Power Plants: for tank water-dominated fluids characterized by moderate temperatures (between 120 and 180 ° C), the binary cycle technology is the most commonly used. The geothermal fluid is used to vaporize, through a heat exchanger, a secondary fluid with a boiling temperature lower than water, (such as isopentane). This liquid makes a closed loop, expands in the turbine and is returned to the heat exchanger after condensation. The geothermal water, after passing through the heat exchanger, is re-injected into the reservoir.

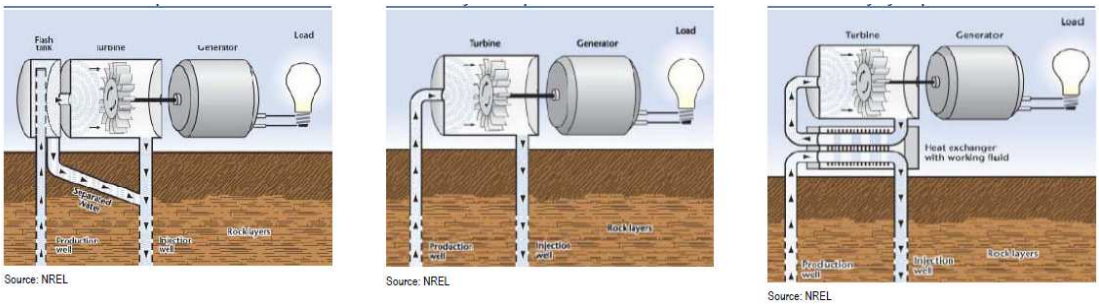

Figure 1.9- Flash cycle power plants, dry steam and binary cycle.

Central hybrid: in water dominant reservoirs, in which the fluid has very low temperatures, it can be used to pre-heat another fluid (usually water) through a heat exchanger, which is then vaporized by the heat generated by combustion of fossil fuel or biomass.

Combined Cycle Power Plants: is a type of system where a single-cycle flash and binary cycle are coupled.

Electricity costs of geothermal plant are dependent on several factors: the temperature and the depth of the resource, the well productivity, the infrastructure and the funding of the project. The capital cost for a geothermal power plant is in the order of € 2500 per kW installed. The life of operation of a system is typically ranging from 30 to 40 years. Therefore it can be planned to recover the investment costs within the first 15 years of operation, then the costs of the system decrease by 50 % to 70%, considering to cover the costs of operation and maintenance.

These systems are characterized by a considerable investment for the construction of the plant which are necessary for the following activities: surface exploration (6% of the total), perforation (53%), construction of the plant (36%), steam ducts (5%).

Therefore, the voice with higher cost, is that due to the drilling of wells: drilling geothermal is much more difficult, and costly in comparison to that of oil wells due to high temperature, and the corrosiveness of the fluids.

Each geothermal well can cost several million of euro, and each system can contain from 10 to 100 wells. Normally such wells are deep 200 - 1500 meters for systems at low and medium and temperature, and 700 - 3000 meters for those at high temperature.

1.5.2 Other uses of geothermal Energy

In addition to electricity generation, geothermal heat can also be used for direct applications, exploiting water at temperatures between 20 and 150 ° C. Depending on the temperature of the fluid, there may be a variety of applications in fish farms, greenhouses, district heating, industrial, balneology. The district heating is the most common form, amongst the possible direct uses of geothermal energy; it consists in using the geothermal fluid to heat directly, by means of heat exchangers, the water circulating in the terminal units of the heating plant of the dwellings.

More frequently heat pump are used, by means of fluids at very low temperatures. It is a thermal machine capable of transferring heat from a colder body to a warmer environment, by means of external energy that can be electrical or mechanical. In several countries geothermal energy is exploiting at low temperatures (7-40 ° C), such as Sweden, Japan, the United States, Switzerland, Germany and France.

1.5.3 Environmental impact

Geothermal energy is a viable alternative to traditional energy sources which allows low environmental impact that may result by a correct exploitation. Albeit in limited quantities, there are the some impact, which have to be considered:

Emissions of non-condensable gases are naturally present in the geothermal fluid. They do not condense at environmental temperature and pressure; after expansion of the fluid in the turbine, they are at from the condenser and released to the atmosphere. The amount and the composition of these gases can be very variable, but usually are mainly formed by from carbon dioxide, hydrogen sulphide, methane, hydrogen and traces of radon. These are substances already present in the atmosphere, and the only care is them in the environment, in order to avoid local harmful effects.

Wastewater liquids: The geothermal fluid, after being used for the production of electricity, should be reinjected into the ground. It may contain a variety of natural substances; some of (such as boron, arsenic, mercury, lead and sulfur) are potentially harmful to humans and the environment, if present in high concentrations.

Noise: Noise emissions of a geothermal plant are reduced and limited to a very specific period of time during the drilling of wells, when very high values of sound intensity can be reached. Subsequently, during its operation, the noise produced depends mainly on the opening of relief valves, which, however, are equipped with silencing systems. Ultimately, the noise is a problem easily solved today, and practically irrelevant.

Impact aesthetic: The geothermal plants resemble many industrial complexes. A big impact in the past was due to the cooling towers of fluids (heights from 15m to 20 m). Today, however, impact is equal to that of a normal building.

These considerations are valid for geothermal systems that use a direct water from the geothermal reservoir, i.e. when the system of wells is an open system. In the case of a system connected to the heat pump the use of closed circuits in geothermal probes, an environmental pollution is caused, if the probe, for various reasons, breaks by venting the fluid from the probe itself, and it is mixed with the ground water. If the heat transfer fluid is water, there are no problems of aquifer pollution. If instead, the heat transfer fluid is a mixture of water with a percentage of antifreeze fluid, pollution in groundwater, which may be a important choice in order to avoid environmental disasters. An example of an antifreeze fluid, compatible with the environment is propylene glycol. More details are described in section 2.2.3.

1.5.4 Geothermal Energy: past, present and future

The exploitation of geothermal energy by man has ancient origins: In Europe the Greeks, Etruscans and Romans as well as, at different times, the Indians of America or the Maori of New Zealand. employed the warm waters, which flowed naturally to the surface for bathing, and space heating for the treatment of skin disorders, and eyes.

As early as 1777, it was used boric acid water geothermal area of Larderello, and in 1827 there was the first real use in direct form of geothermal energy, the heat of which, was used instead of wood for the evaporation water to extract boric acid, thanks to the French Larderel, giving his name the area.

The attempts to exploit this energy for the electricity production date back to 1900 and were carried out in Tuscany. In 1904 in Larderello, Prince Piero Ginori Conti, lit five light bulbs using a dynamo of 0.75 hp, driven by a reciprocating engine, utilizing steam from a shower head. In 1912 in Lardarello the first geothermal power plant in the world, was built.

Between 1905 and 1936, drilling techniques were improved and reached an installed electric capacity of 73 MW from the twenties. The first geothermal wells were dug in Japan in 1919, and the U.S. in 1921. However, only after the Second World War, many countries were attracted by geothermal energy, considering it economically competitive with other forms of energy. In 1958, a small geothermal power plant went into operation in New Zealand and another in Mexico in 1959, and in 1960 the first geothermal power plant in the United States at The Geysers. And so forth, until you have electricity generated from geothermal steam in 21 countries, spread over all five continents. The top ten in 2000 were: U.S.A. (2228 MWe), Philippines (1909 MWe), Italy (785 MWe), Mexico (755 MWe), Indonesia (590 MWe), Japan (547 MWe), New Zealand (437 MWe), Iceland (170 MWe), El Salvador (161 MWe) and Costa Rica (143 MWe).

Over the past 30 years, the development of geothermal power has grown considerably, with 15% per year for the first two years of the period, but down to 3% per year over the last 10 years, due to the economic depression that occurred in the several Far Eastern countries, and the low cost of fossil fuels. The direct use of geothermal heat, in contrast, is characterized by a growth rate over the last three decades, at around 10% per year thanks to the contribution of geothermal heat pumps.

Seventy-two are the countries that have national data on the development of geothermal energy, and from here it is evident that it is spreading the use of natural heat in recent years. There is a greater focus on development programs that produce electricity and heat in cascade (especially those that use fluids at temperatures around 100 ° C). These uses of low-medium heat, allow to improve the efficiency of the system and may be economically feasible.

Overall, with reference to 2000, the installed capacity worldwide was 7974 MWe (megawatts electric) for the generation of electricity and 15,144 MWt (megawatts thermal) for direct use. In 2010 there was an increase of only 300 GW of geothermal electricity installed, and for 2020, according to Bloomberg New Energy Finance, the increase will be more than 5GW.

Even trough geothermal energy that moves slowly compared to other renewable energy sources, there are countries such as El Salvador, Kenya, Philippines and Iceland which generate more than 15% of electricity from geothermal sources, and several have recently introduced incentives to encourage the development of geothermal exploitation, in response to growing demand for electricity. The IEA (International Energy Agency) states that geothermal can provide 1.6TWh of electricity, i.e. 3.5% of global demand by 2050.

Table 1.2- Geothermal power installed in 2010.

Table 1: Current installed capacity (MW)

	Installed base (2010)
Chile	0
China	24
Costa Rica	166
El Salvador	204
Ethiopia	7
France	1
Germany	7
Guadeloupe	15
Guatemala	52
Iceland	575
Indonesia	1189
Italy	863
Japan	502
Kenya	167
Mexico	958
New Zealand	769
Nicaragua	88
Papa New Guinea	56
Philippines	1966
Portugal	29
Russia	82
Turkey	82
US	3102
Others	2
Total	**10906**

Source: IEA

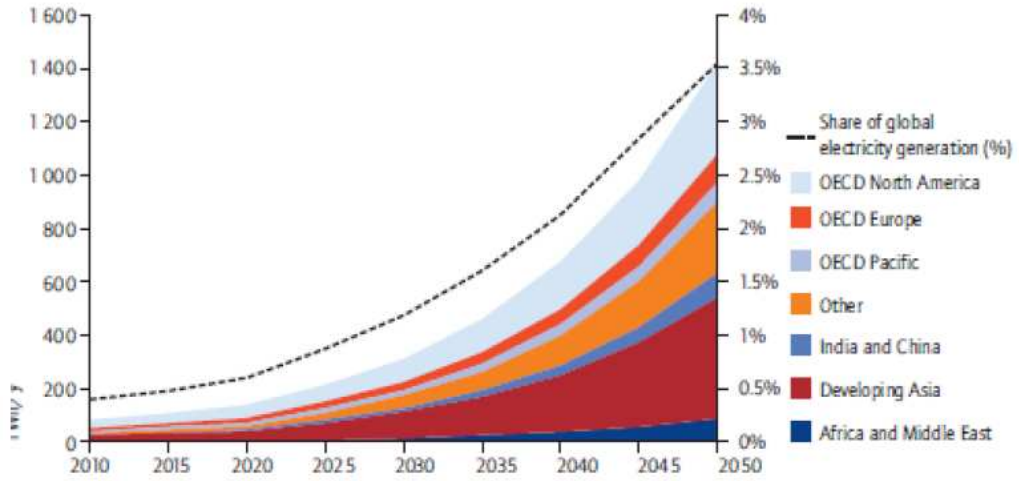

Figure 1.10- Development of geothermal Energy respect to the world's electricity production. Source: IEA.

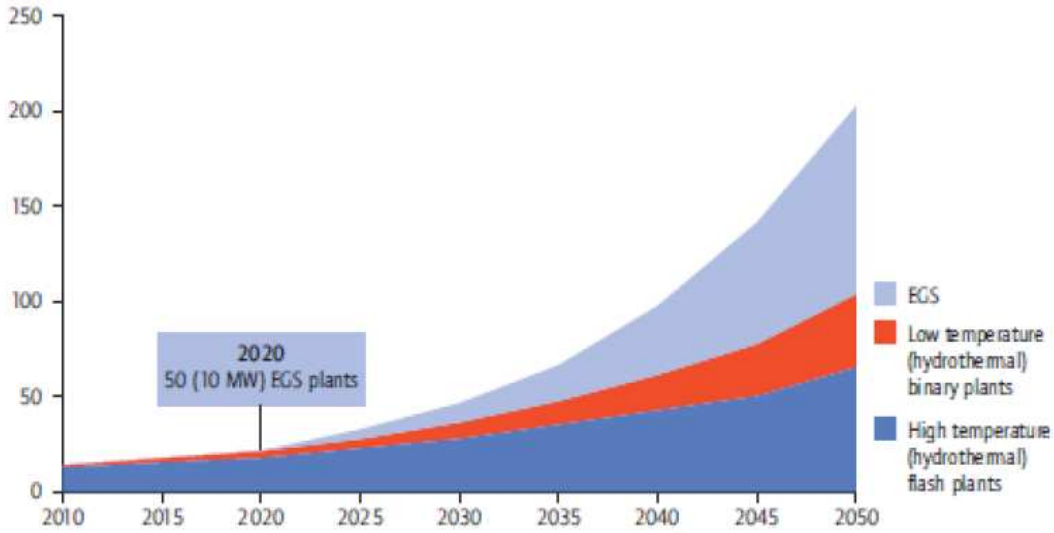

Figure 1.11- Development of geothermal capacity installed by technology. Source: IEA.

Europe

In **Italy** there are currently more than 800 MW of installed capacity, more than 1, 5% of total electricity production in the country, placing the country third in the world's top producers of electricity from geothermal energy.

Concerning the high enthalpy geothermal fluid used for the production of electricity, there are four fields in operation: the most important is in Larderello with 282.5 MWe installed; 111.5 MWe are installed in the region Monte Amiata, Piancastagnaio, 160 MWe in the Tuscan region of Travale-Radicondoli; 268 MWe are in Lago and finally 40 MWe in Latera in Lazio.

The nation with the wider use of geothermal energy is **Iceland**. The island is part of a dorsal expansion of mid-ocean emerged, set to a Hot Spot, and the geological origin is due to an important geothermal anomaly. In 2009, 99% of 16,839 GWhe generated of electricity was based on renewable sources. of which 27% geothermal, and derives 50% of its total consumption of primary energy.

Geothermal energy in Iceland has been always important, but nowadays it is playing an increasingly role in Icelandic energy affairs. It is exploited in space and swimming pools heating, snow melting and electricity production; geothermal energy is now an indispensable part of every Icelander's life.

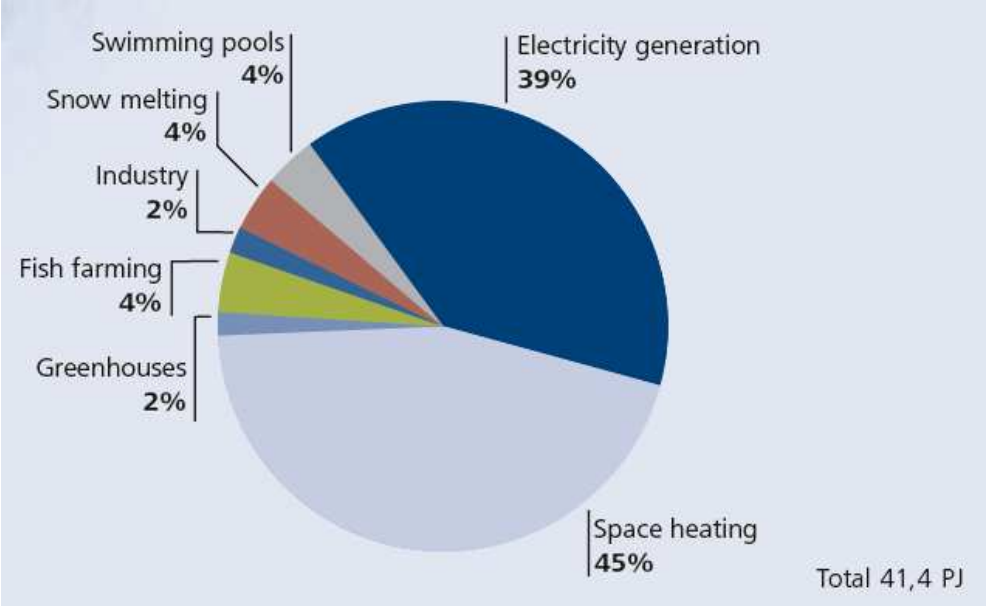

Figure 1.12- Utilization of geothermal energy 2009.

Geothermal space heating is very common in Icelandic buildings; it accounted for 89% in 2005, the other buildings are heating by electricity (10%) and oil (1%). In the last years with the increasing of the population, increased also the utilization of geothermal energy for space heating. A great part of the existing heating system have been expanded and some small heating utilities have been established in rural area (there are some 200 small, rural utilities). About the geothermal energy use to melt snow from streets and pavements in the urban areas, in 2005, the total area system was estimated to be around 835000 m^2, and the system annual energy consumption was approximately 360 GWh.

The first geothermal power plant of 3 MW started in the 1969 in Bjarnaflag, North Iceland, it is still open. The Krafla power in North Iceland started in 1977, in the first 20 years its power was 30 MW, the capacity was increased to 60 MW in 1997. The Svartsengi co-generation power plant started operations in 1977, it is located in Reykjanes peninsula, 40 km from Reykjavik, and serves about 16000 people. The installed capacity for the electricity production is 47 MW. In Reykjanes peninsula 100 MW power plant is under construction, in Nesjavellir high-temperature field, Reykjavik Energy is operating a co-generation plant. It started in 1990 producing hot water for Reykjavik area, 27 km away. At the end of 1998 it started to generate electricity with 60 MW installed capacity. In 2001 was completed an expansion of 90 MW and another 120 MW in 2005. In Husavik, Northeast Iceland, there is a low-temperature geothermal field that has one of the first Kalina binary-fluid 2 MW generators in the world, and it was put into service in 2000.

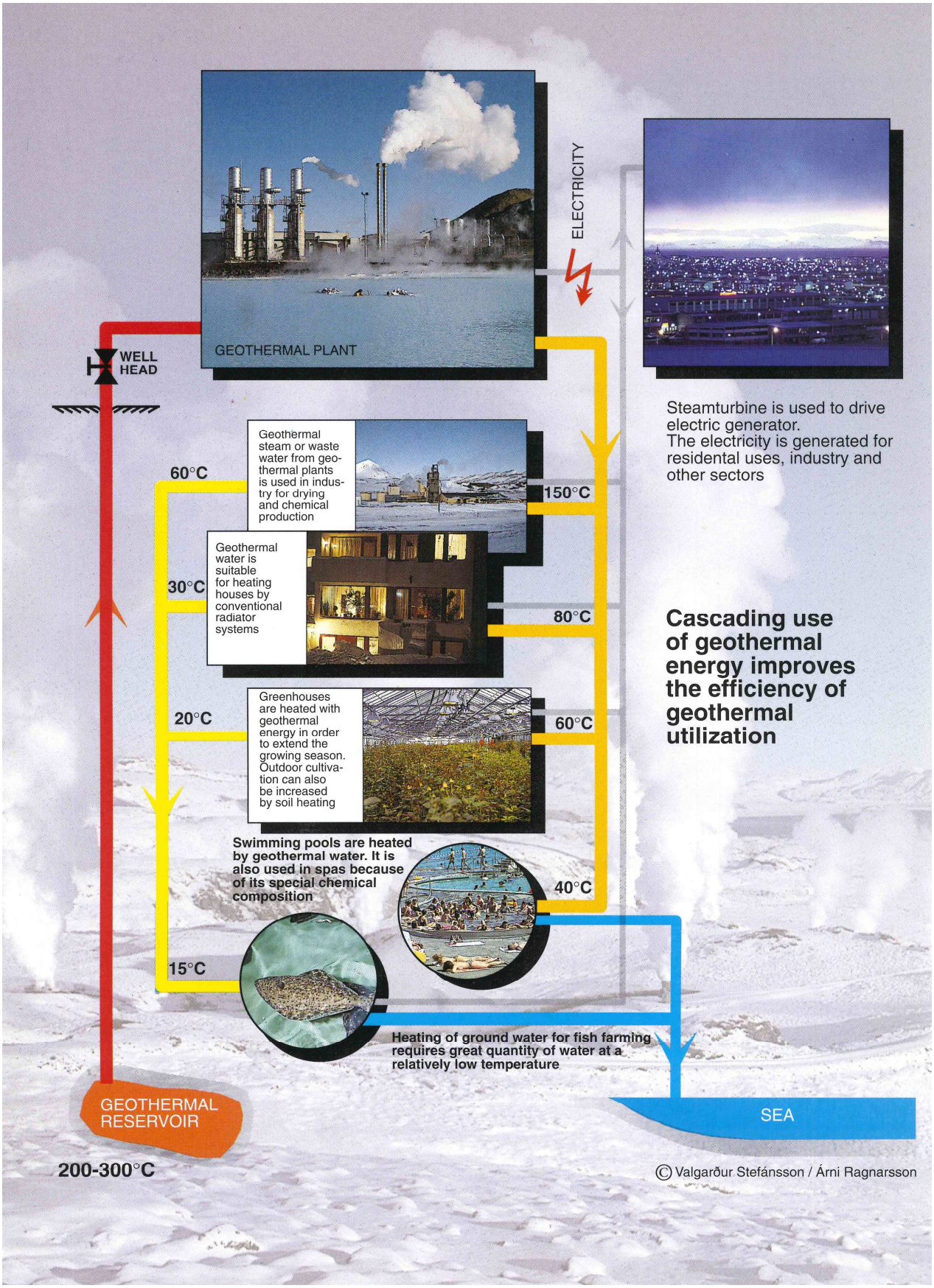

Figure 1.13- Scheme of cascading use of geothermal energy in Iceland.

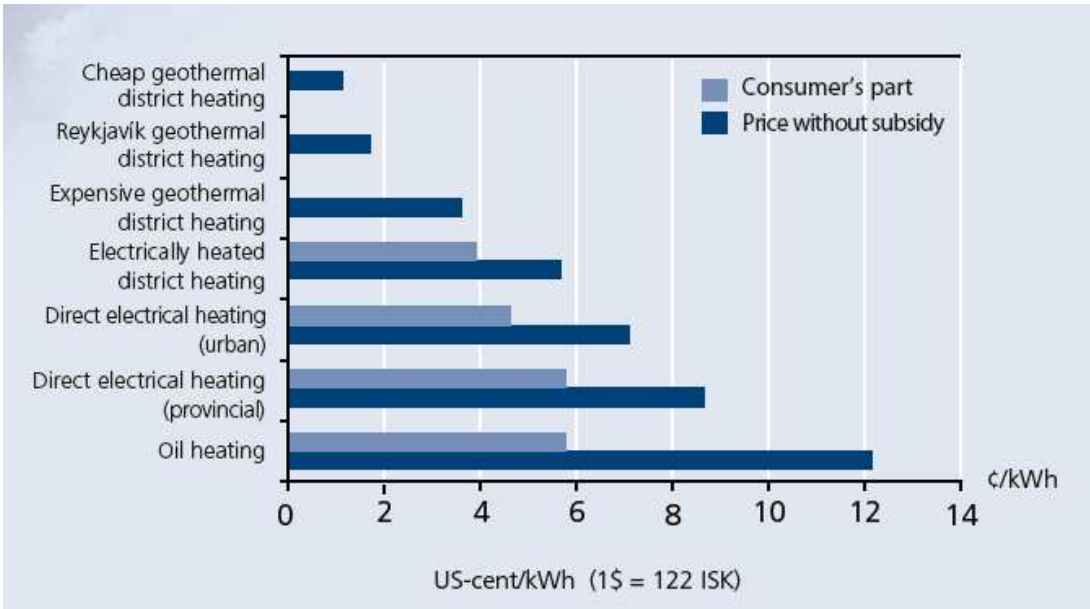

Figure 1.14 - *Comparison of energy prices for residential heating mid-year 2010.*

In Iceland the electricity price is generally lower compared to other European countries, like in the other Scandinavian countries and Western Europe, but the distribution and transmission costs are higher. The price for the hot water and space heating may vary, depending on the energy source.

The primary energy consumed in producing electricity from geothermal energy, according with the standard calculating method, is ten time, the electricity produced; the efficiency of the generation process is 10% if no heat is returned to the geothermal reservoir by injection of the effluent water. When geothermal energy is utilized directly for heating there are no international standard methods for calculating primary energy.

The energy intensive industry is the main reason for the increasing demand for electric energy. In 2008 geothermal plant generated 24,5% of the total 16500 GWh produced, 78% used by the energy intensive industry (Geothermal development and research in Iceland, Orkustofnun, 2010).

Iceland has an extensive energy reserves, but it is not unlimited. There is uncertainty in the assessment of the extent. For the potential generation of the electricity the energy reserves are estimated at roughly 50 TWh per year, 60% from hydropower and 40% from geothermal resources.

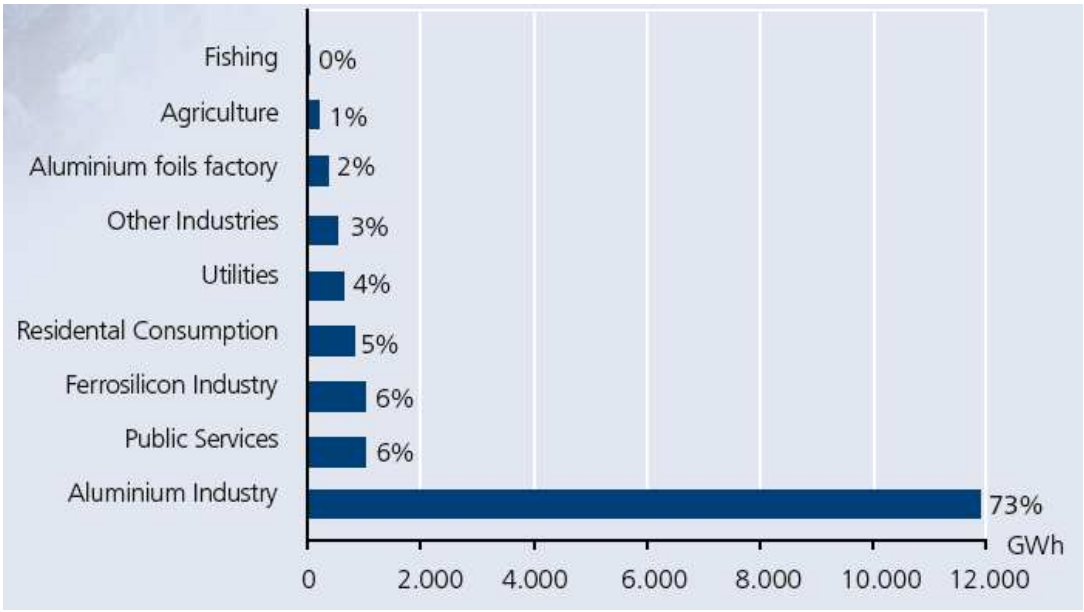

Figure 1.15 - Electricity consumption, GWh/year 2011.

Turkey is opening up the sector and the ambitious program to reach 550 MWe capacity for 2013. **France** and **Russia** have significant production, but stationed in non-European regions. Although at low levels, **Austria**, **Germany** and **Portugal** have started to produce geothermal energy, and this shows that the generation of electricity from geothermal sources can be obtained even with fluid at relatively low temperatures (100 ° C), in regions where there geothermal anomalies are present. Amongst other European countries Greece and Hungary are very promising countries for geothermal exploitation.

North America

The **United States** is one of the most advanced countries in geothermal energy, with over 3 GWe of installed capacity, and cover a bigger share of global geothermal market. There are 26 fields in operation at high temperature, it is primarily water systems dominant distributed in the Imperial Valley in California, in addition to the giant vapor-dominated field, The Geysers, which is the largest geothermal field discovered in the world. In addition to California, there are geothermal prospects in other states on the west coast in Alaska. The field of low temperatures geothermal energy is also exploited (3766 Mtep in 2000), used mainly for civil heating.

Central America, has very large geothermal resources, and countries such as **Costa Rica**, **El Salvador**, **Guatemala, Mexico**, and **Nicaragua** are developing several projects in the field. Among these, Chile, dependent on neighboring countries for the import of natural gas, currently has no system, but given the high geothermal potential, the government has recently kicked off 70 exploration projects. **Bolivia** also presents an interesting market, with plans for a potential of 400 MWe.

Asia and Oceania

In the archipelago of the **Philippines**, geothermal energy for electricity generation is a very important resource, since the 70s. In 2000, almost 22% of electricity demand was met by geothermal steam. This nation has one of the highest growth rates in the world, with regard to this energy source: it was decided to add 526 MWe of installed capacity by 2008. However, the field of low temperatures is not very developed.

On the other hand, many reservoirs are located in developing countries like the Philippines, where the geothermal resource, can play an important role. In fact, there is still a limited consumption of electricity, compared to industrialized countries, and their economy can benefit from the use of local renewable sources. The Philippines, have set themselves the goal of 1.2 GWe installed by 2020, and have recently privatized state-owned enterprises in the sector, to accelerate investment.

Indonesia, expects to achieve alone 4 GWe of geothermal capacity over the next decade.

Africa

There is a large geothermal potential along the **Rift Valley**, in the eastern part of the continent. In **Kenya**, the government has proposed to achieve the 25.1 GWe of new capacity installed in 2018. Even in **Ethiopia** there is movement in the field.

1.6 References

Axelsson G., Gunnlaugsson E., 2000. Background: Geothermal utilization, management and monitoring. In: Long-term monitoring of high- and low enthalpy fields under exploitation, WGC 2000 Short Courses, Japan, 3-10.

Bank of America, "Merrill Lynch Renewable Energy Report", Geothermal, 22 July 2011 Us Department of Energy .

Benderitter Y., Cormy G., 1990. Possible approach to geothermal research and relative costs. In:Dickson, M.H. and Fanelli, M., eds., Small Geothermal Resources: A Guide to Development and Utilization, UNITAR, New York, pp. 59—69.

Bertani R., 2005, World geothermal power generation in the period 2001 – 2005, Geothermics 34 pp. 651 – 690.

Dickson, M.H and Fanelli, M., 2004. What is Geothermal Energy?, UNESCO publication.

Dickson, M.H and Fanelli, M., Cos'è l'energia Geotermica, Istituto di Geoscienze e Georisorse, CNR, Pisa, Italy, febbraio 2004

ENEA, Rapporto Energia Ambiente 2009, analisi e scenari, Agenzia nazionale per le nuove tecnologie, l'energia e lo sviluppo economico sostenibile

Hochstein M.P.,1990. Classification and assessment of geothermal resources. In: Dickson, M.H. and Fanelli, M., *eds*., *Small Geothermal Resources: A Guide to Development and Utilization*, UNITAR, New York, pp. 31—57.

Muffler P., Cataldi R., 1978. Methods for regional assessment of geothermal resources.*Geothermics* , 7, 53—89.

Nicholson K., 1993. *Geothermal Fluids*. Springer Verlag, Berlin, XVIII—264 pp.

Orkustofnun, National Energy Authority, Energy statistic in Iceland, 2011.

Renner J.L., Geothermal Energy in the United States, IEEE power engineering society energy development and power generating committee, IEEE 2002 summer power meeting, Chicago, July 22, 2002.

Unione Geotermica Italiana, Geologia tecnica ed ambientale, - "La Geotermia, Ieri, oggi, domani" -, 2007

Web site:

Landsvirkjun Annual Report 2009. (2009).

http://www.landsvirkjun.com/media/enska/finances/Annual_report_2009.pdf

MIT, 2006. The future of geothermal Energy. Impact of Enhance Geothermal System (EGS) on the United States in the 21th Century. Assessment by a Massachusetts Institute of Tecnology-led interdisciplinary panel (J. F. Tester, Chairman), 372 pp.

http://geothermal.inel.gov/publications/future_of_geothermal_energy.pdf

Regione Toscana: Miniere e geotermia.

http://www.regione.toscana.it/sportelloenergia/leftmenu/geotermia/index.html

http://www.geothermal.uwa.edu.au/home/energy

2. LOW TEMPERATURE GEOTHERMAL ENERGY

2.1 Introduction

The low temperature geothermal energy, allows the heating and cooling of buildings by means of a heat pump connected to geothermal probes inserted in the subsoil, where, inside a heat transfer fluid circulates allowing the heat exchange with the ground. The system is applicable in any type of subsurface as it exploits the almost isothermal soil. In reality, the only limitation of the technology is related to economical costs and to the use of terminal units at low temperature, i.e. radiant floor or low temperature radiators. Among the various techniques that can be used to take advantage of this almost infinite source of heat, the most widespread, especially in the north - Europe and North - America, is the use of ground coupled heat pumps, which can operate reversibly . The same heat source can be used for heating and cooling the buildings.

2.2 Geothermal heat pump

For the pursuit of environmental protection, in line with the principles of sustainable development and respecting the CO_2 emissions heating and cooling by using low-temperature geothermal heat pumps are a promising technique.

In the majority of cases the subsoil has an almost constant temperature which oscillates between 5 ° C and 25 ° C, excluding those areas affected by situations attributable to phenomena of hydrogeological anomalies. In general, this temperature remains constant from 10 m to 100 m depth. Within 10 m of depth, the soil instead is affected by temperature, day / night and summer / winter skin effect, hence the temperature varies as shown in Figure 2.1.

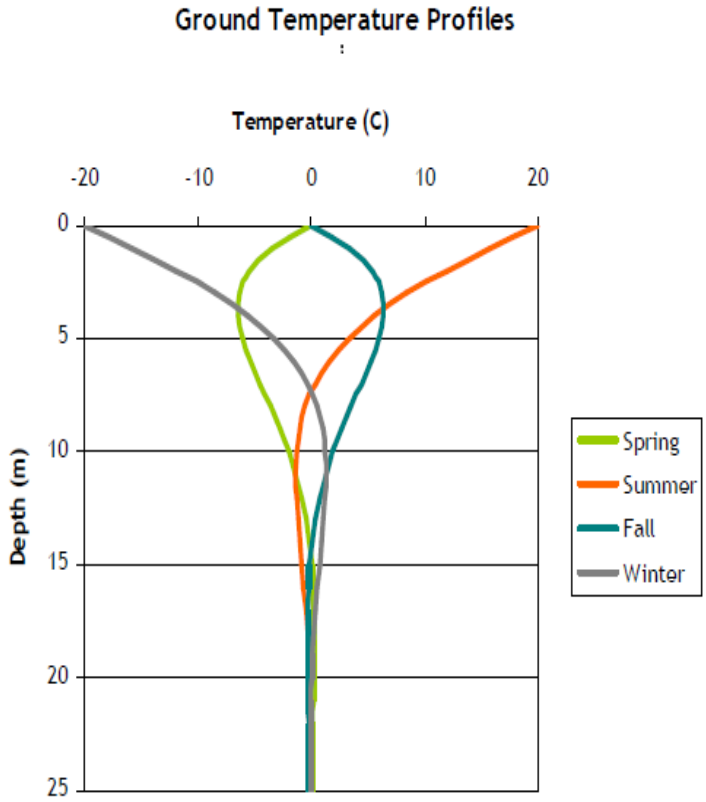

Fig. 2.1: "Skin effect" of the ground to vary the depth.

Over 100 m, the temperature begins to rise with an increase of 3 ° C per 100 m of depth. However, the temperature gradient, i.e. the value which increases the temperature of the ground, closer to the centre of the earth is not constant everywhere and at any depth. the same argument is valid for the temperature of the subsurface which is also variable depending on the considered location, the possible presence of aquifers, their origin and their periodicity.

The portion of the subsoil generally interested by Ground Source Heat Pumps (GSHP) is that which goes from a few meters up to more than 300 m depth. Commonly considered the costs of drilling are preferred depth "contained" about 100 m.

Energy is transferred daily to the Earth's surface from solar radiation, rains, winds, etc. As a result of this continuous exchange of energy, underground works like a "rechargeable battery" (Fig. 2.2), providing heat during winter and recharging thermal energy during summer.

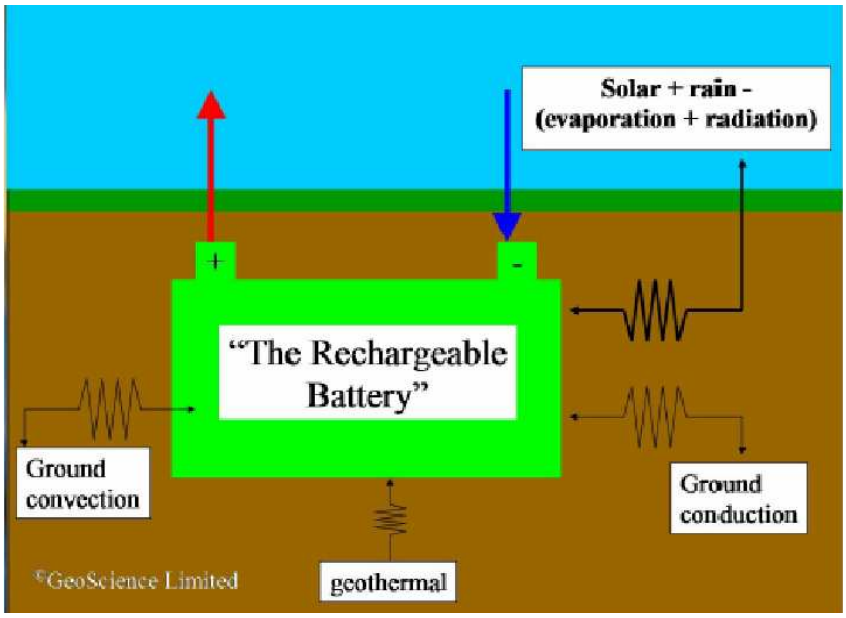

Fig. 2.2: The ground can be considered as a rechargeable battery.

The geothermal system that allows use from the natural energy of the subsoil is a system composed of a reversible heat pump coupled with the Ground Heat Exchangers (GHE).

During the winter the soil has a temperature generally higher than that of the outside air, the fluid down in depth through the GHE subtracts thermal energy to the ground, returning on the surface at a higher temperature. This energy is transferred in the heat exchanger of the heat pump (evaporator) bringing the vector fluid in the heat pump circuit, from the liquid state to vapour. Subsequently, it is sucked into the compressor which, operated by an electric motor, provides the mechanical energy required to compress the fluid, thus determining an increase in pressure and consequently in temperature. The refrigerant inside the heat pump circuit passes trough the heat exchanger of the heat pump condensing (vapour). At this stage there is a new change of phase of the fluid, which passes from the vapour to liquid; transferring heat to the heat transfer fluid of the system terminals, for heating, environments or for the production of water warm meter for building heating uses. The cycle ends with an expansion valve with lowers the pressure and the temperature for the evaporator, thus returning to the initial conditions of the cycle (Fig. 2.3a).

The same system, with proper changes plant, can provide air cooling; in this case the cycle is reversed and the system releases in to the ground the heat extracted from the building. (Fig. 2.3b).

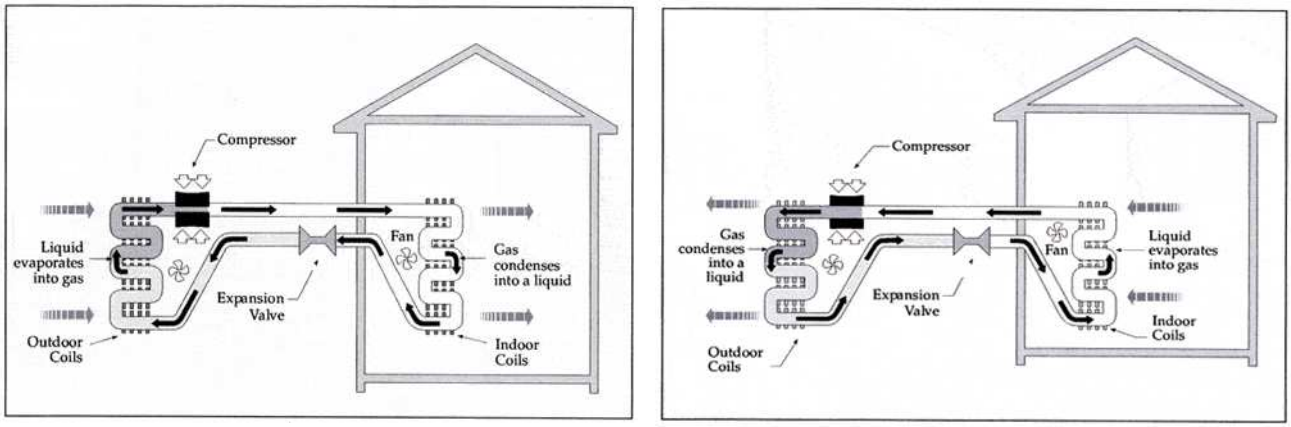

a *b*

Fig. 2.3: Operating of a reversible heat pumps heating mode a) and cooling mode b).

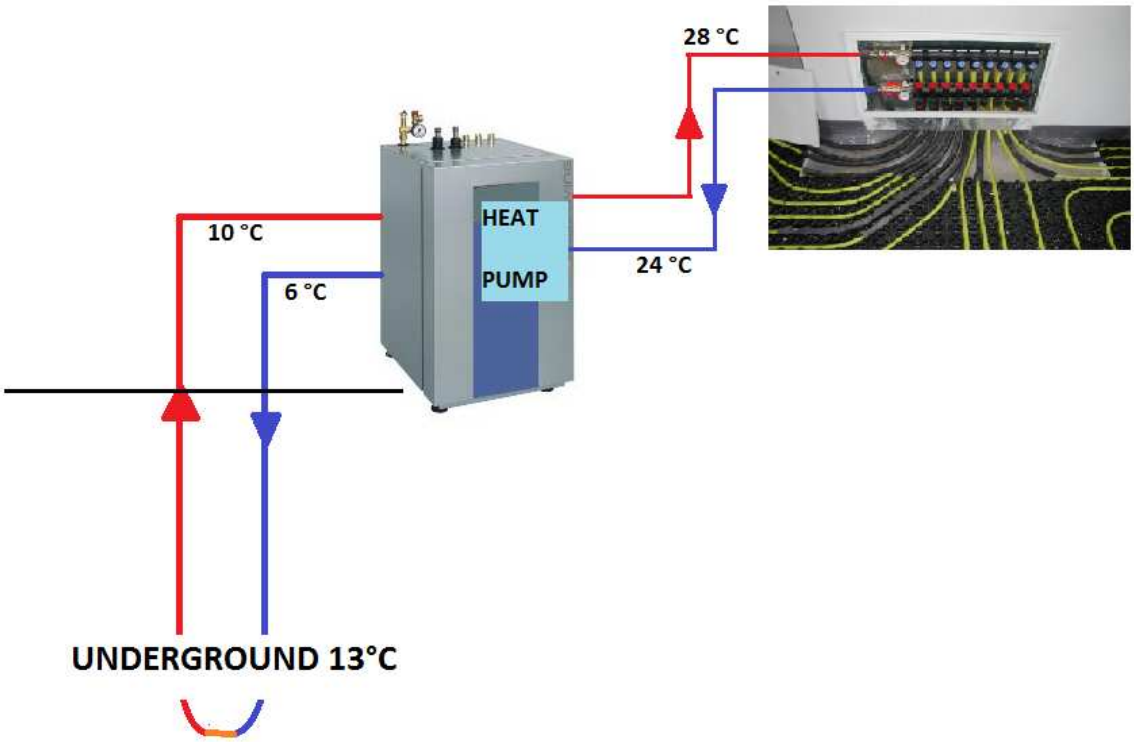

Fig. 2.4: Example of typical temperatures in winter.

A plant which operates at low temperature is composed of:

- Heat pump, usually installed inside the building;

- Geothermal probes, on GHE systems;

- Fluid, inside the borehole heat exchangers;

- The distribution system of heat at "low temperature", such as (floor heating, radiant panels, fancoils, etc.

2.2.1 Heat pump

The heat pump (HP) is a thermal machine capable of transferring the extracted heat from a low temperature source (cold source), towards an external environment at a higher temperature (warm well). Its capacity is to force the heat flow in the opposite direction with respect to what is defined as the natural flow. However, the second law of thermodynamics is not violated because the heat pump performs forcible transfer of heat, using outside work, which can be electricity (compression machines) or heat (absorption machines). The term heat pump refers to the heating operation mode. The HP becomes reversible when the same machine is able to operate also as a chiller for the summer period, when it transfer heat from the room (cold source) towards a warm well. The heat pump, as well as the cooling machine, is composed of a closed circuit where the refrigerant performs a reverse cycle. The only difference between the two systems is the useful effect desired: in the first case it consists in providing heating to an environment while in the second case the goal is it subtract heat from a room (schematized in Figure 2.5).

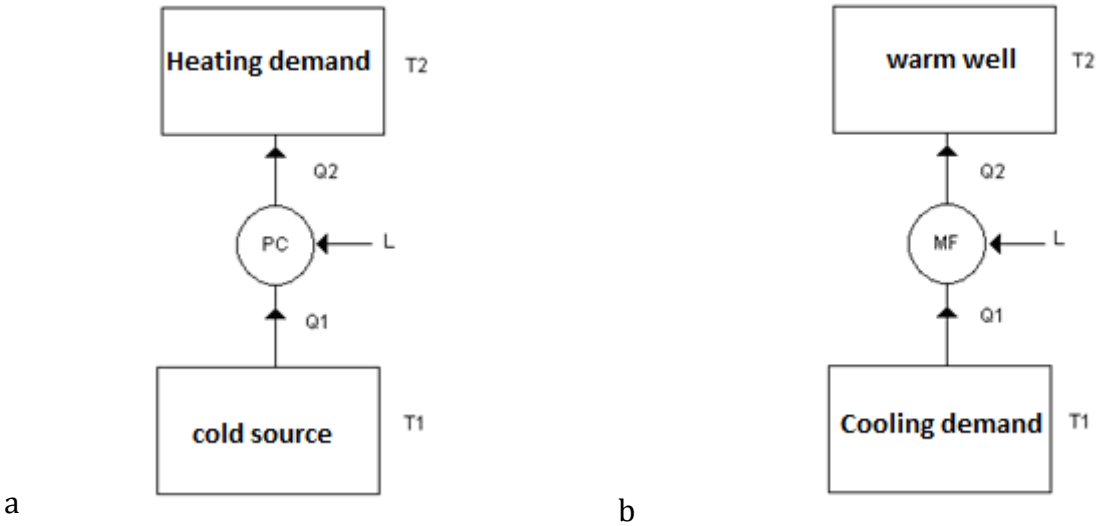

Figure 2.5: Scheme of a reversible cycle: heating operation a) and cool operation b)

The main mechanical components, which constitute a heat pump in a closed circuit are:

1. The compressor: its function is to increase the pressure of the refrigerant fluid and therefore the temperature, to achieve suitable levels of condensation.

2. The condenser is a heat exchanger in which the thermal power is transferred from the fluid that condenses towards the hot well.

3. The evaporator: it is a heat exchanger that allows the extraction of energy from the source at a lower temperature. The subtraction of heat occurs by exploiting the passage of the refrigerant fluid from liquid to vapour phase;

4. Lamination unit: Used to close the loop and to reduce the pressure between condenser and evaporator. It consists of a capillary tube (cheaper solution) or a valve (more expensive, but usually with higher performance).

5. Safety devices and auxiliary devices: devices for control and safety are useful when the heat pump operates outside the standard conditions: pressure gauge of high and low pressure, manometer for the pressure of the liquid and a thermostat for defrosting if needed. Among the auxiliary devices there is the four-way valve, used in pumps reversible cycle, and the accumulator where the fluid is collected for avoiding refrigerant excess.

A plant scheme is presented in Figure 2.6:

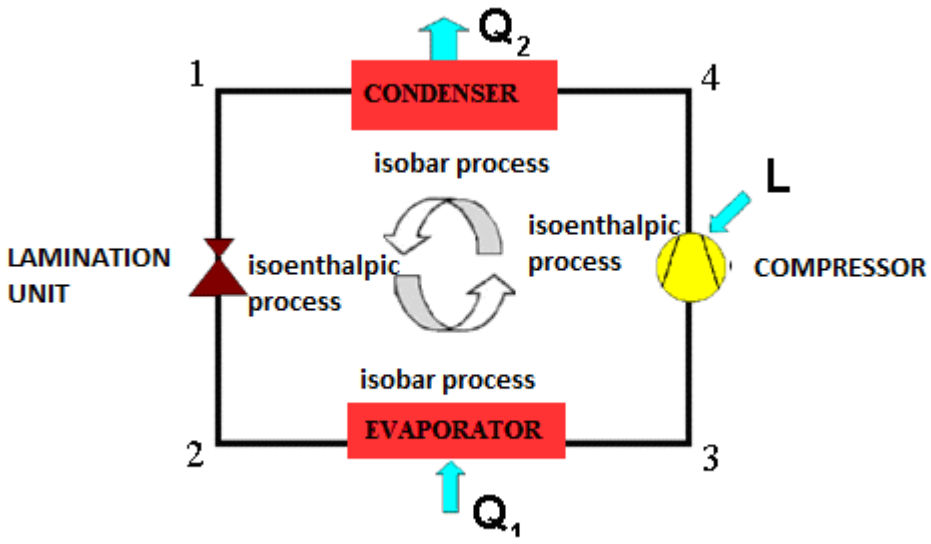

Fig. 2.6: schematization of a heat pump.

The reverse cycle consists in the evaporation of the fluid that absorbs heat from the cold source. It is then compressed by the compressor and condensed in the condenser where it gives up heat to the hot fluid. Finally, the condensed fluid is laminated and returns in the initial conditions to be again evaporated. The transformations of the refrigerant can be seen in the classical thermodynamic diagrams in Fig. 2.7.

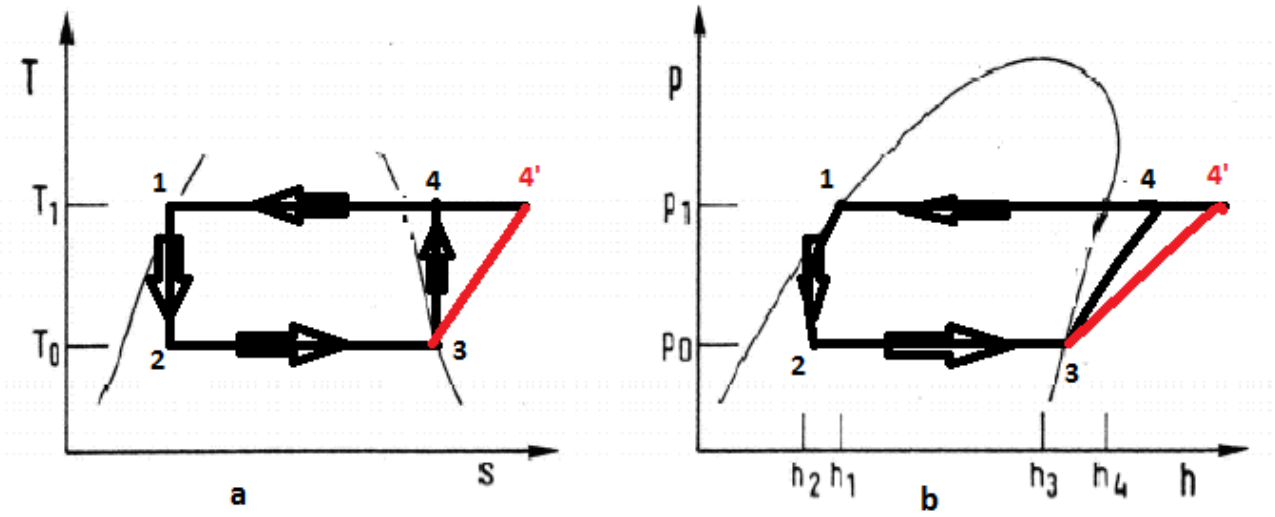

Fig. 2.7: Reverse cycle in the diagram T – S a) and p – h b).

To evaluate the efficiency of a system is of fundamental importance to know the temperatures of the rooms to be heated or cooled, and the heat transfer fluids to be used. The heat released from a heat pump (Q_2) is the sum of the heat extracted from the source (Q_1) and the necessary energy supplied by the compressor (L), to activate the cycle:

$$|Q_2| = |Q_1| + |L| \qquad (2.1)$$

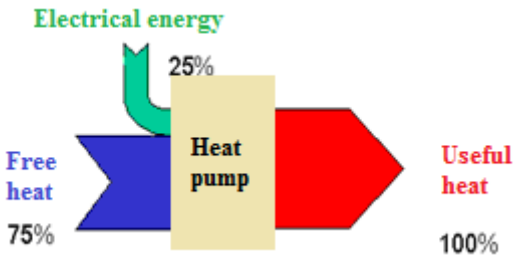

Fig. 2.8: Scheme diagram for a heat pump.

In Fig. 2.8 the energy flows in the case of a heat pump can be seen.

The performance of a compression a heat pump, referring to certain and precise conditions of temperature, is indicated with the term Coefficient of Performance, COP. It is defined as the ratio between the quantity of thermal energy supplied by the heat pump (Q_2) at temperature T_2 and the electric energy supplied to the compressor (L).

$$COP = \frac{|Q_2|}{|L|} \qquad (2.2)$$

In summer operation (cooling conditions), the chiller subtracts the thermal energy Q_1 at the temperature T_1 by means of the energy L. In this case the efficiency is defined through the Energy Efficiency Ratio (EER):

$$EER = \frac{|Q_1|}{L} \qquad (2.3)$$

The COP and EER are not thermodynamic efficiencies (which has values between 0 and 1) and therefore their values can be greater than one; this does not mean that it yields more energy than it absorbed. The system as a whole must always satisfy the first principle of thermodynamics, expressed by equation (2.1).

The maximum theoretical value of COP of a heat pump operating between two temperatures T_1 and T_2 can be calculated according to Carnot's cycle: (Figure. 2.9).

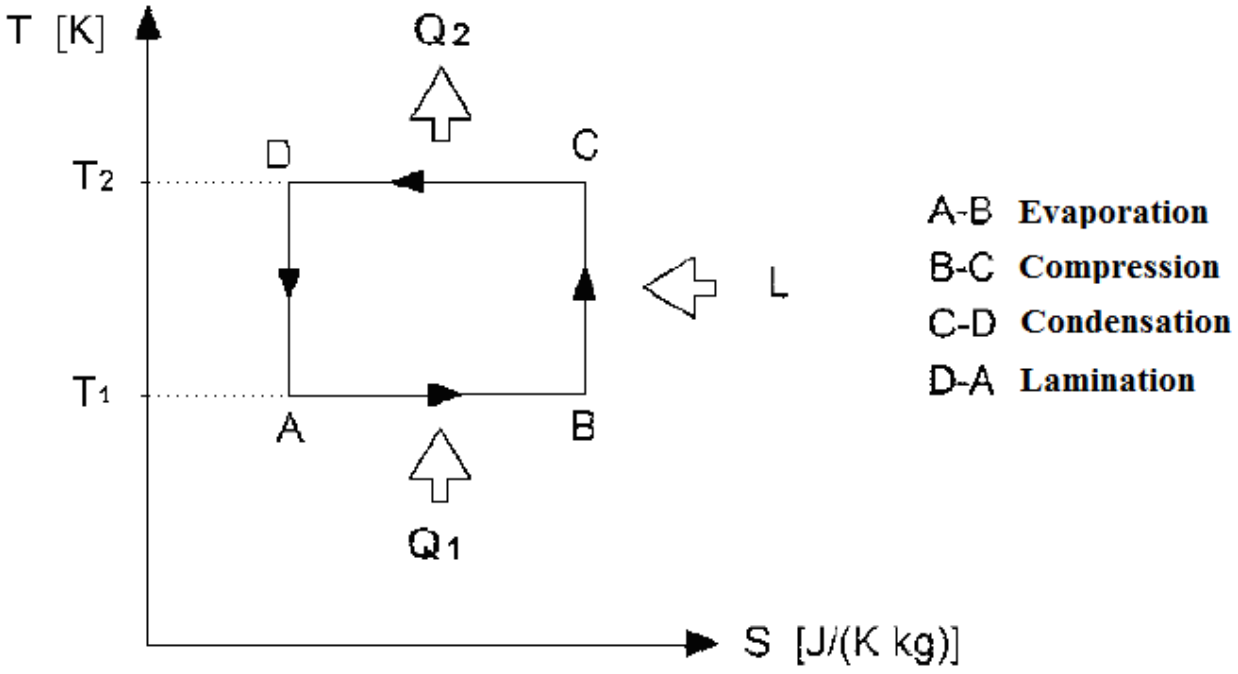

Fig. 2.9: Carnot cycle.

$$COP_{CARNOT} = \frac{|Q_2|}{|L|} = \frac{|Q_2|}{|Q_2| - Q_1} = \frac{T_2}{T_2 - T_1} \qquad (2.4)$$

For a chiller operating between T_1 and T_2 the Carnot efficiency can be written as:

$$EER_{CARNOT} = \frac{Q_1}{|L|} = \frac{Q_1}{|Q_2| - Q_1} = \frac{T_1}{T_2 - T_1} \qquad (2.5)$$

Even if the Carnot cycle can be reached in theory, it can be seen that the COP and EER are dependent on the difference between T_1 and T_2 (ΔT). This sentence can be generalized also for usual machines, as can be seen in Fig. 2.10, where the trend of the COP is presented, for real machines compared with the ideal Carnot cycle with the same level temperature difference between the hot tank, and the cold source. As can be seen the lower the ΔT the higher the COP.

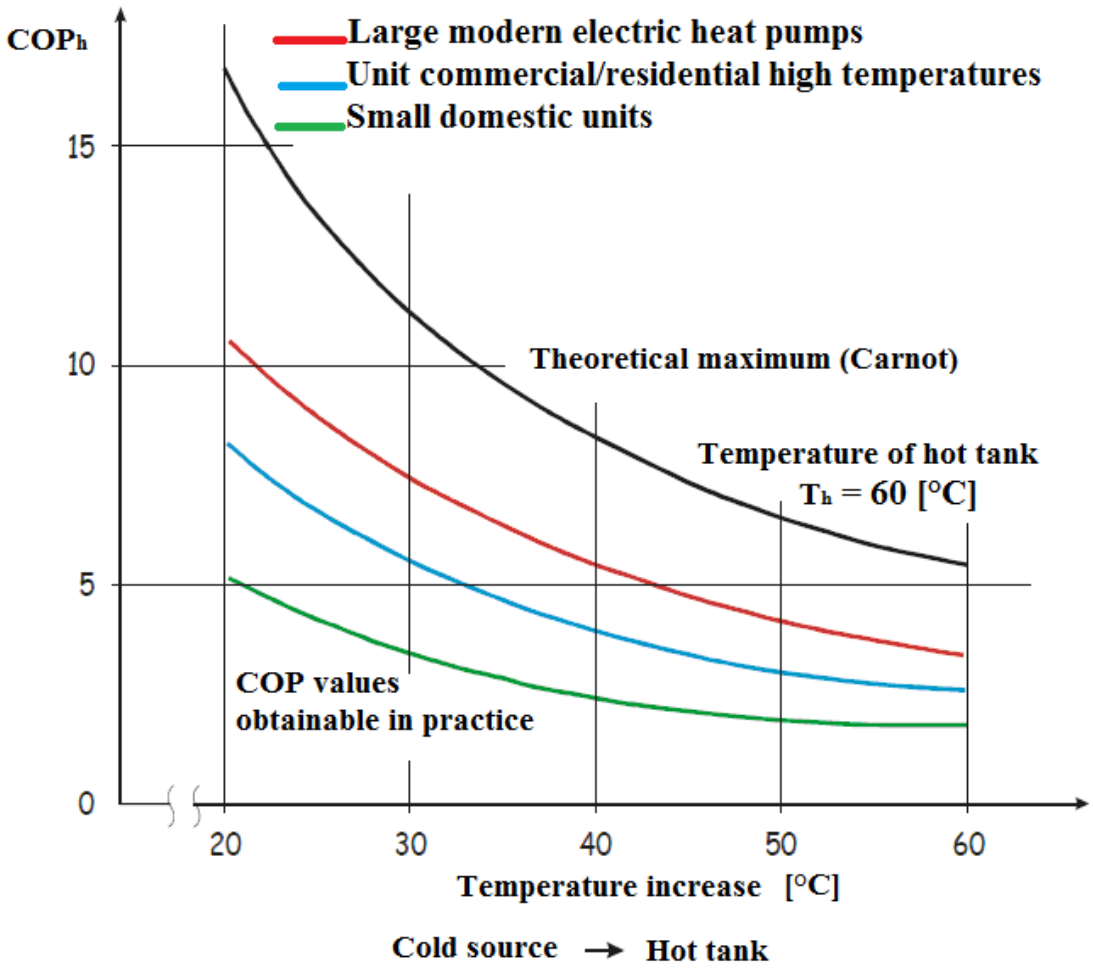

Fig. 2.10: influence of ΔT between the hot tank and cold source at the COP pump.

This reasons which lead to lower COP / EER values in real cycles are due to the irreversibility which characterize the real cycle compared to the ideal Carnot. Such irreversibility is attributable to internal causes and external. The first cause consist of friction losses in the flow of fluid along the exchangers, and along the connecting pipes between the various organs of the cycle (negligible) and losses in the compression of the fluid, characterized in the real case by its own isentropic efficiency (not negligible) .

The second cause is due to temperature differences between condensing fluid and hot tank one part, and between the evaporating fluid and cold source on the other. This is due to the fact that in real heat exchangers the condensing refrigerant liquid is at higher temperature compared to the warm well, while the refrigerant has lower temperature compared to the cold source (Fig. 2.11).

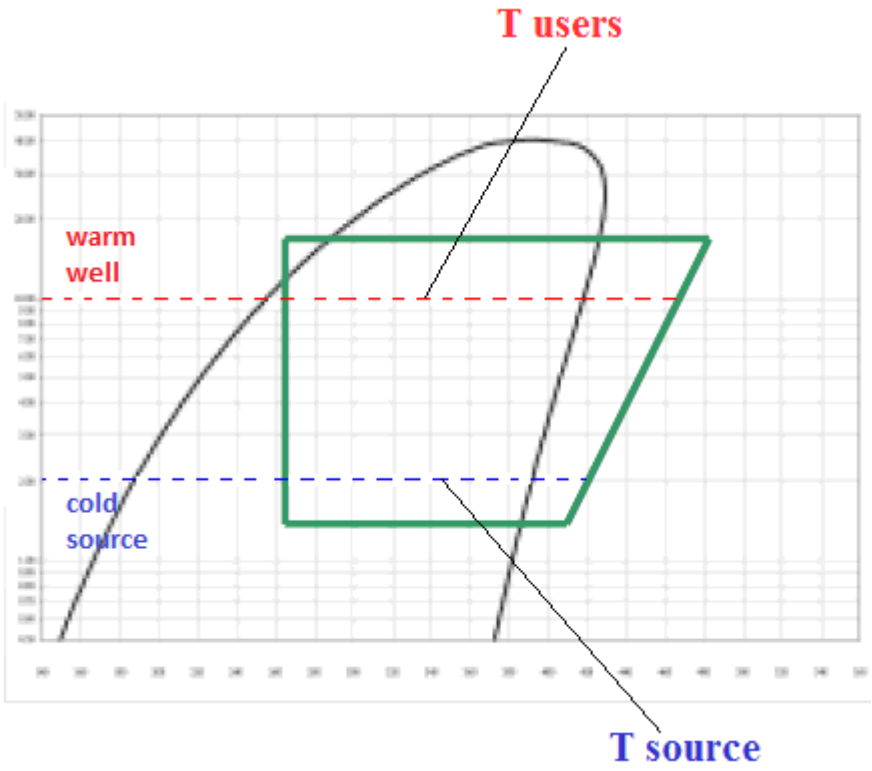

Fig.2.11: Differences between temperatures of the refrigerant fluid inside the cycle and the warm well and cold source temperatures.

2.2.2 Heat exchange with the ground

ASHRAE identifies a classification of heat pumps depending on the type of heat exchange in the ground:

Heat transfer by direct means: that is, through an open circuit with extracted directly of water from the territory;

Exchange of heat by indirect means: that is, a system of pipes closed circuit that directly exchange heat with the ground, to which inside the circus a heat transfer fluid; these systems can be divided into two subcategories:

- Systems closed circuit secondary heat pump exchanges heat energy from the ground by a heat transfer fluid (water or mixture of water - antifreeze fluid);

- Systems a closed circuit and direct expansion refrigerant: heat is transferred directly between the coolant and the ground.

In this chapter, the interest focuses on the indirect exchange with the ground and amoung then, the work has been carried out on secondary fluids, therefore these tecnologies will be further shown in detail.

2..2.1 Horizontal heat exchangers

The horizontal heat exchangers, are interred in horizontal trenches excavated in deep usually no more than 2 meters. For this reason, these probes are strongly affected by the climatic conditions of the atmosphere in the form of solar radiation and, precipitation. This is essential to consider their correct positioning, avoiding therefore, the installation in shady areas if the system is studied during the winter for heating, or vice versa use shady areas if the principal use is in cooling season.

The horizontal arrangement allows to avoid perforations and therefore high initial costs, while it requires substantial extensions of the excavation area. It becomes impossible the realization of this technology in city centers. In addition, the thermal flow exchanged between the probe and the subsoil is influenced by the length of the pipe, the depth of installation and by the distance between the tubes. It is important to remark that with increasing distance between the pipes the thermal interference between the branches decreases. Increase the number of tubes for trench or the total length of tube per meter of excavation means reducing the area required and therefore the cost of excavation and backfilling with the counter of a significant increase thermal interference between the probes, with consequent increase of the total circuit length (Figure 2.12)

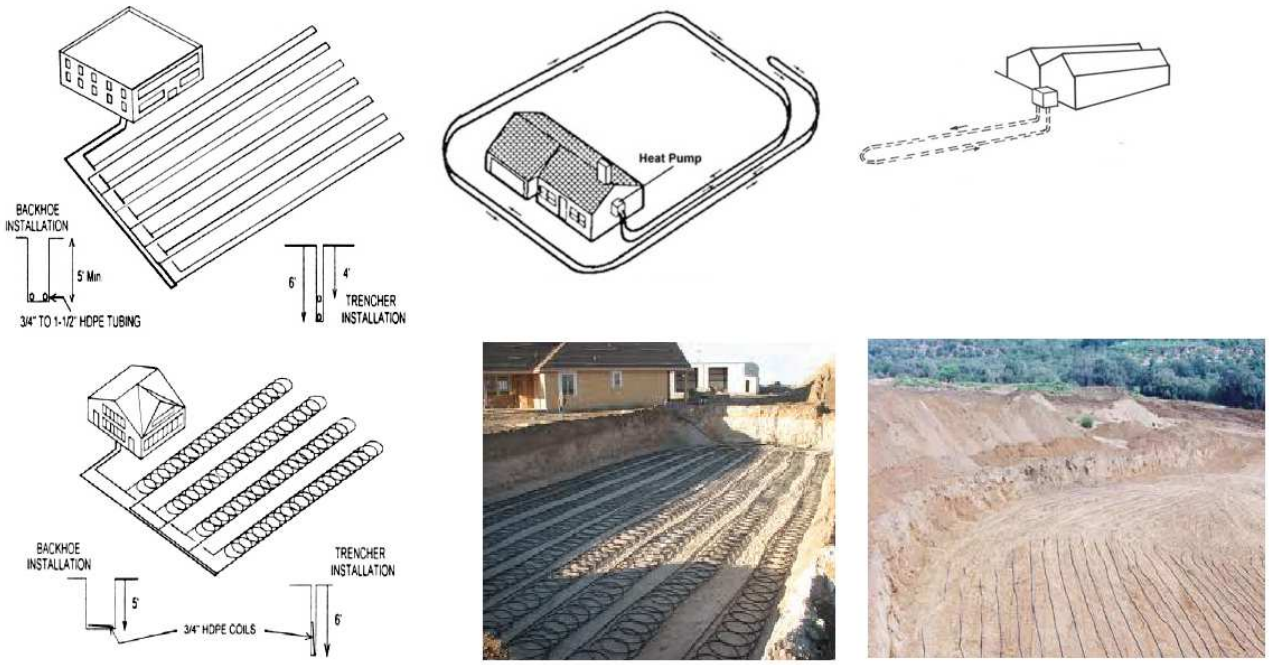

Fig. 2.12: Certain types of configuration installation of geothermal probes horizontal development.

2..2.2 Vertical heat exchangers

The vertical heat exchangers due to the considerable depths, have the advantage to be affected negligibly to climatic variations atmospheric.

As for the pose, the vertical probe requires a vertical drilling of the ground to the desired depth and diameter. Then pipes are installed and finally the filling closed the hole from the bottom to the top of the drill. (Figure 2.13). Typical values found in the literature for vertical probes are represented in Table 2.1.

Fig. 2.13: Phases of drilling and installation for the installation of geothermal probes vertical.

Table2. 1: Sizes typical for geothermal ground in vertical development.

Drilling depth [m]	20 – 180
Diameter of the perforation [mm]	100 – 150
Material of pipe	Flexible tube HDPE (high density polyethylene)
Nominal outside diameter of pipe [mm]	20 – 40
Distance between the probe [m]	6 – 8

It is quite common to use different boreholes with different patterns.

The space available, the characteristics of conductivity of the soil and the presence of water in the aquifer are elements that influence the choice of the arrangement of probes. In fact, any consideration of thermodynamic problem is confronted with the objective limits that are found in any drilling project.

To avoid thermal interference between the probes is necessary to maintain a minimum distance between the centers the probes with a range variable between six and eight meters, depending on the conductivity of the soil preferably least 7m . The thermal influence of a probe on another, in fact, can cause, over the instantaneous loss of efficiency of the system, a thermal irreversible change of the ground, with a consequent visible impact on the environment and a progressive deterioration of the thermal capability to extract/release heat from / to the underground. In extreme conditions, with the temperature of the heat transfer fluid glycolate constantly below 0 ° C, the phenomenon called *ice lencing* may occur: the ground is not able to cope with lowering of temperature, and therefore, being saturated, permanently freezes also producing mechanical damage to the probes because of the pressure exerted by the increase in volume of the frozen zone.

The geometry of the systems of probes is based on all of these factors and therefore varies with respect to each case. The most common geometries consist of the disposal of probes in parallel rows, possibly staggered honeycomb (Figure 2.14).

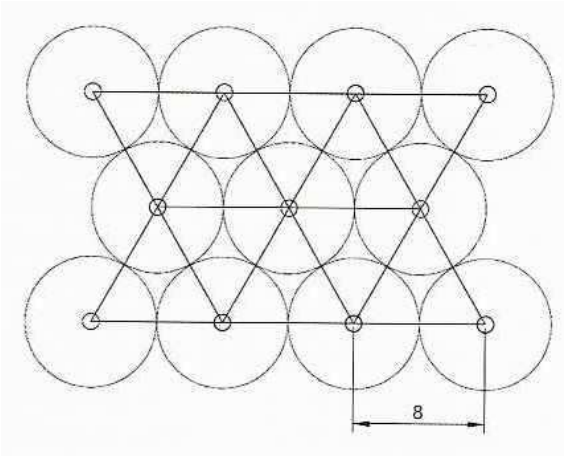

Figure 2.14 – The geometry for the disposition of probes honeycomb.

In this manner it is possible to optimize the distance of 7m between a probes. For areas with a significant amount of wells, such geometry can determine the thermal variations in the ground since, although the distance between probes is respected, the total number may be excessive for a limited amount of space.

It is also important to consider the type of configuration of the hydraulic connections on the surface that can be in series, in parallel or hybrid configurations (series / parallel) for systems with a large number of probes. (Figure 2.15). The difference between the configurations consists essentially of unequal flow rates and pressure drops, therefore, case by case, on the basis of economic factors and the characteristics of the plant different solutions can be chosen.

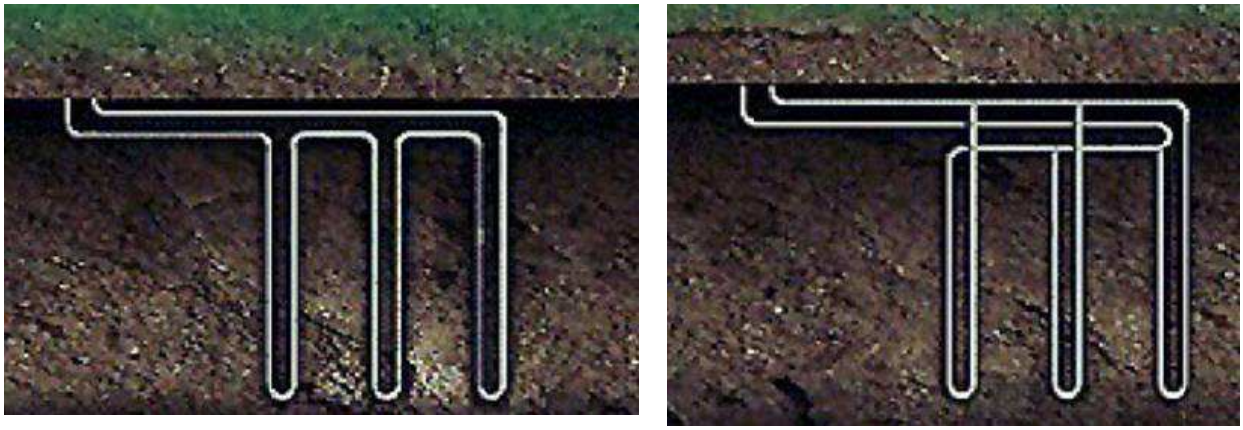

a b

Fig. 2.15: vertical probes connected in series a) and in parallel b).

The geothermal probes are made of polyethylene, and may have different types of cross section:

- single U-tube (Fig. 2.16a): in the well one pipe is inserted, presenting a U fitting between supply (down stream) and return (upstream); to or to avoid breakage, thus avoiding the welding, continuous pipe is positioned;

- double U-tube (Fig. 2.16b): in the two tubes U-tubes are inserted; in the bottom part of the borehole two U – shape terminations are present. The water can circulate in parallel (most common) on in series;

- coaxial tubes (Fig. 2.16c): it consists of concentric tubes, which may also be built in different material. These types of section allow the advantage of a reduced space of drilling, a large exchange surface, best contact between soil and probe; where allowed by the geology of the soil, it is possible to install the probe using infixion and percussion techniques, avoiding drilling. On the other hand, in case of perforation it is difficult to ensure the restoration of the impermeable soil horizons risking the communication between the aquifers.

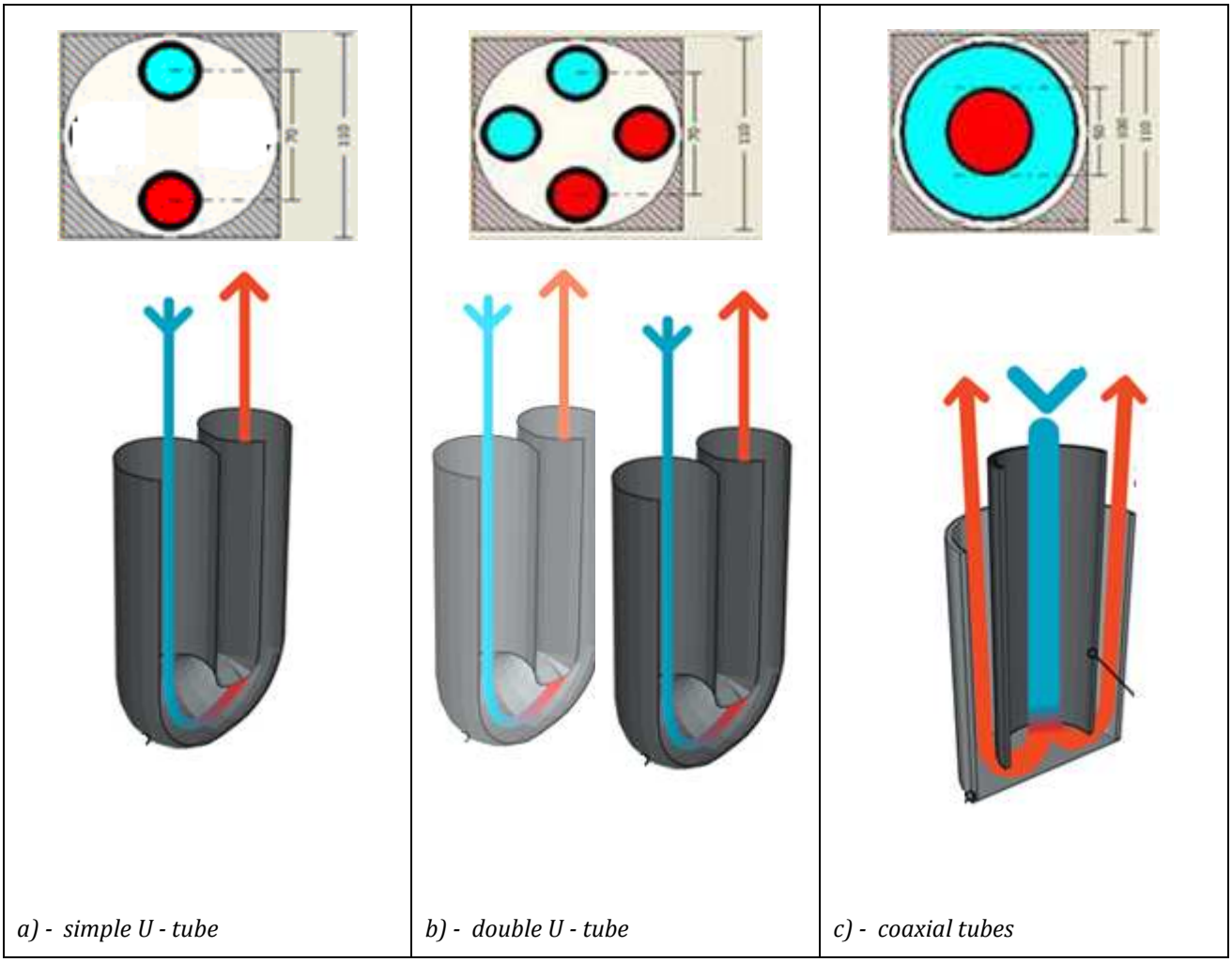

a) - simple U - tube | *b) - double U - tube* | *c) - coaxial tubes*

Fig. 2.16: Cross – section vertical geothermal probes (dimensions in mm, drawing not to scale).

The installation of geothermal probes requires a lot of attention in all phases, as it is sealed and therefore it is not possible to make any maintenance on piping in depth.

The materials used for the realization of the tubes is generally the high density polyethylene HDPE. The use of a plastic material for geothermal probes provides significant advantages as it is very easy to handle, flexible and easy to transport on site for the low specific weight, also resistant to corrosion, in the phase of operation of the plant, to any chemical agent; finally it presents important characteristics of mechanical resistance, long-term stability, and reduced internal roughness, compared to other materials, resulting in low hydraulic resistance, and therefore low pressure drop.

The borehole is the heat exchanger, i.e. the intermediary between the soil and the heat transfer fluid, allowing to exchange or transfer the thermal energy; therefore, the thermal characteristics of the material of the pipe and of the ground are quite important. The pipes made of polyethylene have a conductivity variable from 0.38 to 0.40 W / (m K). In the realization of the tubes the mechanical stress of pressure between fluid and ground, normally considering the pressure at the bottom of the borehole (100m depth means a nominal pressure of 10 bars).

In literature: (Delmastro and Noce 2011), the temperature range for the use of the polyethylene can vary from - 60 ° C to + 70 ° C; during operation, to avoid deterioration due to thermal shock, the recommended temperature range is much lower, varying from - 20 ° C to + 30 ° C. In addition, attention has to be paid on sun exposure of the tubes before being placed in the ground: it is recommended not to expose the pipes outdoors for a long time (about two years), as they are subject to deterioration and therefore loss of mechanical characteristics.

For a wider temperature range the cross-linked polyethylene PEX should be used. In fact, it has a temperature range up to 90 ° C. in comparison with the HDPE, PEX is more resistant to pressure, and presents characteristics of thermal conductivity around 0.24 to 0.30 W / (m K); the costs are also higher.

Another important phase is that of filling the space between the probe and ground. In fact the filling material is important for the purposes of the heat exchange between ground and pipes. The filler material may consist of quartz sand and cement mortars.

It is important to careful by choose the granulometry of the sand, as it must guarantee a thermal conductivity at least equal to that of the soil in situ; for this reason it is preferred to use quartz sands. Attention should also be paid to the machining step of filling the hole, this can be dried by natural gravity of sand, or for pumping in a mixture with water. In any case, during the filling phase it should be ensured that along the probe no air voids; are present in fact, the areas with no continuity with the material (sand - soil) do not ensure the exchange of heat since the air will act as thermal insulation.

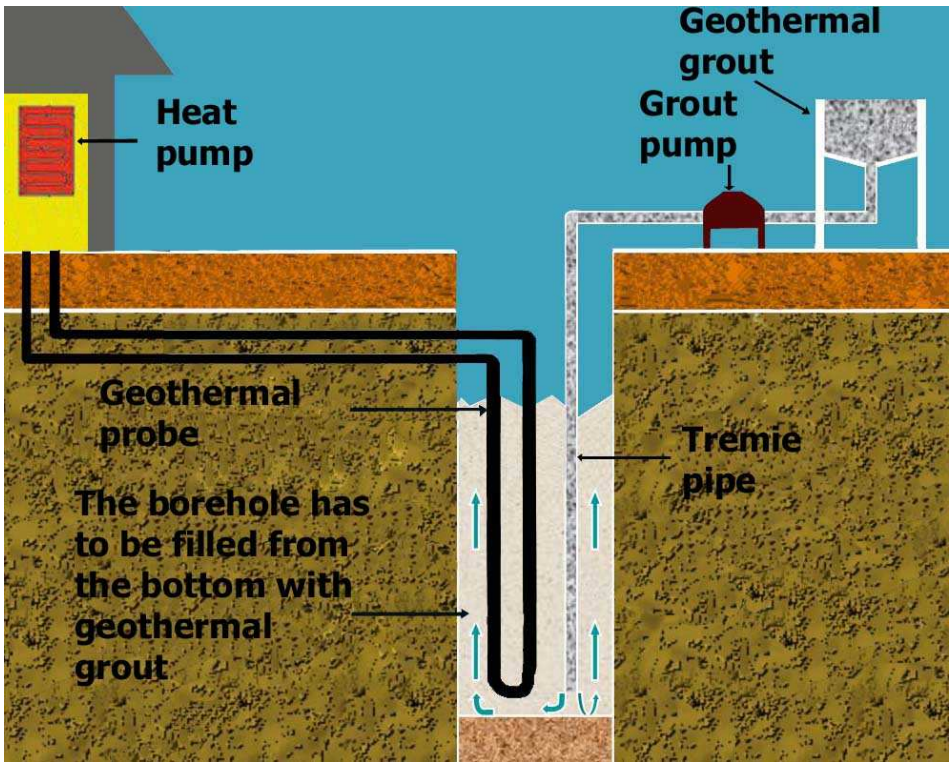

Fig. 2.17: Filling phase in the installation of a vertical GHE.

The cement mortar must respond to important properties, among which the main ones are:

- Thermal conductivity,
- Density;
- Rheology;
- Permeability;
- The maturation time;
- The heat of the maturing process;
- Change in volume during maturation;
- Resistance to frost;
- Separation of the phases (bleeding effect).

The thermal conductivity, the cement slurry is the fundamental parameter with respect to all those listed above, because it describes the characteristic of thermal coupling between the GHE and ground. Interesting considerations are presented by Delmastro and Noce (2011), in which highlighted that improving thermal conduction of the filling lowers thermal resistance between the pipes and the ground, but, at the some issue, creates a short – circuit effect between supply and return water. (seen Figure 2.18):

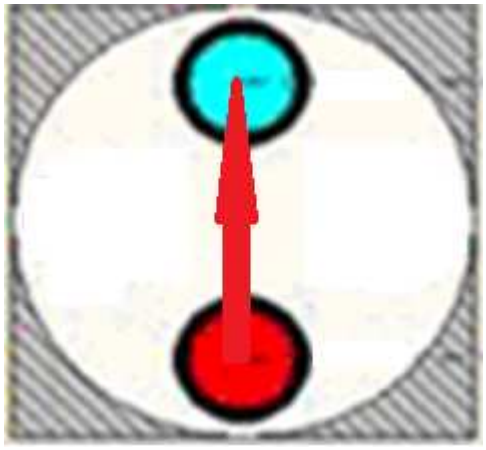

Fig. 2.18: Heat flow of short – circuit due to the high thermal conductivity of the cement grout filling.

Studies in the literature show the importance of the distance between the tubes just to reduce the short – circuit effect above mentioned, in particular Hellstrom (2006) shows that the use of spacers (Fig. 2.19), used to maintain equidistant and in the correct position the package of tubes, are effective for this purpose.

Fig. 2.19: example of spacer to be used in drillings

Table 2.2 shows some indicative values of thermal conductivity of different materials used as filling (Reuss, Sanner 2001).

Table 2.2: Approximate values of thermal conductivity of the materials from filling.

Material	Thermal conductivity [W/(mK)]
Saturated sand	1.7 – 2.5
Dry sand	3 – 0.6
Clay	0.9 – 1.4
Bentonite 1,3 kg/dm^3	0.7
Bentonite with sand	1.4 – 1.8
Cement / bentonite	0.6 – 1.2
Premixed thermally enhanced	1.6 – 2.2

The knowledge of the density of the cement slurry is critical to understand, by weighing a sample of mortar; if the content of water, and the formulation of the components is correct, it must have values around 1.5 t/m^3.

The rheology is the viscosity measured with the "Marsh cone", a high viscosity implies a good cementing. The number of Marsh represents the time, expressed in seconds, necessary to allow the emptying of a funnel (Marsh cone) Fig 2.20 of standard form filled with the cement slurry (see UNI EN 445, by ATSTM C 909 and DIN 4126). This number must assume values less than 20s (ranging from 15s – 20s), in order to avoid problems in pumping. The rheology is critical the ability to clog any cavities in the ground, thus avoiding zones of thermal insulation between the probe and ground.

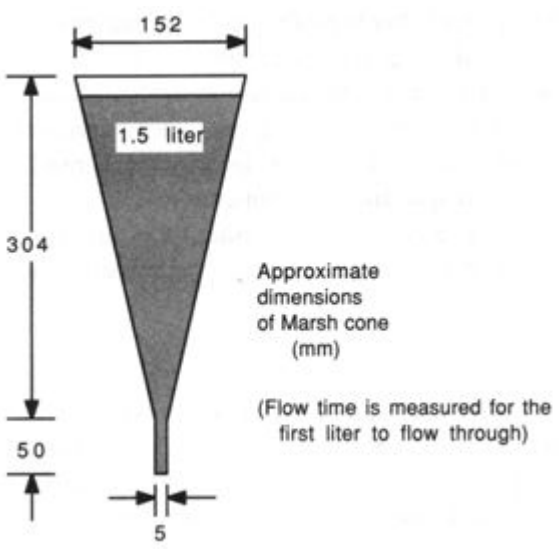

Fig. 2.20: Example and measures of Marsh cone for measuring the rheology.

A low permeability is required, in order to minimize the contact between aquifers at different depth one way to achieve this is the addition of bentonite and various additives. Permeability values are sufficiently low around to 10^{-10} cm / s equivalent to the values of impermeable soils.

Another important aspect is the trend of maturation, that is varying from half day to a few days; this variability depends on the presence of ground water, where, in these conditions the maturation requires more time. It can be said that a good mortar for probes must not show phenomena of volumetric change during maturation, since a volumetric expansion would cause deformation of the pipe with reduction of the passage section or complete obstruction, while contractions may give rise to cracks that would reduce the heat exchange with the ground and increase permeability.

During the maturation of the cement mortar, a strongly exothermic chemical reaction occurs. The heat of maturation, may lead to an increase of temperature which can damage the polyethylene pipe. The knowledge of the temperature during the maturation allows to know if such damage is present and the time needed to reset the undisturbed soil temperature (Ground Response Test) in situ for the determination of the thermal characteristics of the soil and of the probe can be carried out. Increases in temperature are of the order of 15 °C to 20 °C.

In winter, if the heat transfer fluid is located at temperatures below 0 °C, the cement mortar may suffer increases in volume, by starting in the time cycles of freezing and thawing such as to fracture the jet. A frost resistance is crucial to avoid increased permeability and reduction in thermal conductivity.

The separation of the phases, or bleeding effect, Fig. 2.21, occurs when the solid part tends to settle on the bottom, while the liquid part is separated partially from mixing floating in suspension. This phenomenon has to be avoided, as it is a sign of a bad quality of the cement slurry.

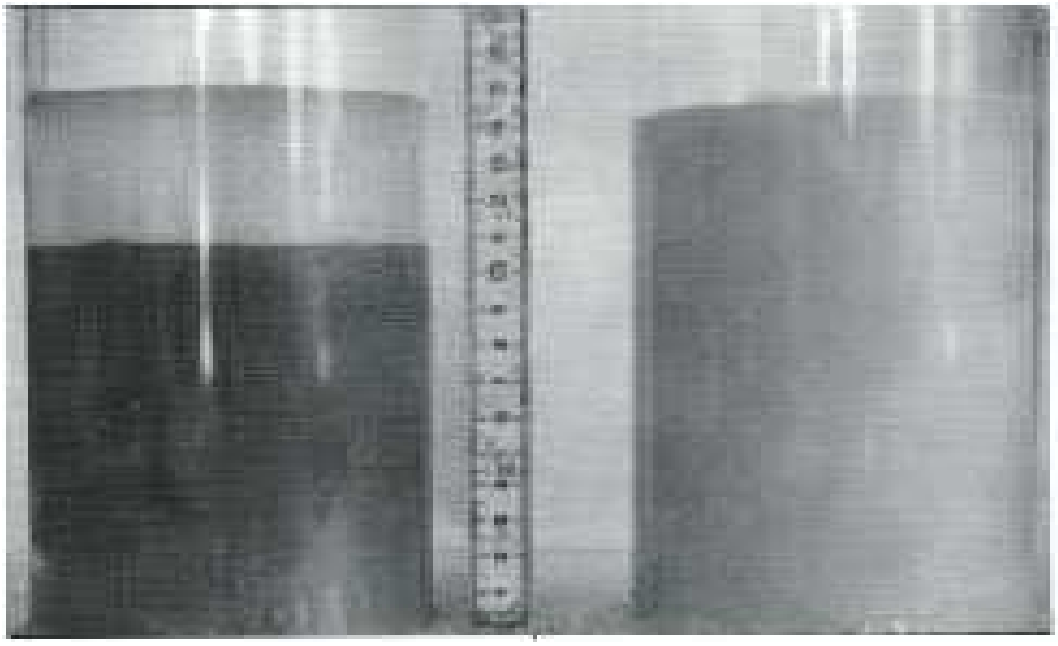

Fig. 2.21: Example of bleeding effect.

2..2.3 Energy piles

Cold foundations energy piles, retaining walls, tunnels, etc. represent a great potential as geothermal resources. In Figure 2.22 a scheme of the geothermal plant, using the foundations cold, such as energy piles and retaining walls is shown.

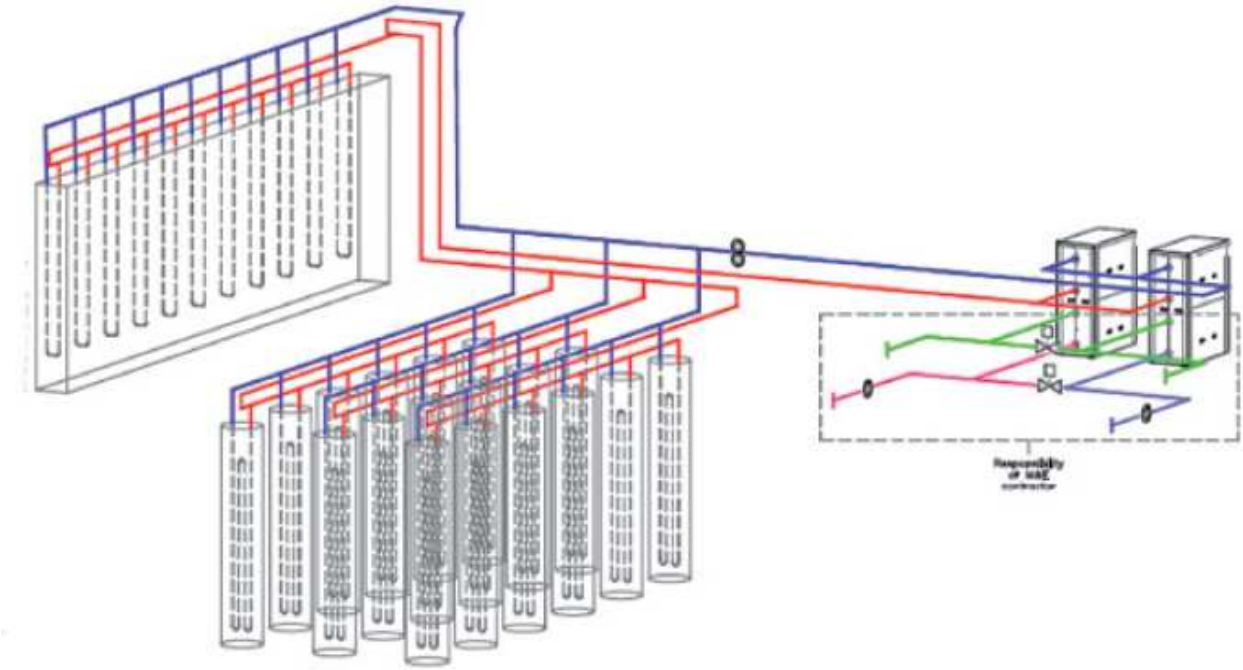

Fig. 2.22: Scheme geothermal plant to "cold foundations" piles, retaining walls.

Since the 80s, geothermal energy has been increasingly realized by using foundations; in Austria and Switzerland, at the beginning foundation slabs have been used, then by piles (1984) and diaphragms (1996). These concrete elements are already required for structural reasons, and there is no need to install new elements as in conventional systems. Figure 2.23 shows the increase in the use of energy piles in Austria since 1984.

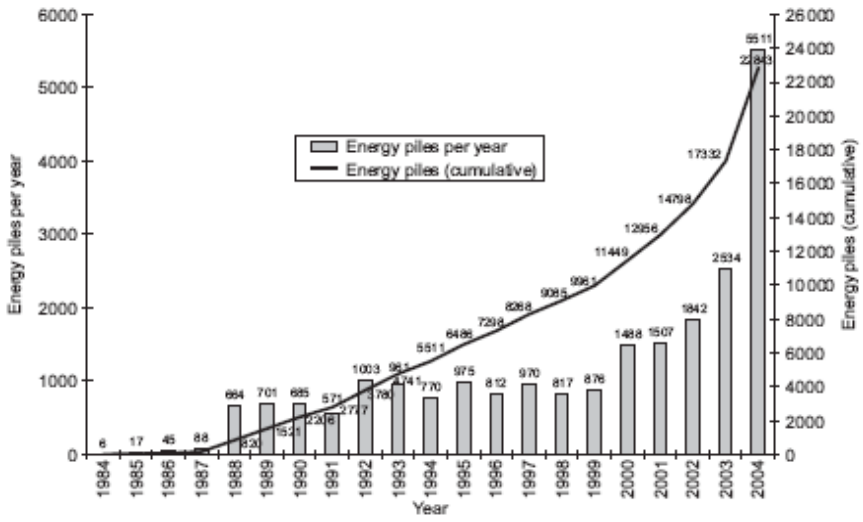

Fig. 2.23 – Number of installations of Energy piles in Austria.

The concrete piles will act as a structural element, transfers ring the building loads in deeper soil layers, while a support wall will give stability to a slope of terrain. Inside the strctures pipes with water flowing will exchange energy, both for heating and cooling the building.

In Figure 2.24, are represented some phases of the construction of energy foundation piles energy to ensure the bearing capacity of the building (structural function), and to satisfy the energy needs heating/cooling (thermal function).

Figura 2.24 – Executive phases of the installation of piles foundations of a building.

So far, the energy piles with reinforced concrete, represented the majority of energy piles installed. The percentage of bored piles (large diameter) is significantly increased since 2000. The continuous contact, between the heat exchanger (pipes) and the reinforcement, during the immersion in the excavation, can damage the integrity of final plastic tubes. The risk of damage of the probes can be reduced by means of an armature of reinforcement that is to be welded to a stirrup helical vertical bars. Making a connection only with metal wire could afford the excessive deformation of the reinforcement during the descent and the insertion of the cage in the pile of concrete. Consequently, the drilling technique should be preferable for the energy piles, and also, in this case, it is recommended a stirrup reinforcement.

Alternative to driven piles, a jacket of ductile steel, containing spheroidal graphite can be used. The poles, consist of elements of standard length of 5 m which can be easily assembled to achieve longer sections during the installation procedure. The tubes are filled under pressure with concrete. To increase friction is also possible the operation of grouting. Since 1985 in Austria more than 1 million poles jacketed ductile steel have been installed. The heat exchangers, are placed within the fresh concrete, and must be fixed against the buoyancy until the concrete has sufficiently matured. The standard diameter of these driven piles is 170 mm, but this can increase considerably depending on the technology of grouting. Nevertheless, the effectiveness of these piles is less than that of driven piles or prefabricated pill with larger diameter, despite the high thermal conductivity of the steel. The small diameter, allows the installation of one probe only, and not of a bundle of tubes. In addition the contact area with the ground is relatively small. In soft soils, the effect of buckling of the pile must be considered as well.

Experience has shown that if the system is used only for heating, or only for cooling, it is advantageous to have a soil with a high hydraulic permeability and with a high hydraulic gradient, these conditions greatly improve the energy exchange between pole energy and aquifer, though, the best solution in terms of economic and environmental is a seasonal operation with an energy balance during the year, i.e. heating in winter (heat extraction in winter) and cooling in summer (heat exhaust in ground), In this case, a low-permeability soil and a small hydraulic gradient factors are preferable. A dry soil requires deeper piles and an area of major change. Depending on the soil properties and the depth of installation of the heat exchangers, 1 kW of heating power needs by approximately 20 m^2 (for land saturated) to 50 m^2 (for grit dry) of the concrete surface in contact with the ground or groundwater.

With the exception of wooden piles, all types of piles can be in practice fitted with a heat exchanger. A pole and a pole wrought cast on site are shown in Figure 2.25.

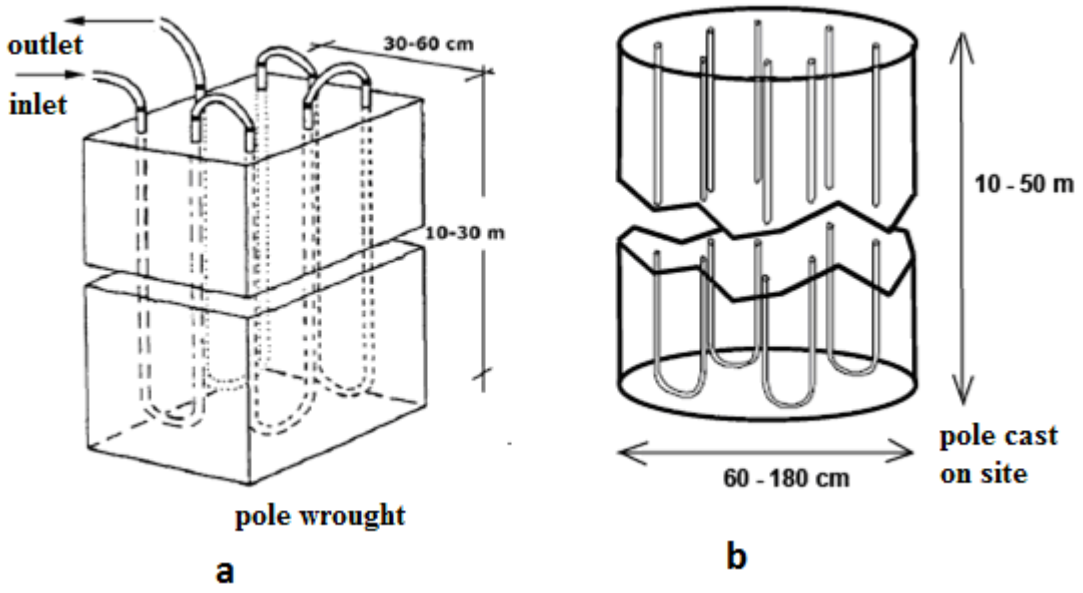

Figure 2.25 – Examples of Energy piles: a) pole wrought b) pole cast in situ.

Figure 2.26a shows a pole prefabricated void and a heat exchanger ready to be positioned (2 tubes U-shaped polyethylene). The empty part of the internal pole is then filled with saturated gravel. In order to optimize the heat transfer with the ground, the tubes should, if possible, be in contact with the inner wall of the concrete pole and be evenly spaced along the circumference.

In piles cast on site, the plastic tubes of the exchanger are fixed to the inner part of the metal structure of reinforcement. Figure 2.26 shows a heat exchanger consisting of 4 U – tubes. Figure 2.26b shows the upper part of the pole. In this case, the four U-tubes are connected in parallel to a plastic manifold. A second manifold is used for the return pipes. Figure 2.26c shows the bottom of the pole, where the tubes are bent forming shape. In practice tubes with small diameter (typically 20 mm) are used. For the entire length of the pole, it is important that the tubes are spaced evenly along the circumference of the metal reinforcement, to optimize the exchange of heat with the ground.

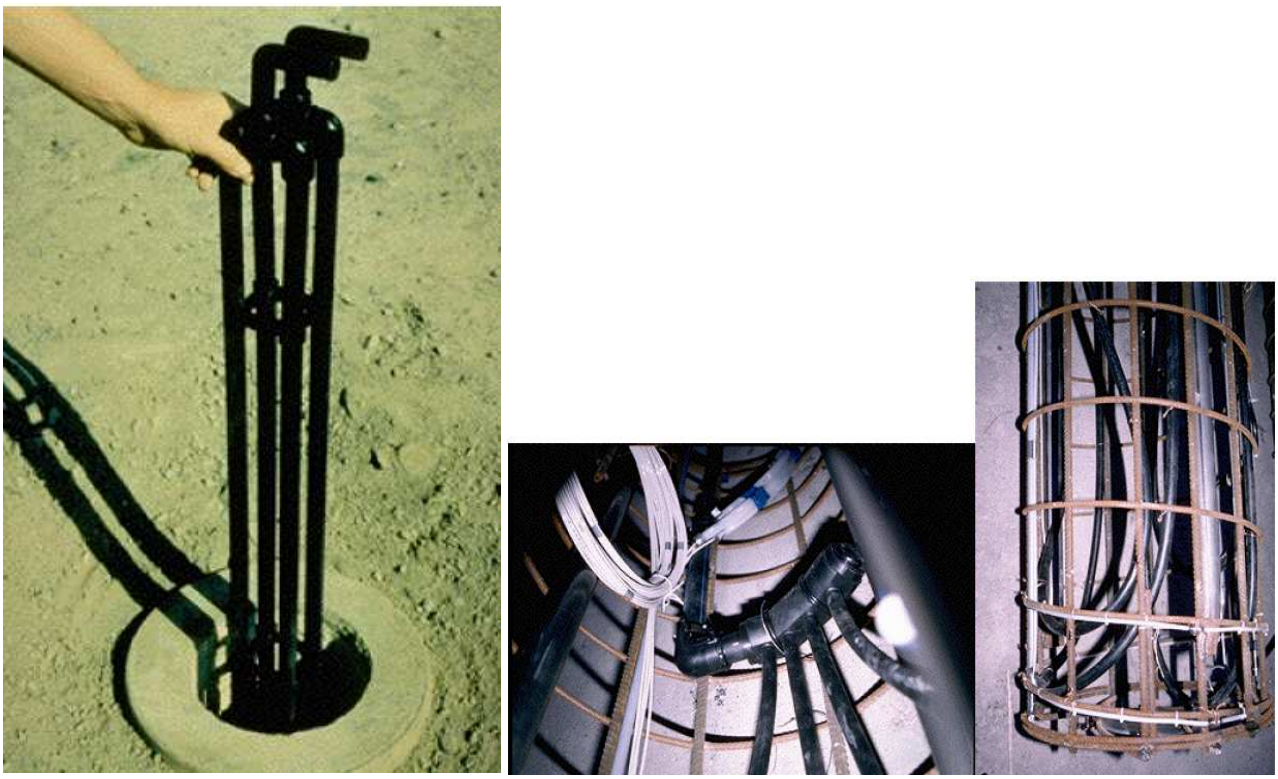

a **b** **c**

Figures 2.26 – a) vacuum prefabricated pile with a heat exchanger consisting of 2 polyethylene U - tubes. b) and c) Pile cast on site. The 4 U – shaped tubes are fixed to the inner part of the reinforcement cage.

The design of the of energy piles is more complex than a classical GHE system because it requires a dimensioning able to avoid that the thermal stresses cause an excessive deterioration of the mechanical properties of the foundations. In particular, it must be avoided freezing of the surrounding fluid whose temperature must not fall below 0 ° C. Recent studies have shown that a pole is subject to energy deformation energy higher than a normal foundation pile already when the temperature rises 15 K.

The installation of geothermal probes must be integrated into the foundation piles at the time of construction of the building, therefore strong synergy between the construction company and the installers of geothermal systems is necessary.

The realization of the energy piles at the factory gives the opportunity to perform pressure tests and thermal performance of the probes, which makes more secure the future installation. In particular, pressure tests to be performed are two: one preceding and one following the pouring of the concrete.

In the situ realization of piles of concrete can occur in two different ways. The first is to stick a steel pole in the ground by means of a conductive element in vibration. The reinforcement cage, in which the tubes are present geothermal, is inserted into the cavity of the pile and subsequently filled with concrete; the steel pile is removed during the injection.

The other mode, which is used for large loads with piles of diameter up to 2.5 m, is to realize the poles through perforation, while the reinforcement cages are inserted at a later time in the hole created.

In both cases, the positioning of the tubes inside the metal reinforcement cages geothermal is carried out in the factory.

2.2.3 Heat tranfer fluid

The heat transfer fluid has the function of transferring the heat from the ground to the heat pump or vice versa. It is generally composed of water to which may be added an antifreeze in case the temperature can fall below 3 ° C. This is especially important in the heating mode of the system since the exchange of heat in the machine can lead to temperature below the freezing point of natural water.

Each fluid has its own specific heat, hence the thermal power exchanged also depends on which type of fluid is chosen for the heat exchange. The most suitable fluid is water. The use of additional antifreeze liquid reduces this value, decreasing the efficiency of heat exchange.

The presence of antifreeze makes the fluid more viscous, with consequent increase in the mechanical work of circulation pump, which leads to increase electrical cost.

In addition, the antifreeze fluid must be replaced around every 10 years, due to the loss of antifreeze characteristics over time, leading to a further voice in the operating costs. These details are important in mild climates, as shown afterwards, since heating energy demand and cooling energy demand are usually needed.

When designing a geothermal system with anti – freeze liquid many aspects must be considered for complying thermal, environmental and health, issues, therefore the fluid should be:

- Non-toxic;
- Non-flammable;
- Stable over time;
- Compatible with the materials of the system;
- Non polluting;
- Non-corrosive;
- Must have low viscosity for limiting the cost of the electric circulation pump;

- Values of specific heat as high as possible.

Various authors have worked on analyzing the properties of each fluid, trying to give more knowledge on this subject. These studies are concentrated in analyzing the antifreeze fluids not only from the point of view of thermal exchange of heat between fluid and ground, but above all from the point of view of environment and health consequences in the case of dispersion of the fluid in particular into aquifers.

Klotzbücher et al. (2007) studied the potential for contamination and the biodegradability of some antifreeze compounds, such as ethylene glycol, propylene glycol, betaine, used in geothermal probes, analyzing results of laboratory experiments on aquifer material. Ethylene glycol and propylene glycol are found to be readily biodegradable, also without forming toxic intermediates or persistent, so it is not expected to contamination of groundwater in the long term, while betaine, although readily biodegradable, has unpleasant odor even at low concentrations, also presenting a potential metal ion complexes, i.e. it can mobilize toxic metals, for complexation or dissolution and precipitation of minerals, in groundwater.

Khan and Spitler (2004) highlight the need for the use of anti-freeze, only to the conditions that the fluid drops at temperatures below 0 ° C. The use of the mixture water - antifreeze has considerable variations on the performance of the heat pump; depending on the antifreeze chosen the length of the probe can be modified as well as the number of probes. The energy consumption of the heat pump and the costs of pumping of the circulation pump also may be affected. The authors, using some simulations, analyze the performance of the system with four different antifreeze mixtures, such as ethylene glycol, propylene glycol, ethyl alcohol, methyl alcohol, finally studying the cost analysis, the long-time operating system, based on the costs of electrical energy for the heat pump and for the circulation pump, considering the costs of antifreeze and installation costs of the plant.

Heinonen et al. (1997) have presented a paper on the evaluation research of antifreeze solutions for systems with heat pumps. In this study the authors examine the risks of the use of six types of antifreeze liquids (methanol, ethanol, potassium acetate aqueous propylene glycol, aqueous magnesium acetate, calcium, urea and water). The study was extended not only to the environmental and health, including the danger of fire, the corrosion, and cost of the life cycle. As a results the authors present a table reported in Table 2.3.

Table 2.3: Categories of risk antifreeze fluids object of study by Heinonen et al (anti – freeze fluid environmental and health evaluation – an update).

Category	Methanol	Ethanol	Propylene Glycol	Potassium Acetate	CMA	Urea
Life cycle cost	***	***	**	**	**	***
Corrosion	**	**	***	**	**	*
Leakage	***	**	**	*	*	*
Health hazard risk	*	**	***	***	***	***
Fire risk	*	*	***	***	***	***
Environmental risk	**	**	***	**	**	***
Risk of future use	*	**	***	**	**	**

*	Potential problems, caution in use required
**	Minor potential for Problems
***	Little or no potential for problems

CATEGORY	NOTES
Life Cycle Cost	1. Higher than average installation and energy costs.
Corrosion	2. High black iron and cast iron corrosion rates. 3. High black iron and cast iron, copper and copper alloy corrosion rates. 4. Medium black iron, copper and copper alloy corrosion rates. 5. Medium black iron, high cast iron, and extremely high copper and copper alloy corrosion rates.
Leakage	6. Minor leakage observed. 7. Moderate leakage observed. Extensive leakage reported in installed systems. 8. Moderate leakage observed. 9. Massive leakage observed.
Health Risk	10. Protective measures required with use (See MSDS). 11. Prolonged exposure can cause headaches, nausea, vomiting, dizziness, blindness, liver damage, and death. Use of proper equipment and procedures reduces risk significantly. 12. Confirmed human carcinogen.
Fire Risk	13. Pure fluid only. Little risk when diluted with water in anti-freeze. 14. Very minor potential for pure fluid fire at elevated temperatures.
Enviromental Risk	15. Water pollution risk.
Risk of Future Use	16. Toxicity and fire concerns. Prohibited in some locations. 17. Toxicity, fire, and environmental concerns. 18. Potential leakage concerns. 19. Not currently used as GSHP anti-freeze solutions. May be difficult to obtain approval for use.

As final conclusions, the ethanol can be used in cases where the risk of fire can be managed, and in case there are no problems of corrosion. Propylene glycol has interesting properties, it is very low environmental risk, health and fire also lower the risk of corrosion. The cons are the cost of glycol itself, since they are considered more than other fluids antifreeze. The potassium acetate has good environmental characteristics and health, but it is important to control the plant during installation to eliminate the risk of losses. CMA and urea can be taken into account once the problems of corrosion and leaks have been fully facing.

Other studies on the antifreeze fluids were conducted by Lokke (1983), the author has analyzed the case of breakage of the geothermal probe, and the outflow of fluid antifreeze in the porous medium. Various types of antifreeze fluid, with various types of porous medium and various types of speed of the aquifer were considered. An interested users result is that the experiments relating to the leaching of ethanol in a controlled amount of oxygen have shown that the degradation occurs as a function of the availability of oxygen. Staples et al. (2001) instead studied the effects and potential environmental risk of ethylene glycol.

From the above mentioned studies, the most commonly used antifreeze fluids are the glycol ethylene and propylene glycol.

Ethylene glycol was prepared in 1859 by the French chemist Wurtz. The production starts from ethylene, which is first oxidized to ethylene oxide and then converted into glycol through a hydration reaction. The gross composition of the ethylene glycol is $C_2H_4(OH)_2$. The molecular mass is approximately 62.1 g / mol. On the market there are various types of ethylene glycol, hence they are admixed with colorants, stabilizers, lubricants depending on the requested function.

Propylene Glycol: is a clear liquid, slightly odorless. Propylene glycol is a compound strongly hygroscopic and viscous. It is perfectly miscible with water in any proportion. The formula of propylene glycol is $C_3H_8O_2$. are the molecular mass is equal to 76.09 g / mol.

Industrial production of propylene glycol is similar to that of ethylene glycol and is based on hydration of propylene oxide; similarly to the ethylene glycol, propylene glycol also the commercial products contain additives.

The propylene glycol is less toxic than ethylene glycol, therefore, preferable in the use of geothermal plants at low temperature, The propylene glycol does not pose a risk to, health, even at high concentrations it is odorless, low toxicity, considered as readily biodegradable, non-toxic to aquatic organisms if released, is not carcinogenic, not mutagenic, not teratogenic .

In the case of accidental breakage of a probe containing a mixture such as water - antifreeze fluid, it is important to analyze the behavior of the pollutant in the porous medium, the pollutant propagation in the soil. The study of the diffusion of pollutants along aquifers, takes place according to the theories of fluid dynamics inside a porous medium, that is, a material in which are present a solid matrix (soil particles) and an empty region consisting of air or water groundwater. The pollutant plume moves along the direction of the movement of groundwater, tending to widen as it moves away from the probe, with the form of elliptical shape, (see figure 2.27). More detailed studies are conducted by Bear and Verruijt, (1987).

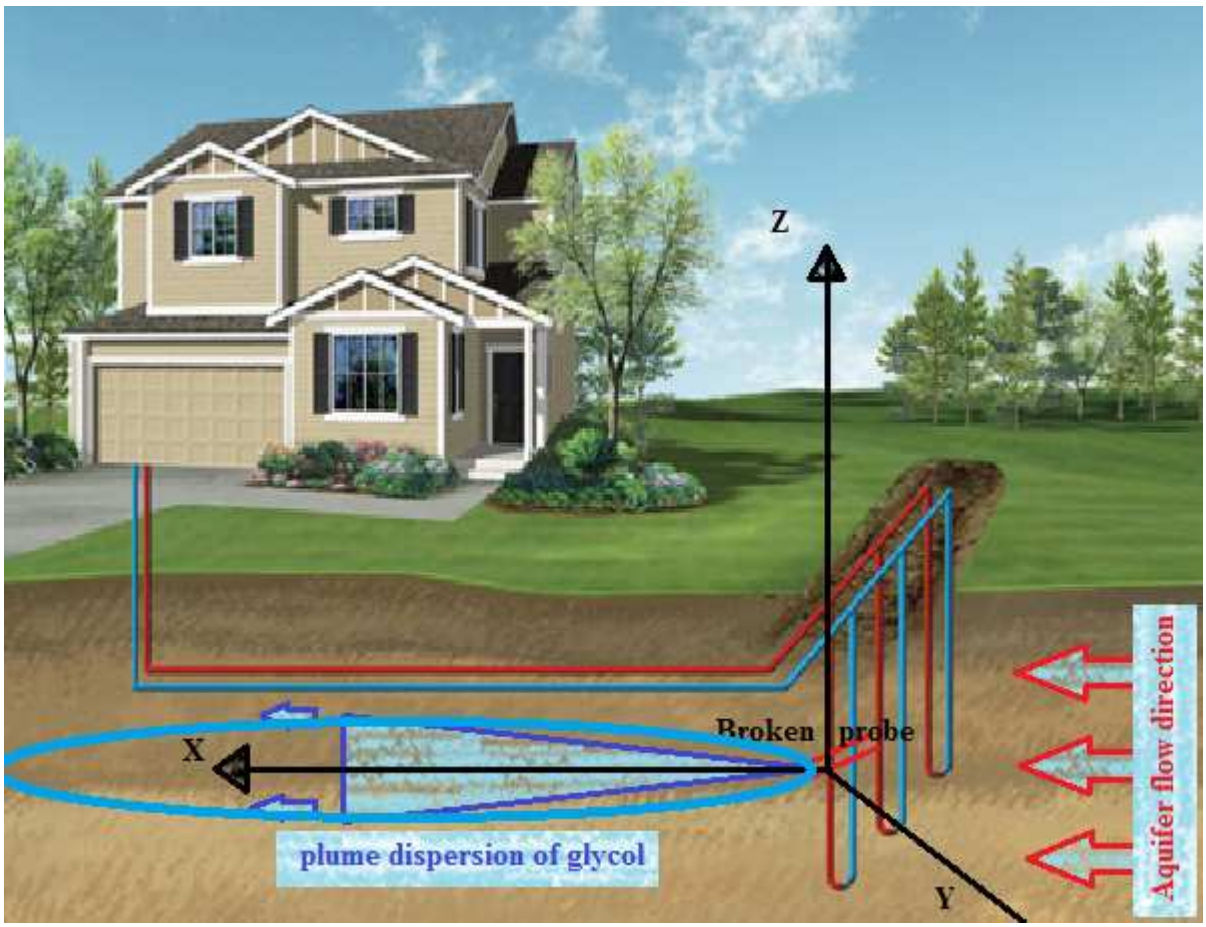

Fig. 2.27 – Scheme point source of pollutant caused by the breaking of a probe.

2.2.4 Heat distribution system "low temperature"

To complete the description of the main components of a GSHP the terminals units are here mentioned briefly.

As shows before, in order to reach high COP the condensing temperature should be heat low in heating period. In cooling period, if possible, the high EER can be reached by high evaporating temperatures.

The types of heat emitters that are usually used, are generally:

1 radiant floor panels with water temperature of the fluid variable from 20 ° C to 30 ° C in heating; during cooling the water temperature is variable from 15 ° C to 20 ° C;

2 fancoils temperature of the fluid variable from 45 ° C to 50 ° C in heating period, during cooling season the water temperature is variable from 6 ° C to 8 ° C;

3 radiators that work only in heating mode water temperature variable from 40 ° C to 60 ° C.

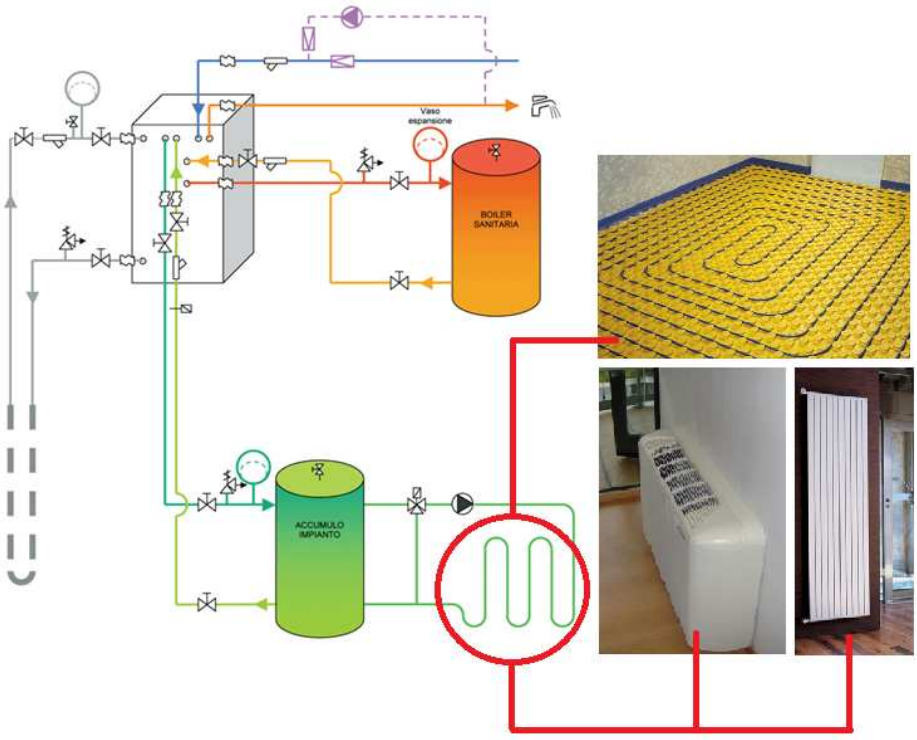

Fig. 2.28: Scheme geothermal heat pump system.

In figure 2.28 is presents a diagram of geothermal plant, with various types of terminal units that can be connected as an alternative or together.

2.3 The design of the geothermal heat pump plant

The design of the geothermal plant is based on the energy needs of the building, and on the geological analysis of for determining the thermal parameters of that soil. Based on the geological study of the ground, the geometry of the probe (diameter of the perforation, arrangement and diameter of the tubes, thermal resistance of the probe, thermal conductivity of the filling material), the characteristics of the heat transfer fluid (flow rate and type of fluid: water alone or a mixture water - glycol), field geometry probes (total number of probes, the same depth and distribution of the field), have to be selected, COP (Coefficient Of Performance) and EER (Energy Efficiency Ratio) of the heat pump, peak of heating, cooling demands, and their duration have to be defined as well. The output data are the temperatures of the heat transfer fluid in the time. Once decided the dimensions of the GHE and their pattern, after the installation of the first borehole, a GRT can be carried alit to check the preliminary hypothesis on the ground. After the GRT measurement, the final tuning of the design of the GHE field has to be carried out.

The calculations can be carried out by means of analytical procedures (e.g. ASHRAE method), by transfer functions (e.g. EED), by finite difference or volume methods (e.g. CARM) or via FEM simulations.

In essence, the process of the design considers the following steps:

1 Study of the energy needs of the building in summer and winter;

2 Preliminary geological study for determining characteristics of the ground;

3 Software theoretical models and models for study the heat exchanged between the probe and the ground over the years;

4 Dimensioning of the total length of the probes or energy piles.

5 Test of the thermal response of the soil, experimental test with the Ground Response Test (GRT);

6 Based on GRT recalculation of the total length of the probes or energy piles for the final design;

7 If needed an additional calculation for determining the thermal plume can be carried out by means of F.E.M. or via analytical procedures.

The design of energy piles is more complex than a classical GHE system, because it requires a dimensioning able to avoid that the thermal stresses cause an excessive deterioration of the mechanical properties of the structure.

In the design of energy piles is crucial first to conduct a geotechnical-structural study, then to analyze the problem from the point of view; finally, the thermal-structural interference has to be studied.

The design of energy piles can follow these step:

Geotechnical aspects:

- Calculation and verification of load-bearing capacity;
- Bearing capacity at the base of the pole;
- Bearing capacity for lateral friction;
- Estimate of subsidence of the foundation pile and all the piling;

Structural aspects:

- Dimensioning of the foundation pile, according to the European standards (Eurocodes), for the calculation of reinforced concrete conglomerates.

Interaction thermal / structural:

- Verification of the minimum and maximum temperatures of the fluid flow in the energy piles throughout the year, in order to avoid compromising the load bearing capacity of the foundation, and the elasticity of the building in case of earthquake, temperatures generally should not exceed 40 ° C in summer and should not be below 0 ° C in winter.

Thermo-technical aspects:

- Dimensioning of the probe embedded in the concrete following the steps of a GHE. In this case the energy piles rarely can meet the heating/cooling power, but they can be used for the base bad, requiring an additional integrative system. Therefore the goal is to see which heating/cooling loads they can cover, once decided the minimum and maximum allowable temperatures for the structural loads.

2.4 Results

In this section is composed of the research results for the low temperatures geothermal energy are shows. They include:

- Simulation with FEM model of the Ground Response Test (GRT);
- Analysis of the thermal field;
- thermo – structural Interaction on the energy pile by using FEM thermal model and FEM, mechanical model;
- Comparison between vertical GHE's with different configurations and operational fluids in mild climates.

2.4.1 Simulation with FEM model Ground Response Test

The simulation of a GRT with a two-dimensional finite element analysis, using the software COMSOL, has been carried out. The model is composed of a domain of land of size 20m by 20 m, and energy from a pole diameter of 1 m inside which are arranged perimetrically 2 geothermal probes connected in parallel (Figure 8.3). The soil has a porosity of 0.25 and it was assumed to be fully saturated. The function *q(t)*, which represents the heat coming out from the probe during testing, was imported into the model as a step function (Fig. 2.30). The test duration of 7 days while the behaviour of the system is monitored for 30 days from the beginning of the tests.

In Table 2.4 shows the physical properties of the soil:

Table .2.4 – Imput data of the model; thermo – physical properties of materials

	k [W/(m K)]	***ρ [kg/m³]***	***C_p [J/(kg°C)]***	***Porosity [%]***
Soil	1.5	1500	1600	25

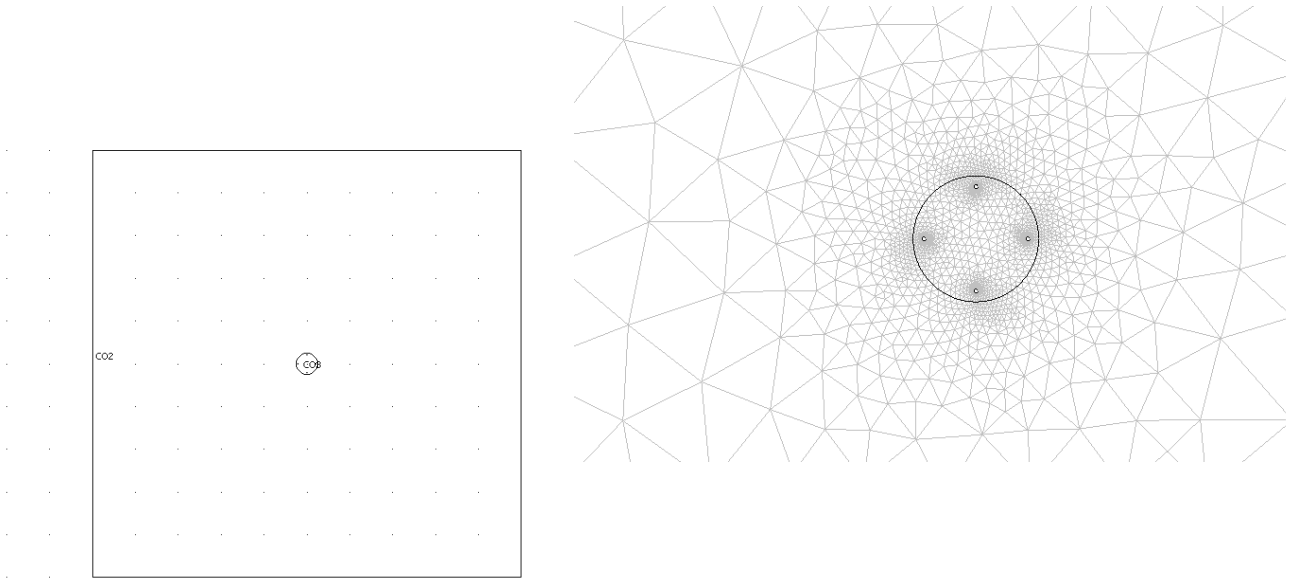

a **b**

Fig. 2.29: Geometry of FEM model a) and mesh the model.

The mesh generated is constituted by triangular elements (Figure 2.29.b). The tolerance used for the convergence of the solution is equal to 10^{-5}.

The boundary conditions of the model are fixed temperature, equal to that of the undisturbed soil (14 °C), along the outer sides of the domain. As alredy exploined, on the edge of the probes, the outgoing heat flow equal to the time-dependent function *q(t)* has been imposed.

A heat flow per meter of drilling equal to 90 W/m, has been choosen; to obtain the imput for the FEM program has been divided by the number of pipes and for their circumference:

$$q = \frac{flow\left[\frac{W}{m}\right]}{n° pipes \cdot 2\pi r_{external\_probes}} = \frac{90}{4 \cdot 2\pi 0.016} = 223.81\left[\frac{W}{m^2}\right] \quad (2.6)$$

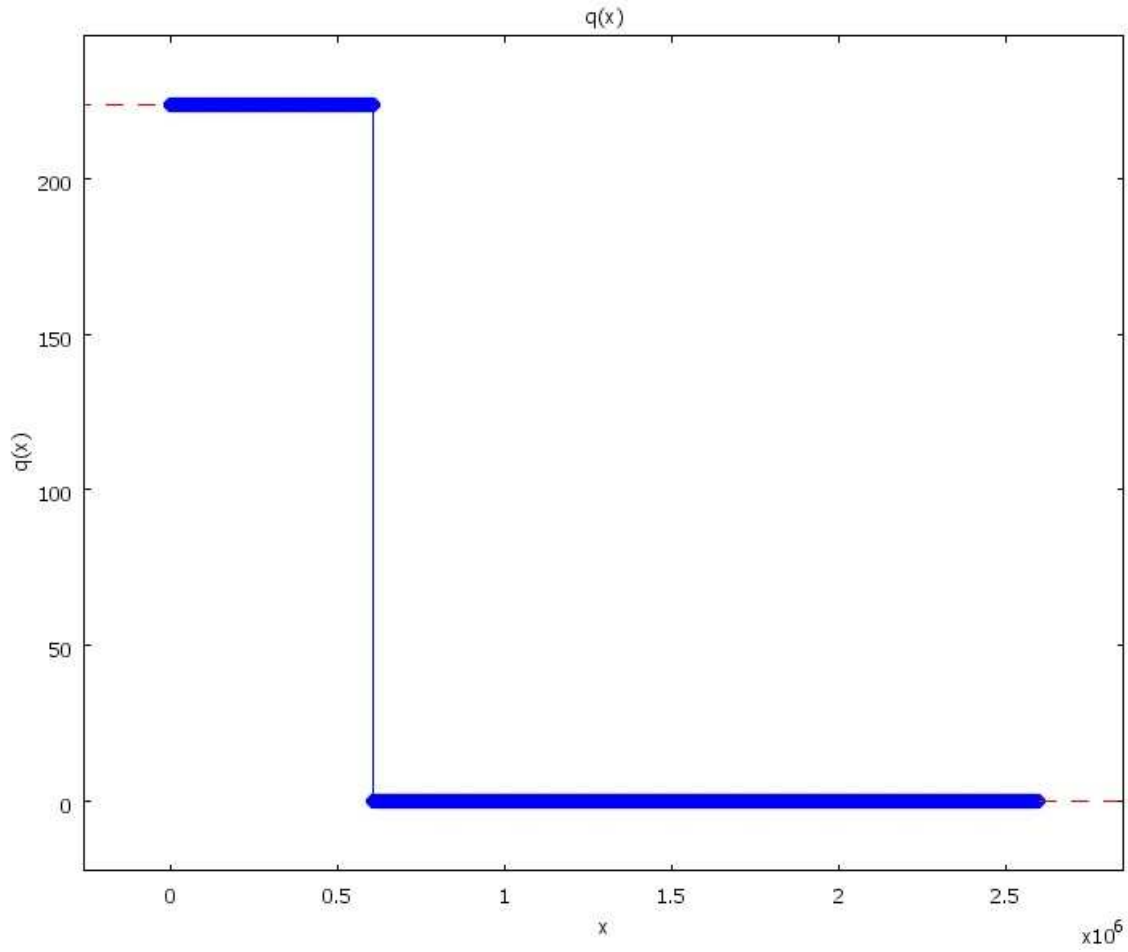

Figure 2.30 – Trend of the input function q(t).

In the model the velocity of groundwater has been set, variable depending on the type of soil to be 10^{-10} m/s up to 10^{-5} m /s.

The graph in Figure. 2.31, represents the temperature distribution on the edge of the pole time. It can be seen that the temperature grows until the seventh day, then it decrease once the heat flow is null, up to tend asymptotically to the undisturbed temperature of departure of 14 ° C.

In the model the contribution of the velocity of groundwater has been added. Results (Figure 2.32) show that the temperature of the system tends to lower, due to the effect of the fluid motion. The effect begins to appear when the a velocity is about 31.5 m/year, up to become important when the velocity reaches values above 300 m/year. These values correspond to velocity of aquifer soils with permeability values that are around $10^{-4} \div 10^{-5}$ m/s (sands, silts).

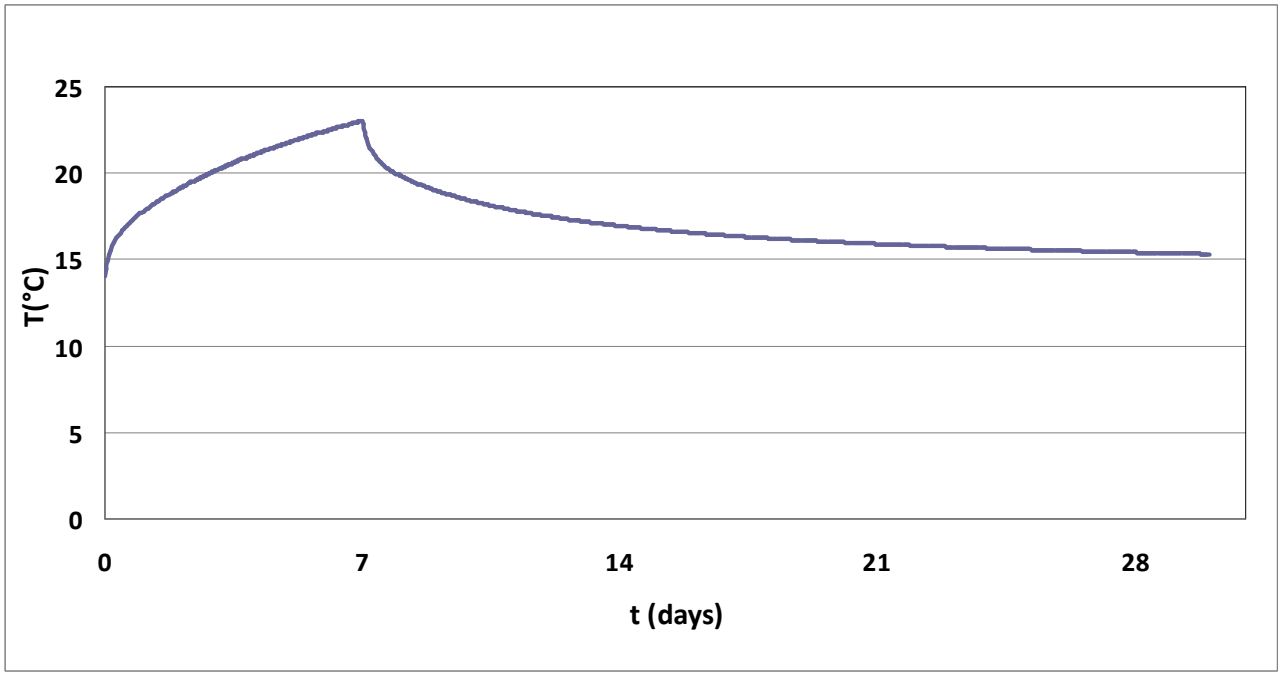

Figure 2.31 – Trend of the temperature at the edge of the pole as a function of time.

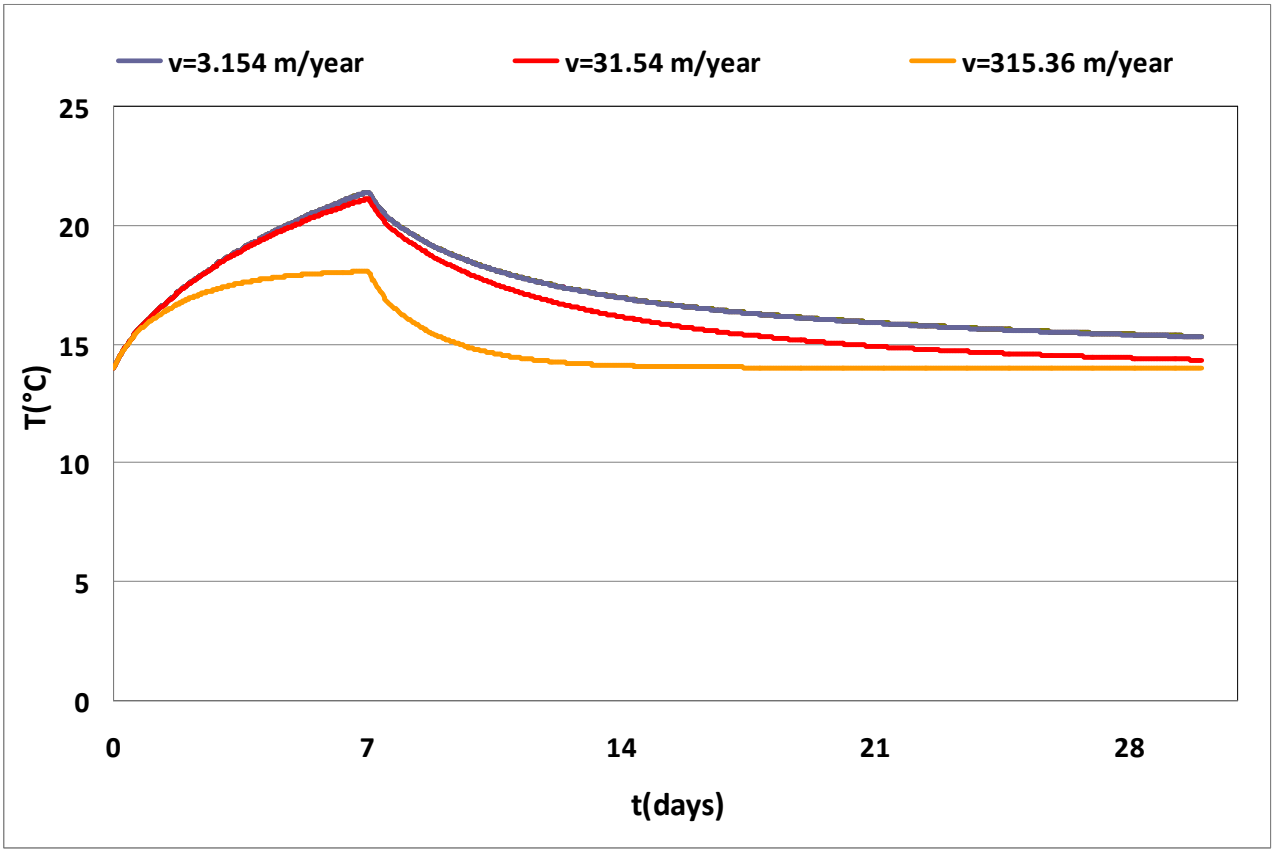

Figure 2.32 – Trend of the average temperature at the edge of the pole as a function of time. to vary the velocity of groundwater.

Looking at the temperatures trend in the geothermal response test, i.e. during the first seven days of the simulation (Figure. 2.33), it is possible to see clearly how the evolution of the thermal field is strongly influenced by the presence of groundwater in movement from velocity values equal to 10^{-5} m/s. As the velocity increases the temperature tends reach an equilibrium condition in a shorter time, that is, approaches the typical temperature distribution of the stationary motion. The effect of groundwater is consistent also observing the trend of the thermal field after the test. The decay of temperature is much greater and faster the higher the velocity of the aquifer.

In this case, the presence of groundwater in motion is thus a positive element for the operation of geothermal systems, as it increases the conductivity of the soil and promotes a greater rapidity of response of the system.

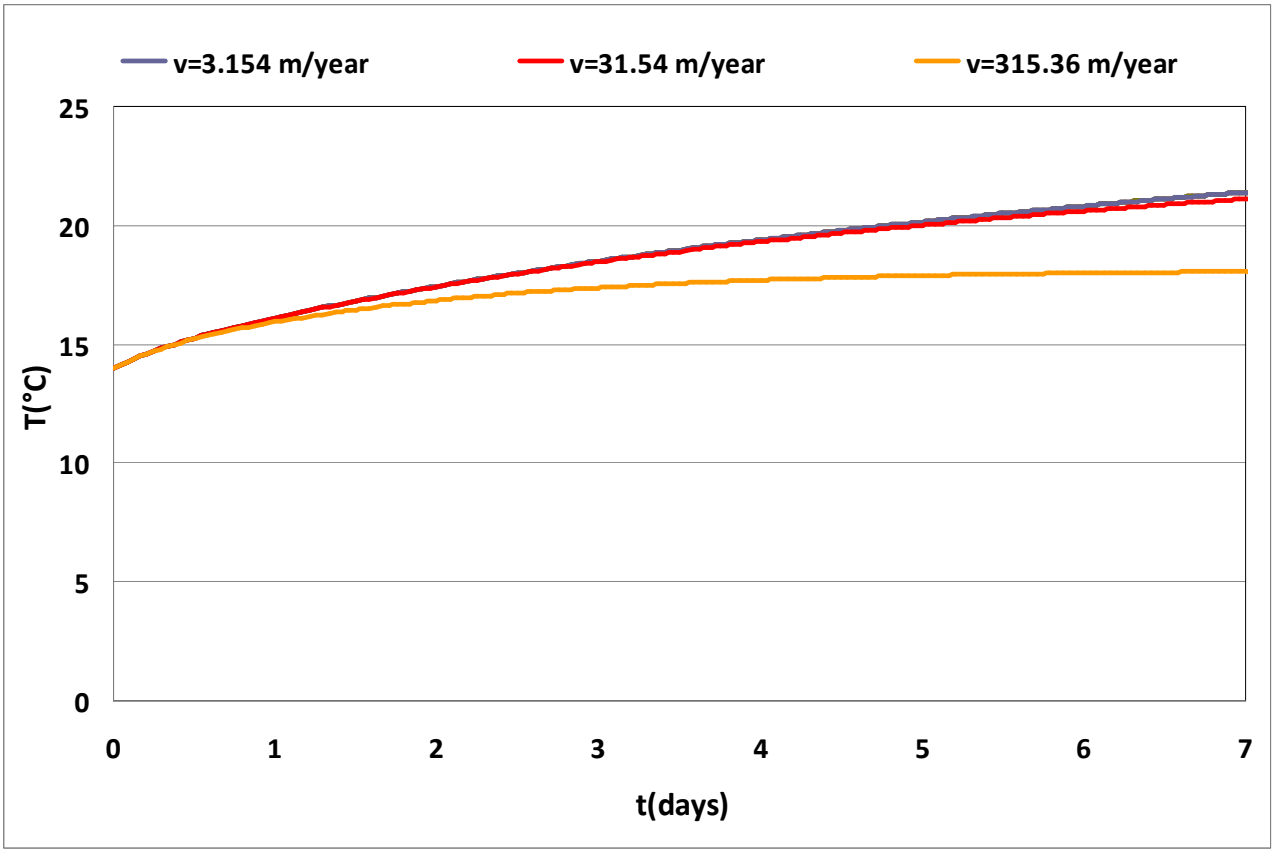

Figure 2.33 – Trend of the average temperature at the edge of the pole as a function of time varying the velocity of groundwater within seven days of heat flow.

The same simulations have been performed on a GRT classical vertical GHE, in order check the differences in behaviour compared to the energy piles. The model is analogous as regards the thermophysical characteristics and boundary conditions to the previous one. The simulation period is always total of 30 days, with the actual test duration of 7 days. The grout diameter is in this case 150 mm, with two U- pipes arranged in parallel 2 cm distance from the edge. The filling is a cement slurry, which thermophysical characteristics equal to those of the concrete.

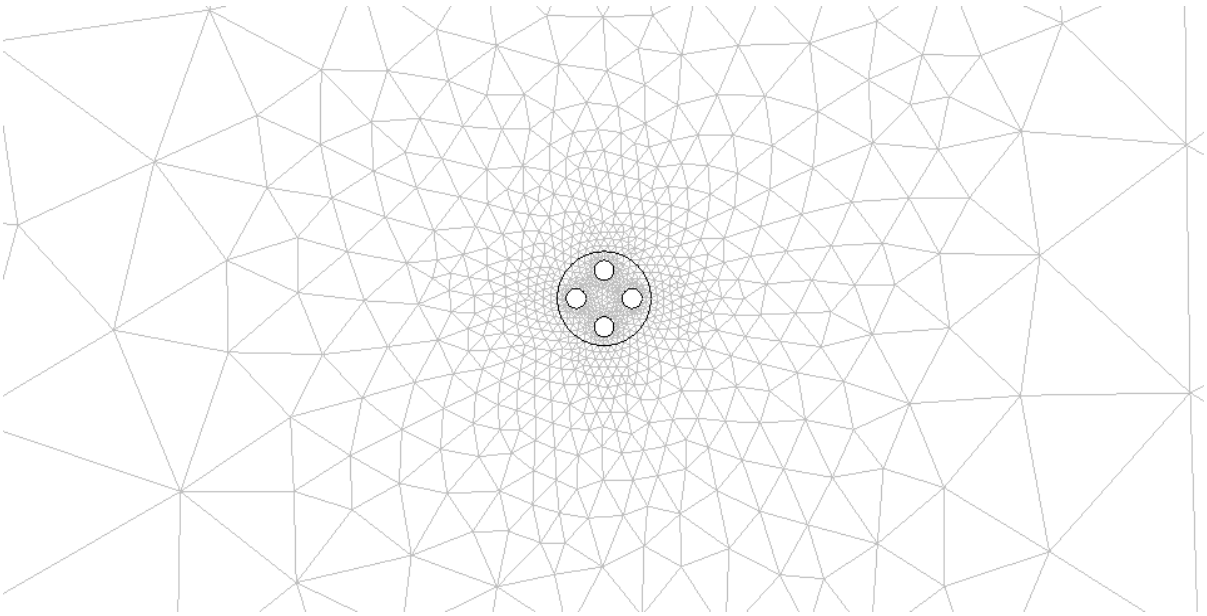

Figure 2.34 – Meshing of the GRT model for vertical GHE of a grout diameter of 150 mm.

Figure 2.35 compares the different distributions of temperature in the time, set the velocity of groundwater equal to 10^{-10} m/s (3 mm /year).

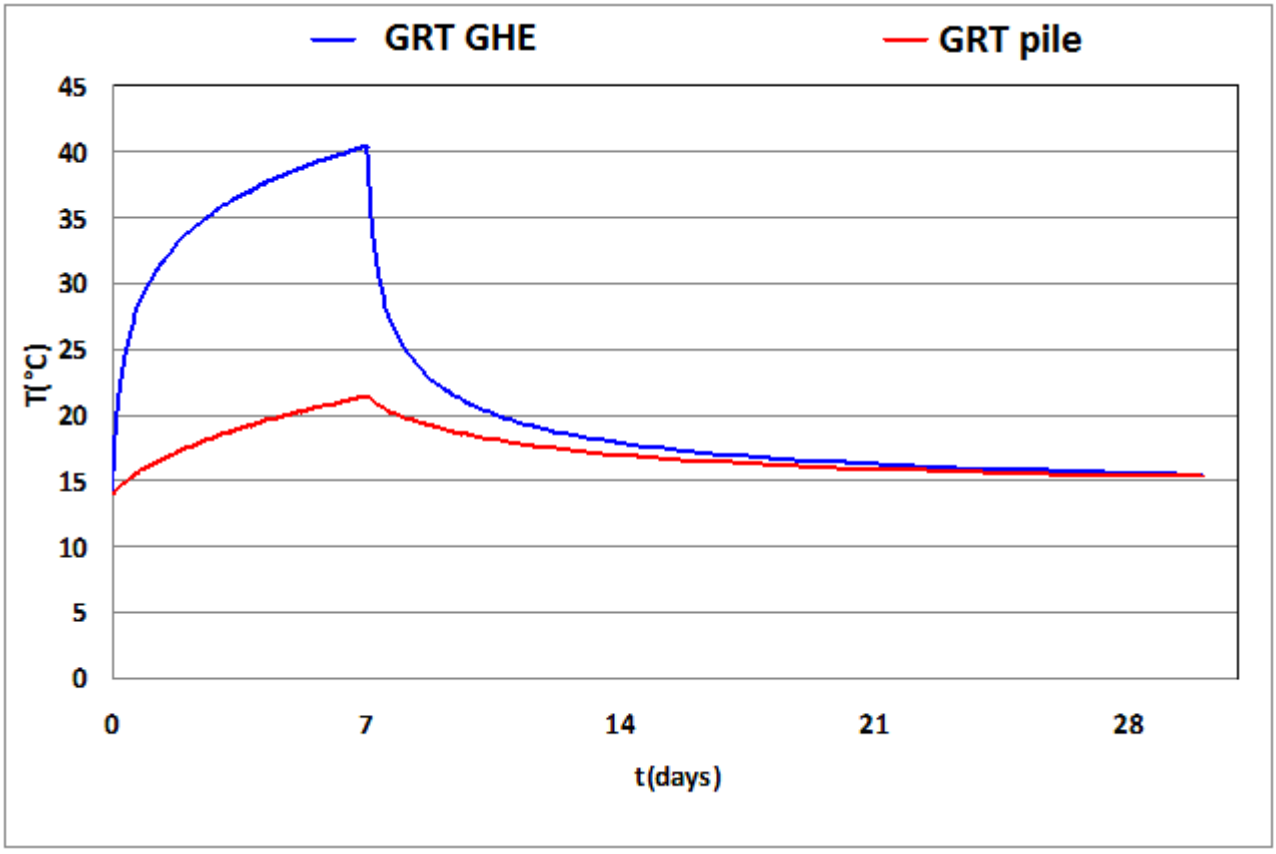

Figure 2.35 – Distribution of temperature versus time obtained from the simulation of a GRT performed on energy pile and an usual GHE.

The comparison shows that in the usual GHE much higher temperatures are reached (around 40°C), compared to the energy pile (around 23°C).

In Figure 2.36 the distributions of average temperature at the edge of the grout with respect to time and depending on the velocity of groundwater are shown.

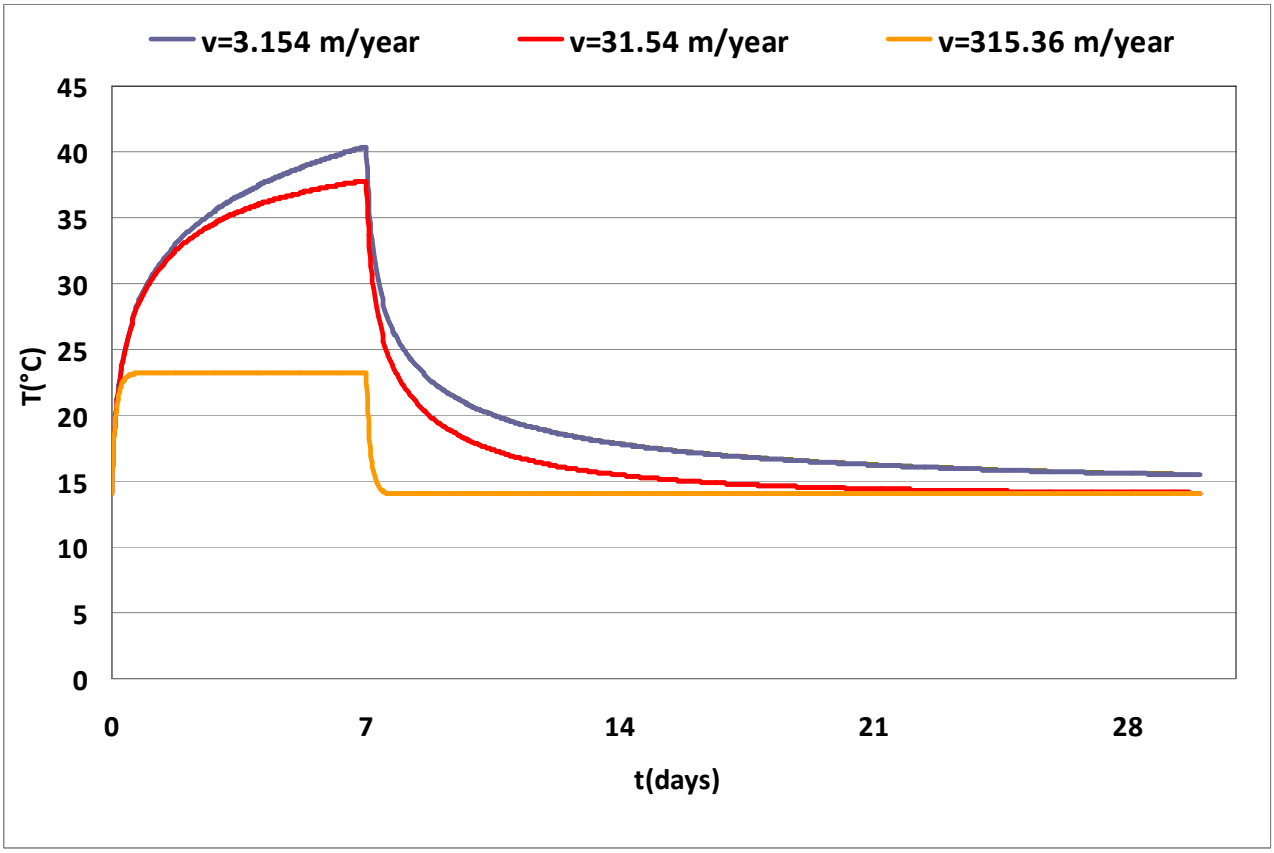

Figure 2.36 – Distribution of the average temperature on the edge of the grout with respect to time, to vary the velocity of groundwater, obtained from simulation of GRT.

The graph shows that the temperature distribution has the same trend presented in the case of the energy pile although in this case temperature levels are higher. Furthermore it is possible to assess that groundwater has a more important effect on the temperature distribution in the usual GHE compared to the case of the energy pile. In case of high velocity aquifer the temperature tends in fact to grow very quickly and then tend towards a constant value already after few days of tests.

The temperature maps presented below, show the effect of the presence of motion of water, in the case of both energy pile and usual GHE.

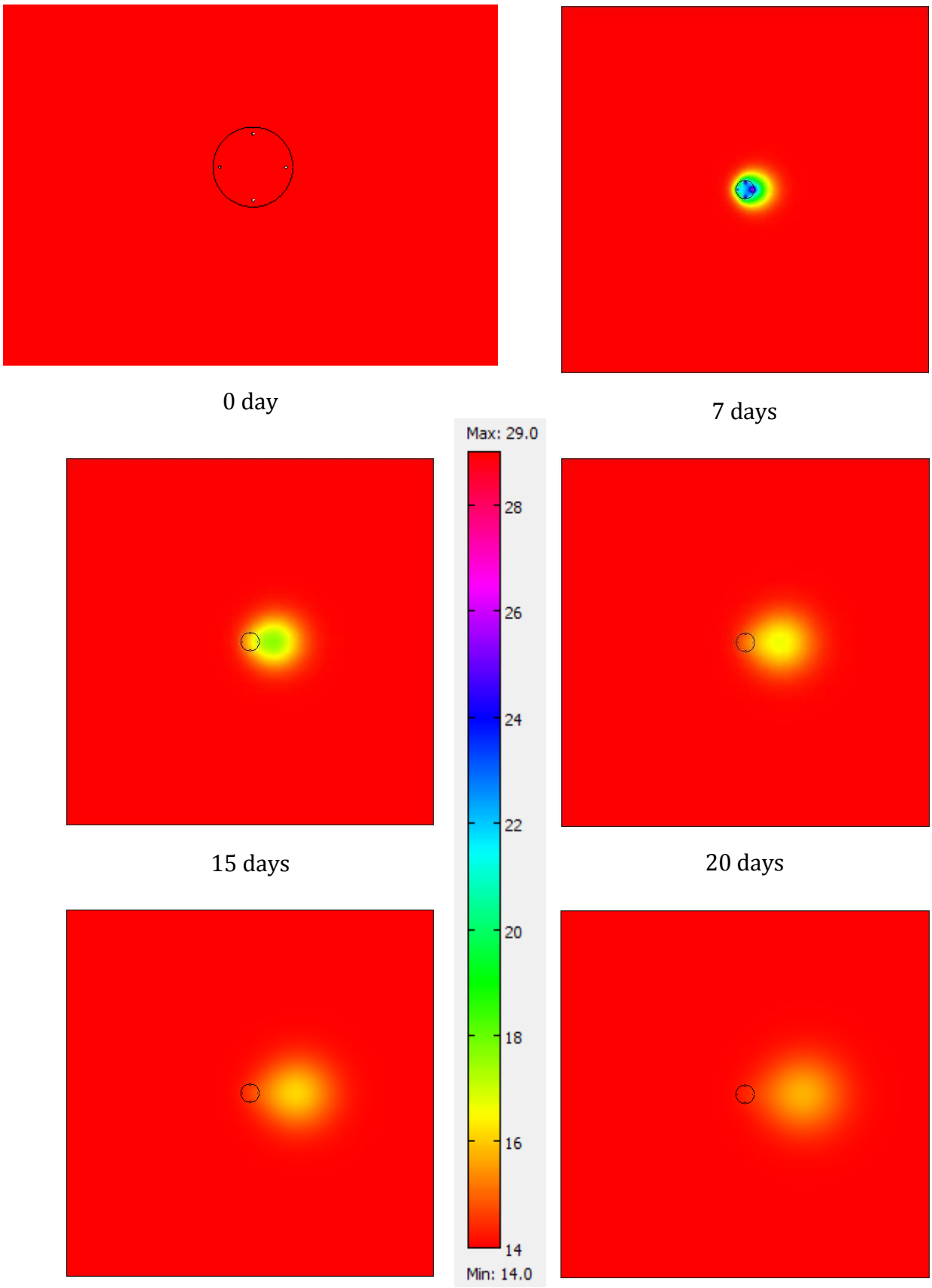

Figure 2.37 – temperature map for the GRT of an energy pile in the case of 31.54 m/year of aquifer velocity

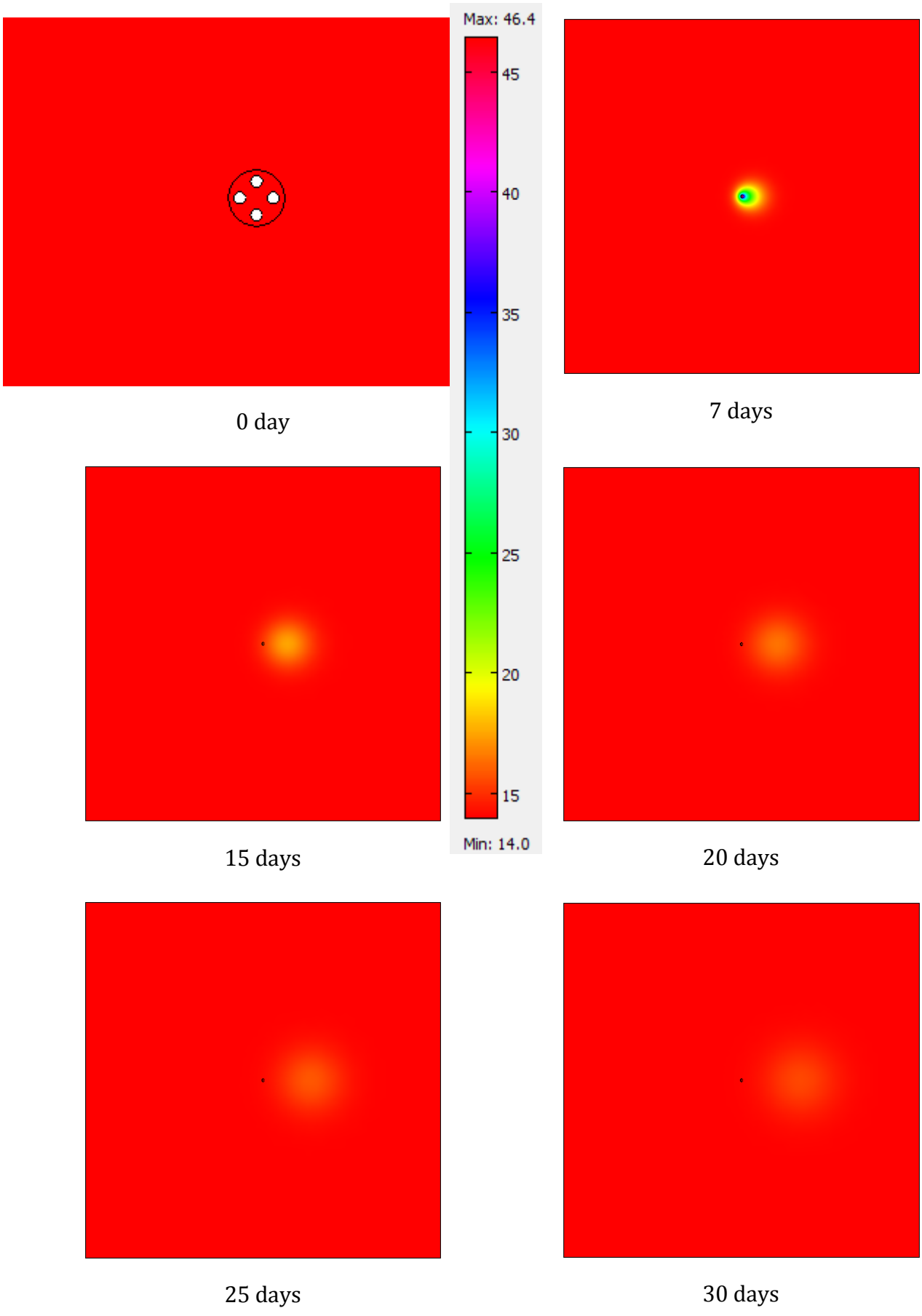

Figure 2.38– temperature map for the GRT of a usual GHE in the case of 31.54 m/year of aquifer velocity

2.4.1.1 Calculation of the thermal conductivity of the soil in the case of energy pile

The calculation of the thermal conductivity is obtained by analysing data reported a graph having in abscissa the ln(t) and the ordinate the average temperature at the pipe calculated by means of the integral of temperature.

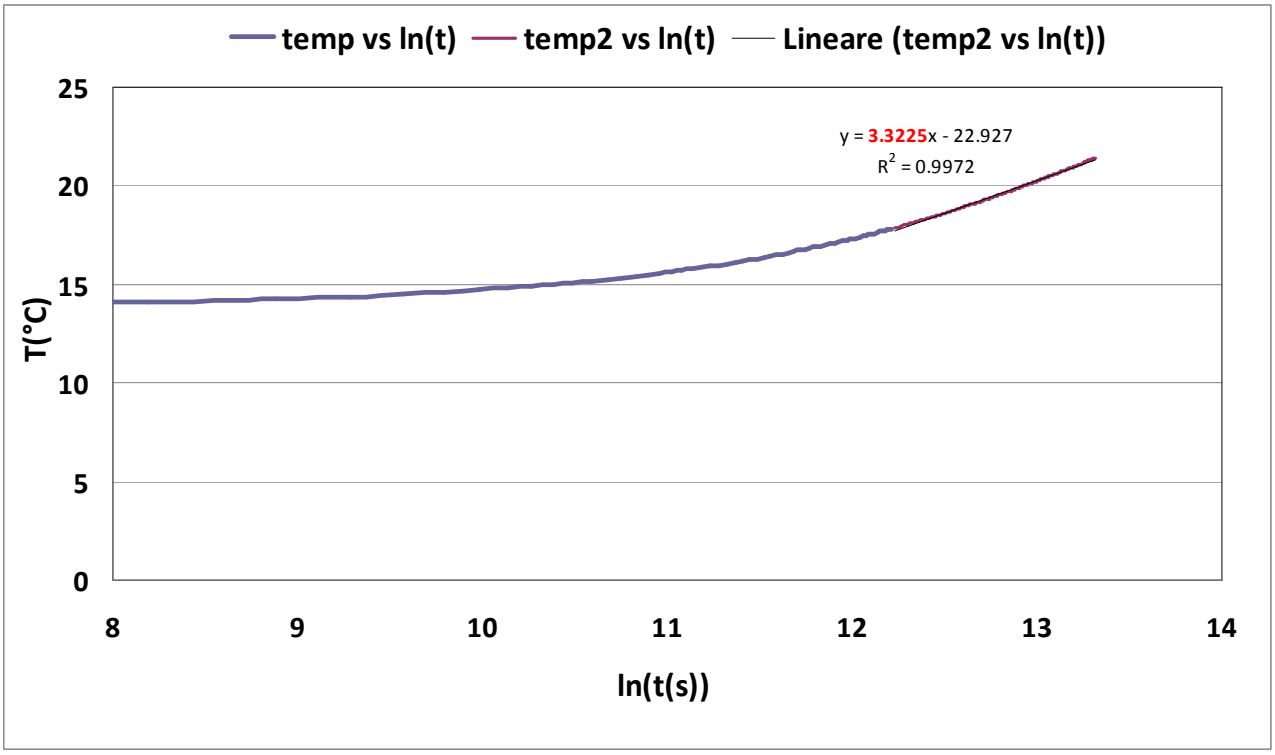

Figure 2.39 – Graphic T - ln t for the experimental determination of the coefficient of equivalent conductivity.

The curve tends to move in a straight line towards the last days of simulation. The thermal conductivity is proportional to the inclination of that portion of this curve:

$$T = k\ln(t) + m \tag{2.7}$$

Where k is the graphical result of the inclination of the curve:

$$k = \frac{q}{4\pi\lambda} = 3.32 \tag{2.8}$$

And λ:

$$\lambda = \frac{q}{4\pi k} = \frac{90}{4\pi 3.32} = 2.16\left[\frac{W}{mK}\right] \quad (2.9)$$

It can be seen that it differs significantly from the coefficient λ imposed as data in input, equal to 1.28 W/(m K).

2.4.1.2 Calculation of the thermal conductivity of the soil in the case of usual GHE

By performing the same procedure for the calculation of the equivalent coefficient of conductivity in the case of the usual GHE, from Figure 2.56 k = 5.41.

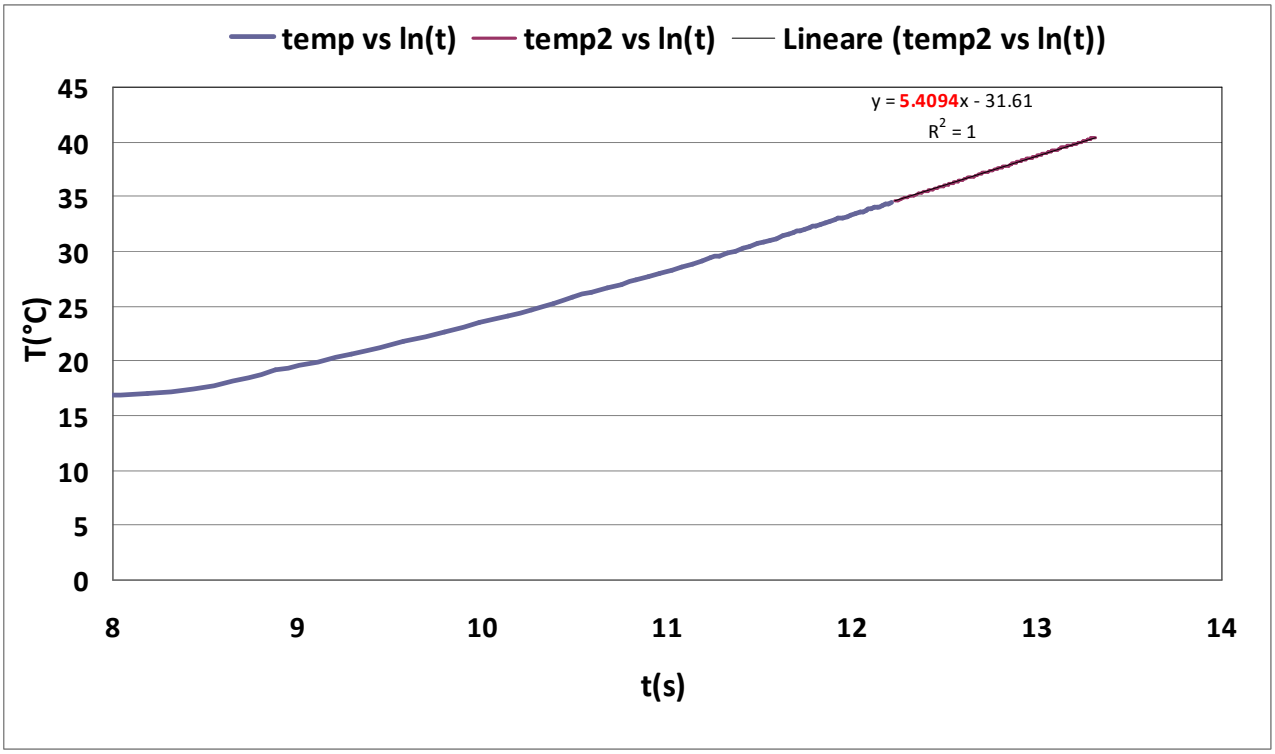

Figure 2.40 – Graphic T - ln t for the experimental determination of the coefficient of equivalent conductivity.

$$\lambda = \frac{q}{4\pi k} = \frac{90}{4\pi 5.41} = 1.32\left[\frac{W}{mK}\right] \quad (2.10)$$

The value is very close to the coefficient of conductivity, characteristic of the model (λ = 1.28):

It can be concluded that the GRT, can be useful for the calculation of the equivalent conductivity of the system in a reliable way when an usual GHE is considered. In the case of the energy pile the estimated value deviates significantly from the real value. This means that the model of linear source does not fit well to energy pile due to the radius of the structure and its mass. Results of GRT on an energy pile could lead to a mistake on the design.

To prove this affirmation, an analysis of transient thermal simulation of a GRT has been carried out with a conductivity equal to that obtained from the graph in Figure 2.40 i.e. with a λ = 2.16 [W/(mK)]. At the end, a comparison of the temperature distribution obtained by simulation with the "real" value of thermal conductivity and that obtained using the value calculated by the analysis of the data can be seen in Figure 2.41.

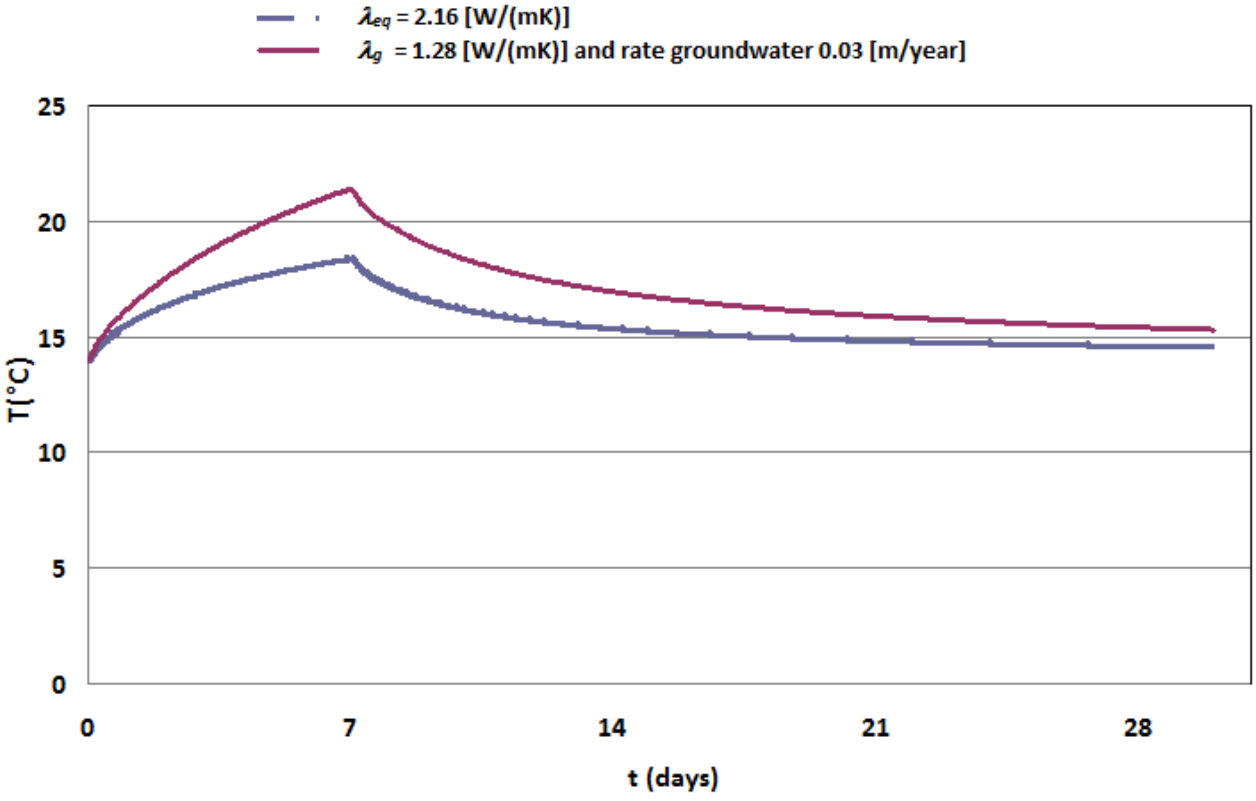

Figure 2.41 – Temperature distribution average to the edge of the pole with respect to time: comparison of the solution with a velocity of groundwater and the solution with thermal conductivity coefficient from the theory of linear source.

The two distributions of average temperature at the edge of the energy pile, obtained with a model with the velocity of groundwater, and with the model derived from the theory of linear source can be seen.

2.4.2 Analysis of the thermal field

The model studied and reported in Figure 2.42, is a two-dimensional FEM model consisting of a square domain of 100 m side; at the centre an energy pile is placed, with a diameter of 1 m. Inside the energy pile, two geothermal probes are arranged, consisting of two U tubes in parallel whose distance from the edge of the pile has been calculated so that it is reflected in their design position, that is linked the reinforcement cage, approximately 8.5 cm from the edge of the pole. The thermo - physical properties of the materials, are reported in Table 2.5.

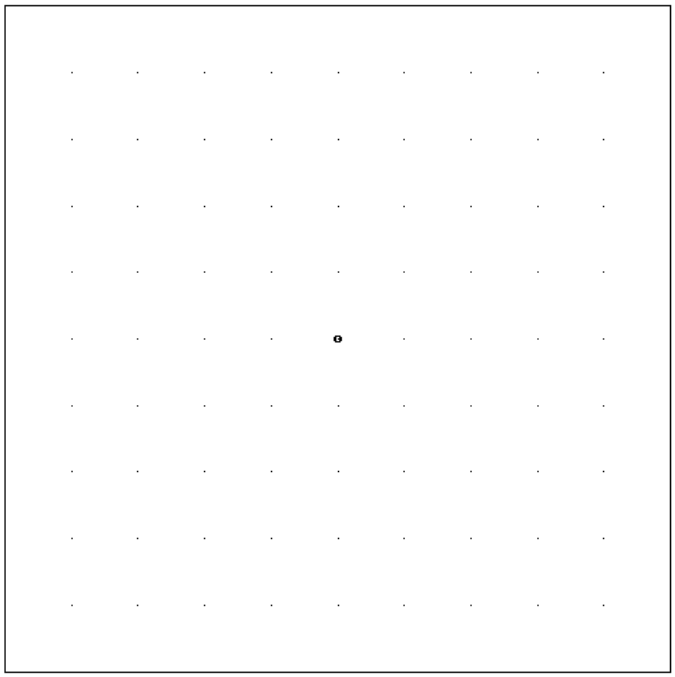

Figure 2.42 – Construction of the model

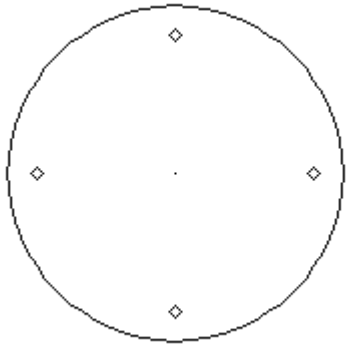

Figure 2.43 – Detail of the energy pile: positioning of the probes.

Table 2.5 - Input data for the model: Thermo-physical properties of materials

	k [W/(m K)]	***ρ [kg/m³]***	***C_p [J/(kg°C)]***	***Porosity [%]***	
Ground	1.5	1500	1600	25	
Concrete pile	1.5	2500	900	-	
water	0.6	1000	4180	-	

2.4.2.1 Sensitivity analysis on the heat flux

In this case the field of temperature has been analyzed with the variation of heat flow imposed. Therefore heat flows have been considered: 20, 30, 50 W /m of drilling.

The domain size was chosen sufficiently large so that the condition of undisturbed soil temperature (14 ° C), imposed on the boundary does not affect the temperature field.

Two cases of operation of the system (a summer case and a winter case) have been considered.

The 2-D model is composed of a mesh of triangular elements with quadratic shape functions. The convergence criterion imposed to the stationary solver has been fixed to a tolerance absolute and relative 10^{-6}. Figure 2.44 shows the thermal mapping of the field:

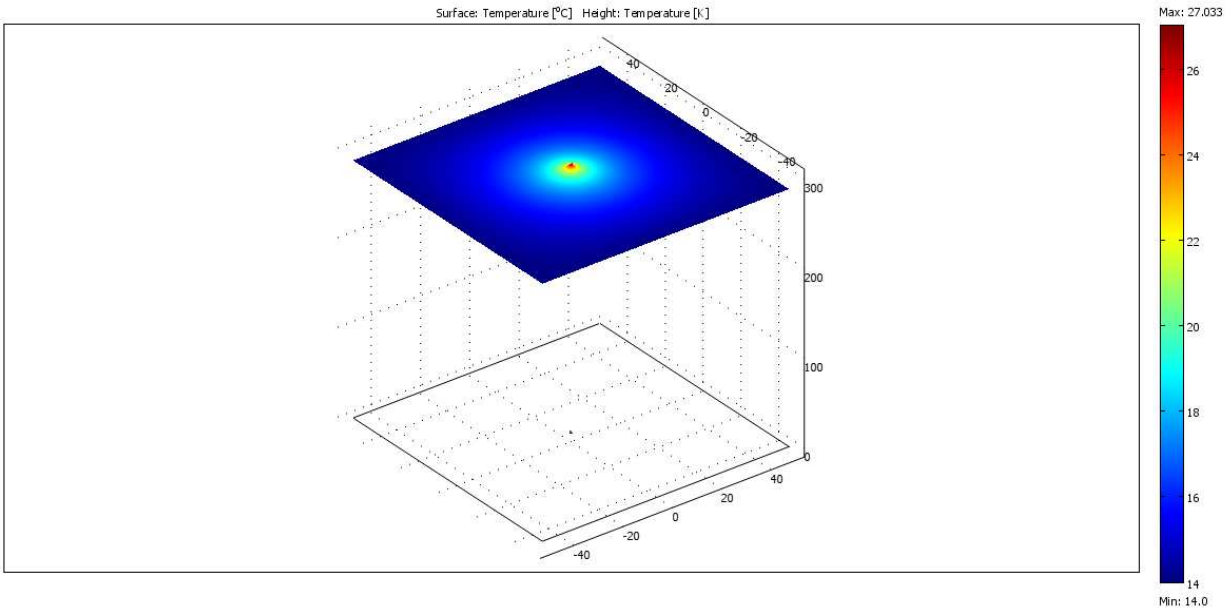

Figure 2.44 – Solution of the temperature field.

The radial temperature distributions obtained, with origin fixed in the axis of the pile, are reported in Figure 2.45, 2.46:

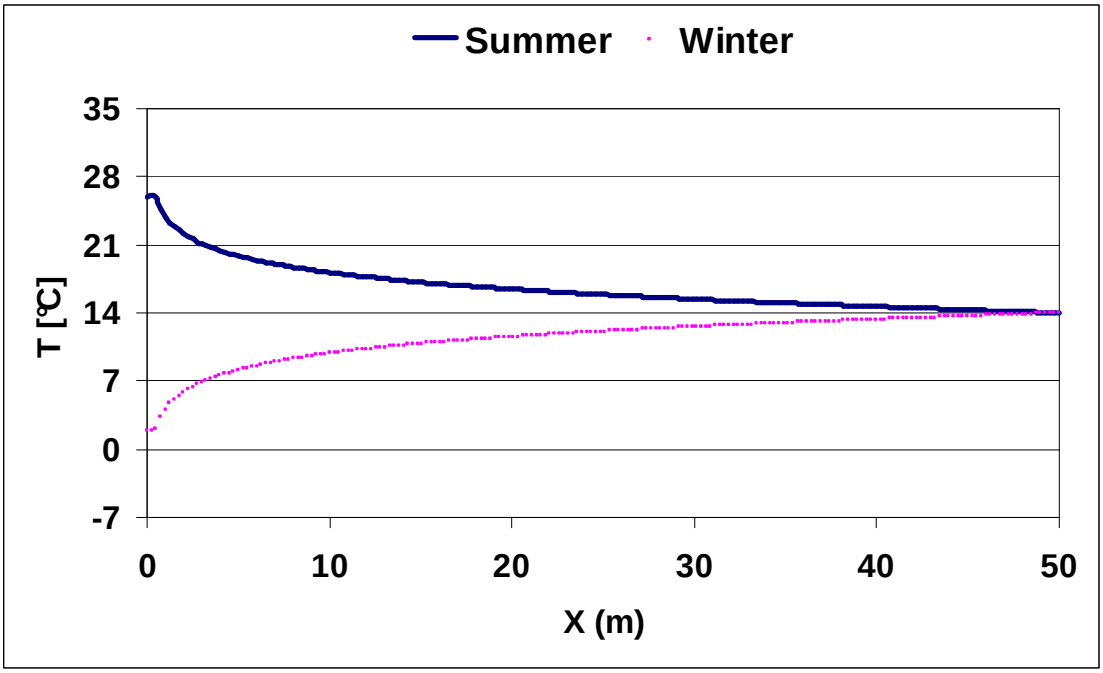

Figure 2.45 – Distribution of temperature in summer and winter regime, q = ± 20 W / m, velocity groundwater absent.

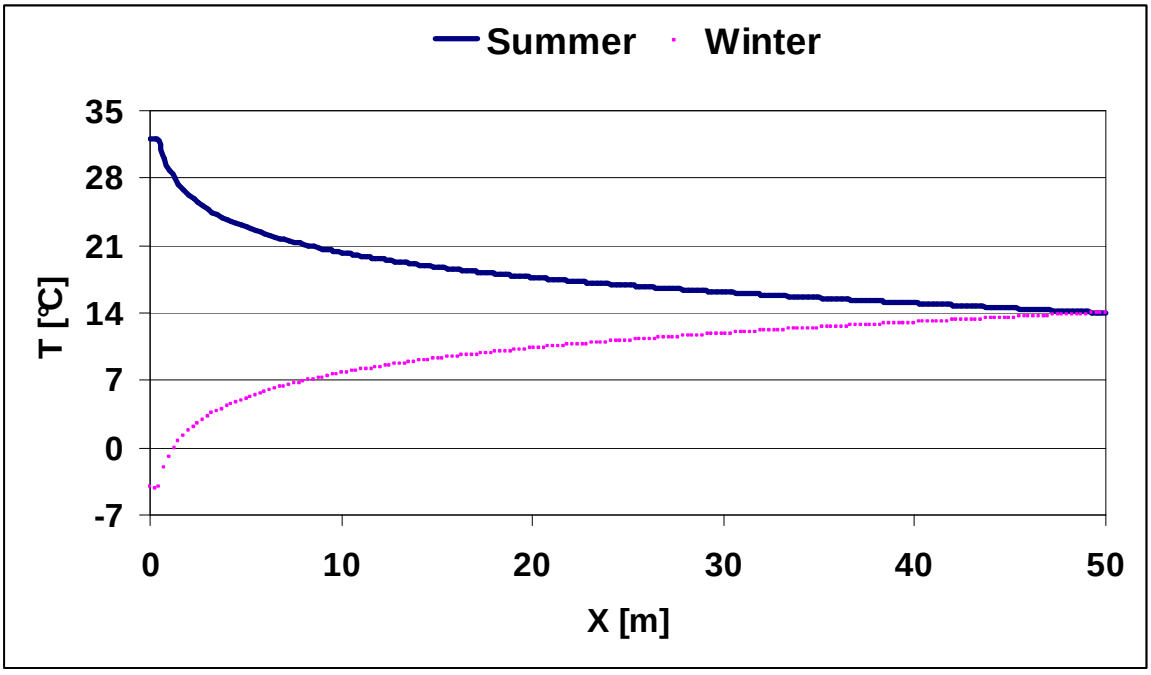

Figure 2.46 – Distribution of temperature in summer and winter regime, q = ± 30 W / m, velocity groundwater absent.

2.4.2.2 Sensitivity analysis on the groundwater velocity

The thermal field has been studied by evaluating the presence of a movement of groundwater in the aquifer as well. It is varied parametrically by a value of 10^{-12} m/s (equal to 0.0315 mm/year) up to a value of 6.10 m/s (equal to 31.54 m/year).

Assuming to fix the hydraulic load equal to 3/1000, the analysis can be seen in terms of permeability rather than in terms of velocity of groundwater. It has therefore a variation of the parameter of permeability from values around 10^{-10} m/s (clays) up to values of the order of 10^{-4} m /s (sands). The results are reported from Figure 2.48 to 2.51.

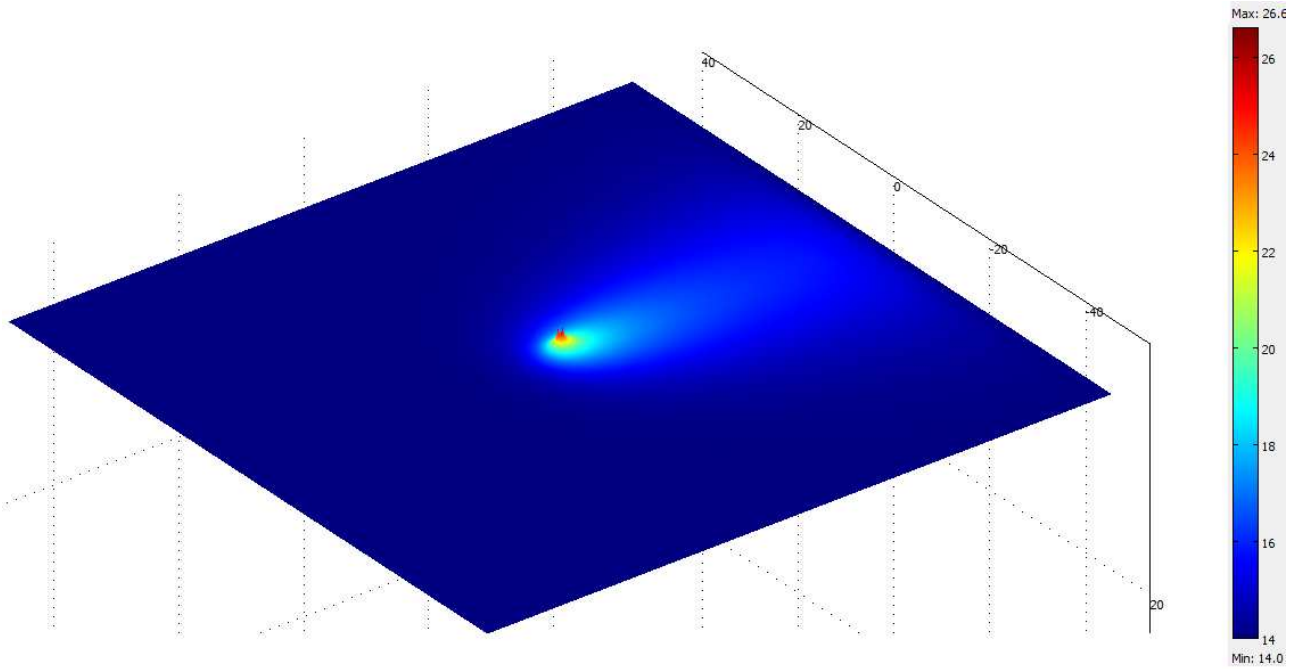

Figure 2.47 – Influence the movement of groundwater, the thermal field: Plume Thermal.

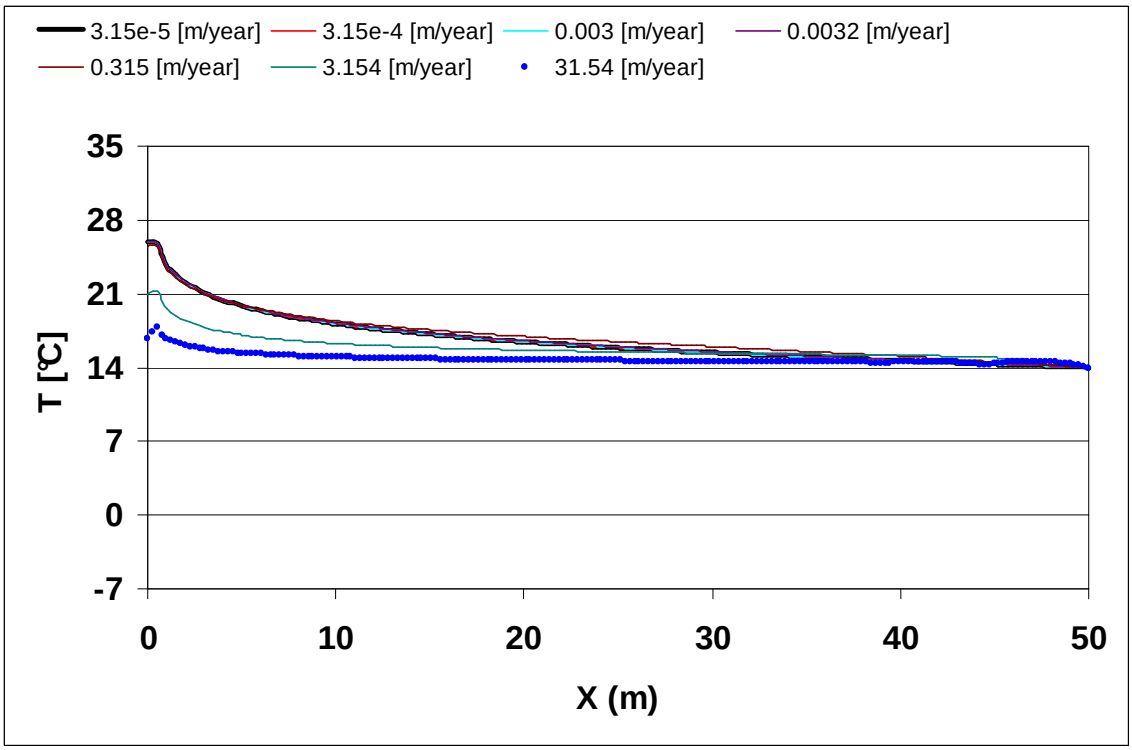

Figure 2.48 – Distribution of temperature in summer conditions, q = 20 W / m, velocity parametric groundwater.

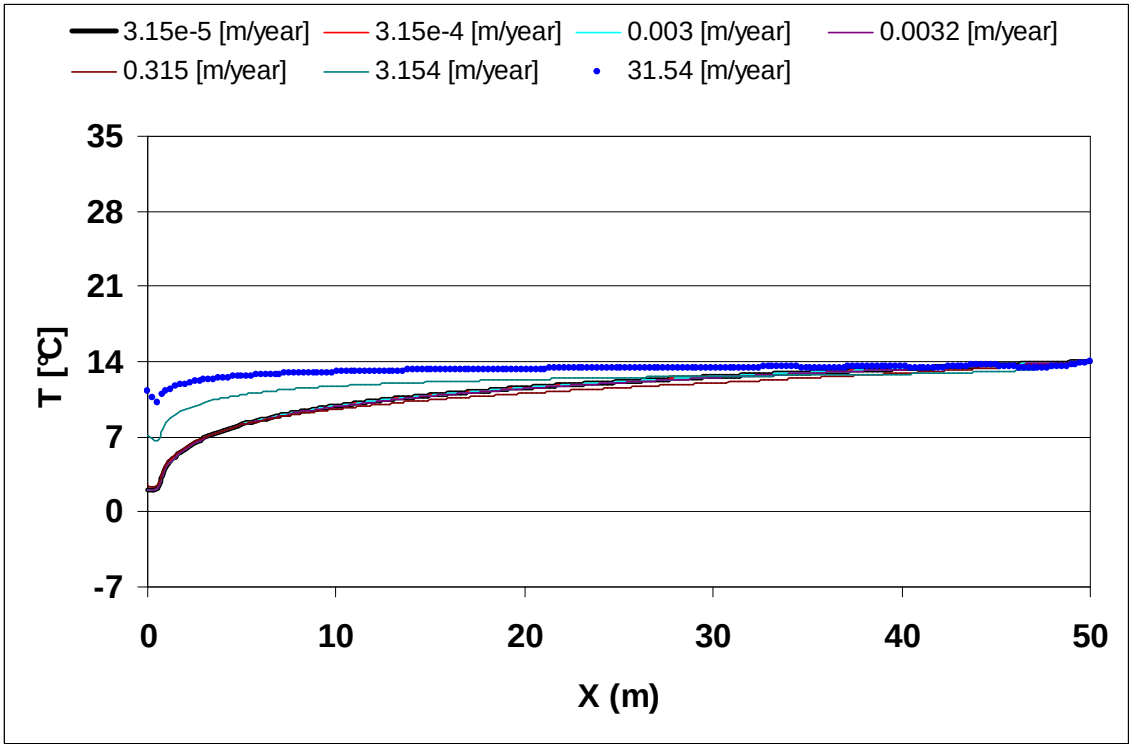

Figure 2.49 – Distribution of temperature in winter conditions, q = - 20 W / m, velocity parametric groundwater.

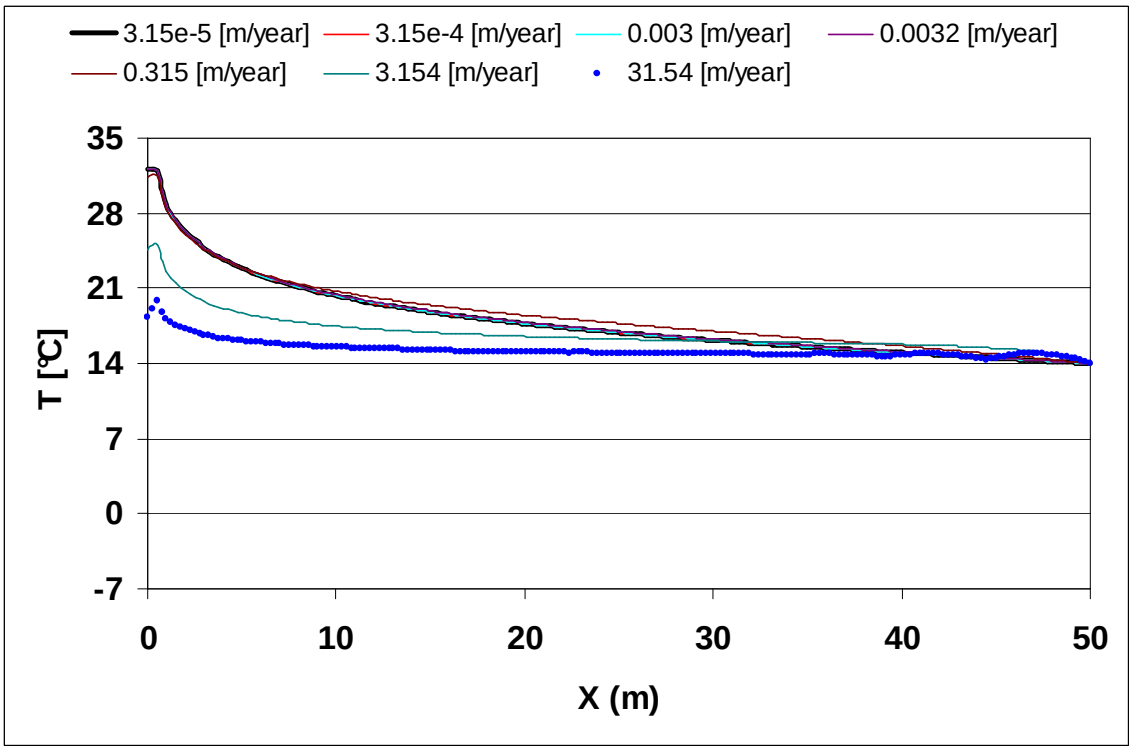

Figure 2.50 – Distribution of temperature in summer conditions, q = 30 W / m, velocity parametric groundwater.

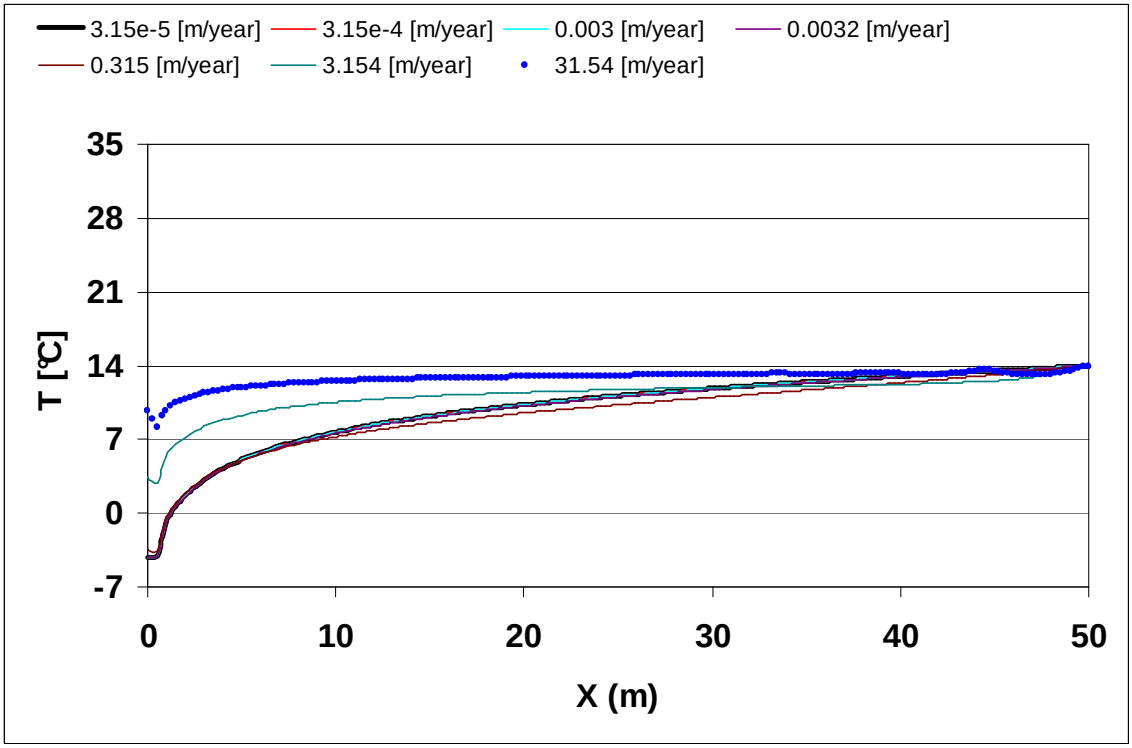

Figure 2.51 – Distribution of temperature in winter conditions, q = - 30 W / m, velocity parametric groundwater.

It may be noted that from the value of effective velocity of 3 m/year (about 10^{-7} m/s) the effect of velocity leads to a significant change on the temperature field, already perceptible at a velocity of about 0.3 m / year. With the increase of the velocity there is a continuous levelling of the thermal field, up to the value of velocity of about 1 m /day, from which the solution tends to become unstable and to diverge towards unreliable results (the motion is no longer laminar or by Darcy). The effect of the water is present for soils of sandy type, and fine sand-silt, (variable permeability between 10^{-6} and 10^{-4} m/s). For gravelly soil type, characterized by velocity of groundwater relevant, a few meters per day, it should solve the equation of the flow field.

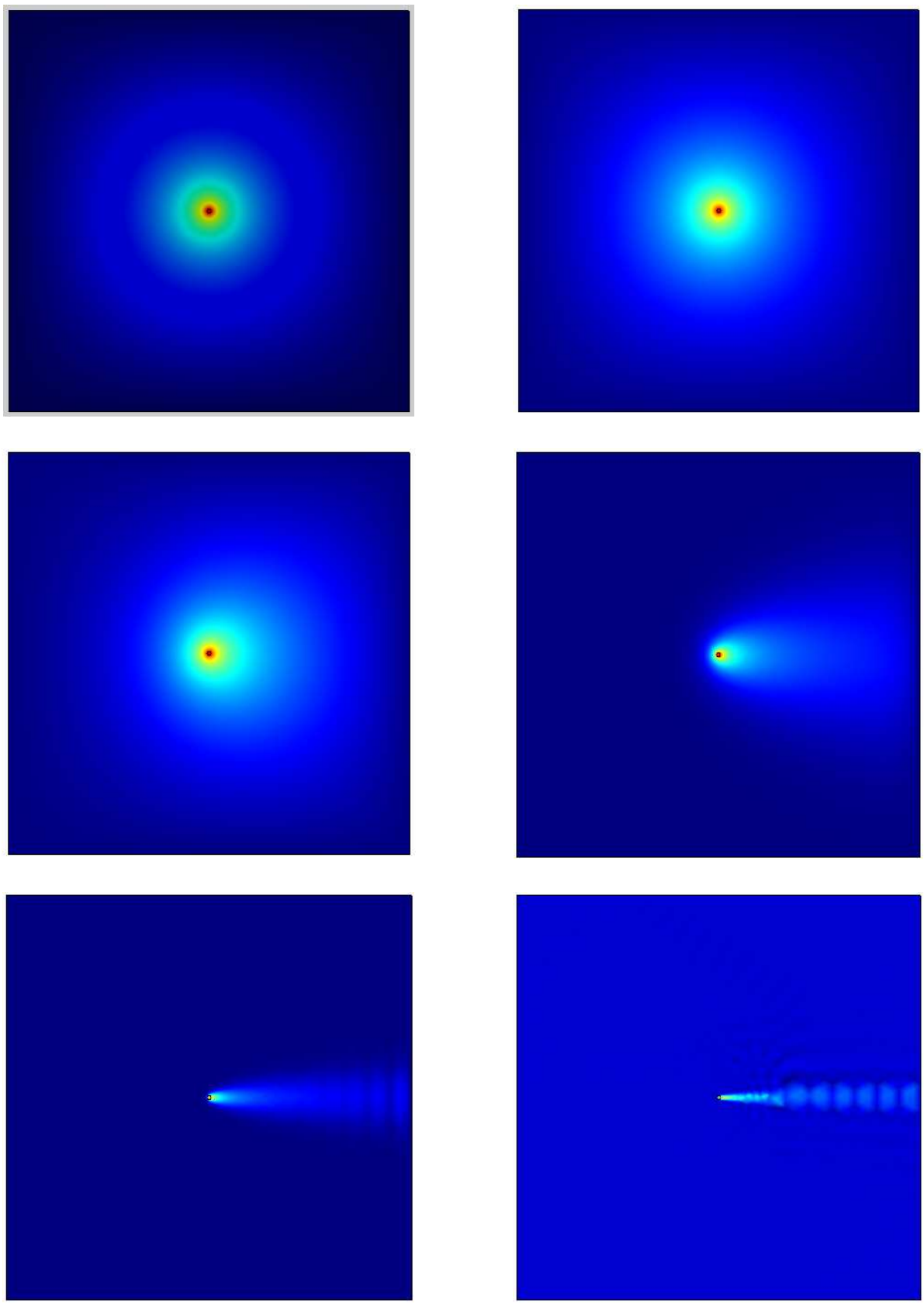

Figure 2.52 – thermal field with various cases of groundwater motion in case summer

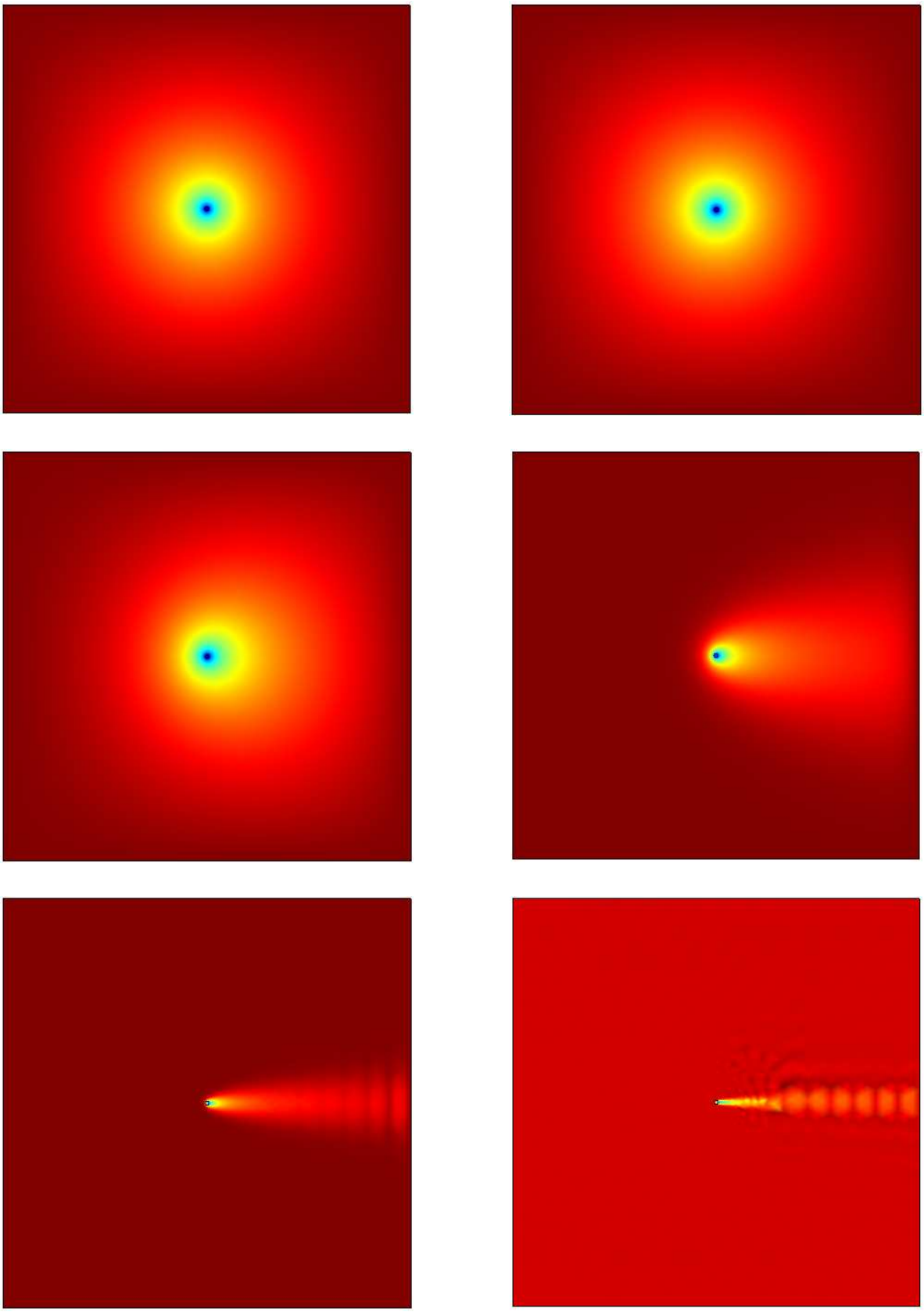

Figure 2.53 – thermal field with various cases of groundwater motion in case winter

2.4.2.3 Calculation of the equivalent thermal conductivity

A further analysis has been carried out on an usual GHE by changing the velocity of the water in the aquifer. By using the line source theory based on the results of a FEM simulation of a GRT the equivalent thermal conductivity has been calculated. Simulations are similar to the ones reported in paragraph 2.4.1.

As for the ground model a λ = 1.5 for the soil has been chosen. In the case there is also water, hence the overall thermal conductivity is:

$$\lambda_{tot} = \lambda_w \phi + \lambda_s (1-\phi) = 1.28 \left[\frac{W}{mK} \right] \quad (2.11)$$

The results obtained are shows in Table 2.6:

Table 2.6: results of the characteristics of the ground derived by the GRT simulations:

	k	**λ_{eq}**
v = 0	2.52	1.27
v = 3.15e-5	2.50	1.27
v = 3.15e-4	2.50	1.27
v = 3.15e-3	2.50	1.27
v = 0.032	2.50	1.27
v = 0.315	2.35	1.36
v = 3.154	1.13	2.83
v = 31.536	0.52	6.07

The results show that the influence of the motion of groundwater (convective component of heat transfer) begins for values of effective velocity of the water of the order of 0.3 m/year (10^{-8} m/s), to become predominant for values of the order of about 3 m/year (10^{-7} m/s), where the calculated equivalent lambda acquires a value twice than the one in pure conduction.

Finally, it is possible to make a comparison between model calculations. The problem of the model system of conduction and convection with ground and water has been, replaced with a purely conductive model in scheme and with a coefficient of conductivity equal to the one calculated. The comparison is made for a value of velocity of 3 m / year. Figure 2.54 shows that one performed the GRT on usual GHE's, the equivalent thermal conductivity and pure conduction is a good method to approximate the heat exchange between the GHE and the soil.

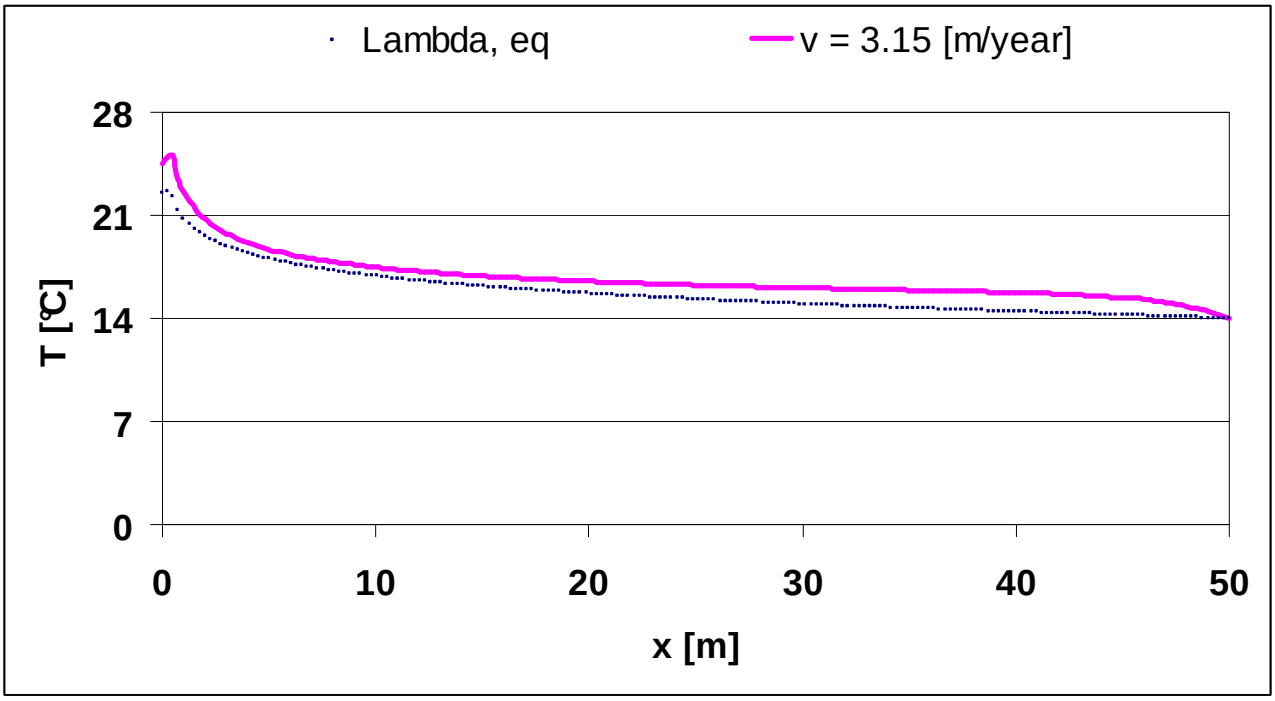

Figure 2.54 – Comparison between the solution with convective motion of groundwater and the solution in regime conductive with λ,eq.

2.4.3 Effect of temperature on structural load of energy piles

Considering a column, with the some composition and size of an energy pile, and applying a temperature variation ΔT (in heating or cooling), a uniform deformation is present:

$$\varepsilon_T = \alpha \Delta T \qquad (2.12)$$

where α represents the coefficient of thermal expansion. In addition there is a variation in length, proportional to the variation of temperature ΔT, equal to $\varepsilon_T L_0$, where L_0 is the initial length of the rod. If the pile is completely bound in the axial direction, any change in its length can not occur. A uniform axial stress equal to:

$$P = \varepsilon_T AE \tag{2.13}$$

where A is the area of the section of the column, while E is the elastic modulus of the column.

If the column is below the ground, which opposes a constant resistance to the energy pile, the expansion/contraction of the pile in response to the change of temperature will be partially constrained hence the effect of the temperature variation will be reduced compared to that for a not constrained column.

In figures from 2.55 to 2.59 a series of mechanisms for the transfer of the load during thermal cycling, are shows. It is assumed that the load acting on the pile is supported by the column, and that resistance that is generated is uniform along the entire length of the pile, which means that the deformation will be constant with depth. It is further assumed that, when the thermal loads are applied to the energy pile, the temperature variation occurs uniformly along the entire length of the structure.

The following cases can be thus found:

1. The pole solicited by only mechanical load is in compression; moving within the soil, the resistance that opposes the load occurs in the interface pile / soil. In this simplified model the mobilized lateral resistance is constant, thus the result of deformation and load decreases linearly with depth (Figure 2.55);

2. When a cooling cycle is applied to the energy pile, in the case both ends are free to move, this is contracted, with development of a tensile stress. By increasing the cooling tensile stress increases, until the deformations reaches the limit of breakage of the pile. (Figure 2.56). Along the upper part of the pile, tangential shearing tensions are generated at the interface between pile and ground; they have the same direction of those caused by a compressive load applied the head. In the lower part, these tensions will have instead the opposite sign.

3. When, a heating cycle is applied to the energy pile, it expands, developing a compressive stress in the pile (Figure 2.57). Even in this case an increase of thermal stress can lead to the breaking of the pile. At the interface between pile and ground will grow, however, the opposite effect than the previous cooling cycle: cutting interface pile/ground is opposed to that induced by the compressive load to the summit of the structure.

4. When a compressive load applied to the head of the pile is associated with a change in temperature in cooling (Figure 2.93) or heating (Figure 2.94), the combined effect of the above mentioned cases happen.

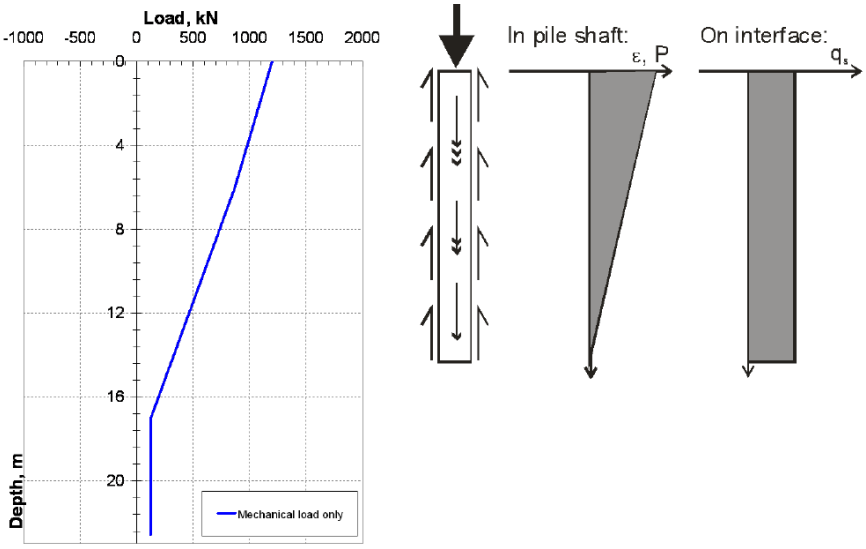

Figure 2.55 – Case of only the load applied on top of the pile.

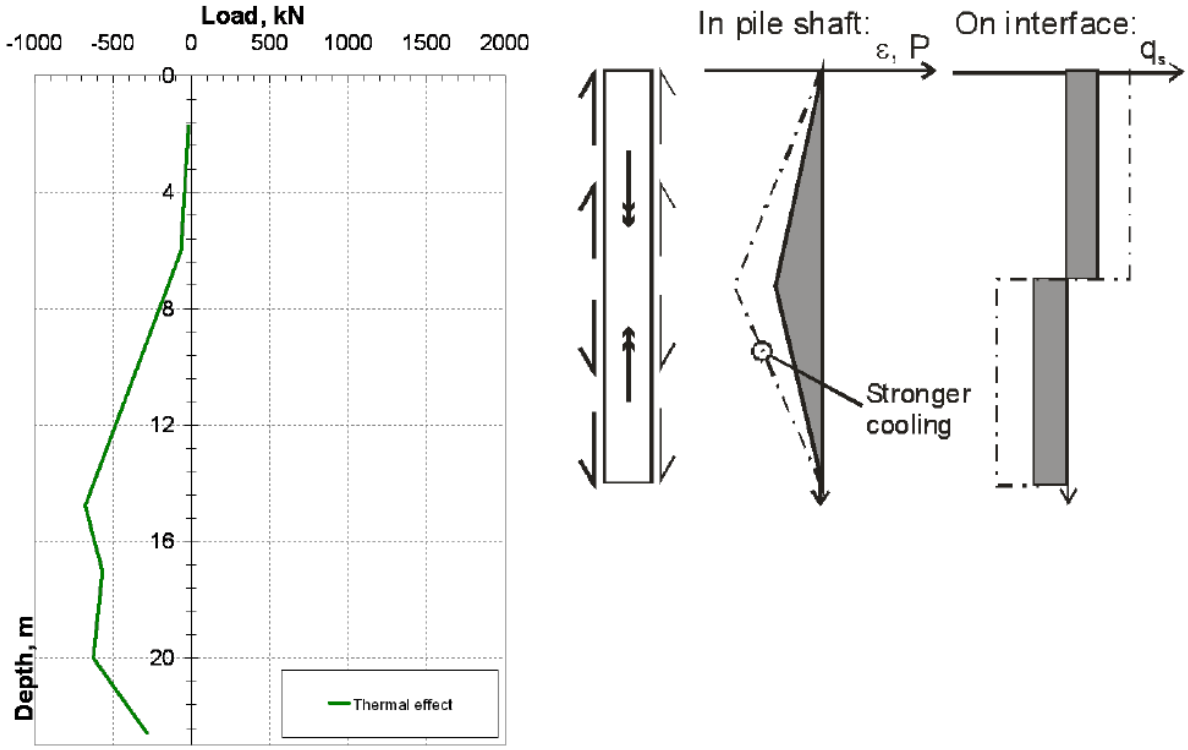

Figure 2.56 – Case of only cooling cycle.

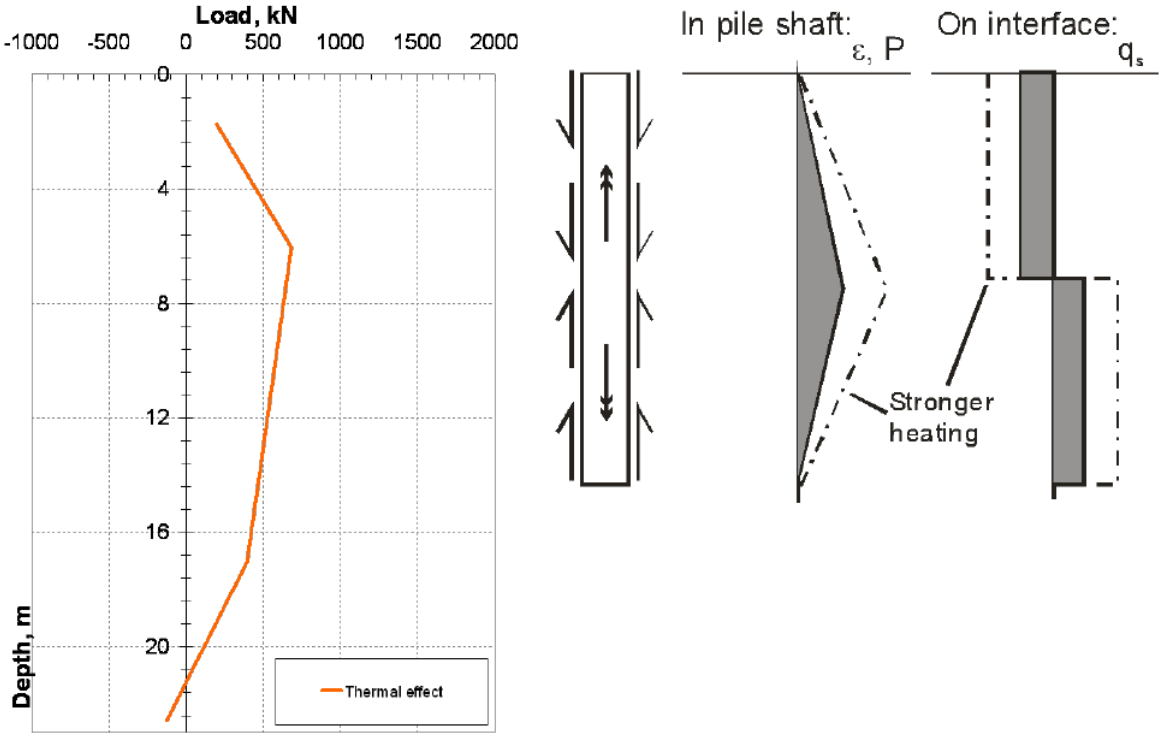

Figure 2.57 – Case of only heating cycle.

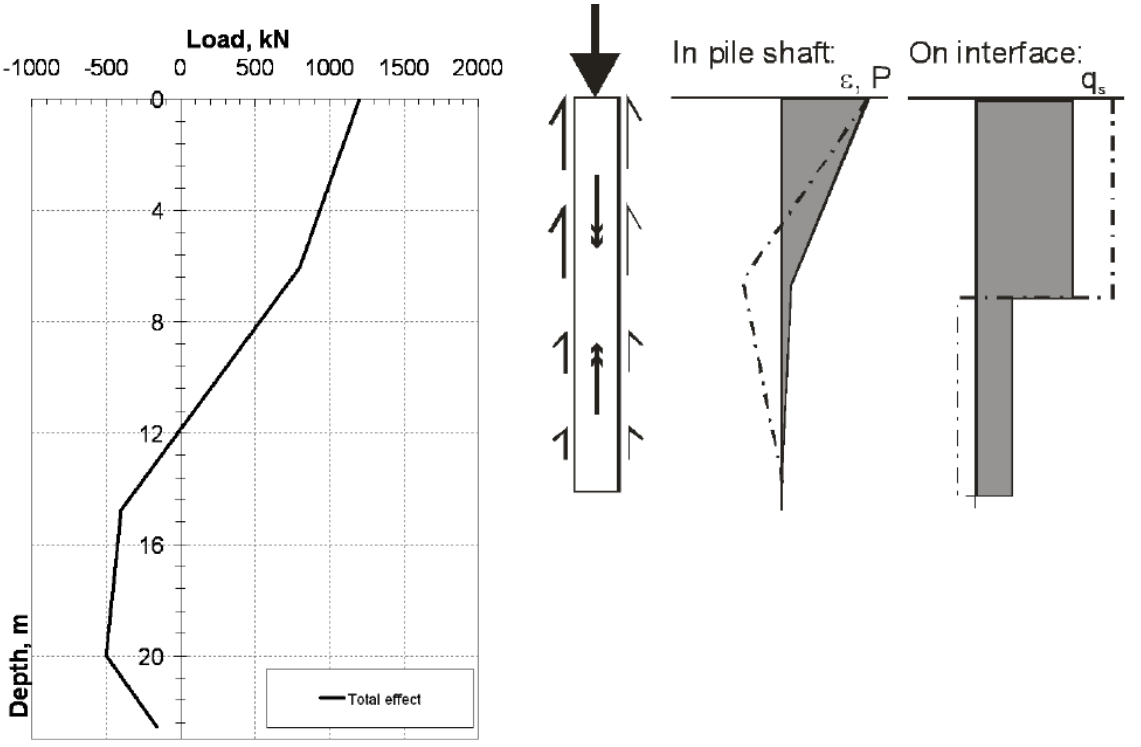

Figure 2.58 – Case of cooling cycle and compressive load.

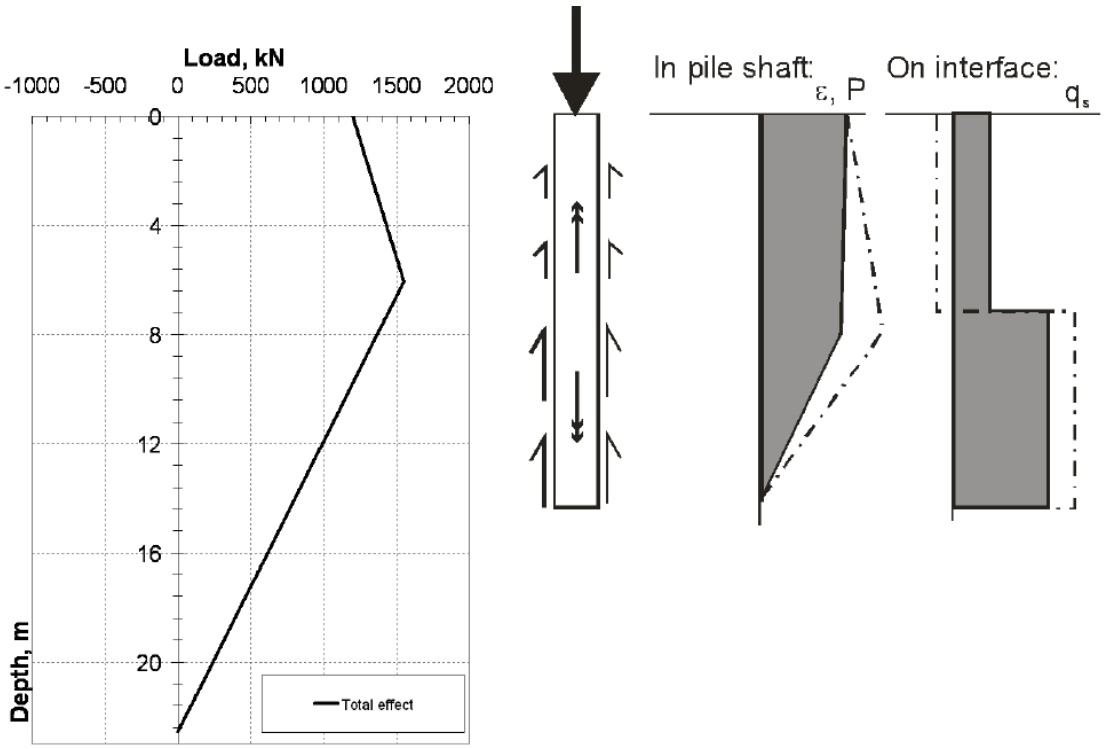

Figure 2.59– Case of cycle of heating and compression loading.

2.4.3.1 FEM model

The entity of the thermo-structural interactions that occur during operation of the energy pile was performed using a three-dimensional finite element model with thesoftware COMSOL Multiphysics.

The intent was to verify the theoretical distributions of tensions, detected in some articles in the literature by means of a calculation model, able to represent a good approximation of the real situation.

The model consist of a central cylindrical element with a length of 25 m and having a diameter of 1 m. The foundation pile is made of concrete and presents 4 cylindrical cavities inside (diameter of 32 mm). The cavities are arranged symmetrically about 8.5 cm from the edge of the energy pile. The volume of soil that constitutes the domain of the problem is a 200m square, having a depth of 55 m. The mesh consists of 3010 tetrahedral finite elements with quadratic shape functions. The thermo-physical characteristics of the materials are reported in tables 2.6.

Table 2.6 – Thermo physical characteristics of materials

	GROUND	CONCRETE
ρ (kg/m^3)	1500	2500
E (MPa)	75	28328
ν	0.25	0.15
α (1/K)	1.00E-05	1.20E-05
n	0.25	0.00
λ (W/m °C)	1.5	1.5
c (J/kg °C)	1600	900
C (J/m^3 °C)	2400000	2250000

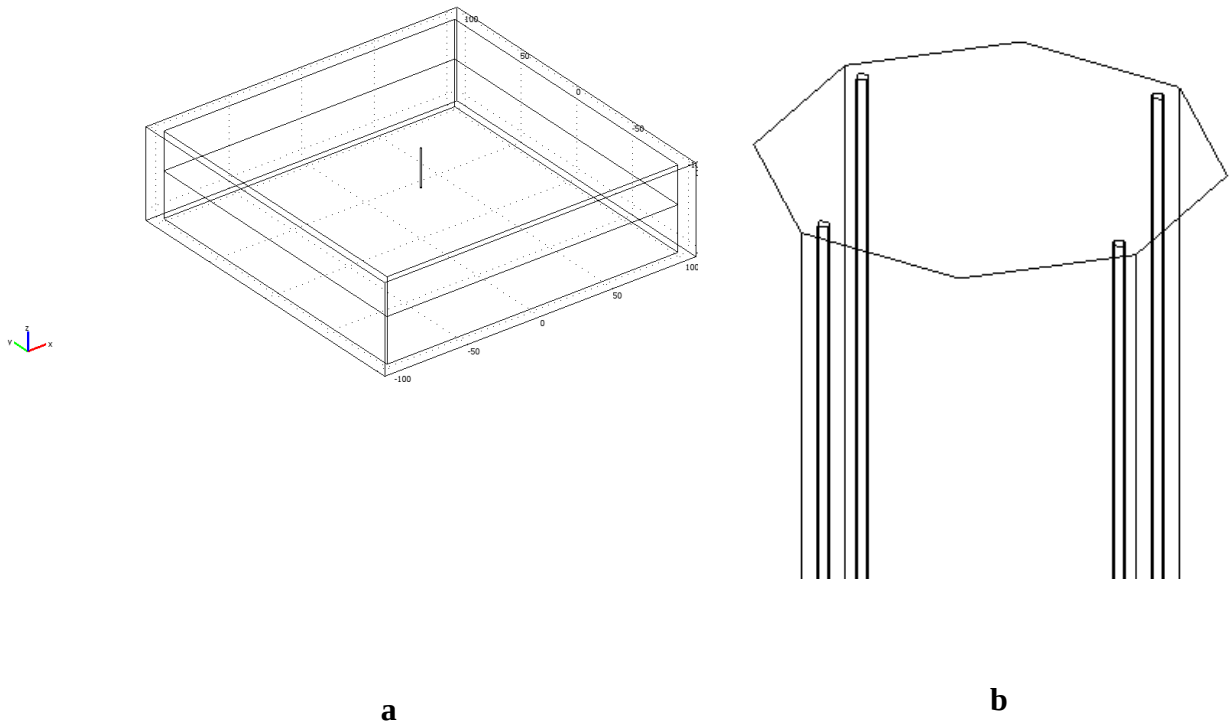

a **b**

Figure 2.60 – three – dimensional geometry of the model a), and Detail of the modelling of the pile and the internal pipes b).

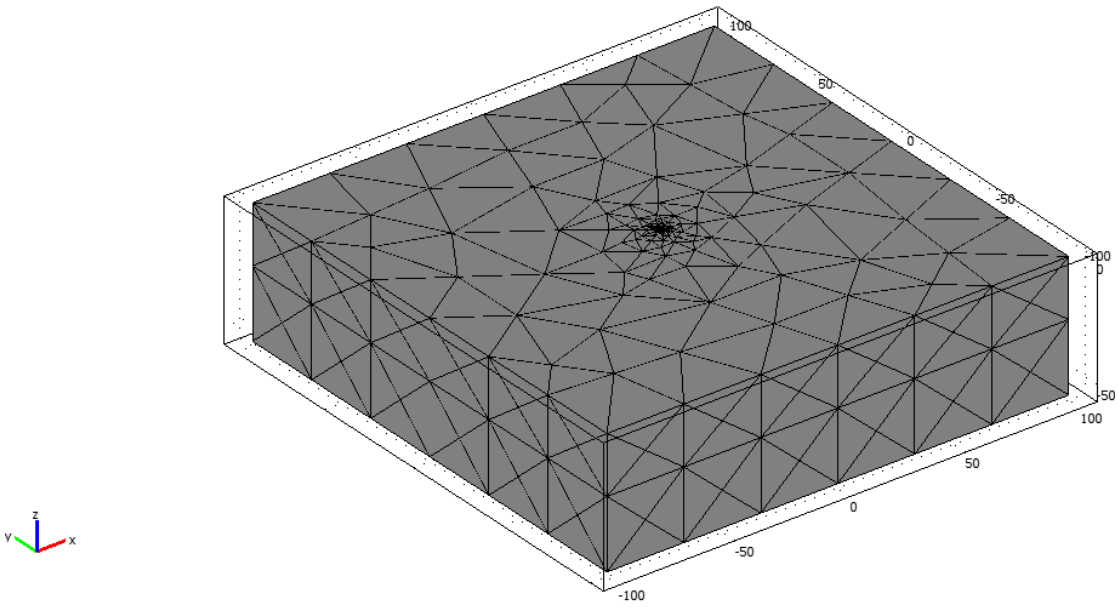

Figure 2.61 – Detail of the mesh generated by the software

2.4.3.2 Thermal model simulation

Summer case

A heat flow has been imposed equal to 100 W/m^2 (simulation of operating conditions in summer regime). The conditions on the boundary surfaces of the domain are fixed temperature, equal to the temperature of the undisturbed soil of 14 ° C. The pile is free to deform, there are no constraints imposed at the summit. At the interface with the ground, the boundary conditions is of perfect friction, i.e. there is continuity between the displacements of the pile and those of the ground. The thermal solver is stationary, the convergence tolerance is set equal to 1e^{-5}.

The solution in terms of vertical tensions σ_z, vertical deformation ε_z, and vertical displacements (subsidence) are shown in figures from 2.62 a, b, c. The abscissa z is measured from the head of the pile.

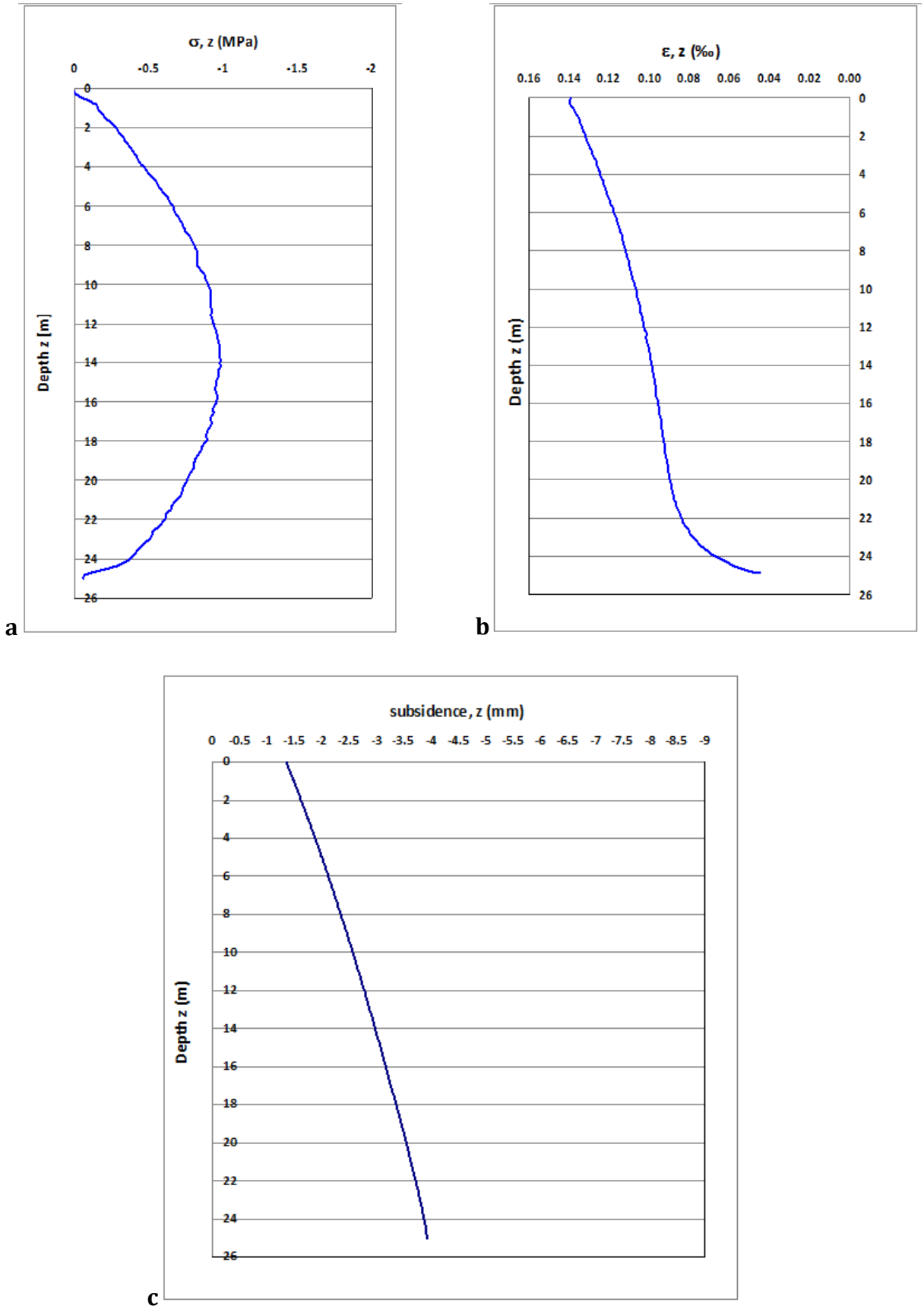

Figure 2.61 – Distribution tensions vertical compression in the pile a), Distribution vertical deformation in the pile b), vertical settlements of the pile case summer c).

In this case, since no applied mechanical loads have been applied to the pile, that is, the pile is free to deform in the vertical direction. Under the effect of the temperature increase, caused by the heat flow that is discharged from the pole in the ground, the pile is not free to expand, this is due to the effect of the soil on the walls of the pole and the contact with the ground . These constraints generated in the pile the tensions of thermal nature (Figure 2.61a), whose trend approximates well the theoretical one described in Figure 2.61. The vertical deformations are not uniform but are influenced by the constraint that the land forces at the interface with the pile (Figure 2.61b).

Winter case

The analysis similar to the previous case, with the only difference that the flow in this case will be entering the pile and hence hose negative sign. In fact in the case of winter operation of the system the purpose is to absorb heat from the soil, inducing, therefore, a decrease of temperature in the surrounding domain.

The boundary conditions of the domain are the same as the previous case.

The solution in terms of vertical tensions σ_z, vertical deformation ε_z, and vertical subsidence are shown in figures 2.62.

It can be noticed that the tensions, the deformation and the vertical displacements have similar trend to those described in the model of operation in summer case, but with opposite sign. The tensile stresses in the pile are, induced by the reduction caused by the decrease of temperature, prevented by the reaction caused by the soil at the interface of the pile. These tensions are maximum at th center of the structure, as described in the theory, and reach a maximum value of 0.5 MPa.

The following Figures 2.63 and 2.64 show the temperature distribution along the axis of the pile and the temperature in the radial direction from the edge of the pile in both winter and summer cases.

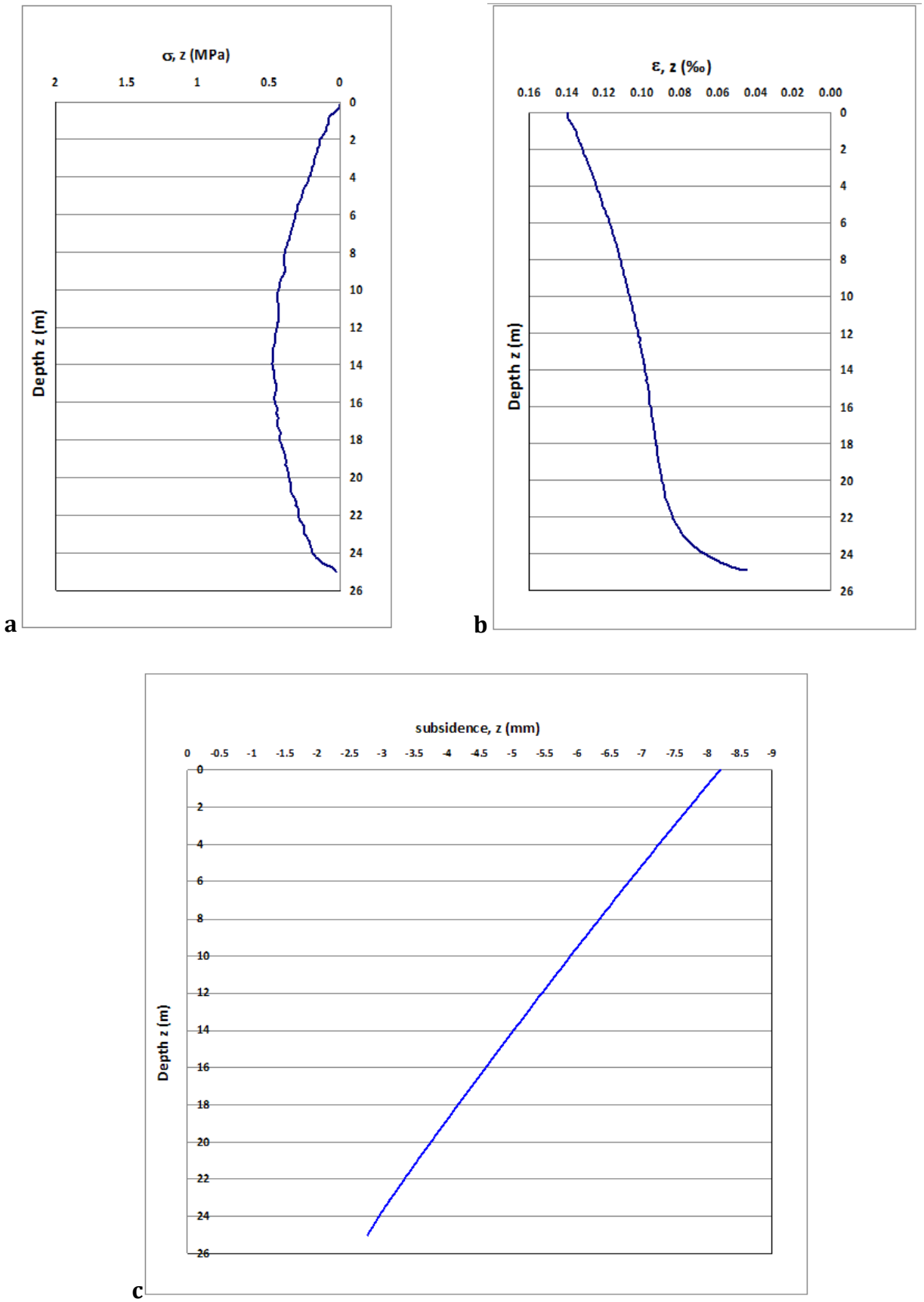

Figure 2.62 – Distribution tensions vertical compression in the pile a), Distribution vertical deformation in the pile b), vertical settlements of the pile case winter c).

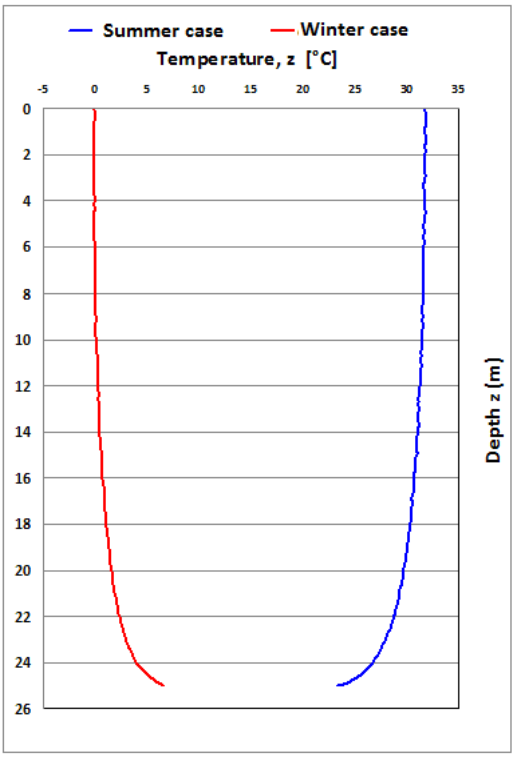

Figure 2.63 – Temperature distribution in the axis of the pile to vary the depth z.

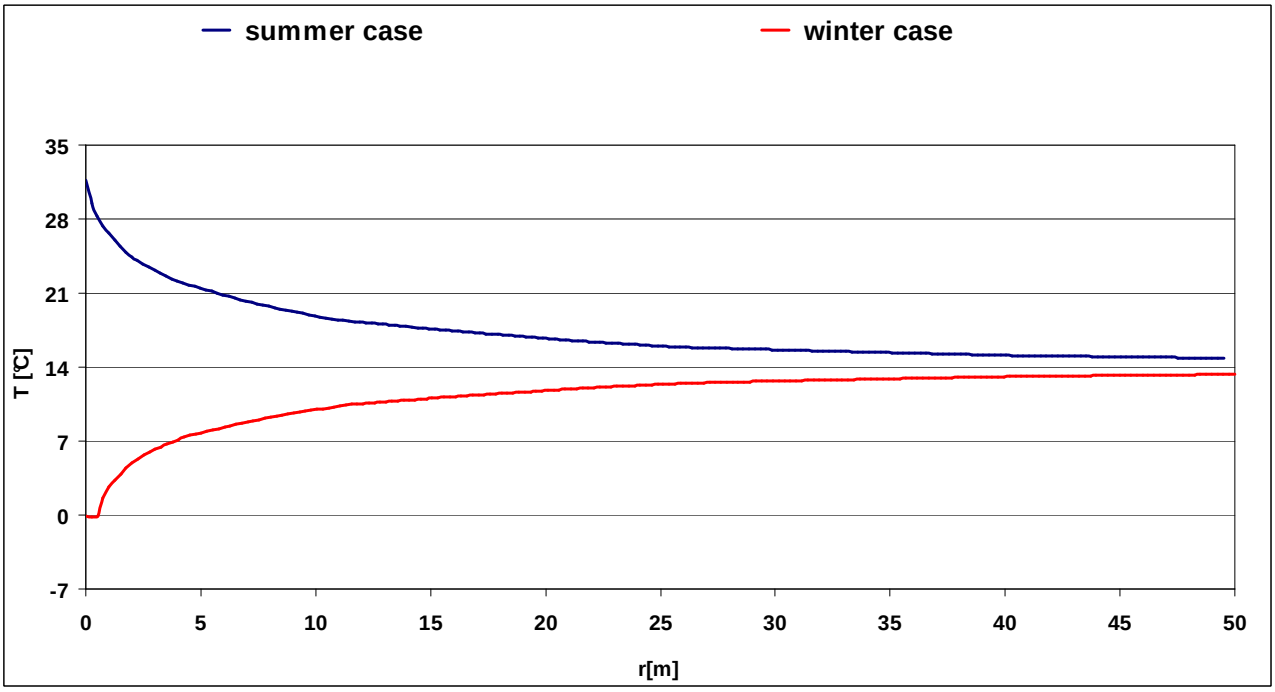

Figure 2.64 – Radial temperature distribution from the edge of the pile.

2.4.3.3 Mechanical model

A model for the evaluation in the pile in presence of a load applied on its head (1300 kN). This value is the same as that used in geotechnical and structural design of the foundation. This value is a typical average value of normal stress acting on a foundation during the life of a structure.

The model used for the evaluation of stress is the same as presented previously. In this case there is no condition on the temperature, as the objective of this analysis was evaluate only the mechanical effect induced by the load in terms of tensions, deformations and displacements, as well as to evaluate the fit of the model comparison with the theoretical solution presented previously.

The geometry of the system, as well as the thermophysical characteristics of the materials, are therefore the same, while the conditions imposed in this case are: symmetry constraint on the walls of the model, the load imposed on the surface of the pile head, equal to the force of 1300 kN , distributed on the surface of the head as a distributed load (Figure 2.65).

In this case, in the model it is possible to take into account the reduction of area reagent due to the presence of the probes, because they are actually modelled as holes. Particular attention must be placed fact in this respect: the presence of the probes, in the vicinity of the reinforcement of the edge, create discontinuities for the purposes of adhesion between the bars and the cement matrix, which can give rise to local complex and dangerous phenomena, especially at high levels of tension.

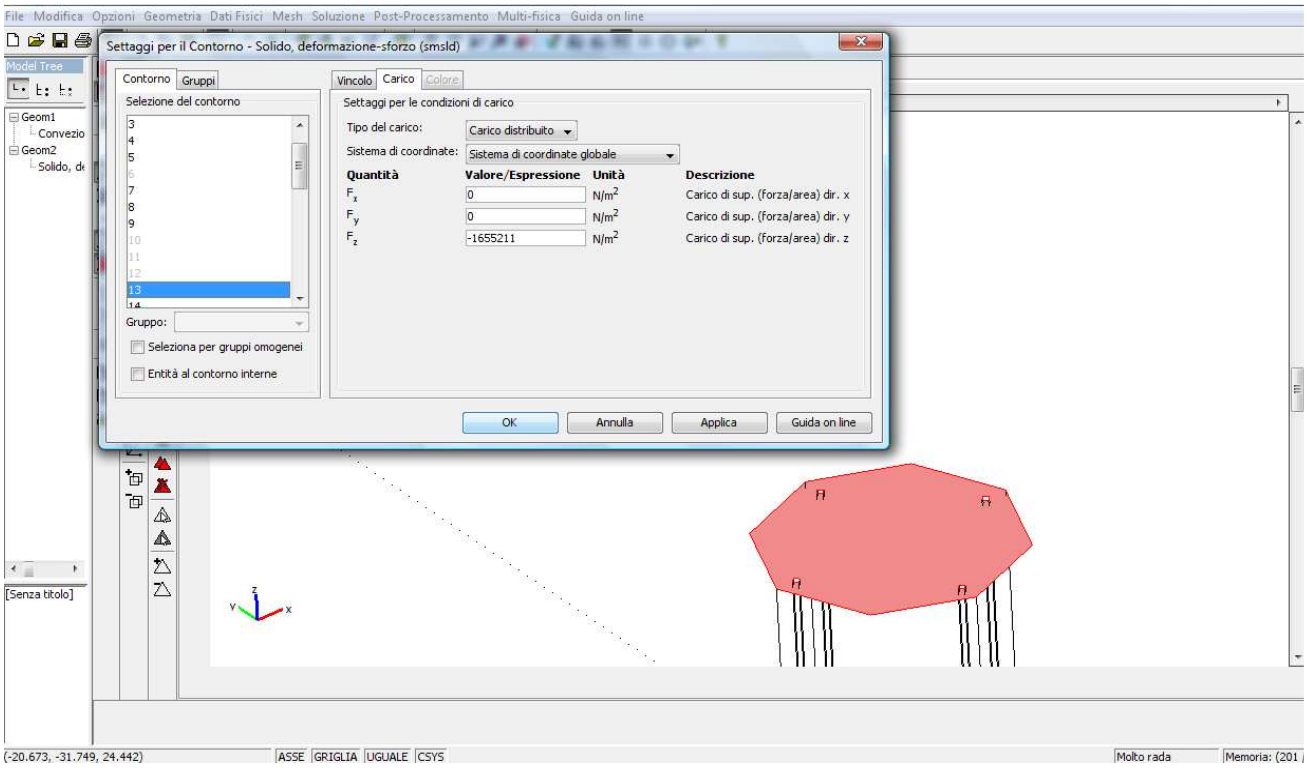

Figure 2.65 – Imposition of the condition of load on the pole head.

In Figure 2.66 the graphs relating the trends of the tensions, strains and vertical displacements referred to the axis of the pile are present.

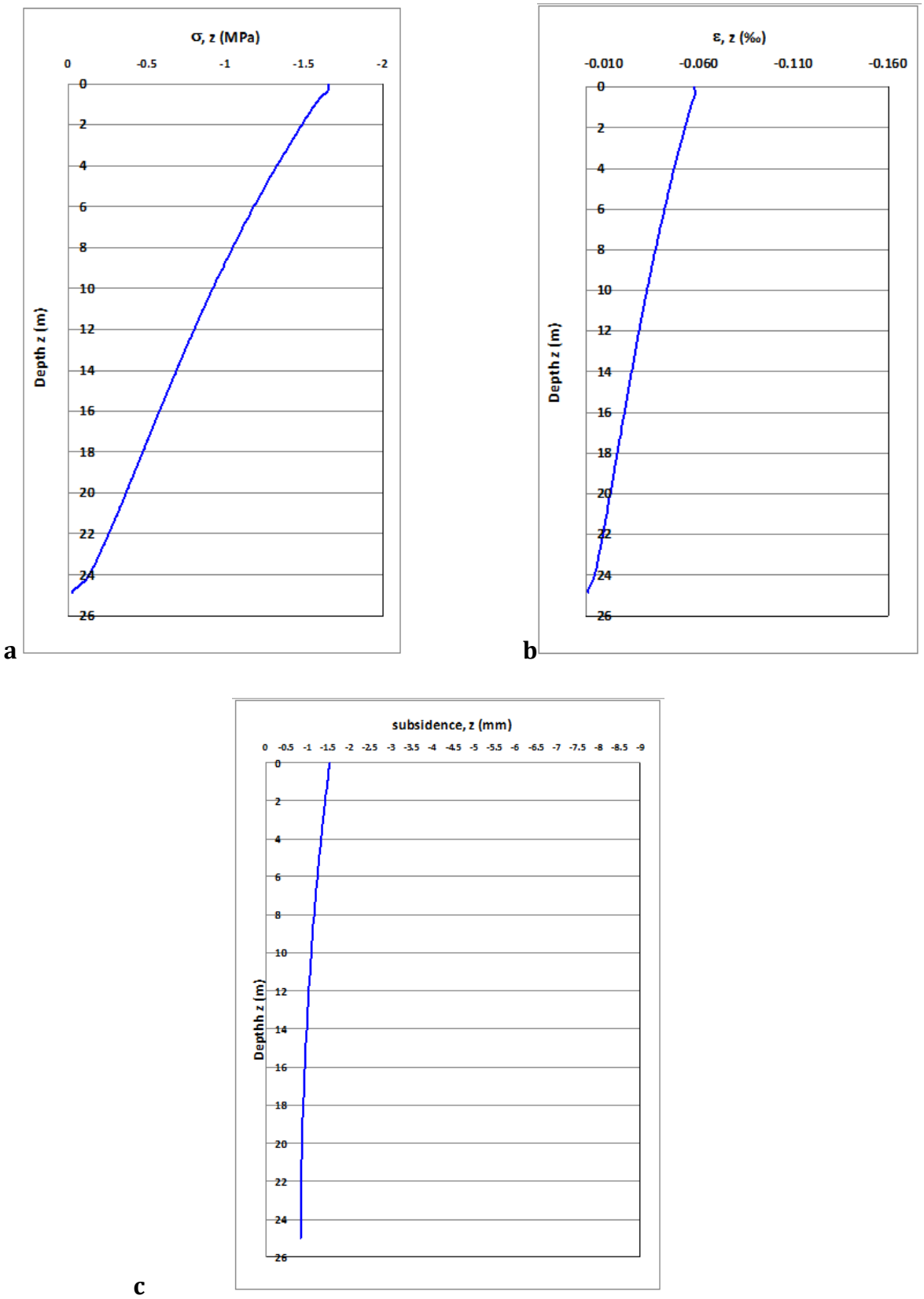

Figure 2.66 – Distribution of compressive stresses inside the pile a), Distribution of vertical deformation ε_z in the pile b), Distribution of the vertical as a function of depth in the pile c).

It can be seen, the maximum compressive stress reached is about -1.7 MPa. From this value, the tensions decrease with linear trend to zero in the vicinity of the tip. This distribution is in agreement with the theoretical charts, as well as the trend of the vertical deformation. The subsidence on the tip is equal to about 1.6 mm,

2.4.3.4 thermal – structural interaction

Finally a superposition of thermal and mechanical effects, which occur in the foundation structure during the course of its load-bearing function, and combined with that of the vertical exchanger with the ground.

It is a starting point for the design of energy piles, since it allows to know the influence of the thermal field on the state of stress, unlike the usual foundation piles. The proposed model is the same as that used by Laloui in Laloui et al. (2006) to draft a thermo-hygro-mechanical model based on experimental analysis of a palificata energy, composed by piles having the size of that under consideration.

The results proposed later, were extrapolated from the three-dimensional FEM model, combining the thermal boundary conditions and the structural constraints imposed in previous calculations. The mesh, generated by the program in an automatic manner, consists of 131 075 tetrahedral elements with quadratic shape functions. The solution was obtained with a stationary thermal solver for calculating the temperatures combined with a mechanical structural solver capable of solving the problem of solid mechanics solicited both from a structural load and from a thermal gradient based on the solution obtained in the previous step for the temperature.

Thermo – structural model: Summer case

The state of stress that is generated inside the structure for combined effect of the structural loading at the top, and of the thermal stresses during operation in cooling mode is shown in the following graph (Figure 2.67).

The overheating due to the increase of temperature in the energy pile leads to an increase of the compressive stresses. The maximum tension, which in the case the structural load is applied alone it at the top of the pile, now is moved downwards and equal to about -1.85 MPa. This effect increases with higher temperatures and therefore the thermal flow exchanged through the probes. The conditions analysed, represent a case almost in operational limit conditons, which may occur, for a few hours per week. In conditions of peak thermal load it is presumed that the temperature of the structure can grow further, causing even a greater state of stress. In general, however, it is desirable to take into account of the effect induced by the overheating of the pile at design and structural verification, because the ratio of tensions induced by the thermal cycle with those caused by the structural load agent, contribute to increase about 30-40% the stress.

Thermo – structural model: Winter case

The state of stress, which is generated inside the structure for combined effect of the structural loading agent at the top, and the thermal stresses during operation in winter conditions is shown in Figure 2.68.

By the trend of vertical tensions, it can be noted that, the cooling of the energy pile, gives rise to a decompression of the structure. At the bottom, this effect is more visible, as tensile stresses are created.

Compared to cases in summer regime that led to an increase in compressive stresses, in this case it tends to have a sign inversion in the distribution of the stress state due to the superposition of the diagrams of tension.

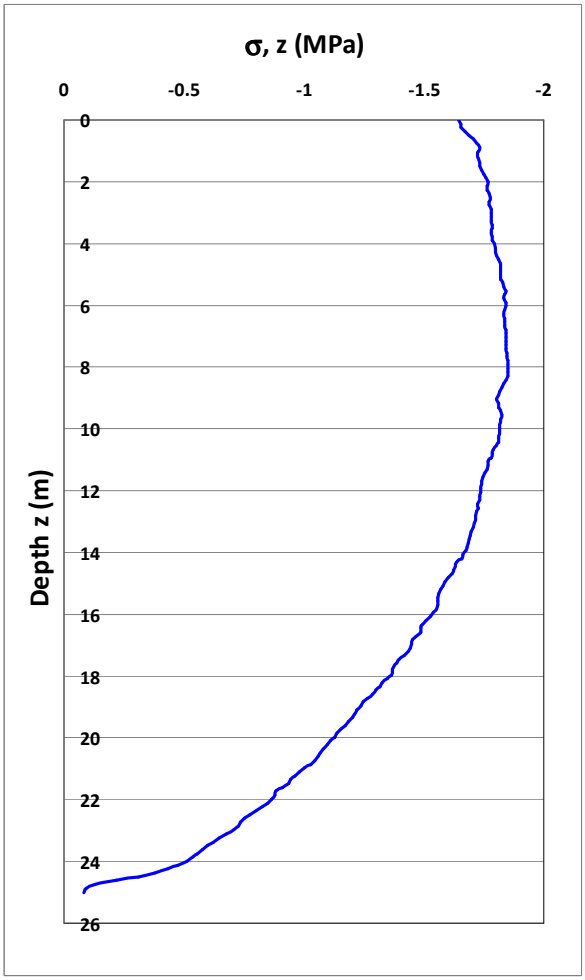

Figure 2.67 – Trend of vertical tensions σ_z along the pile energy (case summer).

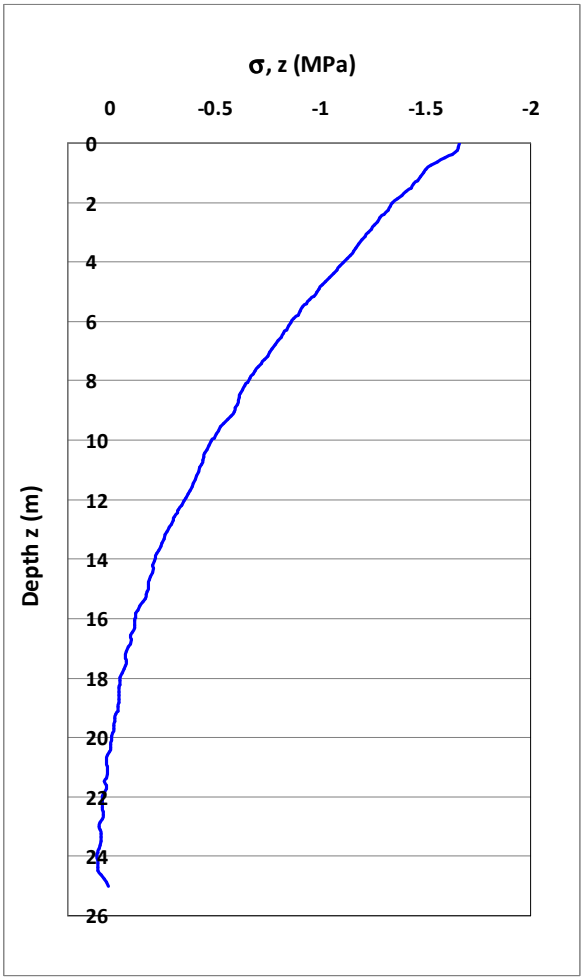

Figure 2.68 – Trend of vertical tensions σ_z along the pile energy (case winter).

2.4.3.5 Final consideration

The results of the analyzes show the differences between the different response to mechanical and thermal loads. Even if the vertical mechanical tension σ_z is greater at the top of the pile (approximately 1.6 MPa in compression), the thermal load, although slightly less of entities is more distributed along the structure. From the data one can formulate the hypothesis that a temperature difference of 1 °C in the energy pile causes a vertical force of about 100 kN.

Below are the results obtained from the model of Laloui, obtained on the basis of experimental studies carried out on a pile having the same geometrical dimensions, and the same static load.

a) *b)*

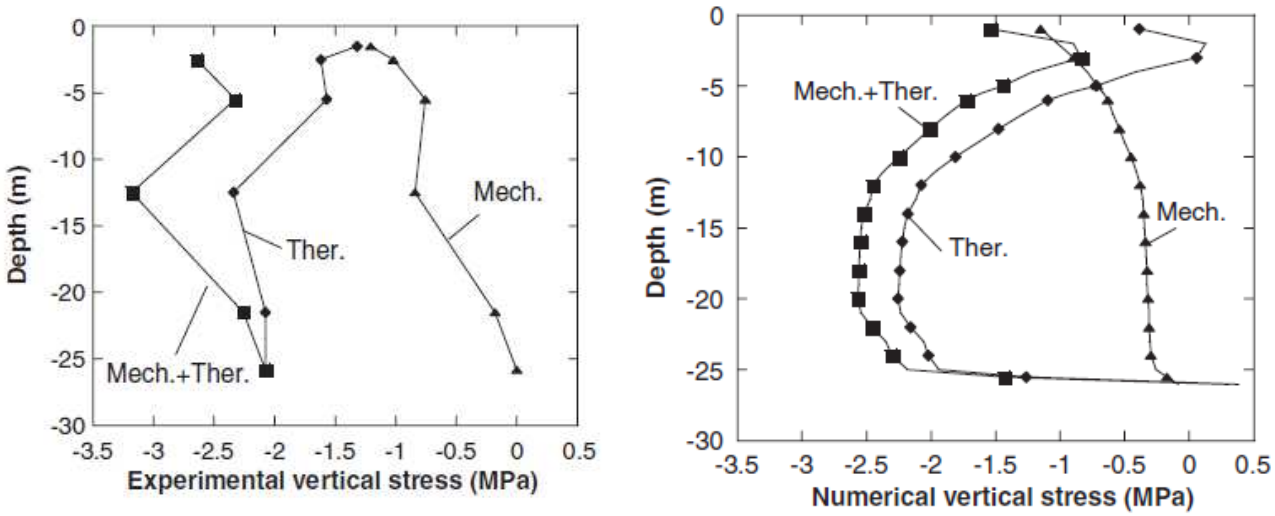

Figure 2.69 – Thermo – mechanical vertical stress in the pile: a) experimental results; and b) numerical simulations by Laloui.

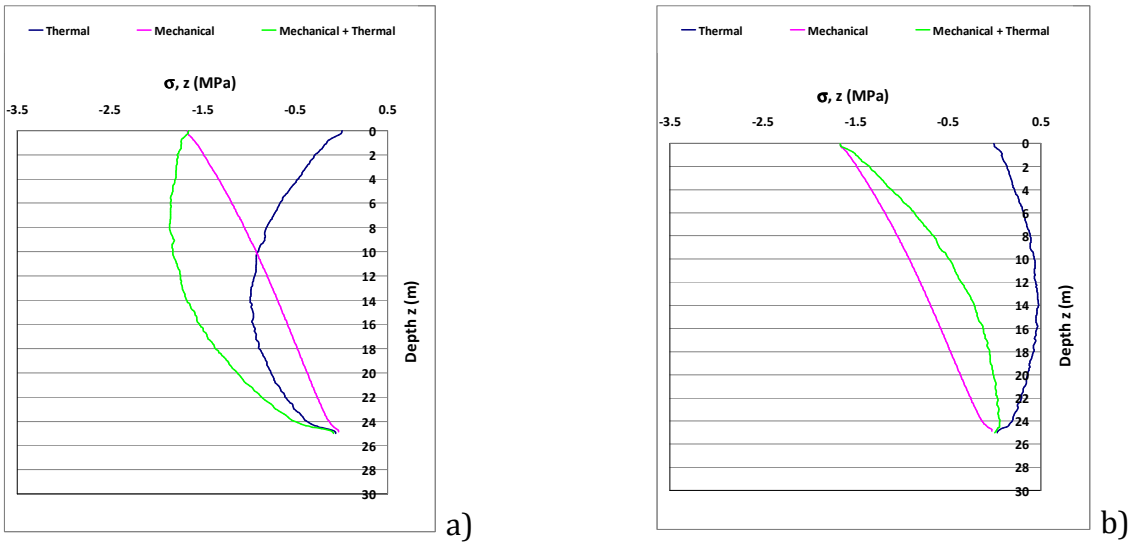

Figure 2.70 – Thermo – mechanical vertical stress in the pile: a) summer case; and b) winter case. Results by COMSOL Multiphysics.

A comparison between Figures 2.69 and 2.70 show that the trends obtained in the simulations (thermal, mechanical and thermo-mechanical) are essentially the same. In the graph obtained by Laloui, values tension are obtained slightly higher. Such diversity, is to be found in the following reasons: the model of Laloui, has as a boundary condition, an imposed temperature, (those obtained experimentally) while the model in analysis, imposes the thermal flux, obtaining as a result, slightly different temperature distributions final. Furthermore, this model simulates a transitory model of the total duration of 28 days, in which a heating phase and a cooling phase are put as solicitation, while in the present model the conditions are stationary, having moreover a different soil stratigraphy.

2.4.4 Comparison between vertical ground heat exchangers with different configurations and operational fluids in mild climates

- Introduction

The Ground Source Heat Pumps (GSHP) present increasing interest and success despite relevant initial installation costs related to the overall size of the closed-loop heat exchangers. The design of heat exchangers is a fundamental part of the overall system design, since the perforation (defined as: drilling, installation of the vertical piping and filling with grout the perforation) is a large part of the overall cost of the system, hence a correct dimensioning is very important.

The overall length of the Ground Heat Exchanger (GHE) leads to the average difference between the temperature of the secondary fluid flowing in the pipes and the undisturbed ground temperature. In order to reduce the installation costs often antifreeze mixtures are used, according to a fairly common practice in the countries of Central and Northern Europe. In these regions the climate is quite cold and the outdoor temperatures are rather low, hence reaching minimum temperatures around 0°C in the GHE leads to better COP compared to Air Source Heat Pumps (ASHP).

In mild climates, like for instance the North of Italy, the outdoor temperatures are higher, therefore undersizing the GHE may lead to results in terms of COP close to the ones which can be obtained by means of ASHP. An interesting aspect in mild climates is the possible use of reversible heat pumps which can be used as chillers in summer period. This results in a possible restoration of the underground energy level and therefore a substantial balance between heat absorbed from the soil in winter and heat transferred to the soil in summer. Depending on the climate, on the level of insulation of the building and on the internal loads, there might be plants which present higher heat loads compared to cooling loads (dominant heating buildings), buildings which may present the same amount of heating and cooling loads (balanced cases), or buildings with a cooling demand which exceeds the heating demand

(dominant cooling cases). The first two cases in a mild climate represent typical residential building situations: in the dominant heating case the building is poorly insulated, while the balanced case is typical of a well insulated building. The dominant cooling case is typical of commercial buildings where the high internal gains and the good insulation leads to a cooling demand higher than the heating demand.

The problem of unbalanced thermal loads is already present in literature (Ramamoorthy et al., Cullin and Spitler, Chen and Yang). Usually, for reducing the installation costs of the GSHP plant, in winter time the heat pump is coupled with a boiler (Yang et al.) or with solar collectors for recharging the ground during summer time (Rad et al. , Wang et al.), avoiding the drift of temperatures in the soil. When cooling loads of the buildings are greater than heat loads alternative cooling sources (cooling towers or air to water chillers) are proposed, e.g. Kavanaugh, Yavuzturk and Spitler.

When dealing with dominant heating cases, it is quite common to use an antifreezing fluid which is mixed with water. Usually glycol is used as antifreeze fluid. The addition of glycol in the water has the advantage of lowering the freezing point to below zero, according to the percentage of antifreeze fluid. On the other hand, it has the disadvantage of reducing the thermal conductivity and of increasing the viscosity of the fluid with respect to pure water. Two antifreeze fluids are usually used: ethylene glycol and propylene glycol. The ethylene glycol is toxic and if it is released into the soil there might be pollution problems in particular in presence of aquifers in the ground. Moreover the ethylene glycol is corrosive, therefore, the plant solutions are complex and they may lead to a raising cost of the plant. Staples et al. have shown the effects and potential environmental risks of ethylene glycol. Lokke studied the leaching of ethylene glycol and ethanol in subsoils. Many other authors have investigated various types of anti-frost fluid, to give a wider overview and to estimate an anti-freezing fluid with less environmental risks, compared to ethylene glycol (Den Braven, Heinonen et al., Khan and Spitler, Klotzbucher et al.).

Propylene glycol is preferable, since it is non-toxic but more expensive and with worse thermal performance with respect to the ethylene glycol. The main problem anyway in using propylene glycol is the potential creation of galvanic corrosion, hence inhibitors are needed and usually added; this may lead to a potential environmental impact which cannot anyway be considered negligible (Heinonen et al. Khan and Spitler, Klotzbucher et al.).

One way to reduce the temperature difference between the evaporating refrigerant fluid and the vector fluid circulating in the GHE is the use of a flooded evaporator, which allows the fluid to evaporate at higher temperature compared to the case of classic dry evaporators. The benefits are related to the increase of COP as well as the possible use of pure water instead of anti-freezing mixture. Interesting studies have been conducted by Casciaro and Thome, Cotchin et al., Fernandez-Seara et al., Minetto and Fornasieri, Zheng et. al..

There are few works in literature looking at GSHP applications in mild climates and none of them looks at the energetic and economical benefits of using anti-freezing mixtures in the

system. For this reason the present paper shows a parametric study based on three different possible thermal loads of the building (balanced, dominant heating, dominant cooling), two possible distribution of the borehole field (L-shape or matrix) and two possible heat pump solutions: a flooded evaporator and a classic machine with dry evaporator. In the first case pure water is supposed to circulate in the BHE, while in the second case anti-freezing mixture has been considered as well. The study looks at the energy performance of the different proposed solutions, carrying out a cost-benefit analysis.

- Methods

In the present work two configurations of heat exchangers in the ground have been considered: a matrix (named M) field and an L-shape field (named L). In all simulations the double U-tube, fed in parallel, have been considered, with 100 m depth, and spacing between heat exchangers of 7 m.

Two types of fluid have been evaluated: water and water – ethylene glycol mixture to 25%. Table 2.7 shows the thermal properties of both fluids respectively at 5°C and 25°C, as representative temperatures close to operating conditions in the present study.

Two different heat pumps have been considered as well, one with normal evaporator and another with flooded evaporator. In the usual heat pump the evaporator outlet fluid is completely transformed into superheated steam, its temperature is slightly higher than strictly necessary to evaporation. In the flooded evaporator heat pump the refrigerant is not completely transformed into steam at the outlet of the evaporator, hence some liquid is still present.

The evaporation in the flooded system offers some advantages. Among them the most interesting, for geothermal applications, concerns the evaporation which requires lower temperature differences between the refrigerant and the secondary liquid than a conventional system, therefore the liquid evaporates at a higher temperature than in the case of a dry evaporator. The main advantage is the possibility to use pure water as secondary fluid in the ground loop, limiting environmental impact in case of secondary liquid dispersions.

Even if there is a benefit in terms of COP of the machine, this is limited, hence, in the model used in the present work, for the heat pump the same temperature difference between refrigerant fluid and secondary liquid has been assumed in the different evaporators, thus leading to a conservative hypothesis.

The analysis has been carried out maintaining the same thermal properties of the soil profile and varying only the heat load of the building. Table 2.8 shows the characteristics used for the probe and the ground in the present study. As might be seen, it was chosen to carry out simulations in a mild climate (15°C as undisturbed ground temperature), since in these weather conditions GSHP may have more chances to work over a longer period, i.e. they can be used for both heating and cooling the buildings.

The monthly energy loads and the monthly peak power are presented in Figures 2.71 and 2.72 respectively. The heating/cooling loads and peak power have been calculated by means of dynamic simulations by using TRNSYS. In the simulations the following periods have been considered:

heating season is from January to mid April and from mid October to the end of December (180 days in winter period)

cooling season is from the mid of May to the mid of September (125 days in the summer period)

no operation in the other periods of the year, i.e. from the mid of April to the mid of May and from the mid of September to the mid of October (60 days)

Three buildings have been examined. In the first case heating and cooling loads are balanced (76 MWh are required in winter, 62 MWh in summer). In the second case a dominant heating load (in winter 76 MWh are required, 31 MWh in summer), while in the third case a dominant cooling load (in winter 38 MWh are required, 62 MWh in summer) are considered respectively.

The arrangement of the probes is shown in Figures 2.73 (L-shape) and 2.74 (matrix). As well known, the L-shape field is more efficient than the matrix arrangement, as the heat exchange between the liquid inside the pipes and the undisturbed ground is enhanced due to the wider surface and limited interference between boreholes. Anyway, several times, due to space problems, a matrix arrangement is used in practice.

An overall view of the different cases simulated with the code CaRM is summarized in Table 2.9: as can be seen, simulations have been carried out by changing the heating/cooling demand of the building, the pattern of the borehole field, the type of evaporator of the heat pump and the secondary fluid used.

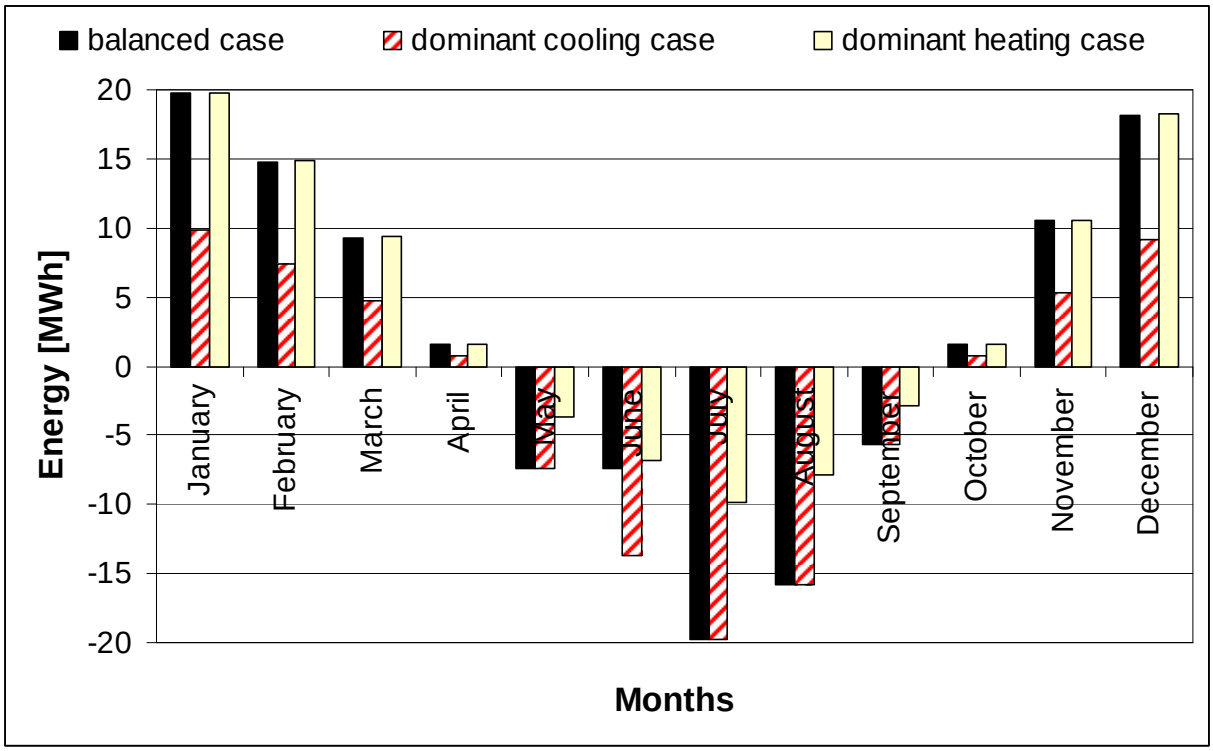

Figure 2.71 – Monthly energy of the building during the year (positive heating, negative cooling): balanced case , dominant cooling case, dominant heating case.

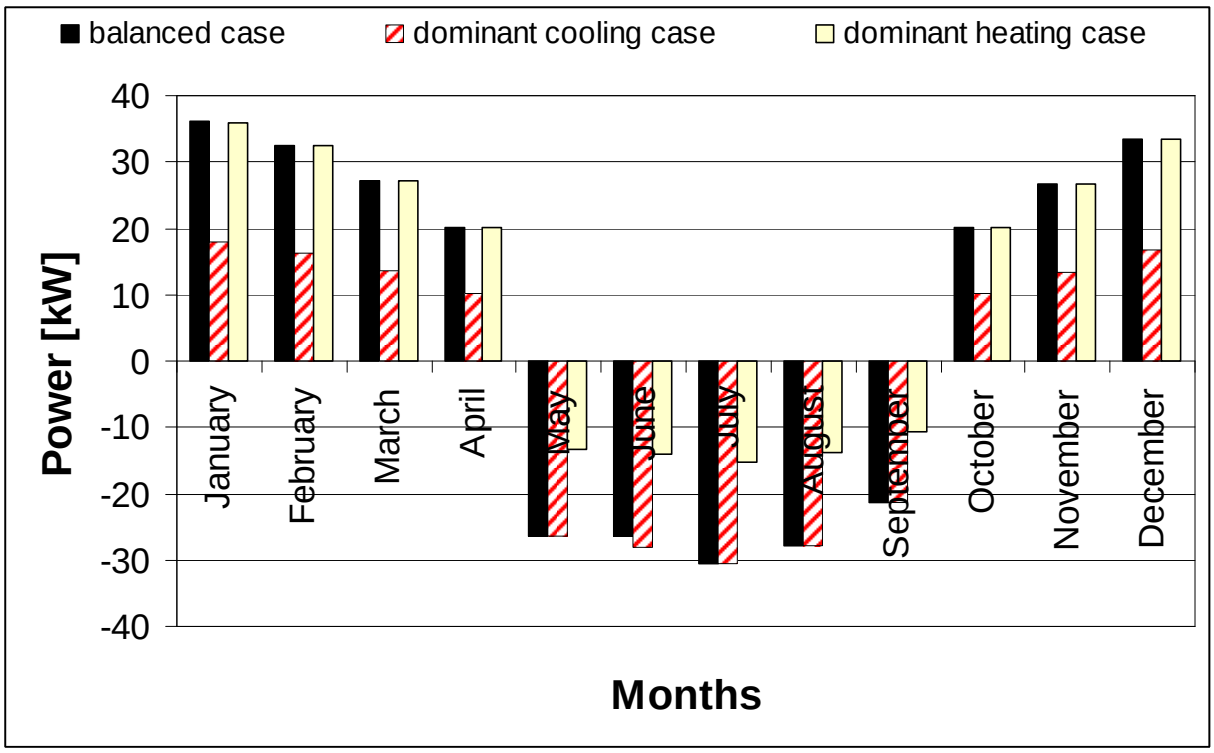

Figure 2.72 – Maximum monthly power of the building during the year (positive heating, negative cooling): balanced case , dominant cooling case, dominant heating case.

Table 2.7 - Thermal properties of the secondary heat carrier fluids: water and water-glycol mixture with temperature 5 °C – 25 °C

		Water		Water – Ethylene Glycol (25%)	
		5°C	25°C	5°C	25°C
Freezing Temperature	[°C]	0	0	-10.9	-10.9
Specific Heat	[J/(kg K)]	4207	4198	3733	3769
Thermal Conductivity	[W/(m K)]	0.57	0.60	0.49	0.50
Density	[kg/m^3]	1000	997	1044	1036
Dynamic Viscosity	[kg/(m s)]	0.0015	0.00087	0.0033	0.0018
Cinematic Viscosity	[m^2/s]	0.0000015	0.00000087	0.0000032	0.0000016

Table 2.8 - Geothermal properties of the probe and ground

TUBE		**Description**
Type		Double U-tube
Material		PEAD
Thermal Conductivity	[W/(m K)]	0.4
Outer diameter	[mm]	32
Internal diameter	[mm]	26
Configuration		Parallel
FILLING MATERIAL		
Thermal Conductivity	[W/(m K)]	1.6
Grout Diameter	[mm]	140
GROUND		
Equivalent thermal conductivity	[W/(m K)]	1.5
Specific heat	[J/(kg K)]	2614
Density	[kg/m^3]	1285
Undisturbed soil temperature	[°C]	15.0

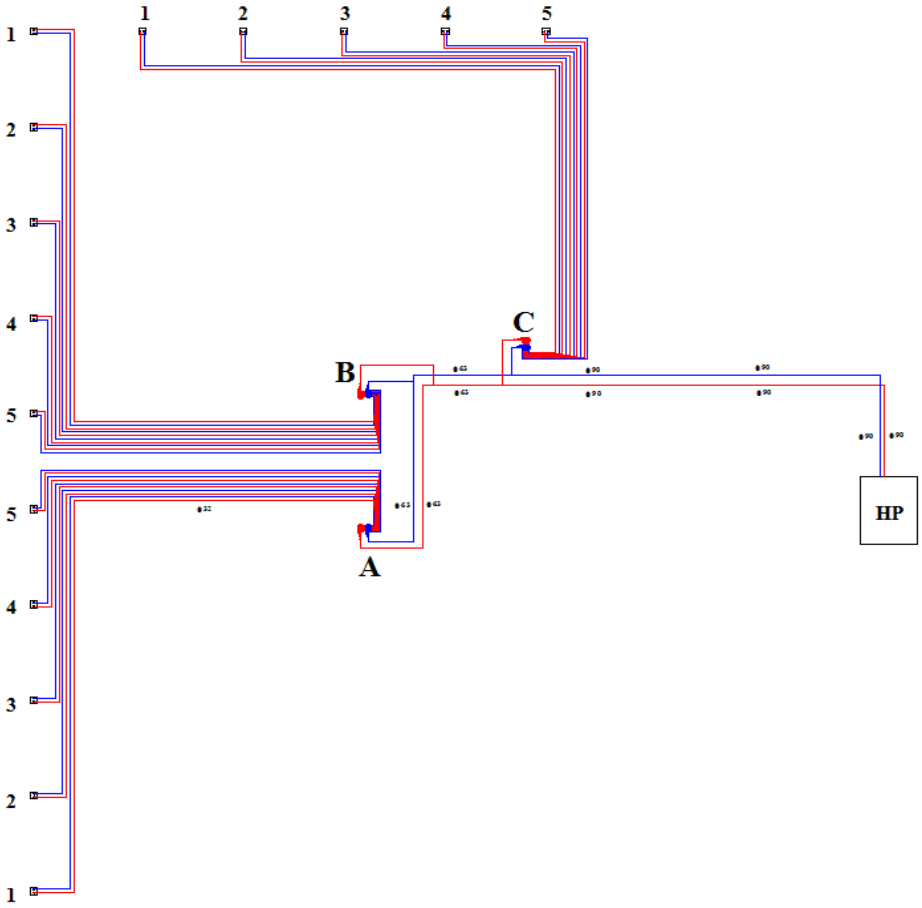

Figure 2.73 - Example of distribution of probes to form an L–shape field (named L)

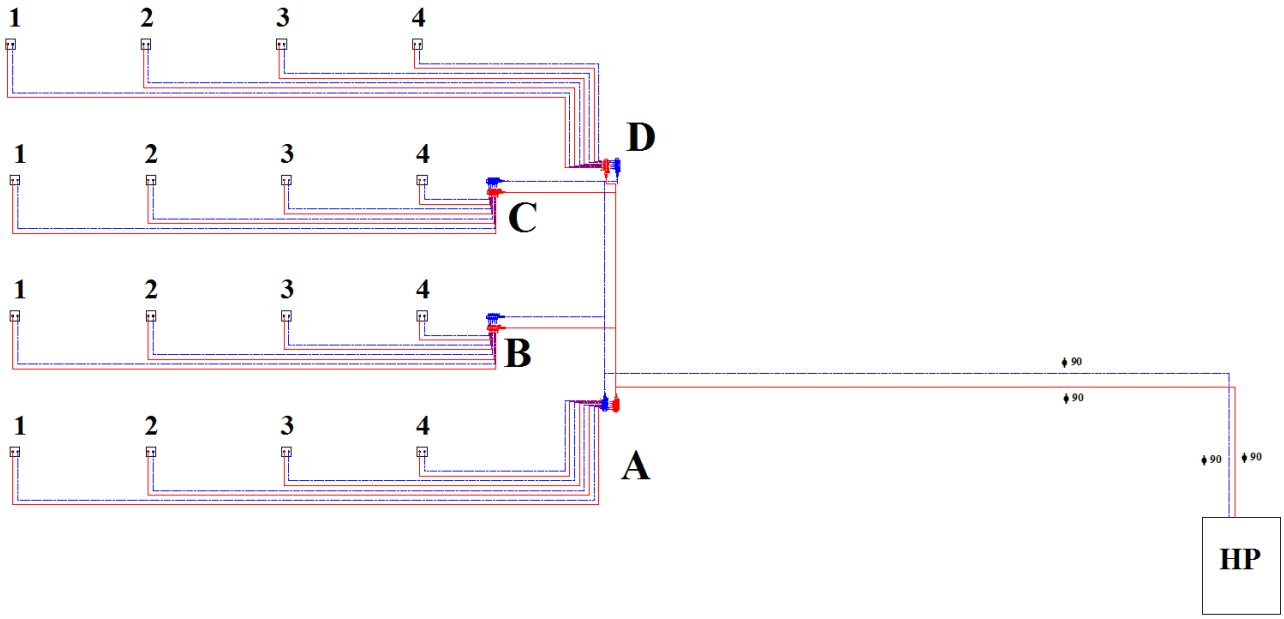

Figure 2.74 - Example of distribution of probes in a matrix arrangement (named M)

- Results

As can be seen in Table 2.9 simulations lead to different values of the amount of boreholes in the ground. These values have been estimated by trying to maintain almost the same conditions in the different cases.

As for the dominant heating load and the balanced load cases, the following conditions have been used as target of the simulations:

in the case of a heat pump with dry evaporator and pure water as a fluid, the minimum allowed temperature (reached in winter) is equal to 5° C;

in the case of a heat pump with dry evaporator and mixture of water-ethylene glycol as secondary fluid, the minimum temperature (reached in winter) is equal to 0°C;

in the case of a heat pump with flooded evaporator and pure water as a fluid, the minimum temperature is set equal to 3° C.

In the case of pure water in the ground loop the minimum allowed temperature has been set for avoiding freezing in the evaporator, while in the case of water – glycol mixture, the minimum temperature has been set in order to achieve an average acceptable COP of the heat pump during the heating season.

As for the dominant cooling load cases, the following conditions have been used as target of the simulations:

in the case of a heat pump with dry evaporator and pure water as a fluid, the maximum allowed temperature (reached in summer) is equal to about 35° C;

in the case of a heat pump with dry evaporator and mixture of water-ethylene glycol as secondary fluid, the maximum temperature (reached in summer) is equal to about 40°C;

in the case of a heat pump with flooded evaporator and pure water as a fluid, the maximum temperature is set equal to 33° C.

In this case the temperatures were considered as a compromise between installation costs and an average acceptable efficiency in the cooling period.

- Energy analysis

The results of the balanced load cases are summarized in Table 2.10 for both the L-shape and the matrix arrangement GHE fields. The temperature is reported in terms of the average value between supply and return temperatures of the fluid in the GHE. Results show the minimum yearly temperature (T_{min}), the maximum yearly temperature (T_{max}) and the seasonal mean temperature ($T_{average}$). As for the energy performance of the reversible heat pumps, the

average seasonal COP and EER of the machine (not including the auxiliary pump for the ground loop) are reported. In the same table the electrical energies used by the heat pump for heating and cooling the building and used by the auxiliary pump are shown as well. Finally the overall electrical consumption (including electricity used for heating, cooling and pumping) is summarized for each case.

The same results for the heating dominant case are resumed in Table 2.11, while in the case of cooling dominant case results are shown in Table 2.12.

As can be seen, in general, when the overall length of the GHE field is reduced for saving investing costs, the energy performance of the heat pump lowers. Due to the lack of knowledge in the frame of GSHP designers very often undersize GHE fields and, for preventing possible freezing problems, glycol is added to water in the secondary fluid loop, even if the building requires more cooling than heating energy demand; in these cases the problem is related to the overheating of the ground rather than to the undercooling in a long term view. As might be seen, in a mild climate a proper sizing of the GHE field allows to work with water without any additional anti-freezing fluid.

Another interesting result regards the average temperatures of the secondary fluid in the ground depending on building loads and on geometry of the GHE field. Looking at the balanced case and the heating dominant case, in winter period the average temperatures are almost the same: when using water as fluid, 10°C for the dry evaporating heat pump and 9°C for the wet evaporating heat pump, while when using water-glycol mixture the winter average temperature is around 9°C (in this latest case temperatures may vary between 8°C to 10°C). When considering the balanced case and the cooling dominant case, in summer period the average temperatures are almost the same: when using water as fluid, 24°C for the dry evaporating heat pump and 24°C for the wet evaporating heat pump, while when using water-glycol mixture the average temperature of the fluid in the GHE is around 27°C.

In Figures 2.75, 2.76 and 2.77 the average seasonal values of the COP (SCOP) and EER (SEER) in the three cases (balanced thermal loads, dominant heating, dominant cooling) are reported. The SCOP and SEER are shown considering only the heat pump operation and considering the system as a whole (including both the heat pump and the circulation pump of the secondary fluid). The lowest values of SCOP and SEER (equal to approximately 3 by analyzing the whole system) occur in the case of water-glycol mixture.

Table 2.9 - summary table of the various types of geothermal plants divided according to the thermal loads: balanced, dominant heating and dominant cooling.

	Dominant energy building			Pattern of the borehole field		Type of heat pump			Number of boreholes
	Balanced	Heat	Cool	L	Matrix	Dry evaporator		Flooded evaporator	
PLANTS	B	H	C	L	M	Water (W)	Glycol (G)	F	N°
BL_W_15	X			X		X			15
BL_G_11	X			X			X		11
BL_F_13	X			X				X	13
BM_W_16	X				X	X			16
BM_G_12	X				X		X		12
BM_F_15	X				X			X	15
HL_W_18		X		X		X			18
HL_G_12		X		X			X		12
HL_F_15		X		X				X	15
HM_W_20		X			X	X			20
HM_G_12		X			X		X		12
HM_F_16		X			X			X	16
CL_W_14			X	X		X			14
CL_G_12			X	X			X		12
CL_F_15			X	X				X	15
CM_W_15			X		X	X			15
CM_G_12			X		X		X		12
CM_F_16			X		X			X	16

Table 2.10 - Energy results in the case of the simulations in the balanced case

	BL_W_15		**BL_G_11**		**BL_F_13**		**BM_W_16**		**BM_G_12**		**BM_F_15**	
	W	**S**	**W**	**S**	**W**	**S**	**W**	**S**	**W**	**S**	**W**	**S**
T_{min} [°C]	5.0		0.0		3.0		5.0		0.0		3.2	
T_{max} [°C]		33.0		43.0		35.0		32.0		40.0		33.0
$T_{average}$ [°C]	10.2	23.2	9.0	27.2	9.4	24.4	10.8	22.9	10.1	26.7	10.3	23.2
COP	3.97		3.57		4.11		4.10		3.06		4.34	
EER		4.73		3.13		4.88		4.95		3.43		5.39
Heat pump [kWhe]	19107	13181	21248	19918	18456	12776	18638	12595	20782	18176	17478	11567
Pump [kWhe]	1659	1086	796	786	1211	831	1645	1056	849	837	1390	940
Total [kWhe]	35033		42748		33274		33934		40645		31375	

Table 2.11 - Energy results in the case of the simulations in the heating dominant case

	HL_W_18		**HL_G_12**		**HL_F_15**		**HM_W_20**		**HM_G_12**		**HM_F_16**	
	W	**S**	**W**	**S**	**W**	**S**	**W**	**S**	**W**	**S**	**W**	**S**
T_{min} [°C]	5.0		0.0		3.0		5.0		0.0		3.0	
T_{max} [°C]		22.0		27.0		23.0		21.0		26.5		23.0
$T_{average}$ [°C]	10.2	17.7	8.2	19.4	9.2	18.2	10.1	16.8	7.7	18.9	8.9	17.3
COP	4.07		3.63		4.27		4.11		3.62		4.34	
EER		6.19		4.04		6.32		6.66		4.12		6.67
Heat pump [kWhe]	2032	1342	920	893	1578	1126	2184	1441	908	887	1528	1065
Pump [kWhe]	18652	5040	20884	7717	17778	4935	18444	4679	20954	7566	17488	4672
Total [kWhe]	27065		30413		25417		26748		30315		24754	

Table 2.12 - Energy results in the case of the simulations in the cooling dominant case

	CL_W_14		**CL_G_12**		**CL_F_15**		**CM_W_15**		**CM_G_12**		**CM_F_16**	
	W	**S**	**W**	**S**	**W**	**S**	**W**	**S**	**W**	**S**	**W**	**S**
T_{min} [°C]	9.0		8.0		9.0		11.0		8.0		9.5	
T_{max} [°C]		35.5		40.0		33.7		35.0		40.5		33.0
$T_{average}$ [°C]	13.4	24.7	13.4	26.8	13.4	23.7	14.5	25.0	14.7	28.2	14.4	24.1
COP	4.10		3.83		4.51		4.18		3.88		4.12	
EER		4.28		3.26		5.14		4.33		3.15		3.87
Heat pump [kWhe]	1510	975	855	839	1519	1074	1622	1057	892	875	1592	1123
Pump [kWhe]	9251	14567	9903	19124	8410	12129	9074	14398	9775	19792	9206	16110
Total [kWhe]	26302		30721		23133		26151		31334		28031	

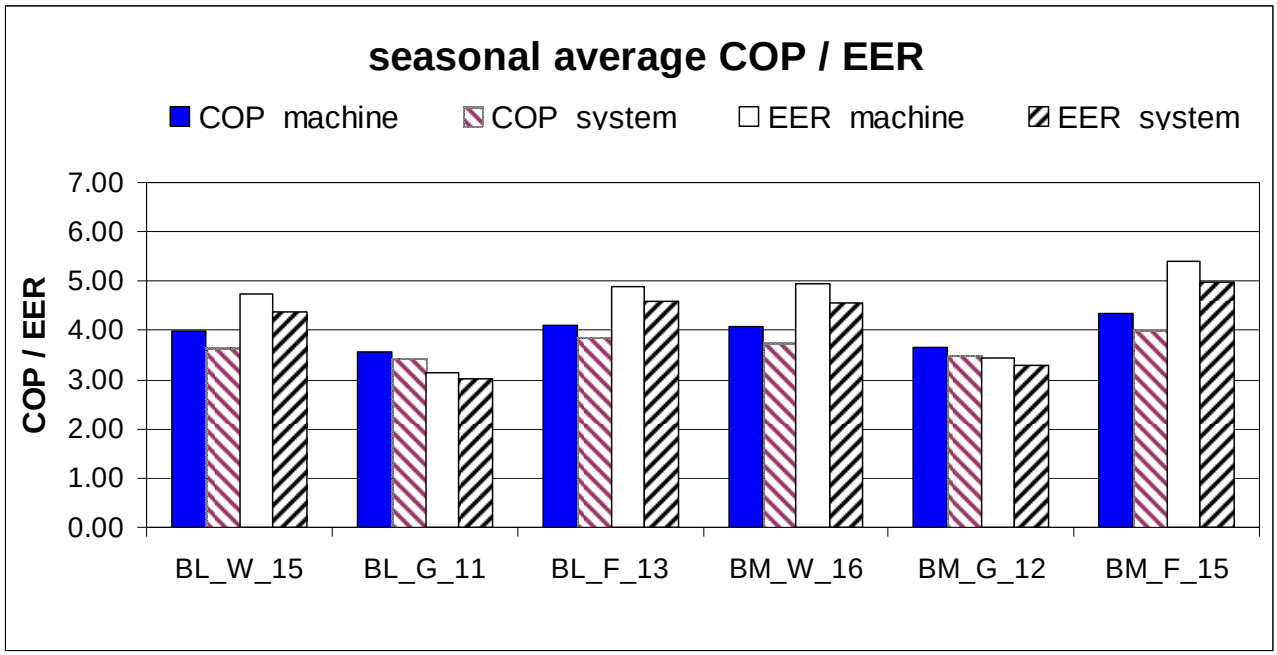

Figure 2.75 – Seasonal average COP and EER in the case of balanced thermal loads

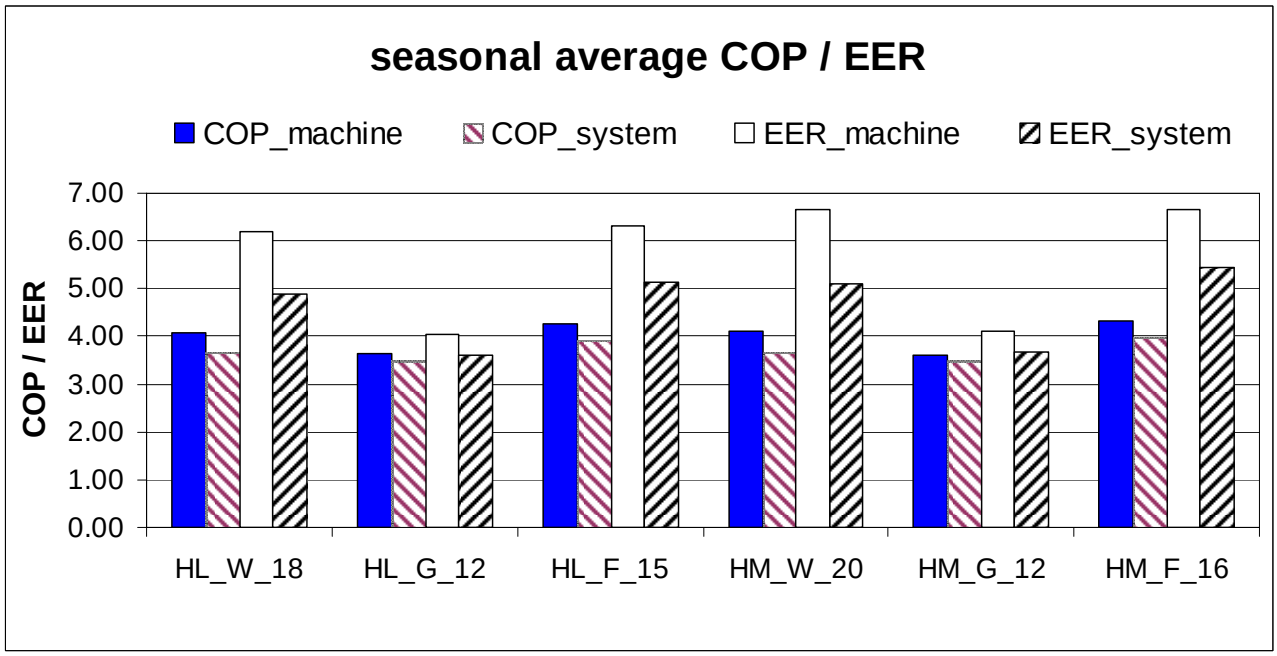

Figure 2.76 - Seasonal average COP and EER in the case of heating dominant thermal loads

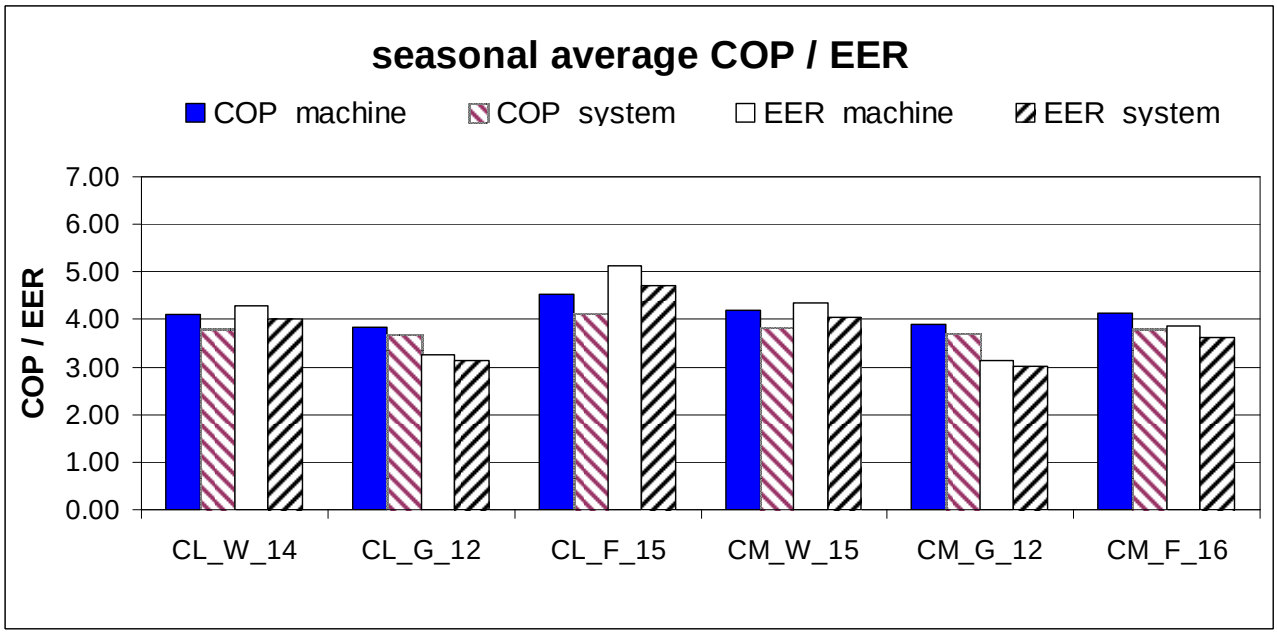

Figure 2.77 - Seasonal average COP and EER in the case of cooling dominant thermal loads

- Economic analysis

The costs have been determined for all the cases, depending on the type of plant. As for installation costs, 45 €/m were considered for the build up of the vertical heat exchanger (drilling, double U pipe, ballast, installation, filling). In the installation costs the cost of the heat pump and the circulation pump have been included in the analysis. In the case of ethylene glycol, an additional cost of 6 €/kg has been counted. The costs take into account also the horizontal part of the material, excavation, laying and backfilling. As for the costs of operation, a rate of 0.165€/kWhe (average cost in Italy) was considered.

Figures 2.78, 2.79, 2.80 summarize the results of the overall costs of the plant (left y-axis), as well as the electrical operating costs (right y-axis), including pumping of the secondary fluid.

As for maintenance costs, 120 € for all systems was assumed. In the case of glycol mixture an additional cost of 4000 € every ten years should be added in order to consider maintenance costs; for conservative reasons anyway this cost has not been considered in the present work.

Looking at installation costs, it can be seen that the costs of installation of an L-shape field is lower than a GHE field with a matrix shape, due to the perforation costs. As can be seen, the choice of the carrier fluid leads to different overall dimensions of the GHE. The most expensive solution is the one using water as secondary fluid and a heat pump with dry evaporator. Glycol can reduce the number of probes, as it allows during winter time to work at temperatures close to 0 ° C, which would not be possible with water and a conventional heat pump. A promising technique for limiting costs is a heat pump with flooded evaporator

which may reduce the number of probes with respect to a conventional heat pump using only water as secondary fluid.

In terms of specific costs (defined as the ratio between the overall installation cost and the maximum heating/cooling power of the machine) in the present study the following vaules have been found:

in the case of balanced heating and cooling energy demands costs vary from 2.1 €/W for the case BL_F_13 to 2.5 €/W for the case BL_G_11;

in the case of dominant heating the costs range from 1.9 €/W for the case HL_F_15 to 2.3 €/W for the case HM_W_20;

in the case of dominant cooling costs vary from 1.8 €/W for the case CL_F_15 to 2.1 €/W for the case CM_G_12.

Calculating the total cost, given by the sum of installation costs and operating costs (electricity and maintenance costs), assuming an inflation rate of 1.5% for a period of 20 years, the different types of systems can be compared, thus assessing the convenience of the investment. The results can be seen in the case of balanced loads in Figures 13 and 14 for L-shape and matrix GHE fields respectively. The results in the case of dominant heating thermal loads are shown in Figures 15 and 16 for L-shape and matrix GHE fields. The results in the case of dominant cooling loads are shown in Figures 17 and 18 for L-shape and matrix GHE fields respectively.

In almost all cases the maximum installation cost occurs when using the water as secondary fluid in a dry evaporating heat pump. The minimum costs are usually related to the case of glycol mixture.

It has to be underlined that the glycol mixture in the case of cooling dominant thermal loads is not necessary, since the most critical aspect is related to summer conditions. In spite of this, for undersized GHE fields glycol is added to water for safety reasons, due to the lack of knowledge on GSHP systems. The economical analysis is anyway not affected by this aspect, i.e. in the case of dominant cooling thermal loads almost the same results could be achieved considering pure water instead of glycol-water mixture.

As for operating costs, usually the cheapest solution is the one with flooded evaporator, since the COP/EER are higher compared to dry evaporator. The use of pure water in a dry evaporating heat pump leads to intermediate costs, while the undersized GHE field with water-glycol mixture represents the solution with the highest operating costs.

When examining the overall costs (Figures form 2.81 to 2.86), despite the undersized system is the cheapest one at the beginning, the flooded evaporator leads to the minimum costs at the end of 20 years. Only when dealing with a heating dominant case the use of dry evaporating heat pump with water is not convenient compared to the use of the mixture water-glycol.

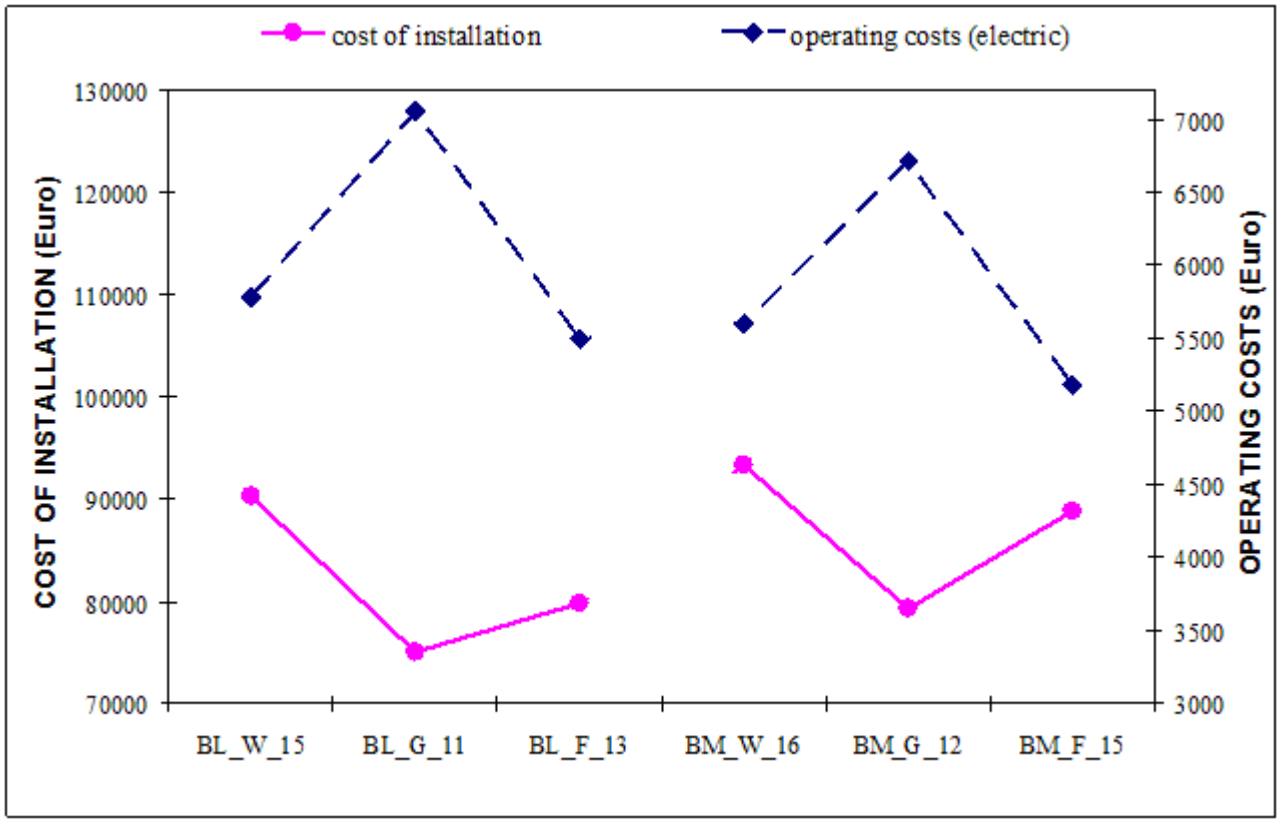

Figure 2.78 - Installation and operating costs for the various systems in the case of balanced thermal loads

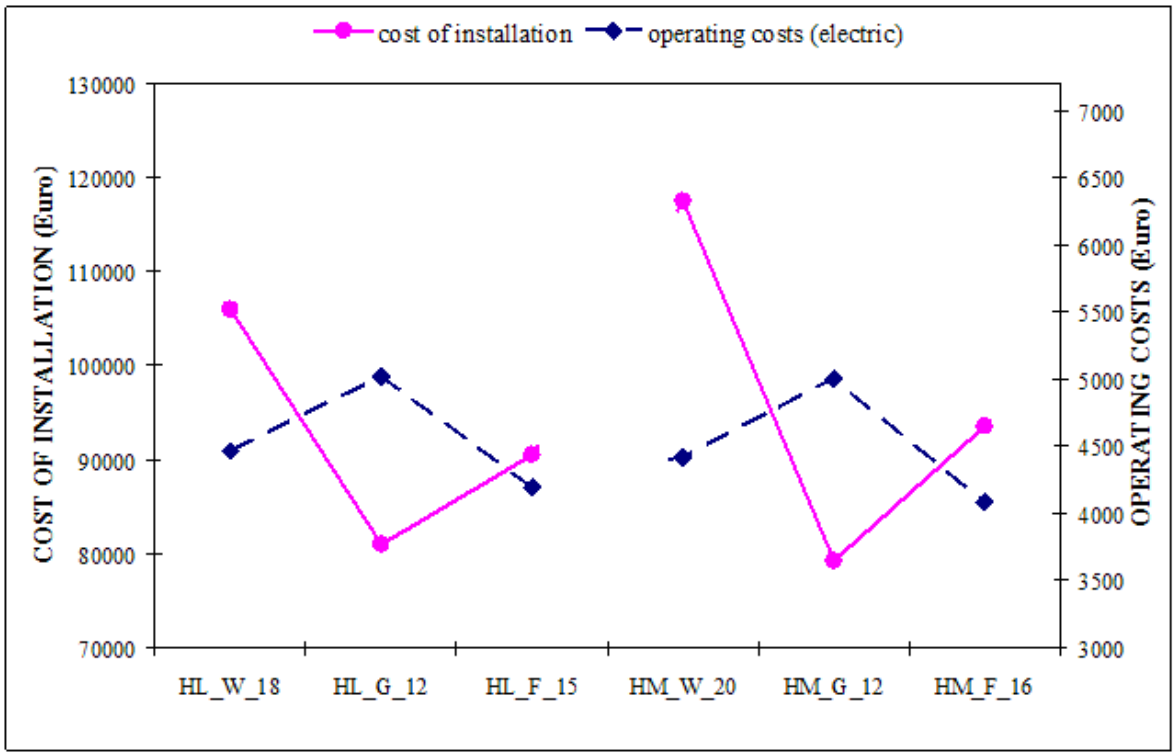

Figure 2.79 - Installation and operating costs for the different systems in the case of dominant heating thermal loads

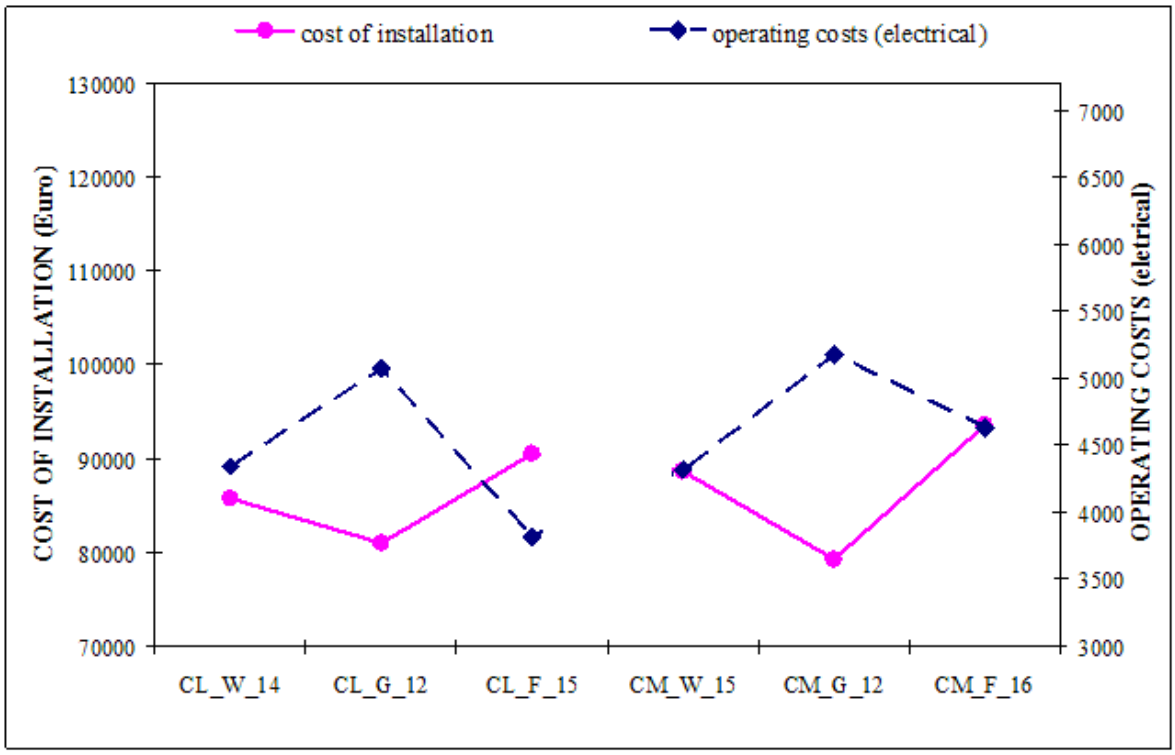

Figure 2.80 - Installation and operating costs for the different systems in the case of dominant cooling thermal loads

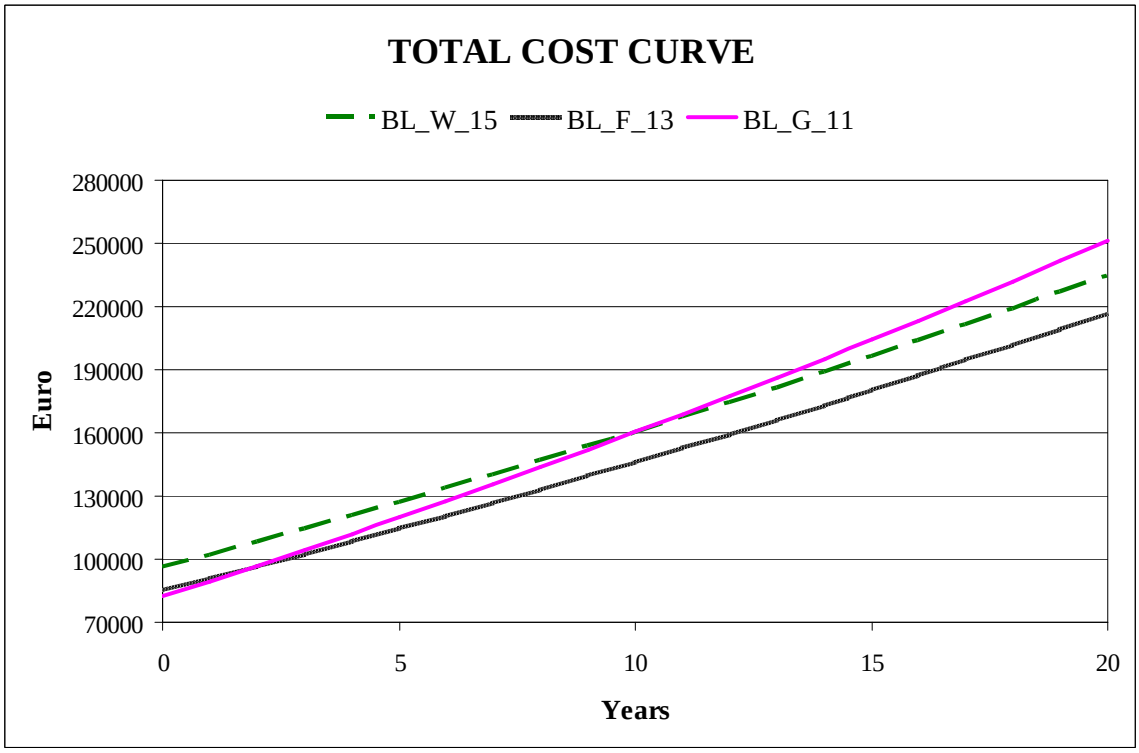

Figure 2.81 - Total cost curves in the case of L-shape GHE field for balanced thermal loads

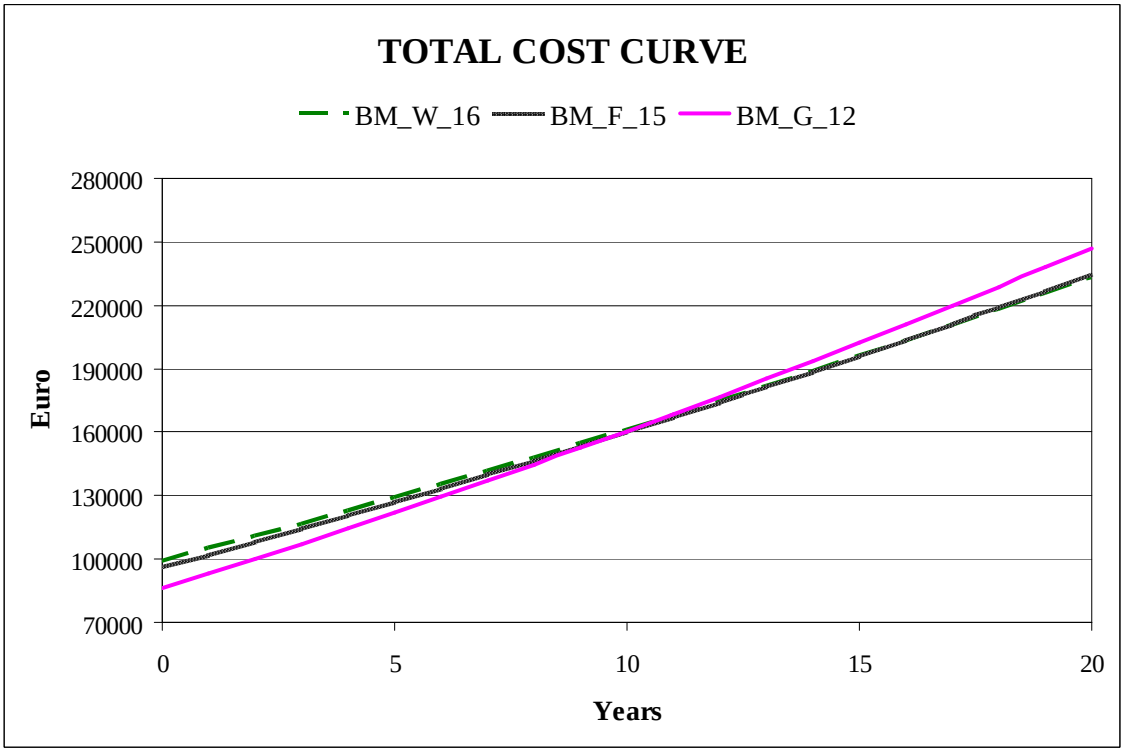

Figure 2.82 - Total cost curves in the case of matrix GHE field for balanced thermal loads

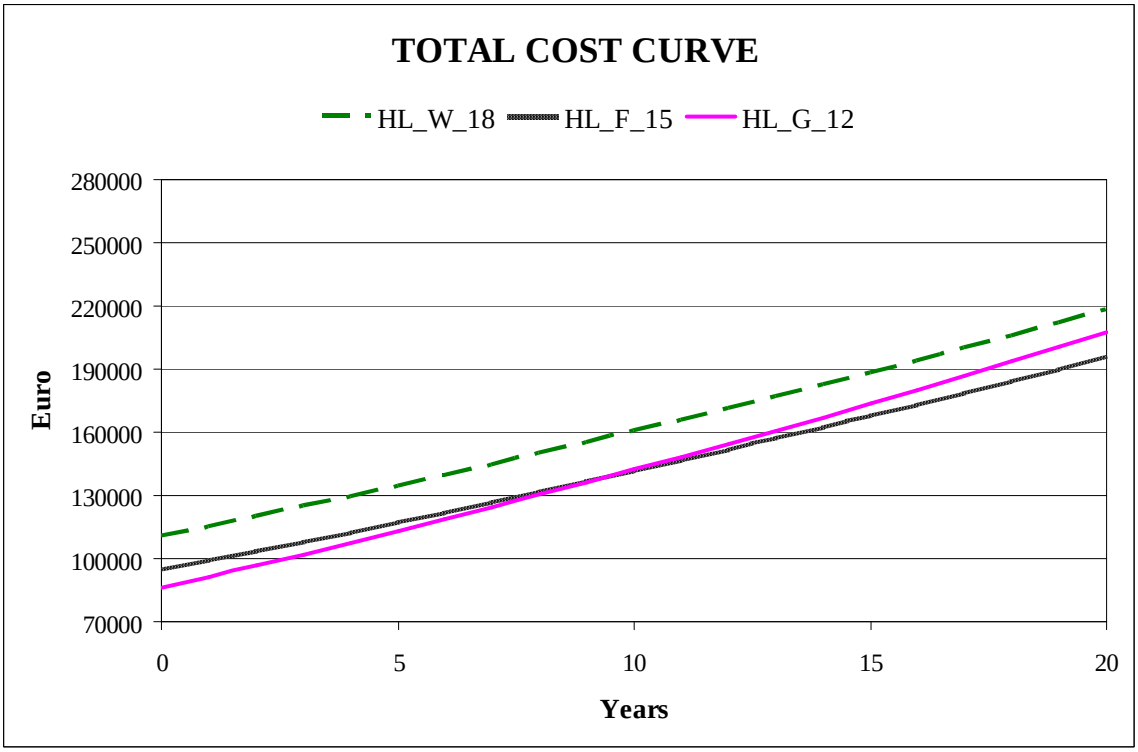

Figure 2.83 - Total cost curve in the case of field probes placed at L: thermal loads Heating dominant case

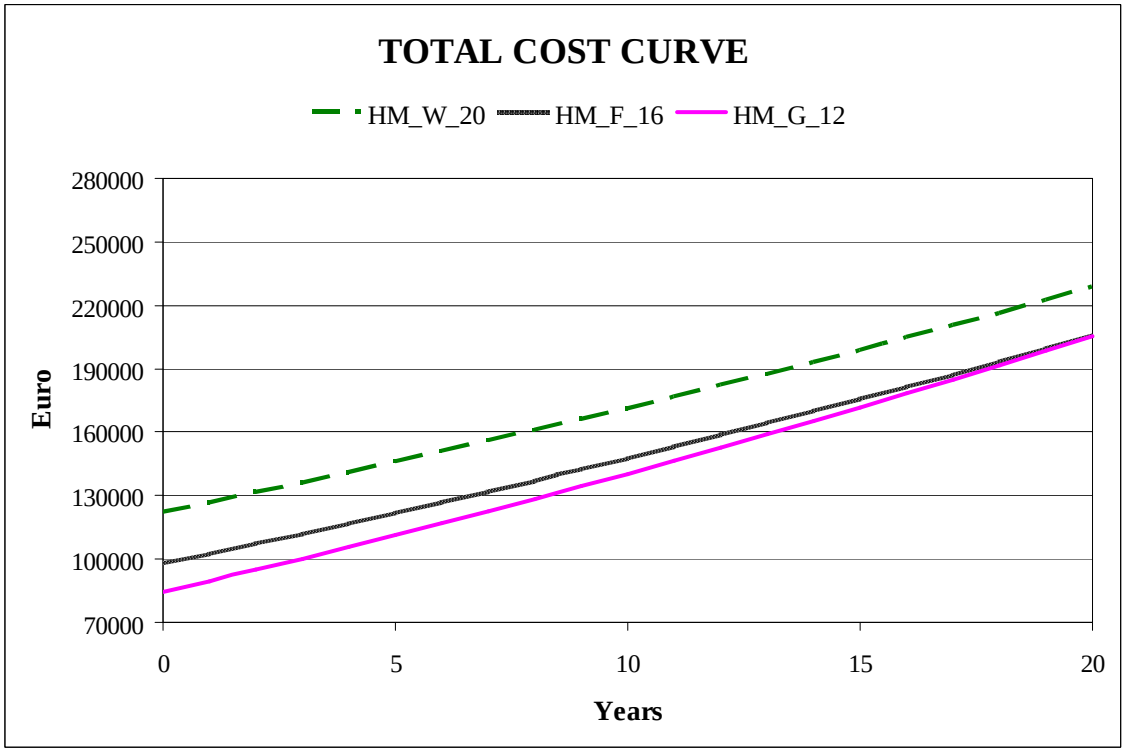

Figure 2.84 - Total cost curve in the case of field probes placed at M: thermal loads Heating dominant case

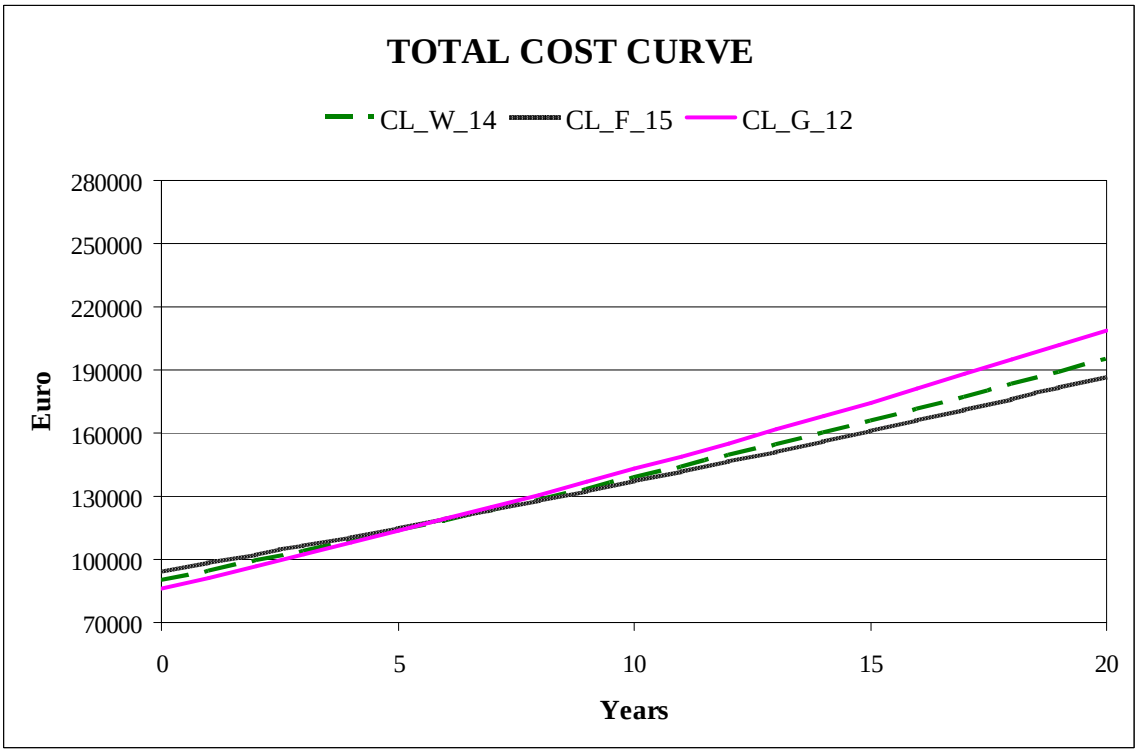

Figure 2.85 - Total cost curve in the case of field probes placed at L: thermal loads Cooling dominant case

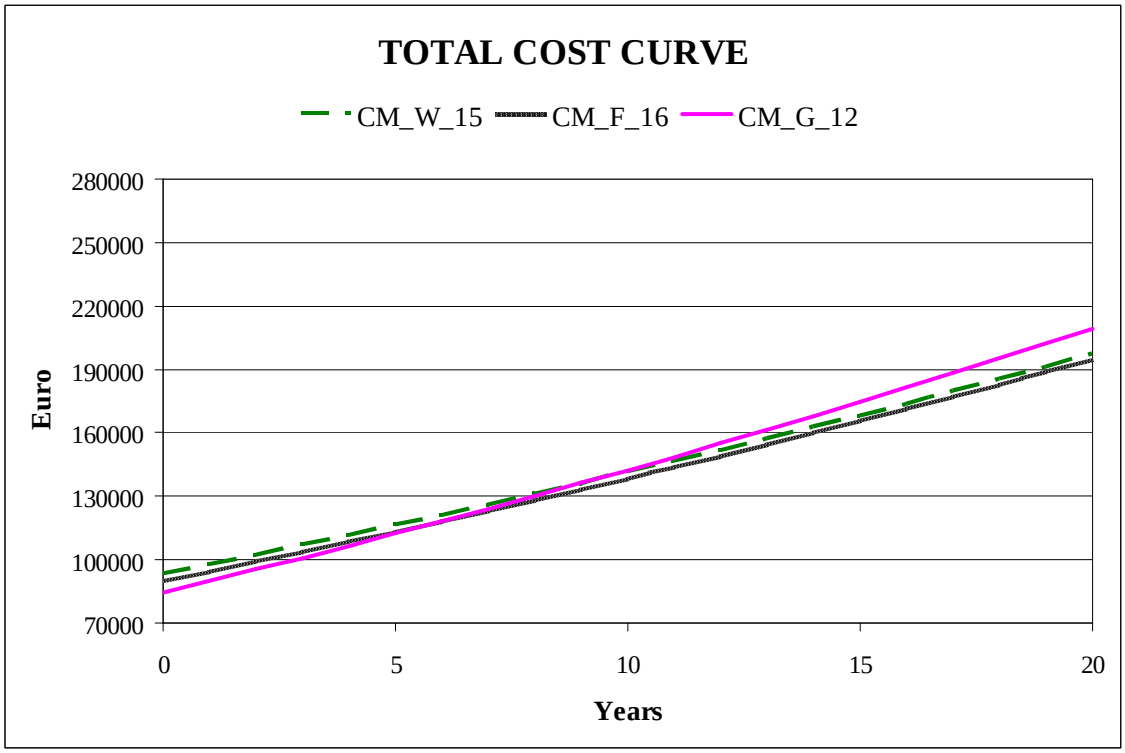

Figure 2.86 - Total cost curve in the case of field probes placed at M: thermal loads Cooling dominant case

2.5 Conclusion

In this part of the Ph.D. thesis describe the research topics that have been addressed on low temperature geothermal energy, with particular attention to the study of the problems of heat exchange between the heat exchanger and the ground, describing the various types of choice that can do, side ground, especially geothermal probes and energy piles.

Studies have focused on simulations of the test (GRT Ground Response Test), modelled in FEM finite element software, COMSOL Multiphysics, both in the case of geothermal probe, which in the case of pile energy. An analysis of the thermal field between pile energy and soil was made, varying the heat flux in the pole, and by varying the same flow with a sinusoidal function of time, both in the case of a single pole that in the case of pole placed in a palificata (where the boundary conditions are posed adiabatic). Furthermore, the model were added movements of groundwater by varying the velocity of the same, the object of study, in the case of choice of the heat exchanger as the pile energy, the focus has shifted to the study of the interaction thermal - structural, finally an energy analysis and a cost analysis was made for a plant with field probes arranged in L, and a plant with field probes arranged in a matrix. In this part of work, we have varied both the heat pump systems: conventional and flooded evaporator, varying the heat transfer fluid to the probes: only with water, and mixture: water - ethylene glycol 25%, and varying the type of climate in which it is placed in the building: load-balanced summer and winter load dominant in winter, and dominant in summer, in order to compare the total costs of the various systems was presented.

Two simulation models of the Ground Response Test (GRT) have been made, both for geothermal probe for both pile energy in FEM software, in order to assess the reliability of the energy piles. It has emerged as after seven days of operation the pile had not yet reached, and even approached, the equilibrium condition. After analyzing the results, it was shown that the thermal conductivity of the ground made the geothermal response test was essentially different from that imposed as input in the program. Compiling results, it was obtained a value of apparent conductivity λ_{eq} equal to 2.33 W / (m K) with respect to the input value, equal to 1.28 W / (m K). It can be deduced, that the thermal inertia of the pile tends to distort the result of the test, while in the case of the geothermal probe, for which it has been performed the same simulation, the result is much more reliable; obtaining, in fact, a relative error equal 3%, comparing the conductivity imposed and that obtained by processing the results. Then becomes advisable, in order to calculate the value of equivalent thermal conductivity, perform a test GRT exclusively on a vertical geothermal probe, in order to know the design data of the thermal characteristics of the soil, and then the design of those geothermal plant on piles energy.

The thermal analyzes carried out, show the temperature range, which is established in the soil surrounding the foundation pile, the distribution of which varies according to the influence of the motion of groundwater. The motion of the ground water, is a beneficial factor, so that the temperature field induced by the operation of the pile energy remains within certain levels, ie does not tend to too high temperatures (higher than 40 ° C) in summer, or at too low temperatures in winter (below 0 ° C), which may involve the risk of overheating / freezing of the soil, and of the structure.

The most direct consequence of the effect of the motion of flap, is that the foundation is able to exchange a greater heat flow with the ground. Furthermore, being a pole energy, then of a structure with mass relevant, the motion of the fluid allows to prevent the pile from overheating excessively, limiting the effect of storage of thermal energy inside. It is also seen as the effect of groundwater is commendable for soils of sandy type, while for cohesive soils of clayey the low permeability does not allow to be affected by this effect.

Analyses carried out in the transitional regime has also been possible to reach to compare the different behaviour of the single pole energy, compared to a energy pile inserted into a piling. In the latter case it is necessary to make further analysis, since the field of temperature tends to be higher, due to the interaction between the different exchangers present. Will then need, use caution and carefully consider the minimum distance between the various energy piles, provided that it is consistent with that caused by static considerations.

From the models, it also emerged as the software used is suitable for a modelling of thermal problems regarding a porous medium such as soil, in which the heat diffusion, through the various phases present is not easily solved.

As regards, the possible interactions thermo-structural, due to the limited installations performed, and studied to date, the thermo-mechanical modelling is limited to that consolidated, consisting of multi-physical models coupled, that solve the equations of motion, the elastic solid and of the thermal field. Particular models are also able to consider the equations of soil mechanics, in order to know the stress and strain of the same, but there have not been considered. This work aims to evaluate the modelling capabilities offered by the program COMSOL Multiphysics. From a comparison between the results obtained from the solution of the model with the analytical solution, as well as with different results found in the literature, it can be seen, they approach with good approximation to the latter.

it is possible therefore, use of finite element modelling to simulate the behaviour of these foundations under the action of mechanical loads and loads of thermal nature. has emerged, as there is a risk of formation of states of traction due to excessive cooling of the pile in winter, and also as it is necessary to keep under control the level of compressive stresses, following the increase in temperature resulting from the operation, in case summer of the system. In particular, from the results obtained in the two limiting cases analyzed (thermal load with T = 0 ° C, thermal load + static load) was observed, as pole exhaust are reached, tensions of 0.6 MPa of traction, while in the presence of the load static tensile stresses are minor and stood on a maximum value of about 0.15 MPa. As regards the case in summer, in the light of the structure of the order of the temperatures reached 32 ° C, there is an increase of the stress state compared to the case purely static. It follows, that the results of these analyzes are needed, to perform a more accurate design of the armature to be used in the pile.

Finally, In this work three different types of GSHP systems were compared : a conventional heat pump with water as secondary fluid in the GHE, a heat pump with water-glycol mixture and a machine with flooded evaporator and with water as vector fluid in the ground loop. Two different configurations of the geothermal field (L-shape and matrix) were also considered. The systems were combined with three types of building loads in a mild climate calculated via TRNSYS: a balanced case (energy need for heating is equal to energy need for cooling), a

dominant heating energy need, a dominant cooling energy need. The overall simulated cases were hence 18, which were analysed by means of the software CaRM.

Results were compared in terms of energy efficiency as well as from the economical point of view, considering both initial and running costs.

In all cases the lowest initial costs were related to the water-glycol mixture, while on the other hand such ystem is usally less efficient: considering the seasonal performance of the heat pump together with the circulating pump in the ground loop, the SCOP/SEER is usually 1 to 2 points lower compared to the corresponding cases using pure water as secondary fluid. This has an impact on the running costs, hence, considering a period of 20 years in the cases of balanced energy needs in heating and cooling seasons and in the dominant cooling cases the conventional heat pump with water has a pay back time of around 10 years compared to the water-glycol mixture. Only in the dominant heating cases the costs are lower in the case of water-glycol mixture with respect to the conventional heat pump with pure water. The use in future of heat pumps with flooded evaporators will lead to lower costs in all cases, avoiding therefore the use of anti freezing mixtures, which have been demonstrated that they can potentially impact the underground environment.

As for the temperatures in the GHE field, the mean value between supply and return temperatures presents an average seasonal value of about 9°C in the case of water- glycol mixture and in the case of flooded evaporator, while ,if pure water is used in a dry evaporator, the mean value is 10°C.

When considering the balanced case and the cooling dominant case, in summer period the average temperatures are almost the same as well: when using water as fluid, 24°C for the dry evaporating heat pump and 24°C for the wet evaporating heat pump, while when using water-glycol mixture the avreage temperature of the fluid in the GHE is around 27°C.

As a conclusion, the use of anti freezing mixtures is not needed in mild climates, i.e. in locations where the average temperature of the ground is around 15°C.

2.6 Reference

Atti del convegno "Geotermia: applicazioni a bassa temperatura". Vicenza (Italy), 26 maggio 2006.

Baietto A., Pochettino M., Salvatici E., (2010), Progettazione di impianti geotermici: sonde verticali e pozzi d'acqua, ISBN 978 – 88- 579 – 0058 – 2, Dario Flaccovio Editore s.r.l.

Banks D. – "An Introduction to Thermogeology: Ground Source Heating and Cooling" - Blackwell, Oxford (2008)

Basta S., Minchio F., Geotermia e pompe di calore, Hoepli Italia, (2007).

Bear J., Verruijt A., Modelling groundwater flow and pollution with computer programs for sample cases, theory and applications of transport in porous media, Vol. 1, J. Bear, Ed. Kluwer, Hardbound 1987.

Bejan A. – "Convection Heat Transfer" – J. Wiley and Sons, NY (1984)

Boennec O. – "Shallow ground energy systems" – Faber Maunsell, London, UK (2008)

Bourne-Webb P.J., Amatya B., Soga K., Amis T. Davidson C., Payne P. – "Energy pile test at Lambeth College, London: geotechnical and thermodynamics aspects of pile response to heat cycles" – Cementation Skanska, University of Cambridge, Geothermal International, UK (2008)

Brandl H. – "Energy foundations and other thermo-active ground structures" – Institute of Soil Mechanics and Geotechnical Engineering, Vienna University of Technology, Austria (2006).

Carslaw H. S. and Jaeger J. C., Conduction of Heat in Solids, 2nd ed. Clarendon Oxford, 1959, p. 396.

Casciaro S., Thome J.R., (2001a), Thermal performance of flooded evaporators, Part 1: Review of boiling heat transfer studies, ASHRAE Transactions, 107 (1) (2001) 919 – 930.

Casciaro S., Thome J.R., (2001b). Thermal performance of flooded evaporators, Part 2: Review of void fraction, two-phase pressure drop, and flow pattern studies. ASHRAE Transactions, 107 (2) (2001) 443 – 453.

Claesson, J. and Eskilson, P., (1987), Thermal Analysis of Heat Extraction Bore Holes, 264 p., PhD-thesis, Lund-MPh-87/13, Lund University of Technology, Sweden.

Chen X., Yang H., Performance analysis of a proposed solar assisted ground coupled heat pump system, Applied Energy 97(2012) 888 – 896.

Comsol Multiphysics – Heat Transfer Module User's Manual and Structural Mechanics Module User's Manual – COMSOL AB. (2008)

Cotchin C., Boyd E., Boiling of refrigerant and refrigerant/oil mixtures in a flooded evaporator Heat Transfer, 3rd UK National Conference Incorporating 1st European Conference on Thermal Sciences, Taylor & Francis, London, 1 (1992) 131 – 137.

Cullin J. R., Spitler J. D., Comparison of Simulation-based Design Procedures for Hybrid Ground Source Heat Pump Systems, 8th International Conference on System Simulation in Buildings, Liege, December 13-15 (2010), pp. 1 – 15.

Den Braven K.R., Antifreeze acceptability for ground – coupled heat pump ground loops in the United States. ASHRAE Transactions, 104(1) (1998) 938 – 942.

De Carli M., Donà M., Vergani D. – "Dimensionare i pali energetici" – AICARR Journal (2010).

De Carli M., Roncato N., Zarrella A., Zecchin R. – "Energia dal Terreno" – Dipartimento di Fisica Tecnica, Università degli Studi di Padova, Convegno AICARR (2007)

De Carli M., Tonon M., Zarrella A., Zecchin R., A computational capacity resistance model (CaRM) for vertical ground - coupled heat exchangers, Renewable Energy, 35 (2010) 1537–1550.

Del Mastro R., Noce G., Manuale di geotermia a sonde verticali, Hoepli Milano (Italy), 2011, ISBN 978 – 88 – 203 – 4539 – 6.

Fernandez-Seara J., Sieres J., Ammonia – water absorption refrigeration systems with flooded evaporators. Applied Thermal Engineering 26 (2006) 2236 – 2246.

Forcellini Merlo F., Rampazzo A. – "Geotecnica" – Univer Editrice

Gehlin S. (2002). Thermal Response Teast, Meathod Development and Evaluation. Doctoral Thesis 2002:39. Luleå University of Technology. Sweden.

Guernsey E.N., Betz P.L., Skan N.H. (1949), Earth as a heat source and storage medium for the heat pump, ASHVE Trans. 55, 321 – 344.

Hamada Y., H. Saitoh, M. Nakamura, H. Kubota, K. Ochifuji – "Field performance of an energy pile system for space heating" – Graduate School of Engineering, Hokkaido University, Japan (2006)

Heinonen E.W., Wildin M.W., Beall A.N., Tapscott R.E., Assessment of antifreeze solutions for ground – source heat pump systems, ASHRAE Transactions, Vol. 103(2) (1997) 747 – 756.

Heinonen E.W., Wildin M.W., Beall A.N., Tapscott R.E., Assessment of antifreeze solution for ground – source heat pump systems. The Second Stockton International Geothermal Conference. March 16 17 (1998).

Heinonen E.W., Wildin M.W., Beall A.N., Tapscott R.E., Anti-Freeze Fluid Environmental and Health Evaluation - An Update.

http://intraweb.stockton.edu/eyos/energy_studies/content/docs/proceedings/HEINO.PDF

Hellstrom G. (2006) Duct heat ground storage Model, manual for computer code, March 1989 workshop of IEA HP Annex 29, January 15 – 17, Sapporo, Japan.

Ingersoll L.R., Plass H. J. (1948), Theory of the ground pipe source fort he heat pump, ASHVE Trans. 54, 339 – 348.

Jun Gao, Xu Zhang, Jun iu, Kiushan Li, Jie Wang – "Thermal performance and ground temperature of vertical pile-foundation heat exchangers: A case study" – College of Mechanical Engineering, Tongji University Shanghai, China (2008)

Jun Gao, Xu Zhang, Jun iu, Kiushan Li, Jie Wang – "Numerical and experimental assessment of thermal performance of vertical energy piles: An application" - College of Mechanical Engineering, Tongji University Shanghai, China (2008)

Kavanaugh, S. P., Rafferty K.. (1997). Ground Source Heat Pumps: Design of Geothermal Systems for Commercial and Institutional Buildings. Atlanta:., American Society of Heating, Refrigerating and Air-Conditioning Engineers, Atlanta, Georgia.

Kavanaugh S.P., A design method for hybrid groundsource heat pumps, ASHRAE Transactions, 104 (2) (1998), pp. 691 – 698.

Khan M.H., Spitler J.D., Performance analysis of a residential ground source heat pump system with antifreeze solution, Proceedings of SimBuild, Boulder, Colorado, August 4 – 6 (2004).

Klotzbucher T., Kappler A., Straub K., Haderlein S., Biodegradability and groundwater pollutant potential of organic anti-freeze liquids used in borehole heat exchangers, Geothermics 36 (2007) 348 – 361.

Laloui L, Moreni M, Steinmann G, Vulliet L, Fromentin A, Pahud D. Test en conditions re´elles du comportement statique d'un pieu soumis a` des sollicitations thermo-me´caniques. Report of the Swiss Federal Office of Energy OFEN, 1999.

Laloui L., Nuth M., Vulliet L. – "Experimental and numerical investigations of the behavior of a heat exchanger pile" – EPFL, Switzerland (2006)

Lancellotta, R. – "Geotecnica" – Zanichelli Ed. (1992)

Lee S.R. – "Energy Piles – Piles as heat exchangers" – Dept. of Civil and Environmental Engineering, KAIST (2009)

Lokke H., Leaching of ethylene glycol and ethanol in subsoils. Water, Air, and Soil Pollution 22 (1984) 373-387.

Man Y., Yang H., Diao N., Liu J., Fang Z. – "A new model and analytical solutions for borehole and pile ground heat exchangers" – The GSHP Research Center, China, Renewable Energy Research Group, Hong Kong Polytechnic University, China (2010)

McCartney J. – "Geothermal Foundations and Thermally-Active Ground Structures" – Dept. of Civil, Environmental and Architectural Engineering, University of Colorado, USA (2009)

Minetto S., Fornasieri E., An innovative system for feeding once-through evaporators in flooded conditions. Applied Thermal Engineering 31 (2011) 370 – 375.

Mogensen P. (1983). Fluid to Duct Wall Heat Transfer in Duct System Heat Storage. Proc. Int. Conf. On Subsurface Heat Storage in Theory and Practice. Stockholm. Sweden, June 6–8, 1983. PP: 652-657.

Nova, R. – "Fondamenti di meccanica delle terre" – McGraw Hill (2002)

Pahud D. – “Sistemi con pali energetici” – SUPSI, DACD, ISAAC, Svizzera

Rad F.M., Fung A.S., Leong W.H., Combined solar thermal and ground source heat pump system, In proceedings of Building Simulation 2009, 11th International IBPSA Conference, Glasgow, Scotland, pp. 2297 – 2305.

Ramamoorthy M. H. Jin, Chiasson A., Spitler J.D., Optimal Sizing of Hybrid Ground-Source Heat Pump Systems that use a Cooling Pond as a Supplemental Heat Rejecter – A System Simulation Approach, ASHRAE Transactions, 107(1) (2001) 26-38.

Rao S. S. – “Finite element Method in Engineering” – Pergamon Press, Oxkord, UK (1999)

Remund C.P., (1999), Borehole thermal resi stance: laboratori and field studies: ASHRAE Transactions 105(1).

Reuss M., Sanner E. (2001), Design of closed loop heat exchanger, Iternational summer school on direct applications of geothermal energy, Chapter 2.5 Bad Urach.

Sanner, B., 1992. ErdgekoppelteW¨armepumpen, Geschichte, Systeme, Auslegung, Installation. IZW-Bereicht 2/92, FIZ, Karlsruhe, Germany, 328 pp.

Staples C.A., Williams J.B., Craig G.R., Roberts K.M., Fate, effects and potential environmental risks of ethylene glycol: a review, Chemosphere, 43(3) (2001) 377 – 383.

Spitler, J.D., Rees, S. and Yavuzturk, C.: More Comments on In-situ Borehole Thermal Conductivity Testing. The Source 3-4/99, 1999

Spitler, J.D., Yavuzturk, C. and Jain, N.: Refinement and Validation of In-situ Parameter Estimation Models. short report, OSU, 1999

Skouby, A.: Thermal Conductivity Testing. The Source 11 - 12/98, 1998

Theis, C.V., 1935. The relation between the lowering of the piezometric surface and the rate and duration of discharge of a well using groundwater storage, Am. Geophys. Union Trans., vol. 16, pp. 519-524.

Tirillò L. – “L’utilizzo della geotermia a bassa entalpia: applicazioni con geoscambiatore a sviluppo verticale” – McQuay Italia S.p.A.

TRNSYS, A Transient Simulation Program - Solar Energy Laboratory, University of Wisconsin, Madison, USA, (1990).

VDI 4640, Verein Deutscher Ingenieure – Dusseldorf (2000)

Viggiani, C. – “Fondazioni“ – Hevelius Ed. (2002)

Zeng, H., N. Diao, and Z. Fang. (2003). Heat transfer analysis of boreholes in vertical ground heat exchangers. International Journal of Heat and Mass Transfer. 46(23): 4467-4481.

Zeng, H., N. Diao, and Z. Fang. (2003), Efficiency of vertical geothermal heat exchangers in ground source heat pump system

Zeng H.Y., Diao N.R., Fang Z.H., Efficiency of vertical geothermal heat exchangers in ground source heat pump systems, J. Thermal Sci. 12 (1) (2003) 77–81.

Zienkevich O., Taylor R. – "The Finite Element Method" – McGraw Hill (1994)

Zheng J.H., Jin G.P., Chyu M.C., Ayub Z.H., Boiling of ammonia/lubricant mixture on a horizontal tube in a flooded evaporator with inlet vapor quality. Experimental Thermal and Fluid Science 30 (2006) 223–231.

Wang H., Qi C., Wang E., Zhao J., A case study of underground thermal storage in a solar ground coupled heat pump system for residential buildings. Renewable Energy 34(1) (2009) 307– 314.

Wood C. J., H. Liu and S. B. Riffat – "Use of energy piles in a residential buildings, and effects on ground temperature and heat pump efficiency" - Institute of Sustainable Energy Technology, School of the Built Environment, University of Nottingham, UK (2009)

Yang W., Li S., Zhang X., Numerical Simulation on Heat Transfer Characteristics of Soil Around U-Tube Underground Heat Exchangers, International Refrigeration and Air Conditioning Conference at Purdue, July 14-17 896(2008).

Yavuzturk C., Spitler J.D., Comparative study of operating and control strategies for hybrid groundsource heat pump systems using a short time step simulation model, ASHRAE Transactions, 106 (2) (2000) 192 – 209.

Web site:

www.geothermie.ch

ANNEX A

A.1 The influence of moving groundwater

If groundwater is in motion, the phenomenon of heat exchange a between GHE and the ground is considerably more complex, since the flow shifts the thermal plume in the direction of the groundwater movement amplifying the amount of heat exchange . The hydraulic conductivity of the soil, is thus another parameter to take into account when investigating heat exchange as it can determine the velocity of the water flowing underground (or Darcy's velocity), known horizontal pressure gradient of underground water:

$$v = k \cdot i \qquad \text{(A.1)}$$

Where:

$v = \frac{Q}{A}$ = Darcy velocity [m/s];

$i = \frac{\Delta h}{L}$ = hydraulic gradients;

k = hydraulic conductivity [m/s].

The various geological formations have different permeabilities which and this also affects the thermal parameters, as shown in the following Table A.1 (Pahud D.):

Table .A.1 – The influence of hydraulic conductivity on the thermal parameters

Type of soil	hydraulic conductivity k [m/s]	Thermal conductivity [W/(m K)]		Volumetric heat capacity [MJ/(m² K)]	
		dry	saturated	dry	saturated
Clay	10^{-8} – 10^{-10}	0.2 - 0.3	1.1 – 1.6	0.3 - 0.6	2.1 – 3.2
Limo	10^{-5} – 10^{-8}	0.2 - 0.3	1.2 – 2.5	0.6 – 1.0	2.1 – 2.4
Sand	10^{-3} – 10^{-4}	0.3 - 0.4	1.7 – 3.2	1.0 – 1.3	2.2 – 2.4
Gravel	10^{-1} – 10^{-3}	0.3 - 0.4	1.8 – 3.3	1.2 – 1.6	2.2 – 2.4

The table shows, that the values of the thermal properties of the soil are much higher in the presence of water.

Moreover, the Darcy velocity influences the storage capacity of the thermal energy in the over long term periods. A Darcy velocity of 0.5 to 1 m per day is able to disperse into the ground the energy transferred from the geothermal and ensure storage.

In practical terms, an aquifer in motion ensures a better heat exchange between the pipe and the ground even in soils judged "poor" thermally.

A.2 Analogy between heat flow and groundwater flow

As the Darcy's law is analogous to Fourier's law and the equation of heat balance has a direct parallel in the theory of flow of groundwater, it is possible to apply the analogy of the equations of Theis, Cooper-Jacob Logan and the radial heat flow equation to a vertical shaft geothermally closed circuit.

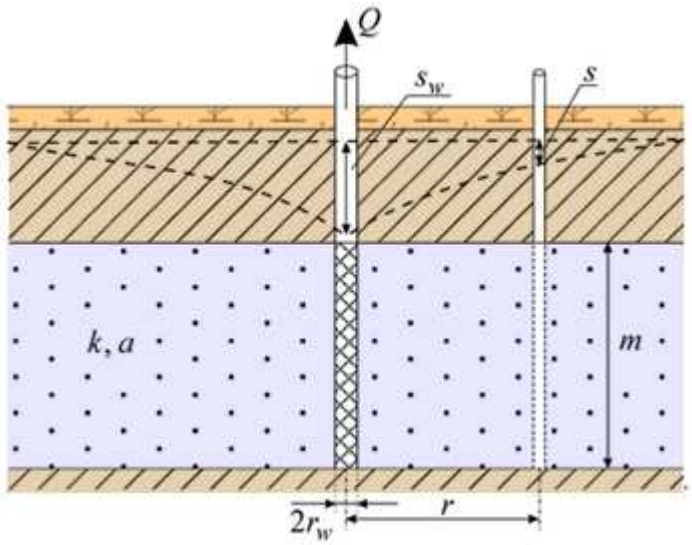

Fig. A.1: Cross – section of a pumped aquifer.

Theis equation (1935):

Theis (1935) solved the non – equilibrium flow equations in radial coordinates based on the relationship between groundwater flow and heat condition. By assuming that the well is replaced by a mathematical drawdown of constant strength and imposing the boundary conditions $h = h_0$ for $t = 0$, and $h \to h_0$ as $r \to \infty$ for $t \geq 0$, the solution:

$$s = \frac{Q}{4\pi T}\int_{u}^{\infty}\frac{e^{-u}}{u}du \qquad \text{(A.2)}$$

For this method the drawdown at a piezometer distance, r from the abstraction well is monitored over time. Theis expressed the transient drawdown, s, as:

$$s = \frac{Q}{4\pi T}W(u) \qquad \text{(A.3)}$$

Where:

Q = flow rate extracted from the well;

T = transmissivity of the aquifer;

W(u) = Theis function;

$$u = \frac{r^2 \cdot S}{(4 \cdot T \cdot t)} \qquad \text{(A.4)}$$

s = drawdown at a given radial distance r from the extraction well at a given instant t after the start of pumping.

Assumpitions:

1. Prior to pumping, the potentiometric surface is approximately horizontal (no slope);
2. The aquifer is confined and has an “apparent” infinite extent;
3. The aquifer is homogeneous, isotropic and of uniform thickness over the area influenced by pumping;
4. The well is pumped at a constant rate;
5. The well is fully penetrating;
6. Water removed from storage is discharged instantaneously with decline in head;
7. The well diameter is small so that well storage is negligible.

Cooper - Jacob equation:

The analysis presented here is of a pumping test in which drawdown at a piezometer distance, r from the abstraction well is monitored over time. This is also based upon the Theis analysis:

$$s = \frac{Q}{4\pi T} W(u) = \frac{Q}{4\pi T}\left(-0.5772 - \ln u + u - \frac{u^2}{2.2!} + \frac{u^3}{3.3!} - .... \right) \qquad \text{(A.5)}$$

From the definition of u it can be seen that *u* decreases as the time of pumping increases and as the distance of the piezometer from the well decreases. So, for piezometers close to the pumping well after sufficiently long pumping times, the terms beyond ln(*u)* become negligible. Hence for small values of *u*, the drawdown can be approximated by:

$$s = \frac{Q}{4\pi T}\left[-0.5772 - \ln\left(\frac{r^2 S}{4Tt} \right) \right] = \frac{2.3Q}{4\pi T} \log_{10}\left(\frac{2.25T}{r^2 S} t \right) \qquad \text{(A.6)}$$

$$T = \frac{Q}{2\pi s_w} \ln \frac{r_0}{r_w} = 1.22 \frac{z}{s_w} \qquad \text{(A.7)}$$

Where:

s_w = drawdown of the groundwater;

r_w = radius of the well;

r_e = distance from the well where the drawdown is approximately zero ($r_e/r_w = 2000$).

There is an important distinction to make difference between hydrogeological heat and geology heat: this difference lies in the boundary conditions for an aquifer and a warm housing. Consider first a typical unconfined aquifer. The bed of the aquifer is usually constituted by some low permeability layer: can be approximated by a contour is not affected by flow. The roof of the aquifer coincides with the surface of the water with a load potentially variable, but that receives (in the long term) Annual approximately constant supply of reloading from rainwater. Conceptually, therefore, there is a constant flow boundary (or, in the case of a confined aquifer, a contour at no flow). The equations of Theis and Cooper – Jacob stipulate that, if water is extracted from a well in the aquifer, develops a cone of depression of the portion of flap around the perforation. The cone of lowering continues to evolve in the space around (in theory) ad infinitum and indefinitely in proportional to the logarithm of time.

A.3 Fundamental equations of the radial conduction: solution of Claesson and Eskilson

A3.1 The initial stages of the extraction of heat

The fundamental equations governing the radial conduction of heat to a 'reservoir' linear into the ground, and other geometries of heat transfer into the subsurface were developed in the 1940's, scientists such as Leonard and Alfred Ingersoll, Otto Zobel (Ingersoll et al . 1948) and Guernsey et al. (1949). However, the Swedes Johan Claesson and Per Eskilson (1987)solved analytical and numerical solutions of the extraction of heat from closed-loop drilling systems in a hot aquifer. It is their job to study that constitutes the basis for the following discussion.

A simple analytical solution proved to be unattainable. The authors were nevertheless able to obtain a discussion of the problem by using the two following simplifying hypotheses:

Hypothesis 1: the geothermal gradient can be neglected, and it can be considered that the aquifer as having initially has a uniform temperature equal to the average temperature along the length of the well perforation. So, if a well of 100 m (before any heat extraction) has a temperature close to the surface around 9 ° C and a temperature at the base of 11 ° C, one could say that the hot aquifer has an average temperature initial T_0 of 10 ° C. If one imagines of a carrier fluid to circulating along the cycle, before operating the heat pump, it will tend to move in thermal equilibrium with the temperature T_0.

Hypothesis 2: that, in the early stages, can be neglect the induced heat from the surface and take into account simply the radial heat flow from the hot aquifer at the well. In other words, in the early stages, the closed-loop system simply by taking heat from the storage tank in the sub-surface.

Returning then to the equation:

$$\frac{\partial^2 T}{\partial x^2}+\frac{\partial^2 T}{\partial y^2}+\frac{\partial^2 T}{\partial z^2}=\frac{S_{vc}}{\lambda}\frac{\partial T}{\partial \theta} \qquad \text{(A.8)}$$

in radial coordinates r, neglecting the geothermal gradient, with the following boundary conditions:

at $\theta = 0$, $T = T_0$ for all values of r and z.

for $r \to \infty$, $T = T_0$ for all values of t.

The solution is not simple, but the problem is still solvable:

$$T_0 - T_b = \frac{q}{4\pi\lambda}E(u) = \frac{q}{4\pi\lambda}\left[-\gamma - \ln(u) - \sum_{n=1}^{\infty}(-1)^n \frac{u^n}{n.n!}\right] \qquad \text{(A.9)}$$

Where E (u) is a polynomial expression to Theis:

$$u = \frac{r_b^{\,2} \cdot S_{vc}}{(4\lambda\theta)} \qquad \text{(A.10)}$$

T_b is the average temperature (° C) of the vector fluid in the well at time t. Here it is assumed that it is identical to the temperature at the wall of the borehole - at a radius r_b from the center of the heat reservoir linear. It is also assumed that any grout or fill around the circuit is infinitely conductive thermally - a geothermal well ideally thermally efficient.

q = share of heat extracted per meter of drilling (W / m); which coincides with the portion of heat extracted divided by the effective depth, taking account of each upper part of the well that will be thermally isolated from the rock;

λ = thermal conductivity of the rock (W / m K);
r_b = radius of the borehole (m)
γ = Euler's constant = 0.5772.

This is the similar thermal equation of Theis. In fact it is more correct to say that the Theis equation was derived from this equation the radial heat flow. As in the case of the approximation of Cooper-Jacob is can simplify this expression by low values of u (large values of t):

$$T_0 - T_b = \frac{q}{4\pi\lambda} E(u) = \frac{q}{4\pi\lambda}\left[\ln\left(\frac{4\lambda\theta}{r_b^{\,2} S_{vc}}\right) - 0.5772\right] \qquad \text{(A.11)}$$

This equation implies that, in the initial phase the temperature of the circulating fluid decreases with the logarithm of time. This approximation is valid for t values within the following range:

$$\frac{5 r_b^{\,2} \cdot S_{vc}}{\lambda} < \theta < \frac{t_s}{10} \qquad \text{(A.12)}$$

If the value of t is smaller than the lower limit given, the reliability of the approximation is less. If t is too large, the log-linear relationship between the time and Tb begins to diverge, even if only slightly, from the real curve, as soon as, the system begins to cause the induction of the heat flux from the surface of the ground and to tend slowly the stationarity.

A3.2 Final stages of the extraction of heat

The instant θ s, after which, the stationary state, begins to be a better description of the evolution of the temperature with respect to the radial flow, is given by Claesson and Eskilson (1987) as:

$$\theta_s = \frac{e^{\gamma} D^2 S_{vc}}{18\lambda} \cong \frac{D^2 S_{vc}}{9\lambda} \qquad \text{(A.13)}$$

where:

γ = Euler's constant = 0.5772;

D = depth of the well (m) above which is the extraction of heat.

The temperature, at steady state of the vector fluid, which converges to the curve of the real temperature is given by:

$$T_0 - T_b = \frac{q}{4\pi\lambda}\ln\left(\frac{D}{r_b\sqrt{4.5}}\right) \cong \frac{q}{4\pi\lambda}\ln\left(\frac{D}{2r_b}\right); \quad \text{if } D >> r_b \qquad \text{(A.14)}$$

where:

$T_{s,\,b}$ = stationary temperature of the fluid manifold, in the well drilled ideal (K) = steady state temperature of the walls of the well, neglecting the thermal resistance of the filler material around the perforation.

A3.3 Transfer of heat in a vertical well geothermal

For conditioning geothermal systems, the heat load released to the ground (G) is in related to the effect of cooling (C) and the seasonal factor of performance (SPFC) of the heat pump through the following relation:

$$G \cong C\left(1+\frac{1}{SPF_C}\right) \qquad \text{(A.15)}$$

The relationships described above for the extraction of heat, can be used in this case, with the except in of the case in which the share of heat extracted is negative and the temperature T_b increases progressively above the value T_0.

ANNEX B

B.1 Software Finite Element Model (FEM): COMSOL Multiphysics

The equations for finite element problems of thermal conduction can be derived through a variational approach, or an approach according to the Galerkin method. In the following sections it will derive these equations by using both methods.

The conduction problems in three dimensions can be solved by transforming the differential equation into an equivalent variational form.

It will, therefore, necessary to search for the temperature distribution T (x, y, z, t) within the solid such that the integral is minimized:

$$I = \frac{1}{2}\int\int\int_V \left[k_x\left(\frac{\partial T}{\partial x}\right)^2 + k_y\left(\frac{\partial T}{\partial y}\right)^2 + k_z\left(\frac{\partial T}{\partial z}\right)^2 - 2\left(q - \rho c\frac{\partial T}{\partial \theta}\right)T \right] dV \qquad \text{(B.1)}$$

and responded to the boundary conditions and initial conditions. Here the term $\left(\frac{\partial T}{\partial \theta}\right)$ must be considered fixed, instead of considering variable. Generally it is not complicated satisfy the boundary conditions of Dirichlet, while, those of Neumann present some difficulties. To overcome this problem, it adds to the functional (Eq. B.1) an integral relative to the boundary conditions, in such a way that when the functional thus obtained is minimized, the boundary conditions are automatically satisfied. These integrals related to the boundary conditions have the expression:

$$\iint_{S_2} qT dS_2 + \iint_{S_3} \frac{1}{2}h(T - T_\infty)^2 dS_3 \qquad \text{(B.2)}$$

It follows, that the functional to be minimized will have the following form:

$$I = \frac{1}{2}\iiint_V \left[k_x\left(\frac{\partial T}{\partial x}\right)^2 + k_y\left(\frac{\partial T}{\partial y}\right)^2 + k_z\left(\frac{\partial T}{\partial z}\right)^2 - 2\left(q - \rho c\frac{\partial T}{\partial t}\right)T \right] dV + \iint_{S_2} qT dS_2 + \qquad \text{(B.3)}$$

$$+ \iint_{S_3} \frac{1}{2}h(T - T_\infty)^2 dS_3$$

B.1.1. Variational approach

In this approach, considering the minimization of the functional I given by Eq. B.3 subject to the satisfaction of the boundary condition and the initial condition. Below is given the procedure step by step for the derivation of the equations finite elements.

Step 1: Divide the domain V in E finite elements of p nodes each.

Step 2: Assume a suitable form of variation of T for each finite element and express $T^{(e)}$ (x, y, z, t) in the element and as:

$$T^{(e)}(x,y,z,t) = [N(x,y,z)]\overrightarrow{T^{(e)}} \tag{B.4}$$

Where:

$$[N(x,y,z)] = \begin{bmatrix} N_1(x,y,z) & N_2(x,y,z) & \dots & N_p(x,y,z) \end{bmatrix} \tag{B.5}$$

$$\vec{T}^{(e)} = \begin{Bmatrix} T_1(t) \\ T_2(t) \\ \bullet \\ \bullet \\ \bullet \\ T_p(t) \end{Bmatrix}^{(e)} \tag{B.6}$$

T_i (t) is the temperature of the i-th node and N_i (x, y, z) is the function interpolating corresponding to the node i and the element.

Step 3: Expressing the functional I, as the sum of the E quantity elementary $I^{(e)}$ as:

$$I = \sum_{e=1}^{E} I^{(e)} \tag{B.7}$$

Where:

$$I^{(e)} = \frac{1}{2}\iiint_{V^{(e)}} \left[k_x \left(\frac{\partial T^{(e)}}{\partial x} \right)^2 + k_y \left(\frac{\partial T^{(e)}}{\partial y} \right)^2 + k_z \left(\frac{\partial T^{(e)}}{\partial z} \right)^2 - 2\left(q - \rho c \frac{\partial T^{(e)}}{\partial t} \right) T^{(e)} \right] dV + \\ + \iint_{S_2{}^{(e)}} q T^{(e)} dS_2 + \iint_{S_3{}^{(e)}} \frac{1}{2} h \left(T^{(e)} - T_\infty \right)^2 dS_3 \tag{B.8}$$

To minimize the functional I it necessarily impose the conditions:

$$\frac{\partial I}{\partial T_i} = \sum_{e=1}^{E} \frac{\partial I^{(e)}}{\partial T_i} = 0 \qquad i = 1,2,\ldots\ldots,M \tag{B.9}$$

where M is the total number of nodal temperatures unknowns. From Eq. B.8 we have:

$$\frac{\partial I^{(e)}}{\partial T_i} = \iiint_{V^{(e)}} \left[\begin{array}{l} k_x \dfrac{\partial T^{(e)}}{\partial x} \dfrac{\partial}{\partial T_i} \left(\dfrac{\partial T^{(e)}}{\partial x} \right) + k_y \dfrac{\partial T^{(e)}}{\partial y} \dfrac{\partial}{\partial T_i} \left(\dfrac{\partial T^{(e)}}{\partial y} \right) + \\ + k_z \dfrac{\partial T^{(e)}}{\partial z} \dfrac{\partial}{\partial T_i} \left(\dfrac{\partial T^{(e)}}{\partial z} \right) - 2\left(q - \rho c \dfrac{\partial T^{(e)}}{\partial t} \right) \dfrac{\partial T^{(e)}}{\partial T_i} \end{array} \right] dV \\ + \iint_{S_2{}^{(e)}} q \frac{\partial T^{(e)}}{\partial T_i} dS_2 + \iint_{S_3{}^{(e)}} h \left(T^{(e)} - T_\infty \right) \frac{\partial T^{(e)}}{\partial T_i} dS_3 \tag{B.9}$$

Note that the integrals of the surface do not appear in Eq. B.9 if the i-th node is not located on S2 or S3. Equation B.4 provides:

$$\left. \begin{array}{l} \dfrac{\partial T^{(e)}}{\partial x} = \left[\dfrac{\partial N_1}{\partial x} \quad \dfrac{\partial N_2}{\partial x} \quad \ldots \quad \dfrac{\partial N_p}{\partial x} \right] \overrightarrow{T^{(e)}} \\ \dfrac{\partial}{\partial T_i} \left(\dfrac{\partial T^{(e)}}{\partial x} \right) = \dfrac{\partial N_i}{\partial x} \\ \dfrac{\partial T^{(e)}}{\partial T^{(e)}} = N_i \\ \dfrac{\partial T^{e}}{\partial t} = [N] \overrightarrow{T^{(e)}} \end{array} \right\} \tag{B.10}$$

Where:

$$\overrightarrow{T^{(e)}} = \begin{Bmatrix} \frac{\partial T_1}{\partial t} \\ \bullet \\ \bullet \\ \bullet \\ \frac{\partial T_p}{\partial t} \end{Bmatrix} \tag{B.11}$$

Therefore, Eq. B.9 can be expressed as:

$$\frac{\partial I^{(e)}}{\partial \vec{T}^{(e)}} = \left[K_1^{(e)}\right]\vec{T}^{(e)} - \vec{p}^{(e)} + \left[K_2^{(e)}\right]\vec{T}^{(e)} + \left[K_3^{(e)}\right]\vec{T}^{(e)} \tag{B.12}$$

Where the matrices $[K_1{}^{(e)}]$, $[K_2{}^{(e)}]$, $[K_3{}^{(e)}]$ e $p^{(e)}$ and are given by:

$$K_{1ij}{}^{(e)} = \iiint_{V^{(e)}} \left(k_x \frac{\partial N_i}{\partial x}\frac{\partial N_j}{\partial x} + k_y \frac{\partial N_i}{\partial y}\frac{\partial N_j}{\partial y} + k_z \frac{\partial N_i}{\partial z}\frac{\partial N_j}{\partial z} \right) dV \tag{B.13}$$

$$K_{2ij}{}^{(e)} = \iint_{S_3{}^{(e)}} hN_i N_j \cdot dS_3 \tag{B.14}$$

$$K_{3ij}{}^{(e)} = \iiint_{V^{(e)}} \rho c N_i N_j \cdot dV \tag{B.15}$$

$$\vec{p_i}^{(e)} = \iiint_{V^{(e)}} qN_i dV - \iint_{S_2{}^{(e)}} qN_i dS_2 + \iint_{S_3{}^{(e)}} hT_\infty N_i dS_3 \tag{B.16}$$

Step 4: Rewrite the Eq. B.12 in matrix form:

$$\frac{\partial I^{(e)}}{\partial \vec{T}^{(e)}} = \sum_{e=1}^{E} \left(\left[\left[K_1^{(e)} \right] + \left[K_2^{(e)} \right] \right] T^{(e)} - \vec{p}^{(e)} + \left[K_3^{(e)} \right] \vec{T}^{(e)} \right) = \vec{0} \qquad \text{(B.17)}$$

where $\vec{T}$ is the vector of unknown nodal temperatures of the system:

$$\overrightarrow{T^{(e)}} = \begin{Bmatrix} T_1 \\ T_2 \\ \bullet \\ \bullet \\ \end{Bmatrix} \qquad \text{(B.18)}$$

Once assembled global matrices of the system, can express Eq. B.17 as:

$$[K_3]\vec{T} + [K]\vec{T} = \vec{P} \qquad \text{(B.19)}$$

Where:

$$[K_3] = \sum_{e=1}^{E} \left[K_3^{(e)} \right] \qquad \text{(B.20)}$$

$$[K] = \sum_{e=1}^{E} \left[\left[K_1^{(e)} \right] + \left[K_2^{(e)} \right] \right] \qquad \text{(B.21)}$$

$$\vec{P} = \sum_{e=1}^{E} \vec{P}^{(e)} \qquad \text{(B.22)}$$

Step 5: Equations B.19 are the equations we need to be implemented after merging the boundary conditions specified on S1.

B.1.2. Galerkin approach

The process according to the theory of finite element Galerkin can be described by the following steps.

Step 1: Divide the domain V in E finite elements of p nodes each.

Step 2: Take a suitable form of variation of T for each finite element and express $T^{(e)}$ (x, y, z, t) in the element and as:

$$T^{(e)}(x,y,z,t) = [N(x,y,z)]\vec{T}^{(e)} \tag{B.20}$$

Step 3: In the Galerkin method, the integral of the residue weighed on a domain of an element is set equal to zero, using as weights the same functions interpolating Ni. solution being B.20 is not exact, substitute the original differential equation solution provides a non-zero result. This non-zero value will constitute the residue. Therefore, the criterion that must be satisfied at any time is:

$$\iiint_{V^{(e)}} N_i \left[\frac{\partial}{\partial x}\left(k_x \frac{\partial T^{(e)}}{\partial x} \right) + \frac{\partial}{\partial y}\left(k_y \frac{\partial T^{(e)}}{\partial y} \right) + \frac{\partial}{\partial z}\left(k_z \frac{\partial T^{(e)}}{\partial z} \right) + \left(q - \rho c \frac{\partial T^{(e)}}{\partial t} \right) \right] dV = 0 \quad i = 1,2,\ldots..,\, p \tag{B.21}$$

The first integral term of the above equation can be written as:

$$\iiint_{V^{(e)}} N_i \left[\frac{\partial}{\partial x}\left(k_x \frac{\partial T^{(e)}}{\partial x} \right) \right] dV = -\iiint_{V^{(e)}} \frac{\partial N_i}{\partial x} k_x \frac{\partial T^{(e)}}{\partial x} dV + \iint_{S^{(e)}} N_i k_x \frac{\partial T^{(e)}}{\partial x} l_x dS \tag{B.22}$$

Where l_x is the cosine director of the direction x normal. Using the same expression for the second and the third integral term, Eq. B.21 can be expressed as:

$$\begin{aligned} &- \iiint_{V^{(e)}} \left[k_x \frac{\partial N_i}{\partial x} \frac{\partial N_i}{\partial x} \frac{\partial T^{(e)}}{\partial x} + k_y \frac{\partial N_i}{\partial y} \frac{\partial T^{(e)}}{\partial y} + k_z \frac{\partial T^{(e)}}{\partial z} \frac{\partial T^{(e)}}{\partial z} \right] dV + \\ &+ \iint_{S^{(e)}} N_i \left[k_x \frac{\partial T^{(e)}}{\partial x} l_x + k_y \frac{\partial T^{(e)}}{\partial y} l_y + k_z \frac{\partial T^{(e)}}{\partial z} l_z \right] dS + \\ &+ \iiint_{V^{(e)}} N_i \left(q - \rho c \frac{\partial T^{(e)}}{\partial t} \right) dV = 0 \qquad i = 1,2,\ldots..,\, p \end{aligned} \tag{B.23}$$

Since, the outline of the element $S^{(e)}$ is composed of $S_1^{(e)}$, $S_2^{(e)}$ and $S_3^{(e)}$, the surface integral of B.23 in $S_1^{(e)}$ will be worth zero (since $T^{(e)}$ is constant and equal to T_0 and its derivative with respect to x, y and z will be null). On the surfaces $S_2^{(e)}$ and $S_3^{(e)}$ the boundary conditions must be satisfied. In this respect, the surface integral of Eq. B.23 will assume the following expression for the contours $S_2^{(e)}$ and $S_3^{(s)}$:

$$\iint_{S_2^{(e)}+S_3^{(e)}} N_i\left[k_x\frac{\partial T^{(e)}}{\partial y}l_x + k_y\frac{\partial T^{(e)}}{\partial y}l_y + k_z\frac{\partial T^{(e)}}{\partial z}l_z\right]dS = \quad \text{(B.24)}$$
$$-\iint_{S_2^{(e)}} N_i q dS_2 - \iint_{S_1^{(2)}} N_i q dS_2 - \iint_{S_3^{(e)}} h\left(T^{(e)} - T_\infty\right)dS_2$$

Using equations B.20 and B.24, Eq. B.23 can be rewritten in matrix form as:

$$\left[K_1^{(e)}\right]\vec{T}^{(e)} + \left[K_2^{(e)}\right]\vec{T}^{(e)} + \left[K_3^{(e)}\right]\vec{T}^{(e)} - \vec{p}^{(e)} = \vec{0} \quad \text{(B.25)}$$

where the elementary matrices $[K_1^{(e)}]$, $[K_2^{(e)}]$, $[K_3^{(e)}]$ and $P^{(e)}$ are the same as those defined in eq. B.12 – B.16.

Step 4: The individual terms of the equation B.24 can be assembled according to the usual procedure so as to obtain the following equations:

$$[K_2]\vec{T} + [K]\vec{T} = \vec{P} \quad \text{(B.26)}$$

Where $[K_2]$, [K] and P are the same as defined eq. from B.20 to B.22. One can see that you have received the same final equations B.19 using two different approaches.

Step 5: The equations B.19 must be resolved after merging the Dirichlet boundary conditions specified on the S1 domain and the initial conditions.

Notes:

The expressions for [K_1 (e)], [K_2 (e)], [K_3 (e)] e P(e) and can be rewritten in matrix form as:

$$\left[K_1^{(2)}\right] = \iiint_{V^{(e)}} [B]^T [D][B] dV \tag{B.27}$$

$$\left[K_2^{(2)}\right] = \iint_{S_2{}^{(e)}} h[N]^T [N] dS_2 \tag{B.28}$$

$$\left[K_3^{(2)}\right] = \iiint_{V^{(e)}} \rho c[N]^T [N] dV \tag{B.29}$$

$$\vec{P}^{(e)} = \vec{P}_1^{(e)} - \vec{P}_2^{(e)} + \vec{P}_3^{(2)} \tag{B.30}$$

Where

$$\vec{P}_1^{(e)} = \iiint_{V^{(e)}} q[N]^T dV \tag{B.31}$$

$$\vec{P}_2^{(e)} = \iint_{S_2{}^{(e)}} q[N]^T dS_2 \tag{B.32}$$

$$\vec{P}_3^{(e)} = \iint_{S_3{}^{(e)}} hT_\infty [N]^T dS_3 \tag{B.33}$$

$$[D]=\begin{bmatrix} k_x & 0 & 0 \\ 0 & k_y & 0 \\ 0 & 0 & k_z \end{bmatrix} \tag{B.34}$$

$$[B]=\begin{bmatrix} \frac{\partial N_1}{\partial x} & \frac{\partial N_2}{\partial x} & \cdots & \frac{\partial N_p}{\partial x} \\ \frac{\partial N_1}{\partial y} & \frac{\partial N_2}{\partial y} & \cdots & \frac{\partial N_p}{\partial y} \\ \frac{\partial N_1}{\partial z} & \frac{\partial N_2}{\partial z} & \cdots & \frac{\partial N_p}{\partial z} \end{bmatrix} \tag{B.35}$$

Once involved all three methods of heat transfer, the differential equation that governs the phenomenon becomes non-linear (due to the introduction of the term irradiation). It will make it necessary then an iterative procedure which will be described later.

B.1.3. COMSOL Multiphysics

COMSOL Multiphysics is a spreadsheet program that allows to model and solve many types of physical and engineering problems based on partial differential equations (PDE). This software allows you to create multiple physical models, ie models that solve coupled physical phenomena simultaneously.

The program is divided into several modules, each of which allows to solve a particular type of problem, depending on the physical nature of the process that is the basis. The modules that were used during the modelling were the form of Earth Science and Structural Mechanics Module.

The Earth Science Module is used to model the soil as a porous medium. In particular the form is used to heat transfer by conduction and convection, that solves the equation of heat transfer in a porous solid with fluid or gas within the pores, also in motion.

The Form Mechanics of Structures is used to solve the equation of equilibrium of the elastic solid in order to find the state of stress and deformation of the structure considered. Furthermore, using the Thermo-Structural Interaction module, you can solve simultaneously the displacement field and temperature range and find the stress-strain generated in the solid based on changes in temperature.

B.1.3.1. *Earth Science Module* – Convection and conduction

This application is able to analyze the heat transfer by convection and conduction in applications involving the geotechnical sciences. Through this type of modelling is possible to describe the heat transported by a fluid in movement described by a speed range. It is assumed that the domain is constituted by a single fluid moving through a solid matrix consists of a number of materials, up to five.

The equation that describes the process of conduction and convection in the ground is as follows:

$$\delta_{ts} C_{eq} \frac{\partial T}{\partial \theta} + \nabla\left(-K_{eq} \nabla T\right) = -C_L u \nabla T + Q_H + Q_G \qquad \text{(B.36)}$$

The dependent variable is the temperature, T. In the equation, C_{eq} is the volumetric heat capacity equivalent; K_{eq} defines the equivalent thermal conductivity; C_L is the volumetric heat capacity of the fluid Mobile. The total velocity of the fluid u is a vector composed of the velocity u, v and w in the three directions. The terms in the second member of the equation, Q_H and Q_G, represent sources of heat generated and geothermal energy. The coefficients of the equation and the heat sources can vary in both space and time, remain constant, being dependent on the temperature T.

The flow of heat transfers includes both inside and through the solid matrix as well as the fluid moving. The total heat flow is governed by the equation:

$$N = -K_{eq} \nabla T + C_L u \nabla T \qquad \text{(B.37)}$$

where N represents the vector of heat flow and the temperature T is the dependent variable. This equation contains two terms: the first describes the thermal flux as proportional to the temperature gradient, the second is the convective heat flux or heat that moves at the velocity of the fluid. In a dry solid, the heat flux proportional to the temperature gradient is the phenomenon of diffusion of heat for only conduction. In porous media, however, the spread may also include variations in the intensity of small scale of velocity and direction.

Because the fluid moving occupies only the interstices between the grains solids, it is possible to describe the convective heat transfers to and from a model element only by the properties of the liquid. For the conduction, it is reasonable to put together the properties of the fluid and components fixed inside the porous medium. In the program can choose to add different materials and to automate the calculation of equivalent properties as follows.

C_{eq} is the equivalent property that describes the volumetric capacity of storing heat. It is typically defined by the volume-average of the properties of the different materials constituting the model.

K_{eq} describes the velocity at which it transfers heat. It is calculated the same as the previous parameter, such as volume-average of the thermal conductivities of the different materials.

The boundary conditions default to define the way in which the model domain interacts with the surrounding environment may be:

- Temperature: specify a temperature on the boundary;

- Heat flow: Specify the incoming flow through the outline;

- Convective flow: this boundary condition is a boundary where the heat enters or leaves by means of a fluid;

- Thermal insulation: There is no heat flux through the boundary (adiabatic boundary);

- Axial symmetry: using this when you have symmetry axes.

B.1.3.2. Structural Mechanics Module

The module of Interaction thermo-structural combines a form of continuum mechanics with a module of heat transfer. The coupling appears in the level of the subdomain, where the temperature calculated by the module of heat transfer acts as a thermal load for the structural model, causing thermal expansion.

The solids expand with increasing temperature, causing thermal deformations which develop in the material. These thermal deformations combined with elastic deformations caused by structural loads give rise to the total deformation:

$$\varepsilon = \varepsilon_{el} + \varepsilon_{th} \tag{B.38}$$

The thermal deformation depends on the temperature T, the reference temperature T_{ref}, and for the tensions from the coefficient of thermal expansion α:

$$\varepsilon_{th} = \alpha\left(T - T_{ref}\right) \tag{B.39}$$

Thermal expansion causes displacements, stresses and strains. To apply the coupling need only specify the coefficient of thermal expansion α and the two fields of temperatures T and T_{ref}. These temperatures can have any mathematical expression and other variables are typically resolved into modules such as, for example, that of heat transfer.

B.2 Model CaRM: FOR MODELS THE HEAT TRANSFER BETWEEN GHE AND THE GROUND

Model CaRM, (De Carli et al. 2009), is based on the electrical analogy to solve the heat conduction equation under unsteady state conditions. For a homogeneous isotropic solid material whose thermal conductivity is independent of temperature and within which no heat is generated, the heat conduction equation is:

$$\frac{\partial T}{\partial \tau} = \alpha \nabla^2 T \qquad \text{(B.40)}$$

where α is the thermal diffusivity of the material. In some cases an analytical solution of the Eq. B.40 is available. However, for most real cases, analytical solutions are difficult to obtain and a numerical approach is preferred. In CaRM a numerical method is used to discretize the heat conduction differential equation, making use of the control volume approach.

The model used in the present study is named CaRM (De Carli et al. 2009), a lumped model which considers the heat transfer in the ground solely by heat conduction. In the model the ground can be composed of several sub-regions, each with different thermal and physical properties. They are mainly determined by the mineral content, the porosity and the degree of water saturation.

In this model, the heat flow between the fluid inside the first part of the borehole near the ground surface level and the outside air is not considered, since the variation due to air temperature penetrates to a depth of a few meters, which causes a very limited influence on the overall performance of vertical heat exchangers (usually borehole length is around 100 meters). The heat transfer between the fluid inside the bottom part of the borehole and the ground beneath is not considered, introducing this way a conservatory calculation.

The model allows to consider different compositions of soils (sub-regions), as shown in Figure B.1: each of them can have a particular undisturbed ground temperature; in this way it is possible to consider a vertical profile of temperature as usual happens in a geothermal site. The model can take into account three different types of ground heat exchangers: single U-tube, double U-tube, coaxial pipes. In the model a maximum radius r_{max}, from the borehole axis, has to be fixed (Figure B.1.a). For a distance, from the borehole axis, $r > r_{max}$, the temperature is equal to the undisturbed ground temperature T_g.

For modelling, the ground surrounding, the borehole is divided into *m* overlapped plates, as can be seen in Figure B.1.b. Also the borehole is divided into *m* plates. Heat transport in vertical direction between two overlapped plates is not considered, therefore the heat flow is one dimension, along the radial direction. The temperature within the annular region is assumed to depend on radius and time. The cylindrical symmetry around the single vertical borehole is assumed: local disturbances due to the U-tube in the borehole are neglected.

Each plate is consequently divided in *n* annular regions at different distances from the axis of borehole (Figure B.1.b – B.1.c). The heat transfer between the pipe wall of the heat exchanger and the grout wall depends on the position of the pipes, the thermal properties of the filling material, as well as the thermal properties of the pipes. All these thermal resistances are assembled in a single parameter, the so called thermal resistance of the borehole (R_b). In CaRM the evaluation of R_b is derived by a finite element numerical model, where the different contributions are split in different thermal resistances, as can be seen in Figure B.2 for the case of a double U pipe: between pipe and pipe, and between the pipe and the borehole wall. Once determined these resistances a contribution of the thermal inertia of the grout is considered as well. More details on the model and on the equations used can be found in (De Carli et al. 2009).

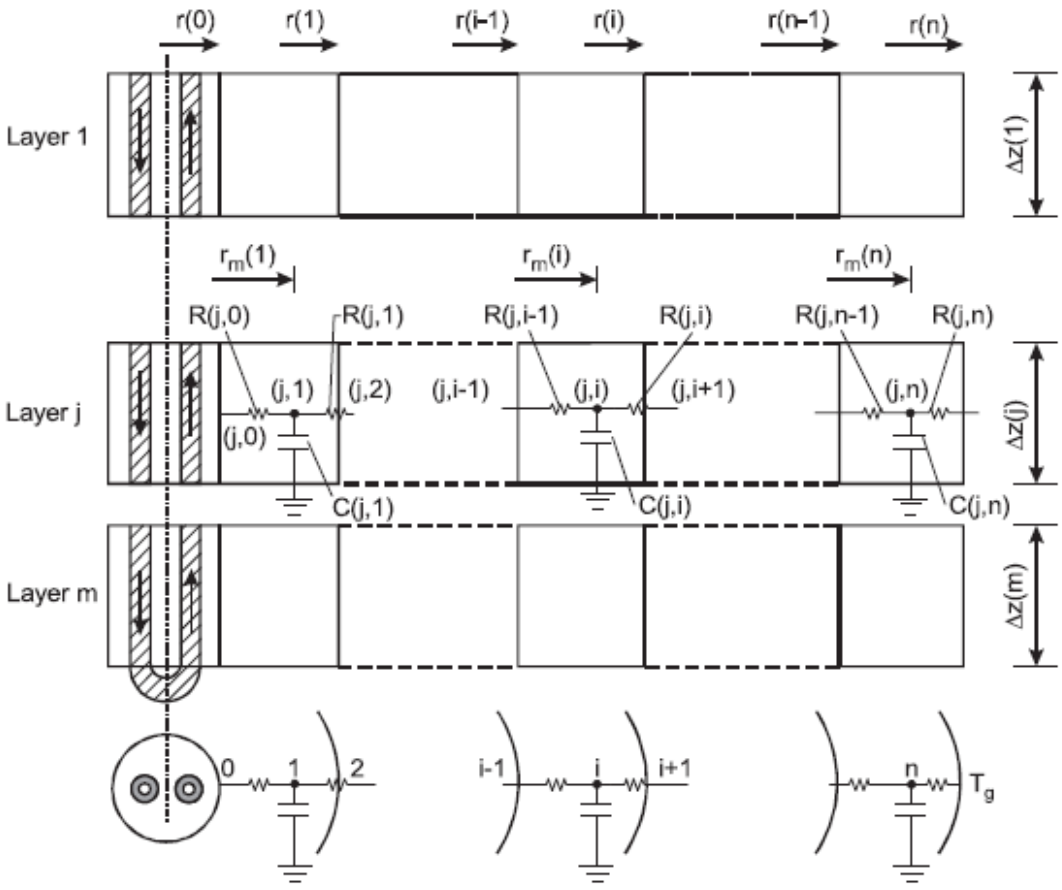

a)

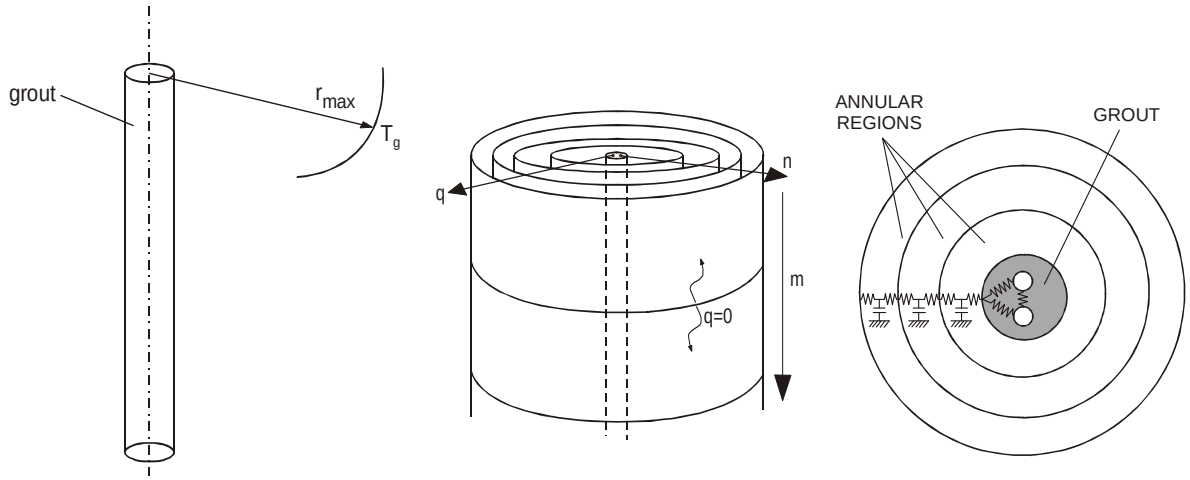

b) c) d)

Figure B.1: General approach of the model CaRM

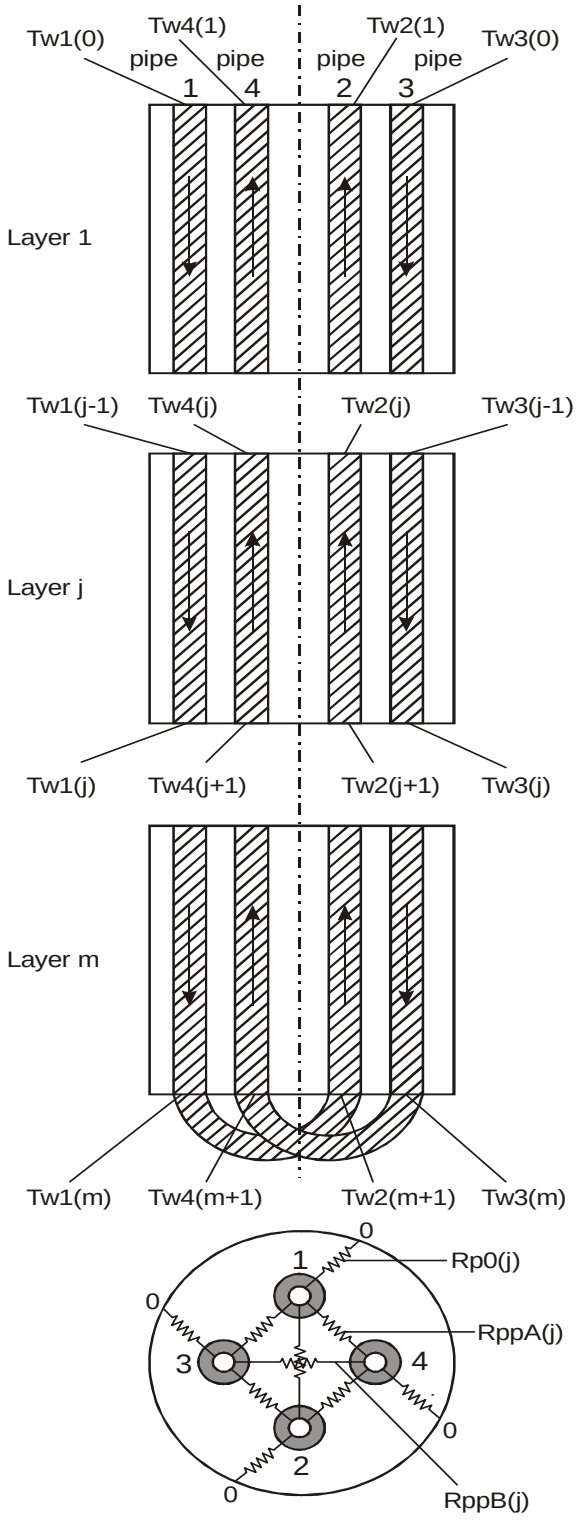

Figure B.2 – Modelling exemplification of the borehole and the heat exchanger in a double U-pipe.

B.3 Dimensioning of the vertical probes (ASHRAE)

For dimensioning the probes follow a method known as ASHRAE, this method provides a calculation procedure using the method developed by Ingersoll in 1954 and revived and implemented by Kavanaugh and Rafferty in 1997. reference equations are based on the cylindrical source model proposed by Carslaw and Jaeger in 1947, and adapted to the use of geothermal probes through the introduction of additional parameters which consider the geometry, layout and design parameters of the heat exchangers.

The method ASHRAE defines the parameters to be considered in the design phase, such as: the temperature of the undisturbed soil (measured in the test GRT), the temperature of the incoming fluid to the heat pump on the ground side, the flow rate and the properties of the heat transfer fluid (only water or water mixture - antifreeze fluid density, viscosity, conductivity, thermal diffusivity and flow regime), thermal properties of the soil (such as conductivity and thermal diffusivity), properties of the probe (probe type: single tube, double tube , coaxial, diameter, layout, type of filler material and its thermal characteristics), characteristics of the field probes (total number probes, distance between them, provision of field, type of circuitry if in series or in parallel), and finally the thermal loads and refrigerants of the days of the project and annual hours equivalent to full load.

The ASHRAE method defines two equations that represent the overall lengths of the probes in the case of heating and cooling:

$$L_C = \frac{q_a \cdot R_{ga} + \left(q_{lc} - \overline{W_c}\right) \cdot \left(R_b + PLF_m \cdot R_{gm} + R_{gd} \cdot F_{sc}\right)}{t_g - \left(\frac{t_{wi} + t_{wo}}{2}\right)_c - t_p} \qquad \text{(B.41)}$$

$$L_h = \frac{q_a \cdot R_{ga} + \left(q_{lh} - \overline{W_h}\right) \cdot \left(R_b + PLF_m \cdot R_{gm} + R_{gd} \cdot F_{sc}\right)}{t_g - \left(\frac{t_{wi} + t_{wo}}{2}\right)_h - t_p} \qquad \text{(B.42)}$$

Where:

c, h	subscript "c" and subscript "h" indicates summer operation (cooling) and winter (heating);
Lc, Lh	lengths of perforation, required respectively for cooling (summer) and heating (winter) the building [m];
q_a	Average heat flow exchanged with the ground in a year [W];
q_{lc}, q_{lh}	Design loads required for cooling ($q_{lc} < 0$) and heating ($q_{lh} > 0$) [W];

$\overline{W_c}, \overline{W_h}$ Electric power absorbed by the compressor of the heat pump / chiller in correspondence of the design load [W];

PLF_m Load factor / time-monthly;

F_{sc} Loss factor, linked to possible short circuit thermal probe between pipe flow and return;

t_g Temperature of the subsoil is not influenced by the presence of the probe [° C], also called undisturbed soil temperature;

t_p Temperature penalty, summarizes the thermal influence between the probes through the soil [° C];

t_{wi}, t_{wo} Temperature of supply and return fluid that feeds the geothermal probes always in two cases: summer (subscript c) and winter (subscript h) [° C];

R_b Thermal resistance per unit length of the probe, between the fluid and the edge probe [(m K) / W];

R_{ga} Equivalent resistance per unit length of the ground, impulse annual [(m K) / W];

R_{gm} Equivalent resistance per unit length of the ground, impulse monthly [(m K) / W];

R_{gd} Equivalent resistance per unit length of the ground, impulse daily [(m K) / W];

The thermal flows, the loads of the building and the penalties in temperature are regarded as positive in heating mode, and negative in the cooling.

The presence of two equations for the length of the probe is due to the fact that a corresponds to the needs winter and the other to the needs summer, so the total length of the probe to be installed in situ corresponds to the greater of the two resulting. For example, in the case of prevailing requirements winter than in summer, the choice to be adopted will be the length of the probe winter, or in the case of summer requirement that prevails over the winter an interesting choice is to be dimensioned according to the load and winter compensate for undersized summer using an auxiliary system, these considerations will be arranged by the designer during the design phase.

Meaning of the terms:

In the calculation of the lengths of the probe, the process of heat transfer is studied in two separate parts, one of which represents the part of soil / rock around the well, the other is the inner portion to the well containing the filling material, the vertical probes and fluid. With such a subdivision is necessary to calculate two types of thermal resistances: one of which is associated with the timing pulses of heat in the soil (thermal resistance of the ground), the other is referred to the cumulative resistance of the heat transfer fluid, the tubes and the filling material of the well (thermal resistance of the well). In the first part of the process of heat transfer is regarded as transitional, while in the second, to simplify, the process is considered as stationary.

The thermal resistance of the ground per unit length is calculated as a function of the period of time in which a particular pulse of heat is applied. Are considered three different heat pulses related to:

- Net annual heat flows (q_a);

- Thermal monthly flows during the month of project (q_p PLF);

- Maximum heat flows during short periods of time during the day of the project (q_p).

The calculation of these heat pulses allows to obtain, through the method in cylindrical source, the thermal resistances associated respectively represented by R_a, R_m and R_g.

q_a : Is defined as the average annual flow of heat absorbed or given up by the soil and is calculated as follows:

$$q_a = \frac{\sum q_k \cdot \frac{EER+1}{EER} \cdot h_c + \sum q_{lh} \cdot \frac{COP-1}{COP} \cdot h_h}{8760} \qquad \text{(B.43)}$$

Where:

h_h, h_c are equivalent hours per year full load for heating and cooling, they represent the number of hours of operation of the system if this worked constantly at maximum load. This approach has the advantage of limiting the number of data necessary for the calculation of q_a, despite this being equivalent to those that require as input data monthly detail.

8760: are the hours in a year.

The values of peak load q_{lc}, q_{lh} are the same as seen in equations calculate the length winter / summer. The EER values are chosen according to the inlet temperature to the heat pump (project datum).

$PLFm$: Is the load factor / partialization, it is very similar to a utilization factor and is defined by the relation, valid for both the summer and for the winter:

$$PLF_m = \frac{\sum_1^{24} Hourly\_Load \times Hours}{Peak\_Load \times 24h} \times \frac{Operating\_days\_per\_month}{day\_per\_month} \quad \text{(B.44)}$$

$\overline{W_c}, \overline{W_h}$: : For the electrical power absorbed by the compressor of the heat pump / chiller in correspondence of the design load, it is had that the building is divided into different zones (i zones) to be conditioned, for each subdivision consider a significant time of day in blocks (for example: 4 hours from 8:00 to 12:00, 4 hours from 12:00 to 16:00, and 4 hours from 16:00 to 20:00), and for each block and for each zone (type in a matrix) locates the maximum load. Next, identify the block having the sum of the loads increased, there has been and will be called a block "b_m". Many heat pumps are considered as the number of zones, and by technical catalogs, find the size needed to cool each zone ($Q_{n,i}$) trying to stay just above the daily maximum load area. From the catalogs is also apparent electrical input power ($W_{c,I}$, $W_{h,i}$).

For each zone, in this case, the Part Load Factor is defined as:

$$PLF_{dj} = \frac{Q_{bm,j}}{Q_{nj}} \quad \text{(B.45)}$$

Finally, sum the product of i Part Load Factor for the respective powers:

$$\overline{W_c} = \sum_i PLF_{d,j} \cdot W_{cj} \quad \text{(B.46)}$$

$$\overline{W_h} = \sum_i PLF_{d,j} \cdot W_{hj} \quad \text{(B.47)}$$

An alternative method simpler, but less precise, for the search of these terms is to consider a single zone covering all the building, in which case will have:

$$PLF_{dj} = \frac{Q_{\max}}{Q_n} \quad \text{(B.48)}$$

Consequently:

$$\overline{W_c} = PLF_d \cdot W_c \quad \text{(B.49)}$$

$$\overline{W_h} = PLF_d \cdot W_h \tag{B.50}$$

Where:

Q_{max} is the maximum load of the building;

Q_n is the nominal load of the machine;

W_c, W_h is the electrical power of the heat pump/chiller in summer and winter.

F_{sc} : Is the term that considers the type of connection between the probes (series and parallel) and the specific flow rate of the field probes, referred to the rated power of the machine. This term evaluates how detrimental is the heat flow between fluid flow and return and between the fluid and the ground. The values of Fsc are tabulated in the literature and generally vary from 1.01 to 1.06 (Kavanaugh and Rafferty 1997), see Figure B.3.

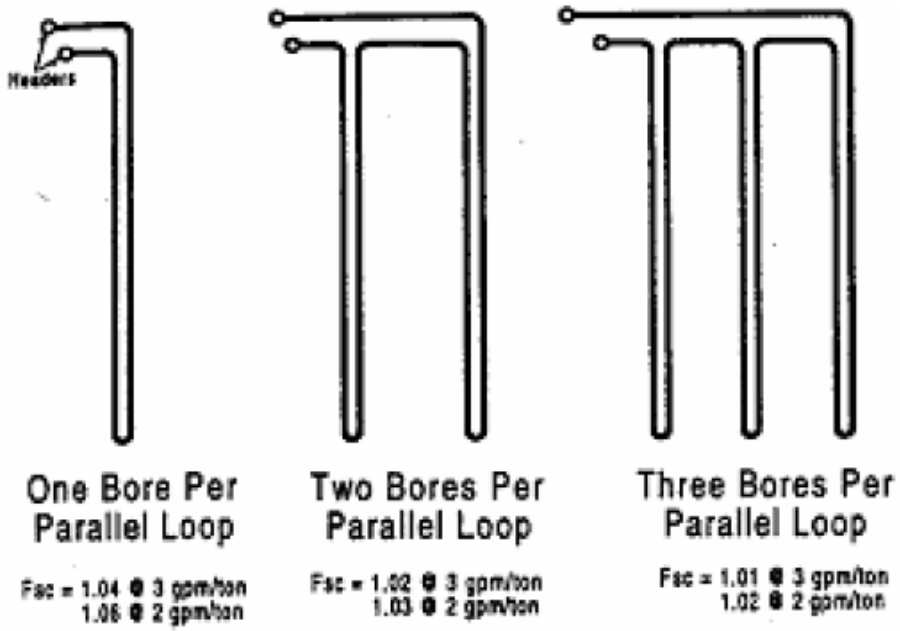

Figure B.3 – Values of Fsc as a function of the connection between the probes and the specific flow. (Kavanaugh e Rafferty 1997).

t_{wi}, t_{wo} : Are the temperatures of the fluid entering and exiting from geothermal probes in the design conditions. The two values are linked by an balance equation:

$$q_{lc} - \overline{W_c} = \dot{m}_w \cdot c_{pw} \cdot \left(t_{wo} - t_{wi}\right)_c \tag{B.51}$$

$$q_{lh} - \overline{W_h} = \dot{m}_w \cdot c_{pw} \cdot \left(t_{wo} - t_{wi}\right)_h \quad \text{(B.52)}$$

They, however, depend on the temperature of the undisturbed soil and by the characteristics of the heat pump, in fact the choice of a value close to that of the undisturbed ground would entail a high efficiency of the system, but with the consequence of a length of the pipes too that goes to affect the initial installation costs. While, the choice of a value of temperature away from that of the undisturbed soil is obtained a minimum length of the tubes but with the consequence of a reduced efficiency in heating and cooling.

Kavanaugh and Rafferty (1997), to dimension heat exchangers in such a way as to be in the range of optimal functionality of the machine, recommend to select ranges of inlet temperature to the heat pump of about 5 - 11 ° C and less than about 11 - 17 ° C higher than the temperature of the undisturbed soil respectively for the heating mode and cooling.

Furthermore authors Baietto et al. (2010), recommend that in the heating mode, to avoid the use of antifreeze solutions in a mixture of heat transfer fluid, it is necessary to select inlet temperatures to the heat pump of at least 3 - 4 ° C, which allow to maintain a threshold of safety above the water freezing.

t_g : Earth's temperature is a matter of design found in tables or special tests.

t_p : The temperature penalty, summarizes the mutual interference of thermal fields of probes through the ground, hitting the temperature difference between the fluid and soil undisturbed. This quantity takes low values if the loads are similar in summer and winter form, higher values if there is a predominance in winter or summer operation. Initially, t_p can be taken at the end there will be the assumption made.

Note the q_a, the length *l* of each probe and the grid choice with which to position the probes, and then analyzed the resulting temperature variation. The t_p assumed to be approximately equal to that obtained by the following empirical relation:

$$t_p = \frac{1 \cdot N_4 + 0.5 \cdot N_3 + 0.25 \cdot N_2 + 0.1 \cdot N_1}{N_{tot}} . t_{p1} \quad \text{(B.53)}$$

Where**:**

N_4 Number of probes surrounded on all four sides by other probes;

N_3 Number of probes surrounded on three sides by other probes;

N_2 Number of probes bordering on two sides with other probes;

N_1 Number of probes bordering on one side with other probes;

N_{tot} Total number of probes;

t_{pl} Temperature of penalization of a probe surrounded by other on all sides.

The determination of t_{pl} is made on the basis of the following assumptions: one considers the parallelepiped of ground, of square section, *ds x ds*, and height *l*, which surrounds the probe (d_s coincides with the distance between the probes in the grid). This portion of the subsoil is capable of accumulating heat, but not to exchange it with the ground, outside of its peripheral surface. The verification is done on the basis of 10 years, on the assumption that this is the period of time required for i annual heat fluxes should be fully operational.

Since, the heat stored by the heat capacity data for the temperature difference (t_{pl}) between the ground and the undisturbed surrounding the probe, have:

$$t_{pl} = \frac{Q_{stored}}{\rho \cdot c_p \cdot d_s^{\,2} \cdot l} \qquad \text{(B.54)}$$

Where:

ρ Density of the soil

c_p Specific heat of the soil

Q_{stored} Heat accumulated after 10 years of operation

The calculation of the heat diffused after 10 years, is made using the solution of the linear source and considering a cylinder with a diameter of 8 - 10 meters, since, on average these distances are affected by the transmission of heat in this period of time. In fact, for a spacing between probes of more than 15 m do not occur perceptible effect, while for distances of less than 5 m, thermal interference occurs, deleterious for the efficiency of the entire system. Not being the temperature gradient constant along the radius of the cylinder investigated, are considered more concentric cylinders and the change in average temperature between them:

$$Q_{stored} = \sum \rho \cdot c_p \cdot \pi \cdot l \cdot \left(r_0^{\,2} - r_1^{\,2}\right) \cdot \Delta t_r \qquad \text{(B.55)}$$

Δt_r is the difference between the temperature of the undisturbed soil and that at a distance r from the source and is determined by applying the solution of the linear source:

$$\Delta t_r = \frac{q_a \cdot I(X)}{2 \cdot \pi \cdot \lambda_g \cdot l} \qquad \text{(B.56)}$$

Where the term I(X) is diagrammed below Figure B.4 (Ingersoll LR, Zobel, Ingersoll AC 1954), as a function of X which is a dimensionless parameter defined as follows:

$$X = \frac{r}{2\sqrt{\alpha_g \cdot \tau_1}} \qquad \text{(B.57)}$$

Dove:

α_g Thermal diffusivity of the ground;

τ_l Time (years)

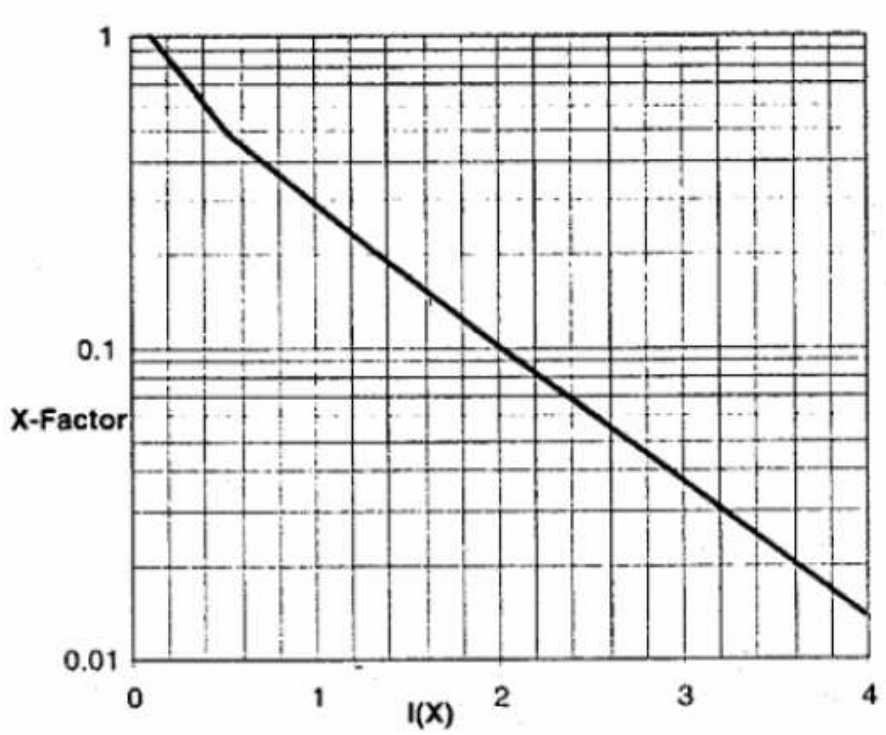

Figure B.4 – Graph for the determination of I(X) , (Ingersoll L.R., Zobel, Ingersoll A.C. 1954).

With the presence of movements of groundwater, the temperature of penalisation can be reduced because the heat is transported from the aquifer far field probes. In this case assumes a lower time of τ_l .

Another method to determine the temperature of penalization Kavanaugh and Rafferty (1997) propose that the tables based on the grid distribution of the probes, the distance between them and to the ratio between the equivalent hours of heating and cooling at full load, estimate the temperature.

R_b : Represents the thermal resistance per unit length between fluid and soil in correspondence with the outer surface of the probe, in contact with the ground itself. It introduces the equivalent resistance of the hole / probe with respect to the ground, where the probe is considered a cylinder introduced into the soil as the radiator or cooling. This term can be considered to be constant with respect to the thermal resistance of the ground, since the heat transfer fluid, the piping and the filling material have a thermal inertia negligible compared to that of the surrounding terrain.

To determine the resistance between the fluid and the edge of the probe, one neglects the heat capacity of the filler, being negligible compared to that of the surrounding terrain.

The thermal resistance is given by:

$$R_b = R_{pp} + R_{gr} + R_t \qquad \text{(B.58)}$$

Where:

R_{pp} Overall thermal resistance of the tubes in which fluid flows;

R_{gr} Resistance of the jet filling;

R_t Resistance of the outer tube which can be lowered into the drilling phase to avoid clogging of the shaft before inserting the probes and make the jet; this tube can be removed ($R_t = 0$) or less consolidated once the jet.

Choices geometrical dimensions (D_{po} and D_{pi}, respectively external and internal diameter) and the material of the U-tube (thermal conductivity λ_p) and calculated the coefficient of heat exchange between the liquid and the tube wall (h_i), the resistance of a single tube is given by:

$$R_p = \frac{\ln\left(\frac{D_{po}}{D_{pi}}\right)}{2 \cdot \pi \cdot \lambda_p} + \frac{1}{\pi \cdot D_{pi} \cdot h_i} \quad \text{(B.59)}$$

While the thermal resistance R_t of the possible outer tube is given by:

$$R_t = \frac{\ln\left(\frac{d_{bo}}{d_{bi}}\right)}{2 \cdot \pi \cdot \lambda_{pt}} \quad \text{(B.60)}$$

For the individual U-tube heat resistance of the grout can be calculated with the following relationship:

$$R_t = \frac{1}{S_b \cdot \lambda_{gr}} \quad \text{(B.61)}$$

Where:

λ_{gr} Thermal conductivity of the material of the grout;

S_b Factor short circuit.

The term S_b is evaluated with the following relation (Remund CP 1999):

$$S_b = \beta_0 \cdot \left(\frac{d_b}{D_{po}}\right)^{\beta_1} \quad \text{(B.62)}$$

Where:

β_0, β_1 are geometric factors shown in the Table B.1 (Remund CP 1999):

Table .B.1 – Coefficients for the calculation of the thermal resi stance of the filling, (Remund C.P. 1999).

Configurazione	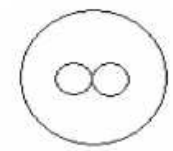 A	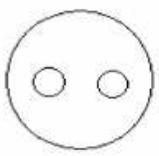 B	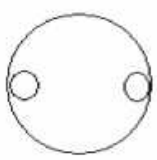 C
β_0	20.10	17.44	21.91
β_1	-0.9447	-0.6052	-0.3796

Being two tubes in which flows the fluid in the pipe, their overall thermal resistance is the result of two resistors in parallel Figure B.5:

$$R_{pp} = \frac{R_p}{2} \qquad \text{(B.63)}$$

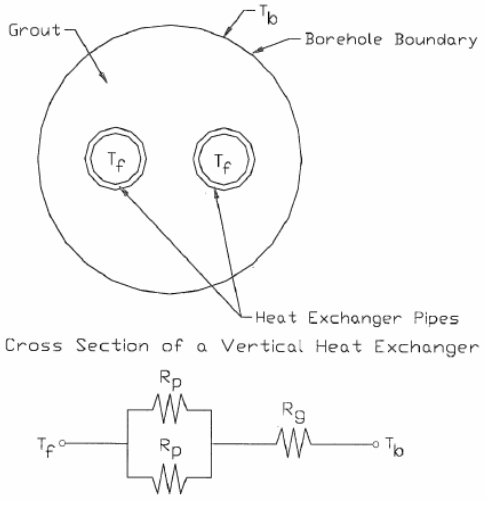

Figure B.5 – Equivalent circuit of thermal resistances of the probe. (Remund C.P. 1999).

R_{ga}, R_{gm}, R_{gd} : Are resistances which refer to the soil surrounding the hole and correspond to the value assumed by this quantity in particular moments of system operation, ie when it has reached a certain stability in heat exchange net (one or more years), in correspondence of the exchange medium that occurs in the month of project, in the moment in which there is a peak in the hours of project.

The first is the thermal resistance equivalent, the land for a thermal pulse annual, generally is 10 years (3650 days after, the thermal flux may have stabilized); R_{gm} represents the equivalent resistance, thermal impulse on a monthly basis (usually designing for the month, 30 days, in which occurs the peak of the load); R_{gd} represents the equivalent resistance, thermal impulse on a daily basis (can be sized for 6 hours, 0.25 days of daily peak).

The calculation of the equivalent resistance of the soil is derived from the solution proposed by Carslaw and Jaeger (1959), in which it defines a number of Fourier which correlates the time during which the thermal exchange occurs with the outer diameter of the probe and the diffusivity of the ground α_g:

$$F_O = \frac{4 \cdot \alpha_g \cdot \tau}{d^2} \tag{B.64}$$

It is assumed that a system of this type suffers mainly three pulses of heat flow, for the following time periods: 10 years (3650 days), 1 month (30 days), peak daily (6 hours = 0.25 days), consequently i periods of pulse:

$$\tau_1 = 3650 \ \ days$$
$$\tau_2 = 3650 + 30 = 3680 \ \ days$$
$$\tau_f = 3650 + 30 + 0.25 = 3680.25 \ \ days$$

Rewriting the relation of F_O for each period, have:

$$F_O = \frac{4 \cdot \alpha_g \cdot \tau_f}{d_b^{\ 2}} \tag{B.65}$$

$$F_O = \frac{4 \cdot \alpha_g \cdot \left(\tau_f - \tau_1\right)}{d_b^{\ 2}} \tag{B.66}$$

$$F_O = \frac{4 \cdot \alpha_g \cdot \left(\tau_f - \tau_2\right)}{d_b^{\ 2}} \tag{B.67}$$

Where:

α_g Overall thermal resistance, of tubes in which fluid flows;

d_b Diameter of the perforation and then the outer diameter of the probe.

From graphics present in the literature are obtained by the respective values of G_f, G_1, G_2, from which knowing the thermal conductivity of the subsoil λ_g, can calculate the thermal resistance of the ground by means of the following relations:

$$R_{ga} = \frac{G_f - G_1}{\lambda_g} \quad \text{(B.68)}$$

$$R_{gm} = \frac{G_1 - G_2}{\lambda_g} \quad \text{(B.69)}$$

$$R_{gd} = \frac{G_2}{\lambda_g} \quad \text{(B.70)}$$

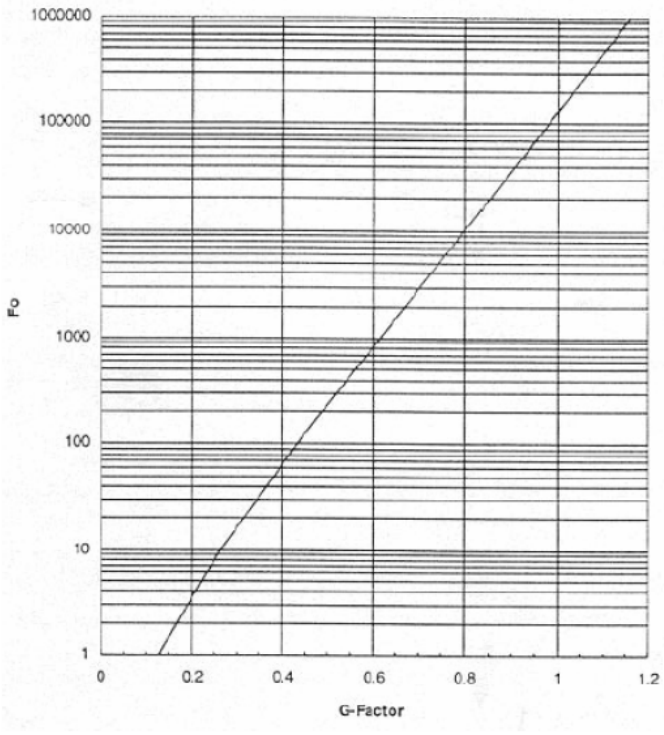

Figure B.6 – Values of G as a function of F_0 (Ingersoll L.R:, Zobel, Ingersoll A.C. 1954).

Another analytical model for the calculation of the equivalent resistance of the hole / probe with respect to the ground Rb is called quasi - three-dimensional proposed by Zeng et al., 2003. the model can be applied to the model integration of dimensioning ASHRAE. It goes to estimate in detail the effect of thermal short-circuit between the probes on the basis of the geometrical and physical characteristics of the actual complex well - probe, whereas both probes to single U that probes to double U. also defines the number of pipes in the well, the spacing between the tubes inside the well, the thermal conductivity of the filler material and to calculate the resistance of well correlated. The method of Zeng et al. (2003) allows to evaluate the influence of the spacing of the tubes and thermal conductivity of the grout on the thermal resistance of well

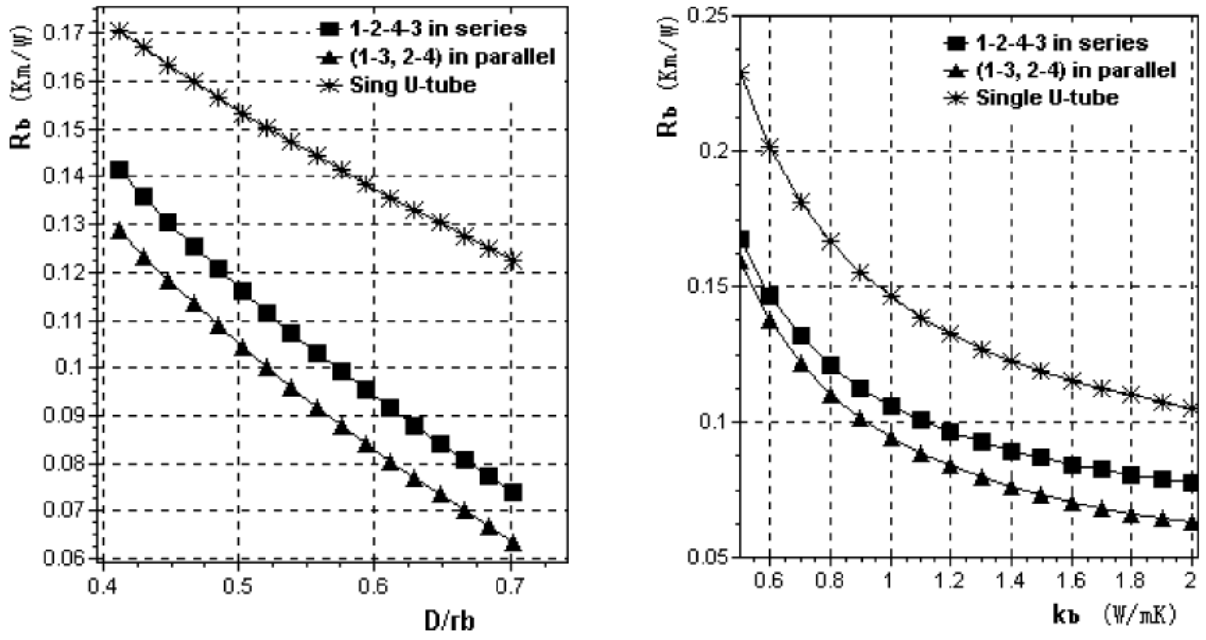

Figure B.7 – Variation of the equivalent resi stance the hole/probe with respect to the ground calculated with the model almost three-dimensional Zeng et al (2003), to vary the spacing between the tubes and the thermal characteristics of the materials of filling of the well pipe single U.

For the best compromise between cost / benefit can dimension the probes reducing the length of working on various aspects, such as:

- Raising the temperature of the incoming fluid to the heat pump in the cooling mode, or lowering the same in heating;

- Installing a hybrid system that compensates for the differences in heating and cooling, this occurs when there is a significant difference between the loads in summer than winter loads;

- By reducing as much as possible the thermal interference between the probes, thus increasing the distance between the probes;

- By varying the parameters that affect the thermal resistance of the well.

ANNEX C

C.1 Ground Response Test (GRT)

In complex cases, it is very important to know the real thermal resistance of a probe or a pole energy, in order to understand its exchange capacity and decide how many exchangers install a function of energy necessary. If for small plants is not wrong to use values of thermal resistance of the heat exchanger estimated based on the characteristics of the pile energy, and use values of thermal conductivity λ soil present in the literature, this is not possible, for systems with a very field probes ample. For these plants, with a power greater than 30 kW and with a greater number of 10 probes, it becomes necessary to perform a test of geothermal response.

In the practice of geothermal plants, this test has a fundamental significance: it allows to calculate the parameters necessary for the design, which are real because measured on site. In the absence of geotechnical data on the types of ground, which are in a certain place chosen for a geothermal system, it is difficult to predict with good accuracy the rock layers present, and their thermophysical characteristics connected. In the case of energy piles, in the construction of the foundation one is able to have direct knowledge of the various layers interested, and these data can then be used to correct the preliminary design.

The GRT, acronym of Ground Response Test, is a test that has the purpose of measuring the thermal properties of the geothermal heat exchanger, installed on a particular subsurface, the thermal conductivity of the ground λ [W / (m K)], and the resistance heat exchanger Rb [K / (W / m)]. The purpose of this test is twofold, as it allows to confirm the thermal characterizations of the soil and of the probe measured at the design stage, in fact it can directly obtain the values to be inserted in the simulation programs of the geothermal field, therefore, the test becomes a validation of design choices. For this reason, the test is carried out in the course of work, or still in the design stage, with the advantage of being able to change the field probes, before the work is finished optimizing plant performance and in the case of reducing the number of probes with the result of lowering the initial costs.

A second purpose, is that the thermal resistivity of the probe depends mainly on the materials used, the quality of the cementation, less instead of the actual position of the probe within the perforated tube, this represents a quality parameter on the execution of the probe.

The first to speak of this process was Morgensen, at a conference in Stockholm in 1983. Later it was developed and perfected by the University of Technology of Lulea, Sweden. The measurement of these parameters provides information thermal type, relative both to the ground in question, that the geothermal probe installed. It is useful to recall that, the test results relate to the thermal properties of the heat exchanger formed by:

• subsoil;

• filling material,

• material, thickness and type of sensor,

• fluid.

The test is carried out on a pilot probe, or a probe within a foundation pile (in case of energy piles), which then becomes part of the subsequent field probes, also needs to be done before they are laid the horizontal connections.

It is necessary to know the thermal properties of the fluid, the geometry of the probe and have some general guidelines on the geology of the site is also well wait for the cement mortar filling has completed maturation approximately 3 weeks after laying.

During the GRT, a defined quantity of thermal flow is fed into the probe. It shall therefore to measure the variations in temperature of the heat transfer fluid returning to the subsurface, consequently determining the heat exchange in those conditions.

From the processing of inlet temperatures, and output of the geothermal fluid from the probe can be derived, using inverse models, both the characteristics of the soil, that a useful set of experimental data on the behaviour of the heat exchangers, necessary for sizing and for checking the correct installation of the geothermal probe.

In carrying out the phases of acquisition, it is recommended the use of a device that respects the standards ASHRAE, shown in Figure C.1:

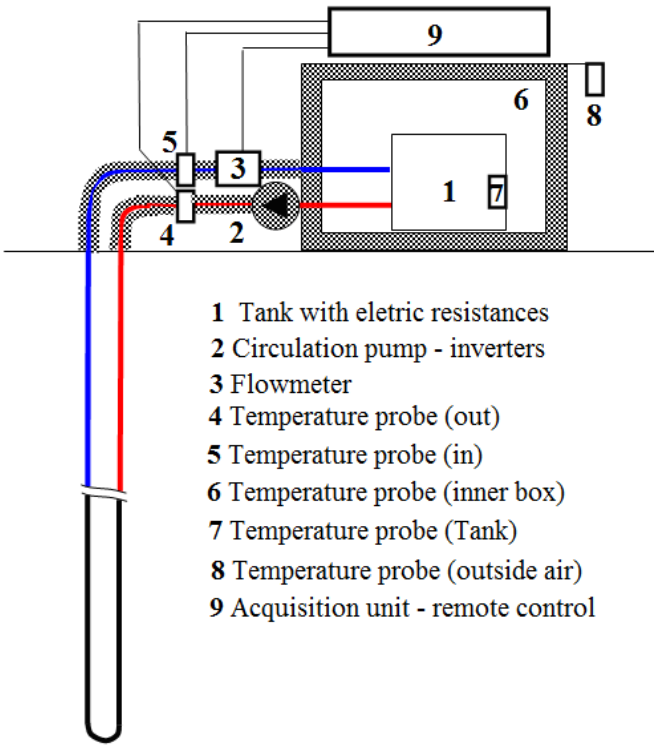

Figure C.1: Scheme of the measuring system.

The apparatus consists of a closed circuit in which water flows. The fluid is heated by some electrical resistances, which may also supplying power of 12 kW, contained within a storage tank (1). The accumulation tank, is equipped with thermal insulation and is inserted within a thermally insulated receptacle (double insulation system); the fluid is set in motion by a pump (2) equipped with a thermal insulation autonomous. Are measured and recorded continuously (start) or at intervals of 1 minute the following parameters: the volume flow of water (measuring 3), (from which we get the mass flow rate), the temperature (thermal sensor 4) and the return temperature (thermal probe 5) water, as well as the electric power absorbed by the resistors and from the pump; this coincides with the thermal power provided to the water, by the Joule effect and for viscous dissipation within the fluid. When the average temperature of the fluid increases very slowly over time (after several hours of test), this power can be considered coincident with the thermal power transmitted to ground.

Figure C.2: Measuring device and hydraulic model of the device.

The circuit follows the following path: the heat transfer fluid exits the tank (1) and, via the pump (2), is made to flow inside the geothermal probe where it exchanges heat with the ground, and finally falls into the tank where it receives power from electrical resistances. The temperature probes (4 - 5) register the inlet temperatures of the water in the probe, T_{in}, and outlet water from the probe, T_{out}.

All the pipes of the test must be suitably insulated, also the pump, filter, valves, bends, the edges were properly insulated, all parts that are in direct contact with the heat transfer fluid and subject to measures that somehow could originate a thermal bridge dispersing into the environment a portion of the thermal power imposed, have been isolated so as not to stagger the test results.

C.2 The physical principles at the base of the test: Analytical methods with Line – source model

the analysis procedure for interpreting the test data GRT is the Line - source model. is based on Kelvin's line-source theory and has been applied to simulate the behavior of the thermal exchange of the geothermal probe (Ingersoll and Plass, 1948; Sanner, 1992). Morgensen (1983) proposed this method to evaluate thermal response test data. The approach adopts the analytical solution for the response to an infinite constant-strength line-source Within a homogeneous, isotropic, infinite medium. Assuming negligible heat flow along the vertical geothermal probes and constant lateral heat flow, the temperature field around the geothermal probe is only dependent on time, t, and radial distance, r, from the borehole axis.

The temperature range is given by Carslaw and Jaeger (1959), using the exponential integral E:

$$\Delta T(r_b,t) = T(r,t) - T_0 = \frac{q}{4\pi\lambda} \cdot \int_{\frac{r^2}{4\alpha t}}^{\infty} \frac{e^{-u}}{u} du = \frac{q}{4\pi\lambda} \cdot E\left[\frac{r^2}{4\alpha t}\right] \qquad \text{(C.1)}$$

The exponential integral E, for high values of the parameter $\frac{\alpha \cdot t}{r^2}$ can be approximated by the following equation:

$$E\left[\frac{r^2}{4\alpha t}\right] = -\gamma - \ln\left[\frac{r^2}{4\alpha t}\right] - \sum_{n=1}^{\infty} (-1)^n \frac{\left(r^2/4\alpha t\right)^n}{nn!} \cong \ln\left[\frac{4\alpha t}{r^2}\right] - \gamma \qquad \text{(C.2)}$$

The maximum error from this simplification is less than 10% for the time $t_c \geq \frac{5r^2}{\alpha}$.

for which the simplified equation becomes:

$$\Delta T(r_b, t) = q \cdot R_g = \frac{q}{4\pi\lambda} \cdot \left[\ln\left(\frac{4\alpha t}{r^2} \right) - \gamma \right] \quad \text{(C.3)}$$

Thus, the temperature at hole wall (r = r_b) and valid for $t_c \geq \frac{5r^2}{\alpha}$, is defined by:

$$T(r_b, t) = q \cdot R_g = \frac{q}{4\pi\lambda} \cdot \left[\ln\left(\frac{4\alpha t}{r^2} \right) - \gamma \right] + T_0 \quad \text{(C.4)}$$

Where:

$\Delta T(r_b, t)$ = temperature difference in the neighbourhood of the borehole; is a function of the radius of the borehole and the time; equals $T_b - T_g$ [K];

t = duration of the test [s];

T_b = average temperature on the walls of the collector [K];

T_g = temperature of the undisturbed ground first intake of heat [K];

q = heat injected into the probe meter [W / m];

R_g = thermal resistance of the borehole in the neighbourhood;

λ = thermal conductivity [W/(m·K)];

a = thermal diffusivity, λ/c [m^2/s]; this value is estimated in a first approximation according to geological analysis to verify the boundary condition;

c = ρc = volumetric heat capacity [$J/(m^3 \cdot K)$];

r_b = radius of the borehole [m];

γ = Euler's constant, equal to 0,5772.

It should be specified, that the temperature along the probe is taken constant since its variability with respect to the radial field is minimal; also, considering the probe of infinite length for short periods of time as such value is much larger than the radius. Another factor, of extreme importance is the thermal resistance R_b of the well between the heat transfer fluid that passes in the tubes and the outer surface of the well, ie the surface in contact with the ground.

That is why the following relationship:

$$\overline{T}(t) = T(r_b, t) + q \cdot R_b = \frac{q}{4\pi\lambda} \cdot \ln(t) + q\left[R_b + \frac{1}{4\pi\lambda}\left(\ln\left(\frac{4\alpha}{r_b^{\,2}}\right) - \gamma\right)\right] + T_0 \qquad \text{(C.5)}$$

where:

The line – source model assumes that $\overline{T}$ corresponds to the average between the inlet (T_{in}) and outlet temperature (T_{out}) of the circulation fluid:

$\overline{T}$ = temperatura media del fluido nel collettore $T = \frac{T_{in} + T_{out}}{2}$

T_b = temperatura alla superficie della sonda [K];

q = quantity of injected power per linear meter [W/m];

R_b = thermal resistance of the well [K/(W/m)].

C.3 The procedure of construction site for testing

For the execution of the test on the heat exchanger, the work plan includes the following steps:

1. Measurement of the temperature of the ground undisturbed.

2. Measurement of the average temperature of the heat transfer fluid as a function of time, for a predetermined value of the power, constant, entered into the ground.

3. Determination of the thermal conductivity of the probe-ground (average value from surface to bottom of the heat exchanger).

4. Determination of the overall coefficient of heat transfer, per unit of length of the heat exchanger, between the water flowing in the heat exchanger and the ground undisturbed, under quasi-stationary.

C.4 Measurement of the undisturbed temperature of the ground

The measurement of the temperature of the undisturbed ground is the first to be made in the test, it is done immediately after the Operating the pump looking at the data measured outlet temperature from the probe. This measurement must be done before the heat transfer fluid passes through the pump, precisely to avoid a heating of the fluid due to the heat formed to friction and Joule effect of the pump, then an alteration of the measure. The water results to be in thermal equilibrium with the ground, since the probe is filled with fluid a few days before the test, this method is considered to be very accurate. (Gehlin 2002).

In practice it has been noticed, that does not occur a total thermal equilibrium, and then the outlet temperature equal to the return temperature, but there is always a minimum of heat input (pressure drop of the fluid in circulation), so various authors Delmastro , Noce 2011 and Basta, Minchio 2010 suggest to calculate the temperature of the undisturbed ground as a weighted average of the water temperatures measured in output from the probe: the temperatures are measured input and output to the probes at intervals of one second, in first few minutes of operation, the water that exits the probe results to be in equilibrium with the temperatures around: the average of the temperature Tout recorded during these first few minutes of operation, weighing on the relative mass flow, therefore represents the temperature of the environment in which the heat exchanger is found.

$$T_g = \frac{\sum_i T_{out,i}\,\dot{m}_i\,\Delta\tau_i}{\sum_i \dot{m}_i \Delta\tau_i} \qquad \text{(C.6)}$$

where with Δτ, is indicated the time interval between two successive recordings, and with the subscript i refers to the summation extended to all recordings of temperature and mass flow relating solely to the water contained in the probe, i.e.:

- Are excluded recordings corresponding to the first seconds of the start of the pump, during which the water flowing in the vicinity of the probe, temperature Tout is the water present in the section of pipe in the air;

- Are considered, the recordings of temperature and mass flow rate until all the water contained in the probe is transited at the probe, temperature T_{out}, whereas the instant of start of the circulation pump. Is also observed the tendency of the average temperature in the probe over time in order to assess the operation of thermal stabilization of the circuit.

C.5 Measure the average temperature of the heat transfer fluid a function of time a function of time, for constant values of power and ΔT (in – out probes) imposed on the system

As recommended by ASHRAE, the measures are executed by providing an electric power to the resistance heating apparatus, almost constant and equal to about 90 W per meter of exchanger.

Is measured continuously (start) and at intervals of 1 minute, the total power $\dot{Q}_{el}$ delivered by the mains to the electrical resistances and the pump. It 'also calculated at intervals of 1 minute the thermal power $\dot{Q}$ provided to the heat transfer fluid with the method of the flow calorimetry, or by means of the relation:

$$\dot{Q} = \dot{m} c_p (T_{in} - T_{out}) \qquad \text{(C.7)}$$

Where, $\dot{m}$ is the mass flow rate of water, cp is the specific heat capacity of water, Tin is the input temperature (or inlet) water in the heat exchanger, T_{out} is the temperature output (or return) of the water from the heat exchanger . In conditions almost stationary, the powers $\dot{Q}_{el}$ and $\dot{Q}$ must be equal (unless of measurement errors and small thermal losses through the insulation).

C.6 Determination of the thermal conductivity of the ground (average value from the ground surface to the bottom of the heat exchanger)

To determine the thermal conductivity using the method "line heat source". This method allows to obtain the thermophysical properties of the soil using analytical solutions of the heat transmission not stationary.

C.7 Determination of the overall coefficient of linear thermal exchange between water of the heat exchanger and soil

Can express the total power exchanged by the probe with the ground as:

$$\dot{Q} = U \cdot L \cdot (T_m - T_g) \qquad \text{(C.8)}$$

where U is the overall coefficient of linear thermal exchange between the probe and ground, W / (m • K), L is the length of the probe, m, T_m is the average water temperature within the heat exchanger and T_g is the temperature of the soil undisturbed. Since the regime is non-stationary, the linear coefficient of overall heat transfer U, is a function of time. The value of U is plotted versus time, during the time interval test. It is particularly relevant the value of U at the end of the test, when the regime is quasi - stationary and the value of U is the minimum. This value is useful for making rapid estimates precautionary, the power that can be exchanged by a probe similar to that examined (in the same soil), for a fixed temperature difference between water and soil undisturbed.

C.8 Duration of test

Yet there is no international agreement on what should be the duration of the test. Currently, apart from some exceptions, it tends to load the underground heat for about 50 to 70 hours this is recommended by studies done by Skouby (1998) and Spitler (1999). The first few hours are not considered in the calculations because the heat flow takes time to stabilize with the subsoil and in general the measured temperature is a function of the probe and the grouting and does not refer to the soil.

The experimental error on tests conducted for 50 hours, is around ± 5%. Test of shorter duration, mean standard deviations higher. In the case of a test carried out for 20 hours, the experimental error on the conductivity was assumed to be equal to 20%.

In any case the duration of the test, must not be less than one time t_M defined by the formula:

$$t_M > \frac{5r^2}{\alpha} \qquad \text{(C.9)}$$

Where:

r Radius of perforation;

λ thermal conductivity;

$$\alpha = \frac{\lambda}{\rho c_p}$$ Thermal diffusivity;

That report shows very well in experimental data, in fact, in the representation on the logarithmic plane of the measures of the test, the linear behaviour of the temperature it is only in times higher, while for reduced times the behaviour is not straight.

From the equation of the duration time of the test shows the dependency of the same from the thermal diffusivity, which in turn depends on the thermal conductivity of the ground. It is important to consider that the thermal conductivity of soil is a parameter that can be evaluated only after the first part of the test, that is, the data to be excluded for the interpretation, to estimate the time limit, the validity is necessary to assign a value to attempt the thermal diffusivity. So should proceed in an iterative manner in the process of interpretation, then based on the value of thermal diffusivity of first attempt determining the thermal conductivity used for the calculation of the thermal diffusivity of the second attempt, then the choice of thermal diffusivity is well is carried out with attention to the type of soil that occurs in site.

It is good that the test is long enough to be a good indicator of reliability of the results, also if the test is done correctly, in the absence of significant fluctuations the water table and the behavior of the soil around the probe has not been heavily influenced by the perforation will the apparent conductivity that remains substantially constant, both on this only the first data after the minimum time of significance of the test, whether one considers all the data in the complex.

The results of the series of measurements performed, are certified by the periodic calibration of instrumentation used: total power, supplied to the fluid by the electrical resistances and from the pump (function of time); volume flow (function of time); temperature, inlet and return (function of time); power exchanged between fluid and soil (a function of time); overall coefficient of linear thermal exchange (function of time).

C.9 Data analysis

When a quantity of heat is injected into a collector, it establishes a transient process expressed by:

$$\overline{T}(t) = \frac{q}{4\pi\lambda H} \cdot \ln(t) + \left[\frac{q}{H} \cdot \left(\frac{1}{4\pi\lambda} \cdot \left(\ln\left(\frac{4\alpha}{r_b^{\,2}} \right) - \gamma \right) + R_b \right) + T_0 \right] \qquad \text{(C.10)}$$

It is the evolution equation of the thermal field, considering the entire length of H [m] of the probe and the total heat exchanged Q [W].

The equation can also be simplified by writing it in a linear form:

$$\overline{T}(t) = K \ln(t) + m \tag{C.11}$$

Where:

$$K = \frac{q}{4\pi\lambda H} \tag{C.12}$$

$$m = \left[\frac{q}{H} \cdot \left(\frac{1}{4\pi\lambda} \cdot \left(\ln\left(\frac{4\alpha}{r_b^{\,2}} \right) - \gamma \right) + R_b \right) + T_0 \right] \tag{C.13}$$

The thermal conductivity of the soil is estimated according to the inclination of the straight line interpolating the measurements on a graph which has the abscissa τ = ln (t) and the ordinate T_f. The thermal conductivity based on the line-source model ($\lambda_{equivalent} = \lambda_{eq} = \lambda_{LS}$) is given by:

$$\lambda_{eq} = \frac{q}{4\pi} \cdot \frac{\ln(t_2) - \ln(t_1)}{T(t_2) - T(t_1)} \tag{C.14}$$

3. MEDIUM TEMPERATURE GEOTHERMAL ENERGY

3.1 Introduction

Medium – temperature geothermal energy, uses in a direct way the ground water; in fact, this method offers significant advantages as it has a higher energy efficiency, as it does not occur the thermal drift, that appeared around the vertical probes in the absence of thermal equilibrium It also has economic advantages, in part of the initial installation costs, and the need for lower surfaces compared to other closed circuit systems. In view of the cost, one must consider the constant maintenance of wells, sampling and re - entry the groundwater, as it can have a profound impact on project costs.

The wells are installed through aquifers (porous media) or fractured rocks, once extracted water, and used for the heat exchange, the heat exchanger, can be subsequently injected.

Or in the aquifer, in the same or different aquifer, through the installation of another well defined replacing well, at a certain distance from the extraction well.

Or in a volume of surface water such as: river, irrigation canal, lake.

The release into surface water, a solution is economically very convenient, even if it is conditioned looking regulatory, and by the capacity of the receiving body to absorb for long periods the flow rates required for the release.

For example De Carli (et al. 2007) defines the use of surface water very favourable in Italy compared to other countries in Northern Europe, because rarely the Italian rivers tend to freeze even in the face of prolonged temperatures external below zero, but the problem is constituted precisely by the seasonal variation of the water flow, which may be important, with reductions in the summer period, when the water is useful in the operation of the machine as a refrigerator. The authors present the development of the temperatures of Lake Maggiore, (Fig. 3.1) as a function of depth throughout the year, highlighting that the water allows its direct use, through the heat exchanger, the air conditioning, for the cooling air.

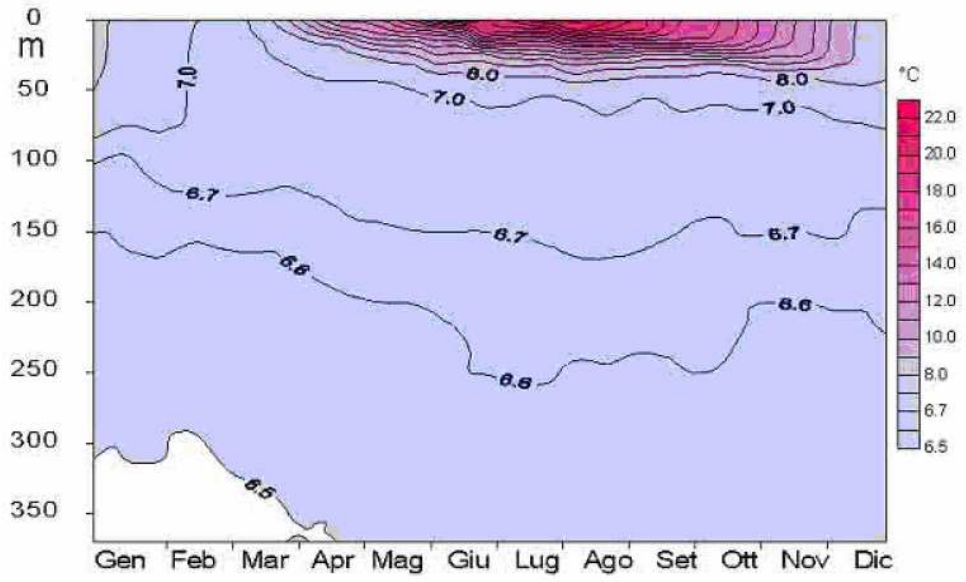

Fig. 3.1 – Trend of the isotherms in Lake Maggiore as a function of depth (year 1996).

The solution of the re-injection in the groundwater is an alternative compared to the previous one discussed above; sometimes it is a mandatory solution, in fact the re-injection into the groundwater has the function to prevent the impoverishment of the same, as it balances the water balance aquifer making more sustainable this form of use from the point of view of preservation of the quantitative resource (Baietto et al. 2010) , with both functions of seasonal storage.

Axelsson (2012) has presented interesting results on the benefits of re-injection geothermal aquifer, first of all his attention to environmental protection, then it also provides an additional charge that acts on increasing production capacity above for geothermal systems that have a limited charging. Another purpose of the re-injection, is the support pressure, to reduce the pressure drop due to the extraction of mass; another fundamental aspect is to compensate for surface subsidence. In fact, extract water from the subsoil, especially in porous media, means leaving voids within the interstices between the solid particles where they were previously occupied by the same water, the presence of a load or the same weight of the soil due to localized subsidence that may cause damage to structure, close to the injection well Fig 3.2, a model of the Terzaghi effective stress.

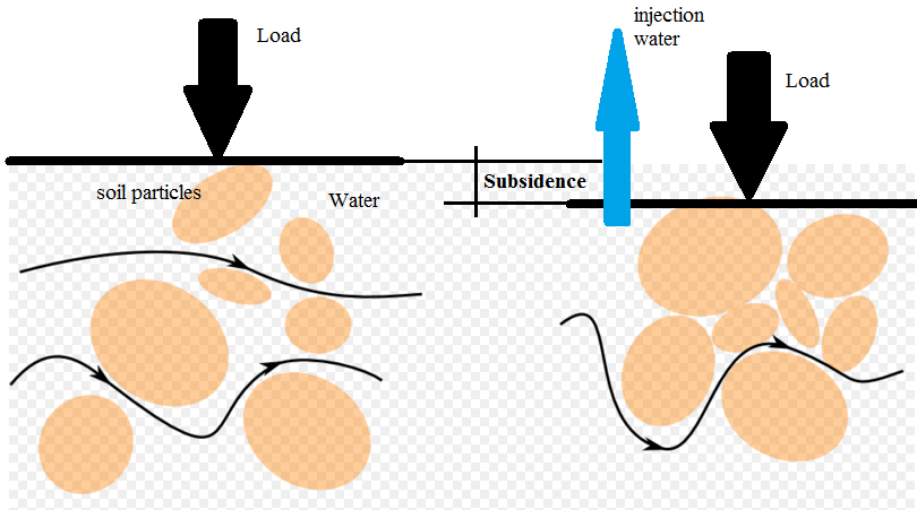

Fig. 3.2 – Scheme of subsidence due to extraction of water from the well (Model Terzaghi).

Finally, the re-injection in the aquifer is to improve or raise the surface characteristics such as hot springs and fumaroles (in Iceland). also in the design, re-injection has been much studied and applied for a decade so it is an integral part of the geothermal operations that use both the terms "injection" and re-injection ".

The same author shows the benefits of re-injection predicted water level changes (pressure changes) in the urban geothermal system under Beijing-city in China until 2160, demonstrating the beneficial effect of reinjection (see Figures 3.3 and 3.4):

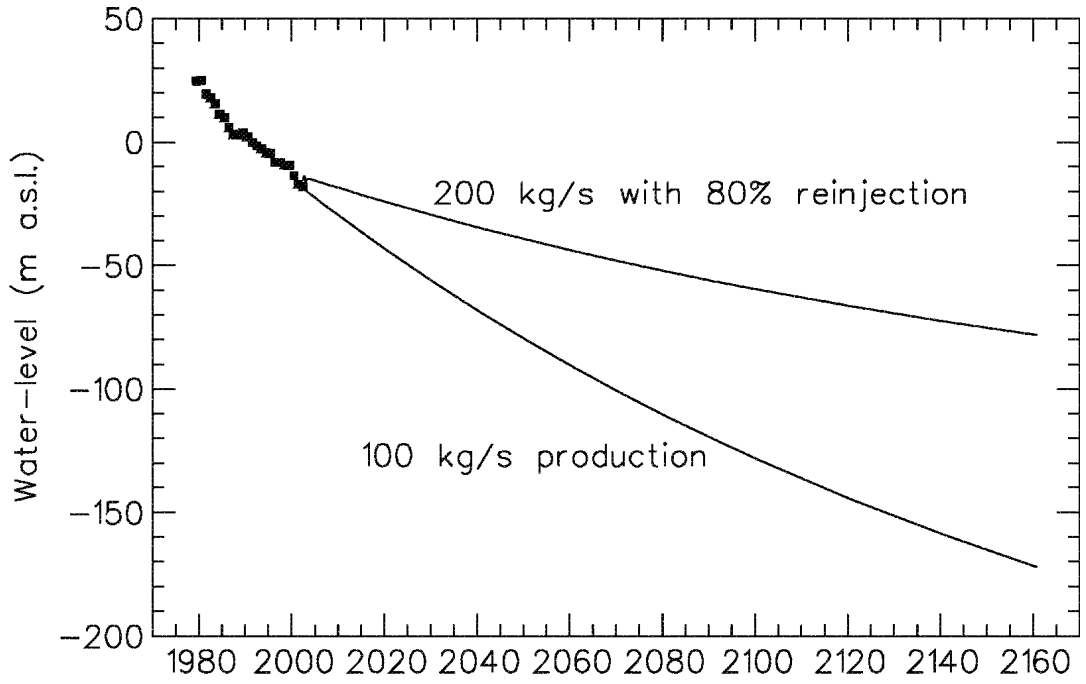

Figure 3.3: Predicted water level changes (pressure changes) in the Urban geothermal system under Beijing-city in China until 2160, demonstrating the beneficial effect of reinjection.

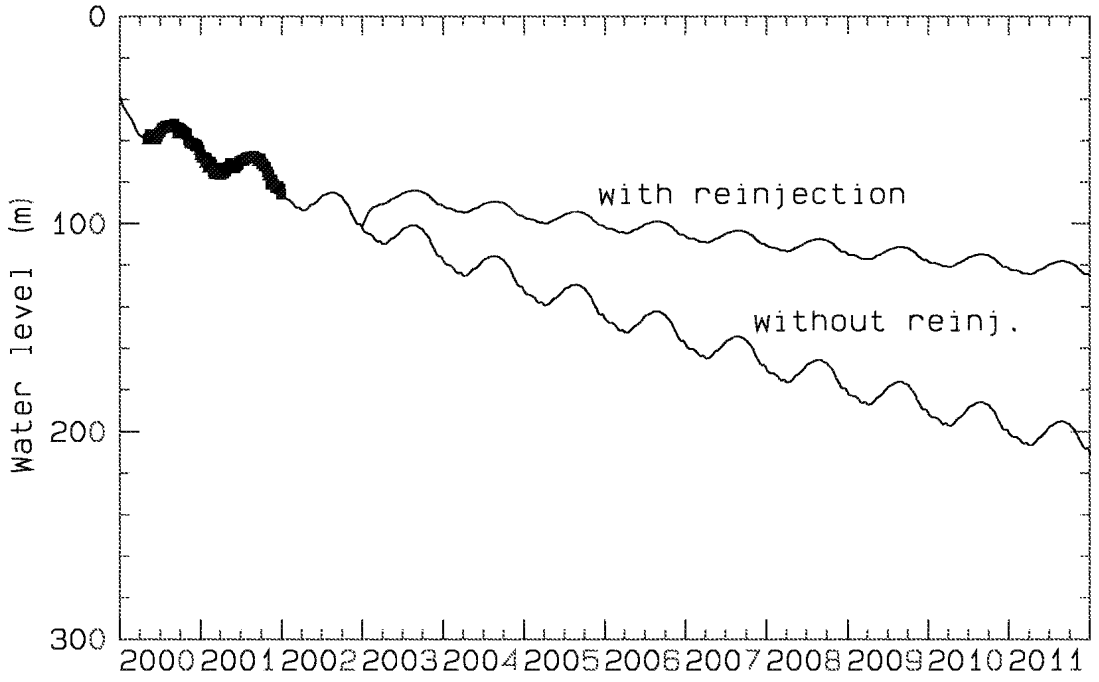

Figure 3.4: Water level predictions for the Hofstadir low-temperature system in W-Iceland, demonstrating the beneficial effect of reinjection.

An example of successful long-term media temperature re-injection is Paris Basin Figure 3.5:; it is composed by limestone for 15,000 km^2, with a depth of around 1500 to 2100 m average temperature of 70 °C. The medium-temperature geothermal systems are composed by a double-scheme with heat exchangers and full re-injection; this operation started in 1969. fifty-four geothermal plants, are still in operation, with others still in the design phase, the production wells away from the wells of re - injection of approximately 1000m.

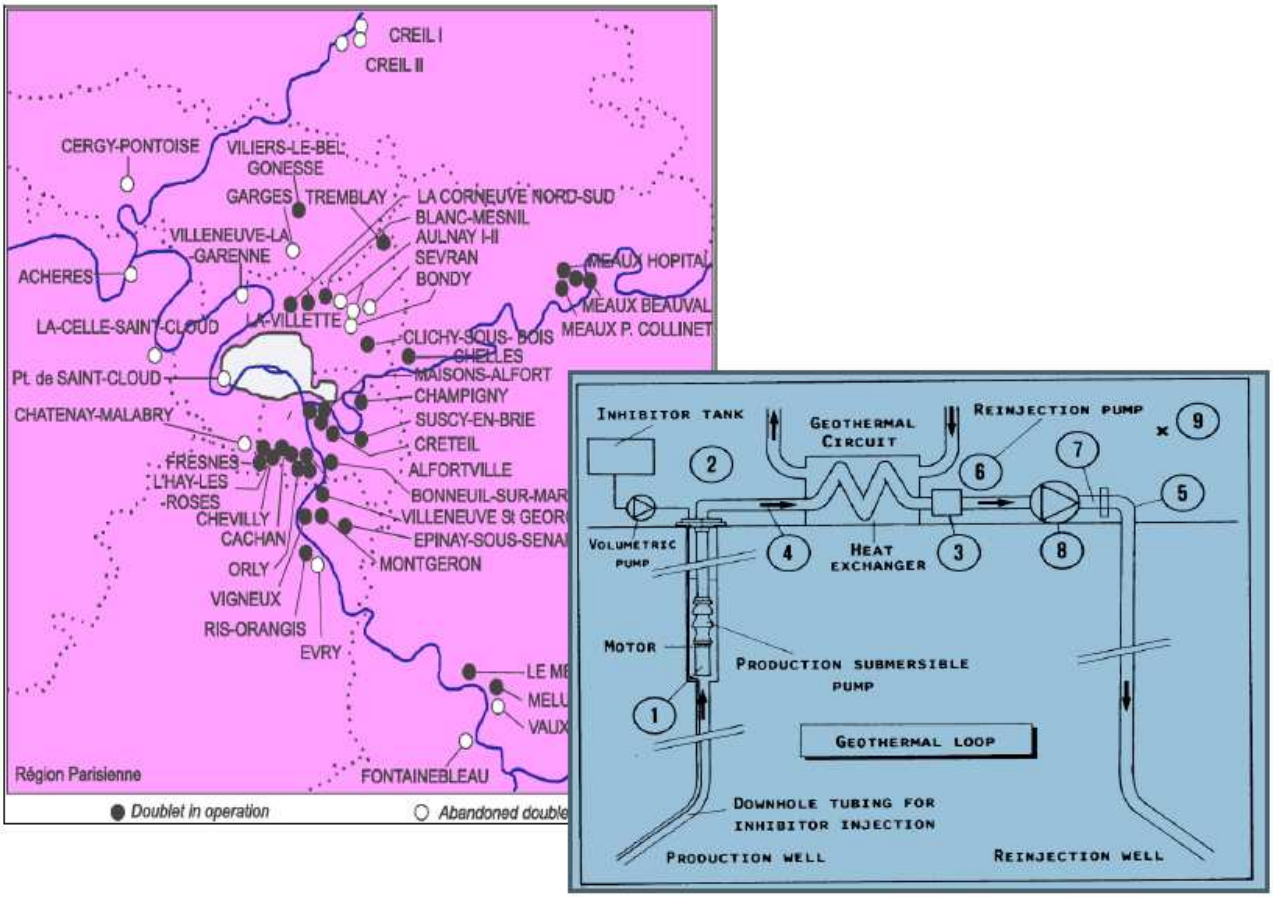

Figure 3.5 – Paris Basin.

As noted above, the re-injection gets important benefits in terms of environmental sustainability and thus a reduction in the risk of land subsidence; for this choice sometimes as a solution forced by regulations, it can present some challenges, for careful evaluation at design,, including a careful study of the distance between the production well and re-injection, in fact it is important to know the volume control of the heat well, so the distance from the undisturbed conditions, will avoid short - circuit for thermal drift. This problem has been studied in this part of the thesis. Other obstacles that may occur for the re - injection are caused by the rapid clogging of aquifers near the injection wells, caused by the precipitation of materials such as sand, up to medium and fine granulometry.

In general, we can thus summarize the main advantages of geothermal energy at medium temperature, which exploits the ground water as a heat transfer fluid are: the energy efficiency is higher, compared to systems having vertical probes to equal energy requirements, the fluid transfer medium is precisely the ground water, for which there are no problems that may exist with fluids anti – freeze; also the extracted water can subsequently be used for other uses, while the main disadvantages are: the hydrogeological particular conditions, a complex design, a constant monitoring of the system when it is in operation,, operating costs both in the relevant pump are in risk of clogging of drains.

3.2 Production wells and re – injection wells

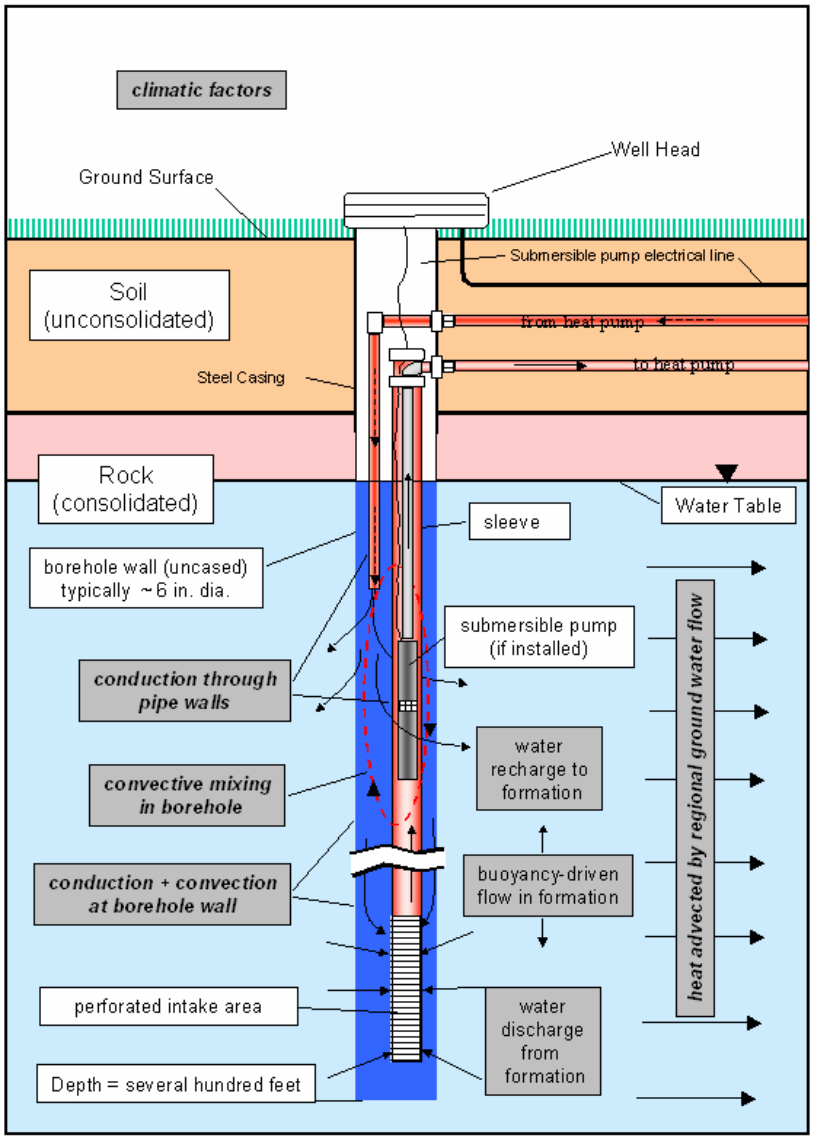

Figure 3.6– Scheme of a well for the extraction of water from the aquifer.(Deng Z. 2004).

The wells installed, in porous media, are constituted by metal pipings, a part of which is closed and a part, concerned aquifer for water extraction, is filtering. The closed pipes perform the function of supporting the walls of the borehole avoiding landslides during operation of the well, while the portion of the filter hose drains, have the task of avoiding cross the water to pass even the solid particles of soil. In case the wells are installed in compact soil or rocks cracked, it is not necessary to use the casing tube, but only the stretch of pipe surface for connection with the pump. In the design phase, and testing in situ, and then analyzed the chemistry of the water and soil mechanics, we proceed with the choice of materials for the pipes of the wells. The most used materials are the galvanized carbon steel, stainless steel AISI 304 or 316, the PVC and the glass fibre. The PVC pipes have crushing strength, less than that of steel pipes, so their use is limited depths, less than 100m.The advantage of these tubes is the resistance to corrosion and a little subject incrustation. The filters that are mainly found in commerce, have rectangular openings and may be bridged or spiral and PVC (see Figure 3.7).

a)

b)

c)

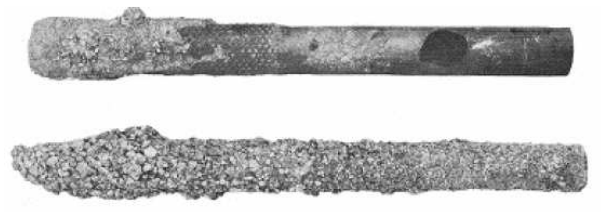

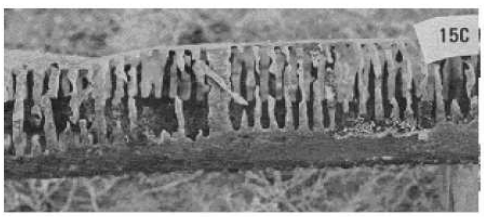

Figures 3.7 – Types of filters for the drainage of ground water in wells: a) Filter continuous light stainless steel, b) Filter bridge stainless steel, c) probable incrustation .

Around, piping filter housing for the gravel to the formation of the drain, he drain must be constituted by rounded grains of siliceous nature, the granulometry must be selected on the basis of the granulometric characteristics of the aquifer and based on the size of the openings of the filters.

The drain is very important, it must not therefore become clogged and therefore must involve the upper and lower sections of the pipe closed, about 2m, while its thickness must not be less than 50 mm and greater than 150 mm.

Important is the cementation, which is carried out in the inter-space between drilling and piping; this is useful to protect the well against pollution by surface water and also to prevent the flow of water from a polluted aquifer to another and reinforce the pipe coating by the crushing; the cementation is constituted by a cement grout and bentonite. The bentonite, in fact, confers plasticity to solid avoiding the inconvenience of withdrawal. The part to be cemented starts above the drain, that is, not less than 2 m from the filters, and must involve a section of pipe closed not less than 15 - 20% of the entire length of the pipe. For wells re - injection into aquifers that are not superficial, cementation must be made from the roof of the aquifer to the ground surface.

3.3 Design and dimensioning

The size of the systems, geothermal media temperature, which exploits the groundwater, aims to estimate the flow optimal groundwater, to guarantee high efficiency of the climate system; it is essential, therefore, the knowledge of thermal needs of the building, the thermal and hydraulic properties of the aquifer, subject to the water request, the quality of groundwater and the chemical characteristics of which it is composed, the depth of the water, the regulations of the place or the possibility of extraction and discharge of deep waters.

An important research topic, studied by various authors (Lauwerier 1955), (Ghassemi 2004), is the study of the distance between the extraction well and well of re–injection; it is in fact important as the spacing between wells must be such as to ensure thermal interference, as lower as possible (Banks, 2009).

The flow of water, which will satisfy the energy needs of the building, will depend on the temperature of the water in the aquifer, the temperatures of way, and return to the heat exchanger, the efficiency of the heat exchanger and the thermal loads of building.

The authors Baietto et al. (2010), define the optimal range of a well, which is the one that causes the least additional hydraulic load losses, due to the turbulent flow under the conditions of maximum yield of the lifting. A method to find the optimal range, is to perform a test of the well, and to analyze the relationship between flow rate of pumping and lowering of the groundwater level; the relationship is represented by a straight line to the initial values of flow rate, while the point curve reflects the presence of additional load losses, due to the turbulent flow. A flow rate just below the attainment of this point corresponds to the maximum optimal, while higher flow rates imply a lower efficiency of the well.

Another important aspect to consider is the most geotechnics, i.e. the subsidence of the ground, that may occur around the wells following the extraction of water. In fact, by extracting water of the aquifer, it is going to change the structure of geo-mechanical aquifer; groundwater lowering increases the voids between the soil particles, the particles of soil are gathering, then compacted occur subsidence that may vary in size, from a few centimetres to meters values, which is dangerous and causes damage to the surrounding works and instability of the well itself.

As regards the study, and the installation of wells of re - injection follow the same techniques views for the production wells, some different precautions are implemented, in order to ensure a regular outflow from the well, towards the aquifer and total absence of solid particles in suspension, In fact, in loose soils, the filtering surface of the well to re-injection should be larger, even twice that of the production well; this to make sure that entrance velocity is reduced, thus increasing the drilling diameter or the extension in depth of the filtering part of the well.

3.4 ATES (Aquifer Thermal Energy Storage)

The technology ATES (Aquifer Thermal Energy Storage) is a particular type of thermal storage which uses the water of the subsoil as a reservoir, taking it from two different wells with sufficient space out between them. During the summer season, the ground water is extracted from the "cold well", and is used for cooling the condenser of the refrigerator (or heat exchanger), and then placed in the subsoil in the "hot well" and, after being used in the evaporator of the heat pump (or heat exchanger), it is injected in the cold well, providing the following summer season. This technology, calls for the slowest possible speed of groundwater, since it has to ensure that the water of the wells will be mixed with each other, and in any case the motion of groundwater should not take away with them, the storage of cold water from a drain and hot water on the other.

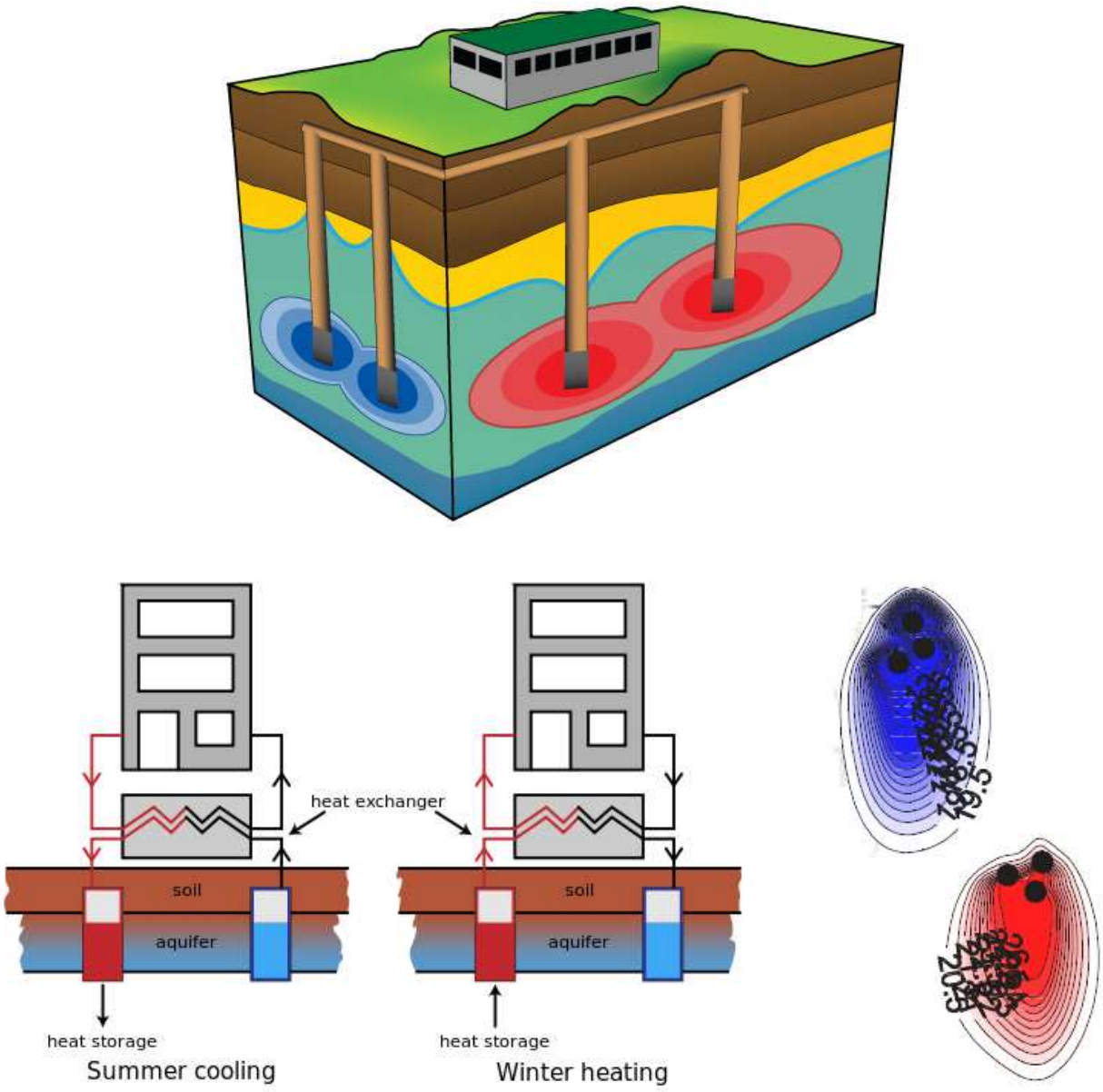

Figure 3.8 – ATES Aquifer Thermal Energy Storage

3.5 Literature review ATES

In this part, it was desired to study the problems related to systems ATES, or in any case the extraction of water from the porous medium, in thermal areas of thermal anomaly, in which, once extracted ground water in a well, said well of production, and conveyed into a heat exchanger for exchanging thermal energy with water resulting from a second circuit, the ground water is rejected in a second well, said well of re-injection, in order to restore the water balance in the aquifer. The object of the study is mainly the knowledge of the minimum distance that must have the two wells, so as to avoid that there is a mixing between the two waters of the two wells; in fact, especially in systems ATES, it is essential that the well production, where there is hot water used for the thermal needs of the building in the winter or cold water for cooling needs in the summer, do not mix with the water of the well of re - injection reservoirs, cold in winter, where the cold water is rejected, or reservoir hot in summer.

The study of he distance between the two wells was conducted according to analytical theories in the literature as the studies conducted by Carslaw and Jaeger (1948) and taken up by Lauwerier in 1955, and Ghassemi, Tarasovs and Cheng (2002), and by Ghassemi and Tarasovs (2004), the theoretical results were compared with the studies conducted by Borbiaux (2011) and then compared with FEM models, implemented in COMSOL Multiphysics. The studies conducted, consider an aquifer, from which it is made to vary the thickness of the same for each simulation (H = 0.1 m, 1 m, 5 m, 10 m, 25 m, 100 m), in which it is made to cross a certain amount of flow along the porous medium, are transient the object of study and the analysis is to see time and space in which the water arrives at conditions of temperature undisturbed same aquifer.

3.5.1 Lauwerier (1955): The transport of heat in an oil layer caused by the injection of hot fluid

The objective of the study conducted by Lauwerier in 1955, was to define a mathematical model capable of explaining, the injection of a hot fluid within a horizontal layer of uniform and constant thickness along the aquifer,, in order to increase the percentage of extraction of the petroleum, reducing the viscosity of the same, by means of the thermal energy exchanged from the hot fluid made to cross in the layer. Moreover, the thickness is considered sufficiently small, compared to the size of the porous reservoir (sand), that inside contains petroleum.

The mathematical model proposed by Lauwerier allows to obtain the temperature field in a porous medium, by means of partial differential equations by relying on two-dimensional Laplace transforms, and the transformation is followed with respect to the variables time and distance.

The model takes into consideration the case where it provides heat to the porous reservoir, through the injection of a hot fluid in injection wells, the case of a linear path of the fluid. The thickness, the permeability and porosity of the reservoir (sand with petroleum) are considered to be uniform, while the hot fluid is considered to be water which is injected at a constant flow rate. In the case of viscous petroleum, it can be assumed that the water and petroleum flow separately; the layer crossed by the hot water is constituted by a uniform layer of constant thickness.

The thermal conductivity of the porous reservoir (sand and petroleum) is considered equal to that of the rock permeable covering, and is nothing taken in the direction of the flow, while infinite in the direction perpendicular, so that the temperature in the latter direction may be considered uniform in the layer of water. Another assumption is to consider instantaneous thermal equilibrium between sand and fluid; this means that the grains of sand have everywhere the same temperature of the fluid that surrounds them.

In essence, the hot water at a temperature T_0, is pumped at a constant flow rate through a number of injection wells along a straight line. Furthermore, the water and petroleum are extracted through extraction wells parallel and distant from those of injection, lying along a straight line.

The model assumes the two-dimensional, since the water flow is assumed linear. A first simplification is to consider that the water flows in a single layer of thickness 2b and that the temperature T_1 is constant in each cross section, and then only as a function of the distance x from the injection well. In Figure 3.9 the section xy defined by the model Lauwerier is represented.

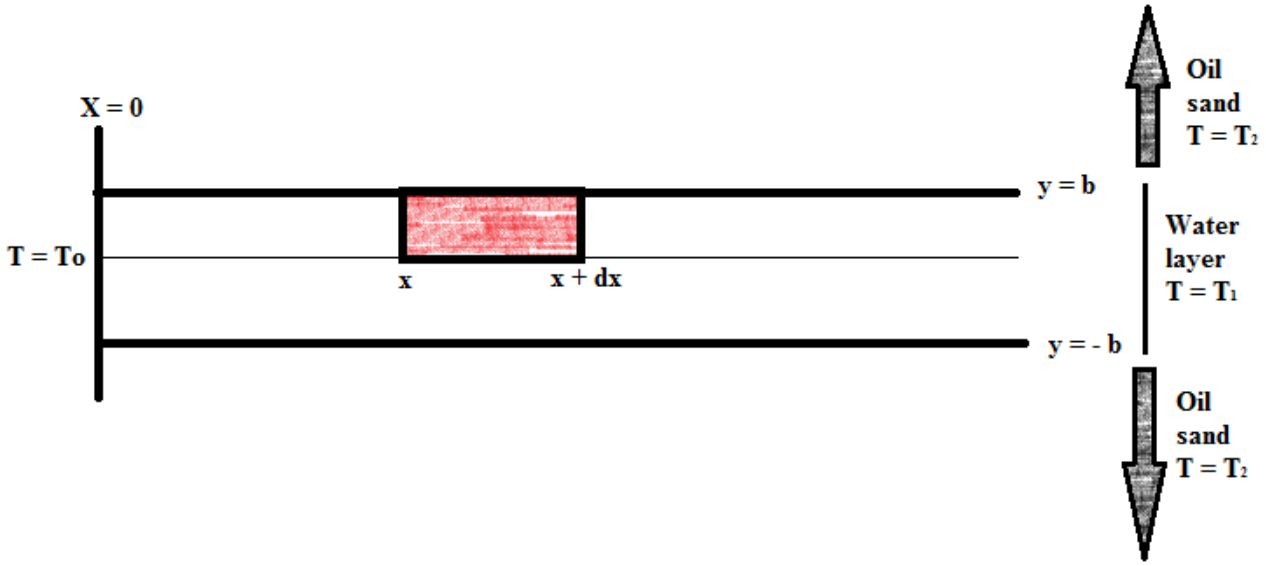

Figure 3.9 – Lauwerier's Model.

The problem can be formulated as follows:

A horizontal layer of water: x> 0, -b <y <+ b, and placed in the middle of a layer of sand imbued with petroleum with initial temperature T_2 = 0 °C. At the beginning also the temperature T_1 of the water layer equals to zero.

From time t = 0 starting from the boundaries x = 0, -b <y <+ b the temperature is kept constant at the value $T_0 > T_1$ thanks to the injection of water at the temperature T_0 with velocity V_w [m / s], in this so it establishes a mechanism of convective heat exchange in the x direction.

A second simplification is introduced neglecting the conduction, in a horizontal direction, that is in the water in the sand. Furthermore it is assumed that there is an instantaneous thermal equilibrium between water and sand.

The temperatures T_1 and T_2 can now be calculated as functions of x, y and the time t.

use the following constants:

$\rho_w c_w$ = volumetric specific heat of water [J/(m^{3}K)]

V_w = linear velocity of water [m/s]

λ_2 = thermal conductivity of the sand satured with petroleum and contour of the rock [W/(mK)]

φ = porosity of the sand

$\rho_s c_s$ = volumetric specific heat of the sand grains [J/(m^3 K)]

$\rho_0 c_0$ = specific heat of the petroleum [J/(m^3 K)]

s_r = residual petroleum saturation in the layer of the water

s_0 = water saturation in the layer of petroleum

Applying the heat balance the shaded region in Fig. 3.9 have :

$$b\rho_1 c_1 \frac{\partial T_1}{\partial t} + b\rho_w c_w V_w \frac{\partial T_1}{\partial x} - \lambda_2 \left(\frac{\partial T_2}{\partial y} \right)_{y=b} = 0 \qquad (3.1)$$

Where:

$$\rho_1 c_1 = (1-\varphi)\rho_s c_s + \varphi(1-s_r)\rho_w c_w + \varphi s_r \rho_0 c_0 \qquad (3.2)$$

It corresponds to the specific heat of the water layer for m^3. In the layer of sand and petroleum the general equation of conduction is:

$$\lambda_2 \frac{\partial^2 T_2}{\partial y^2} = \rho_2 c_2 \frac{\partial T_2}{\partial t} \qquad (3.3)$$

Where:

$$\rho_2 c_2 = (1-\varphi)\rho_s c_s + \varphi(1-s_r)\rho_w c_w + \varphi s_r \rho_0 c_0 \tag{3.4}$$

It is the specific heat of the layer of sand saturated with petroleum, assumed to be equal to that of the rock contour for m^3.

At this point the following dimensionless variables are introduced:

$$x = \frac{b^2 \rho_w c_w V_w}{\lambda_2}\xi, \qquad y = b\eta, \qquad t = \frac{b^2 \rho_1 c_1}{\lambda_2}\tau, \qquad \theta = \frac{\rho_1 c_1}{\rho_2 c_2} \tag{3.5}$$

The equations that describe the model are:

$$\theta \frac{\partial^2 T_2}{\partial \eta^2} = \frac{\partial T_2}{\partial \tau}, \qquad \text{for } |\eta| > 1 \tag{3.6}$$

$$\begin{cases} \dfrac{\partial T_2}{\partial t} + \dfrac{\partial T_2}{\partial \xi} - \dfrac{\partial T_2}{\partial \eta} = 0 \\ T_1 = T_2 \end{cases} \qquad \text{for } |\eta| = 1 \tag{3.7}$$

$$T_1 = T_2 = \begin{cases} T_0 & \text{if } \xi < 0, \\ 0 & \text{if } \xi > 0, \end{cases} \qquad \text{for } \tau = 0 \tag{3.8}$$

The solution of the differential equations is obtained by applying two times the Laplace transform to T2, the first time with respect to ξ for the region - inf <ξ <+ inf, while the second; with respect to time for τ > 0. omitting steps of mathematicians, who can be seen in the article by Lauwerier (1955. It is interesting to note the form of the equation to determine the temperature T2; in fact it is in agreement with the study by Carslaw and Jaeger (1948, or updated in 1959); then:

$$\xi < 0 \qquad T_2 = T_0$$
$$\xi > 0 \qquad T_2 = T_0 erfc \frac{\xi + |\eta| - 1}{2\sqrt{\theta(\tau - \xi)}} U(\tau - \xi) \tag{3.9}$$

The temperature in the layer is equal to:

$$T_1 = T_0 erfc \frac{\xi}{2\sqrt{\theta(\tau - \xi)}} U(\tau - \xi) \tag{3.11}$$

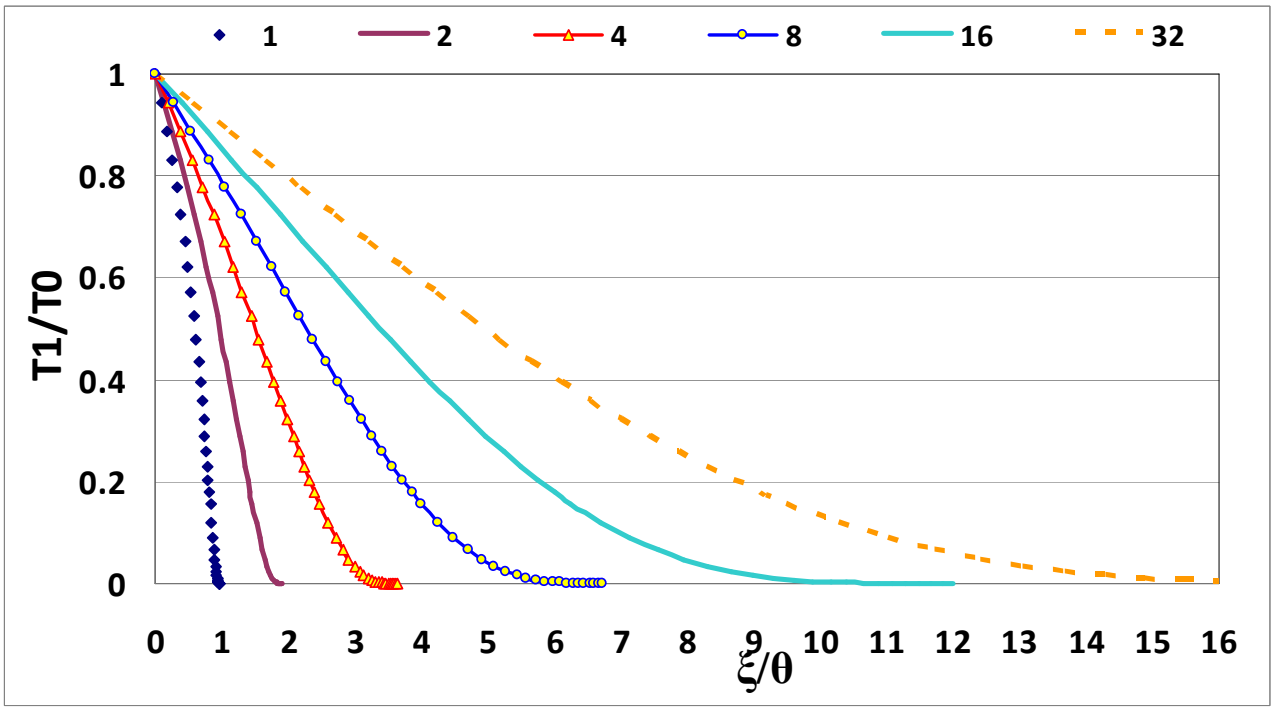

Figure 3.10 – Temperature in the water layer for various values of τ/ θ.

In Figure 3.10 the graph of the ratio $\frac{T_1}{T_0} = erfc \frac{\xi/\theta}{2\sqrt{\tau/\theta - \xi/\theta}}$ is given as a function of ξ / θ for different values of time τ/ θ = 1, 2, 8, 16, 32.

3.5.2 Ghassemi e Tarasovs (2004): Three – dimensional modelling of injection induced thermal stress with an example from Coso

In the study dealt with by Ghassemi and Tarasovs (2004), it is highlighted the extraction of heat from a rock, assuming the fracture: flat with finite size and arbitrary shape, while the geothermal reservoir is considered to be infinitely extended, see Figure 3.11.

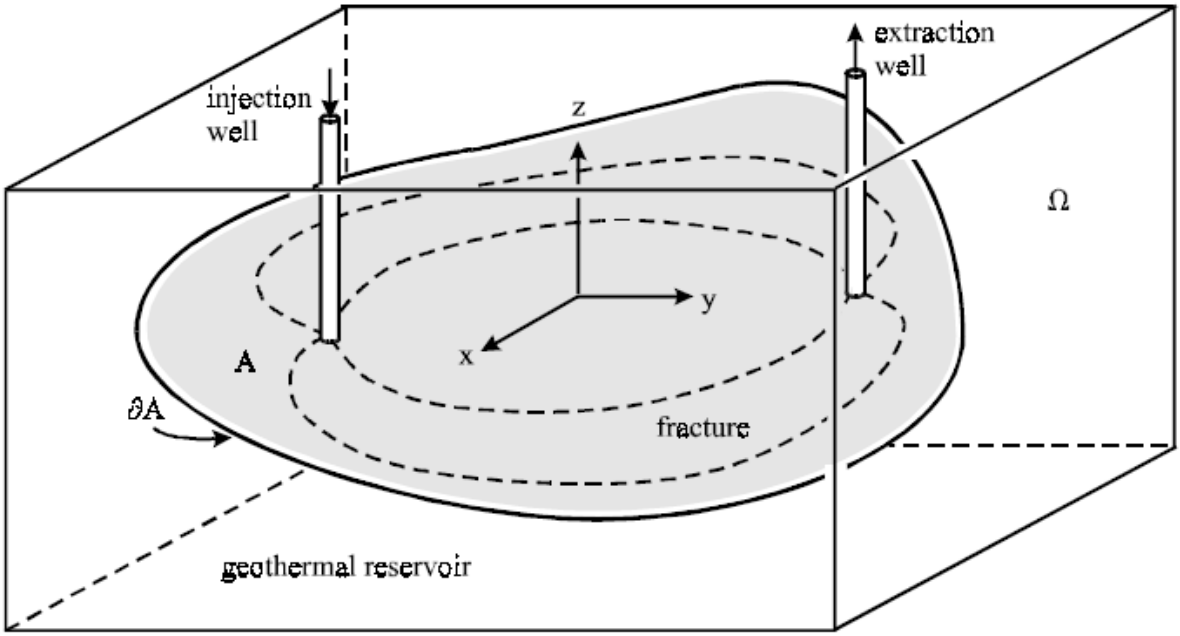

Figure 3.11 – Heat extraction from a planar fracture.

The assumptions made by the authors are:

- The conduction of heat in the reservoir is typically modelled as one-dimensional heat flow, in the direction perpendicular to the fracture.

- The geothermal reservoir is impermeable to water and non-deformable;

- The properties related to thermal conduction are constant;

- Negligible heat build-up, and the effects of dispersion of the flow, the fluid in the fracture;

- The flow of hot water produced is equal to the flow rate injected into the fracture;

- The width of the fracture is small so that the flow is laminar.

Introducing the temperature parameter is dimensionless as:

$$T_D = \frac{T_0 - T}{T_0 - T_{inj}} \tag{3.12}$$

The heat transfer occurs, both in the geothermal reservoir and in the fracture. For the reservoir, the conduction is governed by the equation of the three-dimensional diffusion:

$$\lambda_r \nabla_3^2 T_D(x, y, z, t) = \rho_r c_r \frac{\partial T_D(x, y, z, t)}{\partial t} \tag{3.13}$$

Where:

ρ_r = density of the rock [kg/m^3]

c_r = specific heat of the rock [J/(kg K)]

∇_3^2 = Laplace operator in three dimensions

Ω = the geothermal reservoir infinity (see Figure 3.11)

For heat transport in the fracture equation is (Ghassemi 2003):

$$q(x, y) \cdot \nabla_2 T_D(x, y, 0, t) = \frac{2\lambda_r}{\rho_w c_w} \left. \frac{\partial T_D(x, y, z, t)}{\partial z} \right|_{z=0^+} \tag{3.14}$$

Where:

ρ_w = density of water [kg/m^3]

c_w = specific heat of water [J/(kg K)]

λ_r = thermal conductivity of the rock [W/(m K)]

T_{inj} = temperature of the injected water [K]

The equations are subject to the initial conditions, and boundary. Before starting operations,, the extraction of heat, the temperature of the rock and the fluid in the fracture is assumed constant, equal to T (x, y, z, t) = T_0 while the temperature at the injection point (x_i, y_i, 0) is equal to the temperature of the injected water: T (x_i, y_i, 0, t) = T_{inj}.

The extraction temperature T (x_e,y_e,0,t) is not known. The initial conditions. and boundary can be expressed as a function of T_D:

$$T_D(x, y, z, 0) = 0$$
$$T_D(x_i, y_i 0, t) = 1 \quad (3.15)$$

In the equation (3.14) above, the term in the first member is the convective heat due to fluid flow in the fracture, while the first term in the second member, corresponds to the heat supplied by conduction through the walls of the fracture (two sides); finally the last term, representing respectively the heat dissipated or supplied due to extraction or water injection. It should be noted in (3.14) that the annotation only T_D (x, y, z, t) is used to denote the temperature of the rock and the fluid in the fracture; this is because the temperature is a continuous function through the two means.

The water temperature T_w is equal to the temperature of the rock in the fracture plane z = 0, so, Tw (x, y, t) = T (x, y, 0, t) with x, y belonging to A.

To facilitate the processing of the variation of the time, applying the Laplace transform to the equations above, one obtains:

$$\lambda_r \nabla_3^2 \overline{T_D}(x, y, z, t) = s\rho_r c_r \overline{T_D}(x, y, z, s) \quad (3.16)$$

$$q(x, y) \cdot \nabla_2 \overline{T_D}(x, y, 0, s) = \frac{2\lambda_r}{\rho_w c_w} \left. \frac{\partial \overline{T_D}(x, y, z, s)}{\partial z} \right|_{z=0^+} \quad (3.17)$$

$$\overline{T_D}(x_i, y_i, 0, s) = \frac{1}{s} \quad (3.18)$$

Where the tilde denotes the Laplace transform and the s parameter of the transform.

Note that the initial condition (3.15) has been absorbed into (3.16) so, the equations (3.16) - (3.18) constitute a complete system solution.

The system of equations (3.16) - (3.18) is defined in the three spatial dimensions. It has been shown that by using the Green's function of the equation of the three-dimensional diffusion,, the system of equations can be reduced to two-dimensional integral equation (Cheng 2001). The numerical discretion is performed only on the surface of the fracture, significantly reducing the computational cost. For the temperature on the surface of the fracture (z = 0) we have:

$$\overline{T_D} = \gamma \int_A \left[q\left(x^{'}, y^{'}\right) \cdot \nabla_2 \overline{T_D}\left(x^{'}, y^{'}, 0, s\right) \right] \varpi^{'} dx^{'} dy^{'} \tag{3.20}$$

Where:

$$\gamma = \frac{-\rho_w c_w}{4\pi\lambda_r} \tag{3.21}$$

$$\varpi^{'} = \frac{1}{r} \exp\left(-\sqrt{\frac{\rho_r c_r s}{\lambda_r}} r \right) \tag{3.22}$$

$$r = \sqrt{\left(x - x^{'}\right)^2 + \left(y - y^{'}\right)^2} \tag{3.23}$$

Equation (3.20) is entirely defined on the two-dimensional plane A. Together with the boundary conditions (3.18), form a complete system of solution for the temperature of the fluid in the fracture. The (3.20) contains the temperature gradient is not known, and therefore a finite difference approximation in the numerical solution is required.

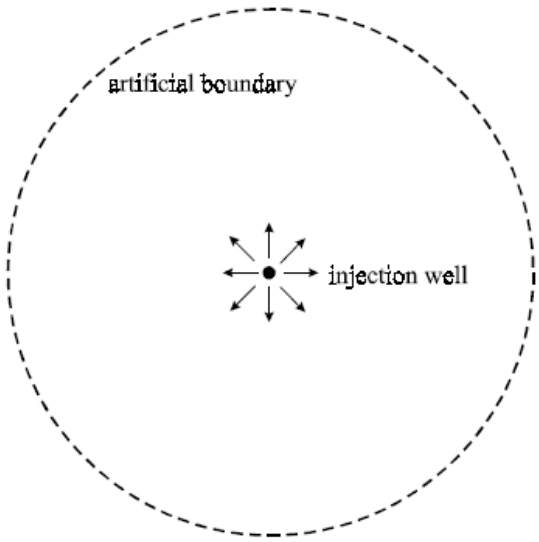

Figure 3.12 – An infinite fracture with an injection well.

This problem can also be solved analytically, if it is assumed that the heat flow in the rock is one-dimensional (perpendicular to the plane of the fracture). The temperature distribution can be written as:

$$T = T_R - \Delta T erfc\left(\frac{ar^2 + bz}{\sqrt{t - Cr^2}}\right) \tag{3.24}$$

$$a = \frac{\pi\lambda}{m_r c_w \sqrt{\alpha}}, \qquad b = \frac{1}{\sqrt{k}}, \qquad C = \frac{\pi h \rho_w}{m_r}, \qquad \Delta T = \left(T_R - T_W\right)$$

with:

λ = thermal conductivity of the rock [W/(mK)]

c_w = specific heat of water [J/(kgK)]

ρ_w =density of water [kg/m3]

α = thermal diffusivity of the rock [m^2/s]

h = thickness fracture [m]

c_r = specific heat of the rock [J/(kgK)]

ρ_r =density of the rock [kg/m^3]

3.6 Results

The results section is composed by the research studies carried out during the PhD, including:

- Solution Lauwerier in a porous medium;
- Study Bourbiaux in system ATES;
- FEM analysis and comparison of studies conducted by Bourbiaux;

3.6.1 Lauwerier Solution in a porous medium

In this subsection, I want to solve the problem of Lauwerier for a porous medium through the use of finite elements. The reference model is shown in Fig 15.61.

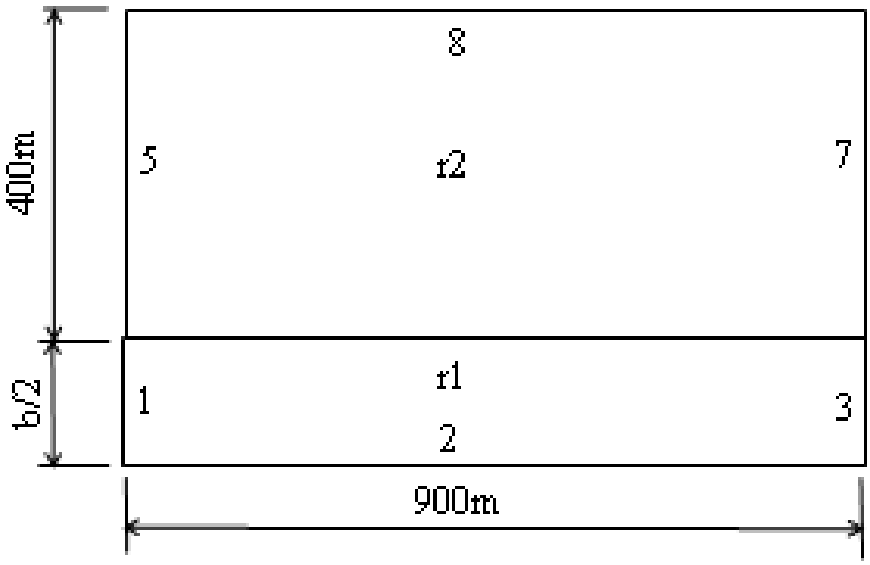

Figure 3.12 – Geometry for the study of a porous layer.

The boundary conditions and domains are as follows:

Table 3.1 . Conditions of domains and boundaries on the COMSOL model porous layer.

	DOMAIN		BOUNDARY					
	r1	r2	1	2	3	5	7	8
TEMPERATURE [°C]	0	0	1	-	-	-	-	-
VELOCITY [m/s]	2.10E-06	-	-	-	-	-	-	-
FLOW OUTGOING	-	-	-	-	✓	-		-
INSULATION THERMAL	-	-	-	-	-	✓	✓	✓
SIMMETRY	-	-	-	✓	-	-	-	-
POROSITY	0.2	-	-	-	-	-	-	-

Starting from the orders of magnitude indicated by its Lauwerier in his publication of 1955:

$\xi = 0.016x$ (x in meters)

$\tau = 1.07t$ (t years)

$\theta = 1.14$

Whereas also in this case a layer of water incorporated between two impermeable layers of rock isotropic, with water and rock having the same parameters of the model developed for the system ATES, see Table 6, one can make the following considerations:

Whereas the ratio τ / θ (with $\theta = \rho_w c_w / \rho_r c_r$) have:

$$\frac{\tau}{\theta} = \frac{\lambda_r \rho_r c_r}{b^2 (\rho_w c_w)^2} t = \frac{1.07}{1.14} t \qquad (3.25)$$

from which it is possible to obtain the semi-thickness b of the fracture, b = 3.66 m. Considering now the ratio ξ / θ:

$$\frac{\xi}{\theta} = \frac{\lambda_r \rho_r c_r}{b^2 (\rho_w c_w)^2 V_w} x = \frac{0.016}{1.14} x \qquad (3.26)$$

from which it is possible to derive the linear velocity of flow within the fracture. Specifically it is V_w = 2.1x10-6 m / s.

The length in the flow direction (x-axis) of the fracture is easily calculated by considering, for example ξ / θ = 16 (see Fig 3.10). In any case this can be freely selected; however, in order to compare the analytical curves, it is necessary to follow the criteria set out above. Is x = 900 m.

At this point, it is noted the geometry of the problem, geometry which in principle is the same as that used for the study of a system ATES. The fundamental difference, in addition to the measures taken, is that this model is 2D, while the ATES, which will be presented in the following pages ,is a 2D-axisymmetric. This has proved necessary to obtain a linear flow with constant velocity V_w.

The analysis used is thermal analysis with thermal exchanges by conduction and convection. The results obtained were collected in a spreadsheet and reported below:

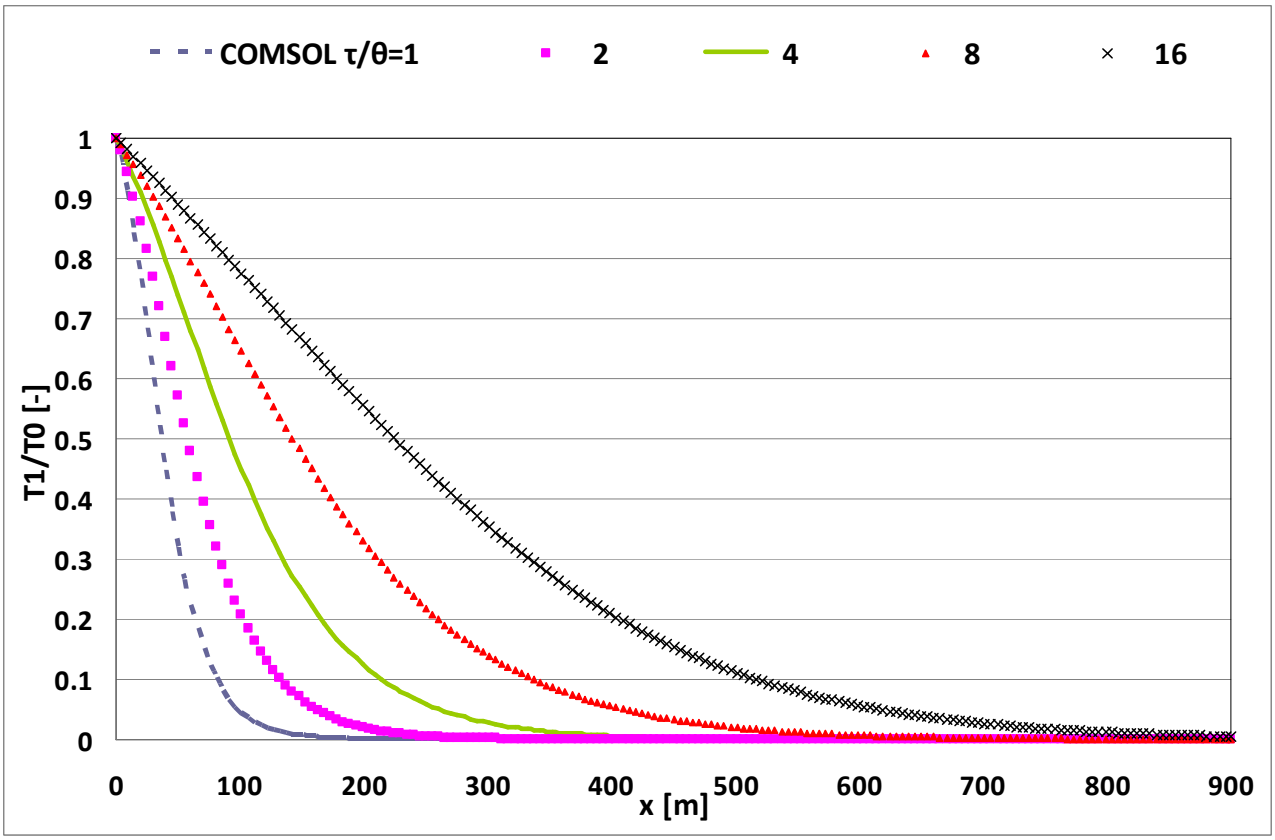

Figure 3.13 - Trend of dimensionless temperature as a function of distance from the well. The curves are parameterized as a function of dimensionless time τ /θ (τ /θ = 16 corresponds to 34 years). Curves made in COMSOL Multiphysics.

The following chart shows the comparison between the analytical results and the results of Lauwerier in COMSOL :

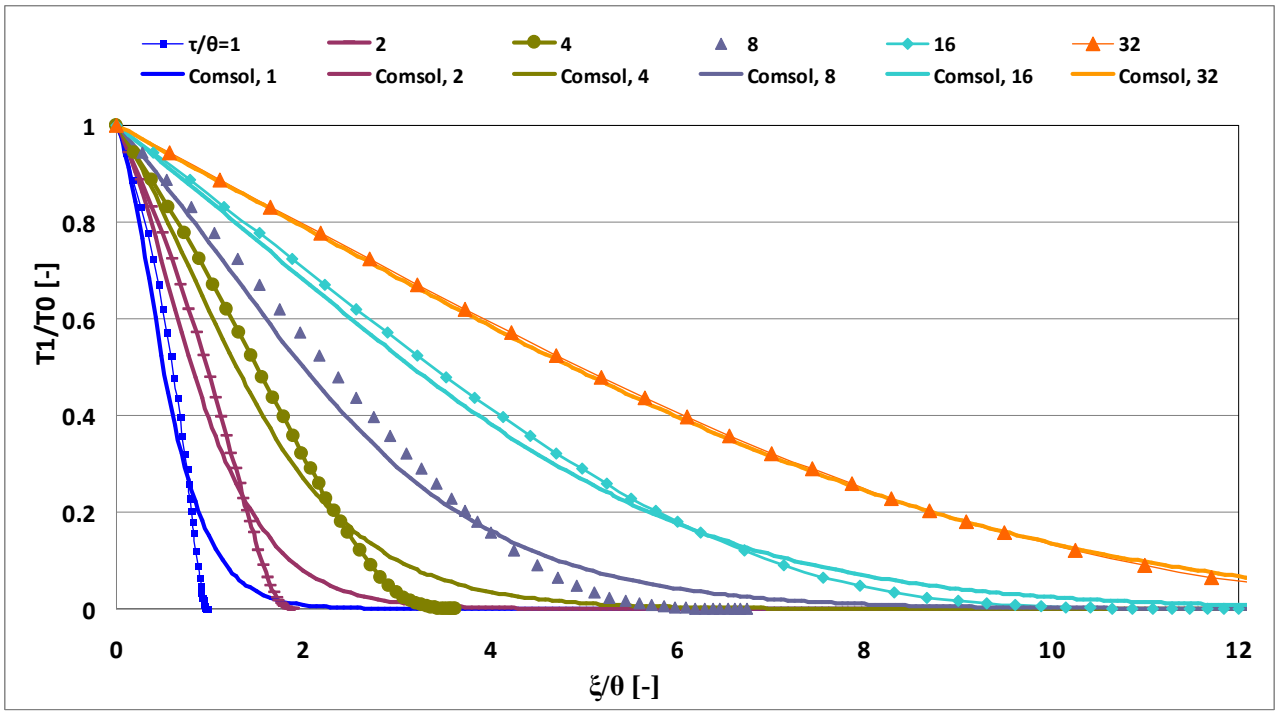

Figure 3.14 – Trend dimensionless the front thermal within a fracture as a function of the dimensionless distance from the injection well. Comparison of the analytical method and FEM. The curves are parameterized as a function of dimensionless time τ /θ.

It should be noted, that the curves 1- 2 – 4 - 8, for T_1/T_0 <0.2, tend to diverge. The results in COMSOL Multiphysics indicate that the thermal front progresses more along the fracture, even if, in reality, the temperature variation is rather contained. This phenomenon, however, tends to annul the increase of the time of analysis; note that for τ / θ = 32 (which corresponds to 34 years), the two curves coincide almost perfectly. After 34 years of analysis, the temperature distribution is as follows:

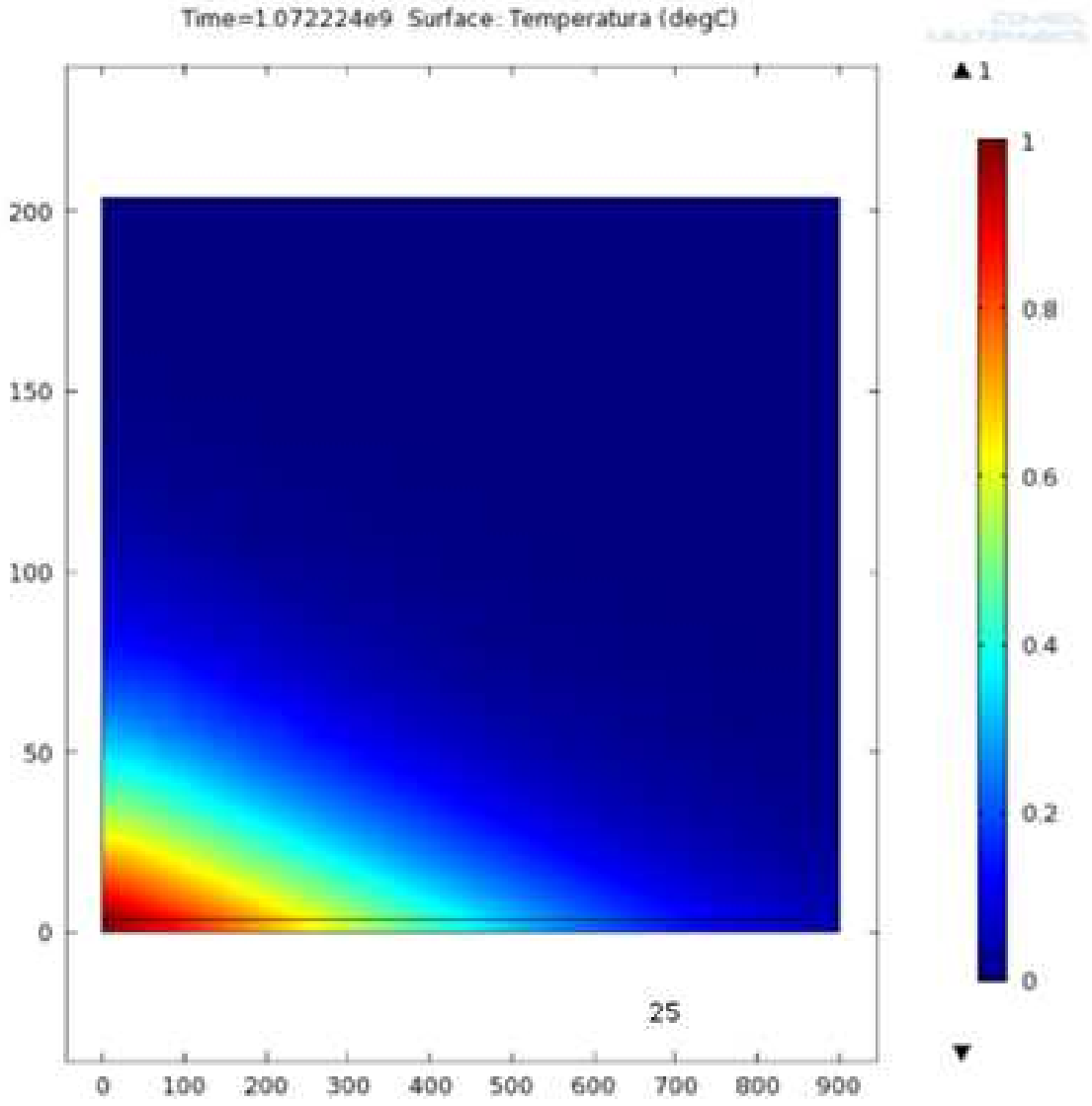

Figure 3.15 – Distribution temperature in the fracture and in the rock after a period of 34 years.

3.6.2 Bourbiaux Study in ATES system

An interesting study was presented by Bourbiaux (2011),in fact it studies systems ATES "Acquifer Exchanger Thermal Storage" for the purpose of accumulating thermal energy reservoirs in saline aquifers occur naturally in the earth's crust. The operation of these systems is seasonal, in summer cold water is withdrawn from the ground, to be used for example in the condensers of the refrigeration machines, to then be re-injected in the same reservoirs, through a second well positioned, at a due distance from the well of extraction. In winter, hot water, accumulated during the summer season, is drawn. Thus, the function of the two wells is alternated as a function of the seasons.

One thing, essential for the proper functioning of this system, is the choice of a suitable distance between the two wells, necessary to avoid thermal contamination , the two bubbles (hot bubble and cold bubble) within the same reservoir.

The Figure 3.16 clarifies the comprehension of the problem:

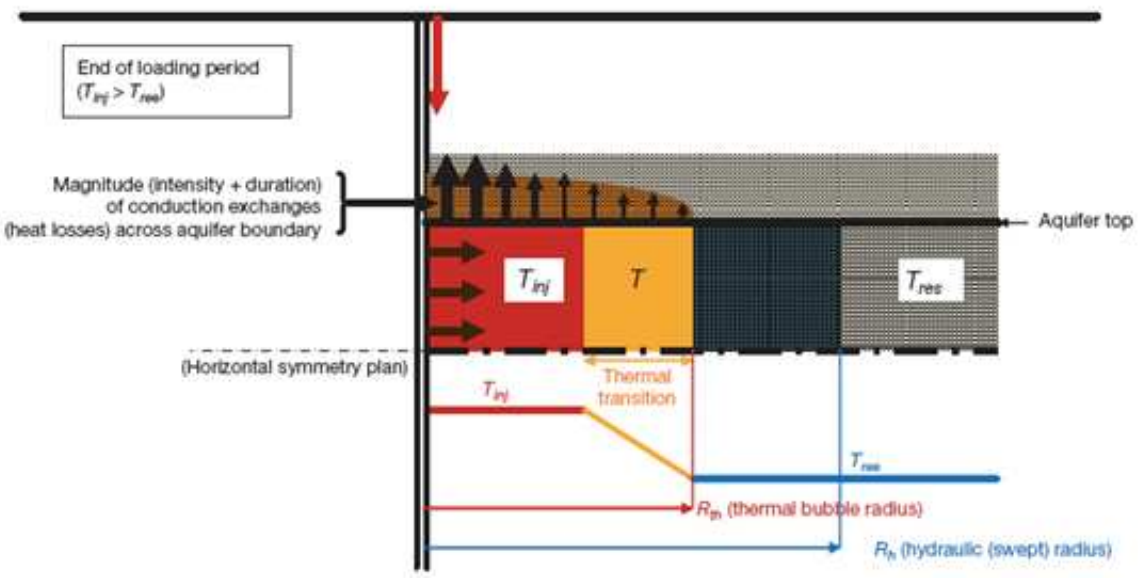

Figure 3.16 – Schematic diagram of a system ATES.

Inside the well, a certain flow of fluid at a temperature T_{w0} (T_{inj} in the figure) is injected; this flow,, with the passing of time, expands radially inside the reservoir, the latter at a temperature undisturbed T_{res}. After a certain period of time, it can show three distinct areas inside the reservoir:

A zone where the temperature is constant and equal to the temperature of the injected water (red zone);

A transition zone in which the thermal temperature degrades until it reaches the initial temperature of the reservoir (yellow zone);

An undisturbed temperature with constant and equal to the initial temperature of the reservoir.

Two important rays, the radius R_{th} thermal and hydraulic R_h are shown. The hydraulic radius refers to the distance travelled by the fluid at the end of the injection period, then it grows with the growth of the total volume of water injected. The radius thermal instead is smaller (by 30 to 70% of the hydraulic radius as a function of the porosity of the aquifer), since the thermal front is lagging behind the front hydraulic. It represents the minimum distance for which it is possible to find the temperature undisturbed of the reservoir.

The thickness H of a porous and permeable, it is possible to estimate the hydraulic radius of the water stored in a cylindrical bubble:

$$R_h = \sqrt{\frac{V_{inj}}{\phi \pi H}} \tag{3.27}$$

It can be defined a form factor as the ratio of the hydraulic radius and the net height of the aquifer:

$$\frac{D_h}{H} = \frac{2R_H}{H} = 2\sqrt{\frac{V_{inj}}{\pi \phi H^3}} \tag{3.28}$$

In addition Bourbiaux, in his article, defines an energy balance between the hot water injected and the volume heated of the reservoir porous:

$$V_{inj}\rho_w c_{pw}\left(T_{inj} - T_{res}\right) = \pi R_{th}^{\ 2} H\left[\phi\rho_w c_{pw} + (1-\phi)\rho_s c_{ps}\right]\left(T_{inj} - T_{res}\right) \tag{3.29}$$

With V_{inj} volume of water injected at a temperature T_{inj}, T_{res} is the initial temperature of the reservoir, ρ_w, and ρ_s, the density of the stored water, and the grains of rock, c_{pw}, c_{ps} and the respective specific heat per unit mass. R_{th} is the radius of the area of the thermal reservoir heated, also called "thermal bubble". Where R_{th} is the thermal radius, the following balance equation, is equal to:

$$R_{th} = \sqrt{\frac{V_{inj}}{\pi H}\frac{\rho_w c_{pw}}{\phi\rho_w c_w + (1-\phi)\rho_s c_{ps}}} = \sqrt{\frac{\phi\rho_w c_{pw}}{\phi\rho_w c_{pw} + (1-\phi)\rho_s c_{ps}}} \tag{3.30}$$

The author studied the phenomenon of heat conduction, which occurs when the hot water is injected into an aquifer, through the boundaries upper and lower sections of the permeable layer, at the same time in which the hot water is propagated along the porous medium (Figure 6). From superposition of transport phenomena, and conduction results a radial profile of non-uniform temperature. A solution for this problem has been developed by Lauwerier (1955) and applied by Bulter (1991) for the study of thermal processes useful for the recovery of petroleum. Bourbiaux presents the results in conditions of radial flow for a cycle of first storage.

The model predicts the presence of a water reservoir, of total height H, with a porosity of 20%. The reservoir is surrounded above and below by a layer of impermeable rock. Other assumptions are:

$T(y,0) = T_{res}$ $(-H/2 < y < +H/2)$;

$T(y,0) = T_r = T_{res}$ in the background infinity ($y < -H/2$ e $y > +H/2$) : T_r varies with depth according to the geothermal gradient, but may nevertheless be regarded as fixed and equal to the initial value the temperature of the reservoir T_{res} (in the example of Bourbiaux T_{res} = 60 ° C) if the flap is between a depth of 10 to 100 m;

The hot water is injected into the aquifer at a constant flow rate, Q, at the temperature T_{w0} (in the example of Bourbiaux T_{w0} = 90 ° C).

The equations that govern the temperature range are:

$$T_1(r,t) = T_{res} + (T_{w0} - T_{res})erfc(X) \tag{3.31}$$

$$X = \frac{x_D}{2}\frac{1}{[\theta(t_D - x_D)]^{0.5}} \tag{3.32}$$

With:

$$x_D = \frac{4\lambda_r \pi r^2}{H\rho_w c_w Q} \tag{3.33}$$

$$t_D = \frac{4\lambda_r t}{H^2 \rho_{sat} c_{sat}} \tag{3.34}$$

$$\rho_{sat} c_{psat} = \phi\rho_w c_w + (1-\phi)\rho_s c_s \tag{3.35}$$

Where:

λ_r is the thermal conductivity of the layer of rock overlying and underlying aquifer;

Φ is the porosity;

θ is the ratio between the volumetric heat capacity of the aquifer and the layer of rock bordering with it (in the exercise is taken per unit);

the subscripts w, s, sat stand for water (water), sand (sand) and saturation (satured);

The radial profile of temperature after 180 days of injection is shown in Figures 3.16, and 3.17, for different heights, H of the reservoir (5, 10, 25, 100 m). The thermal properties of the reservoir and the geological formation are assumed equal.

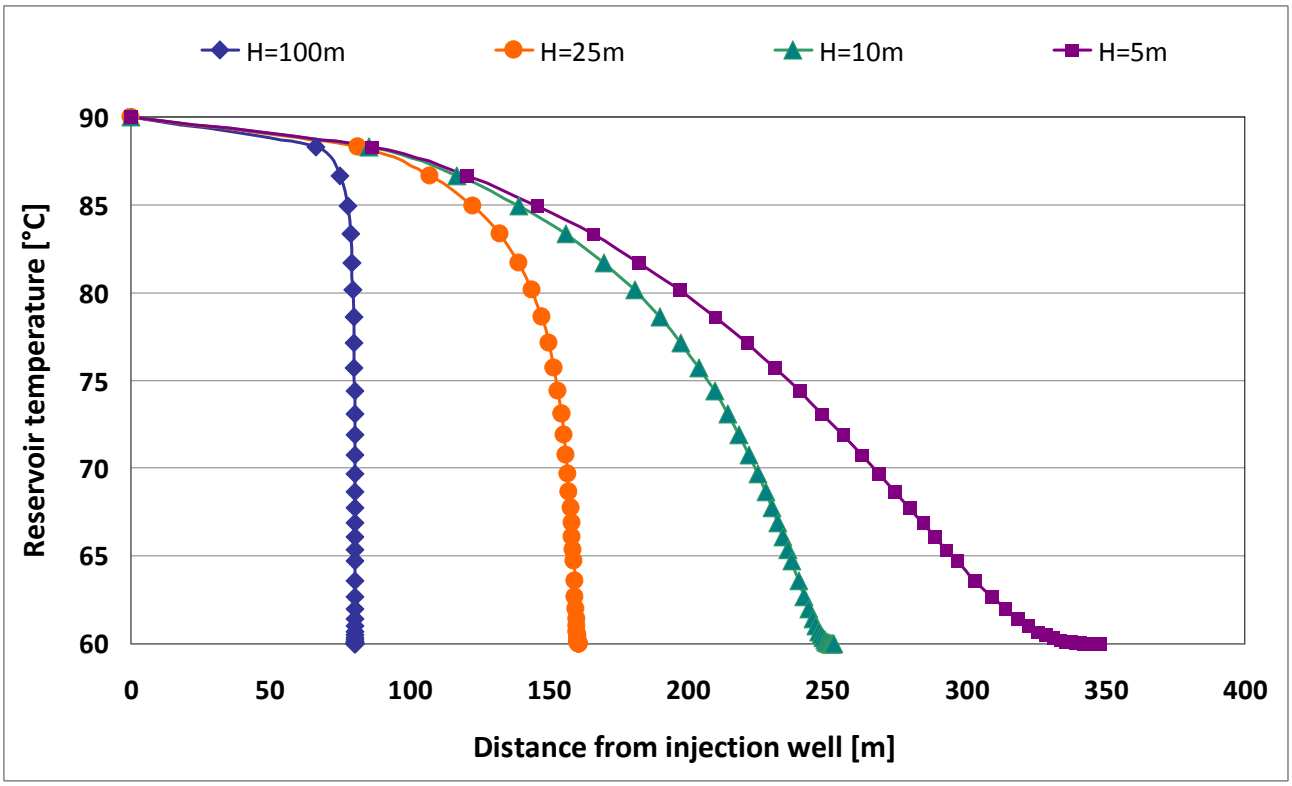

Figure 3.16 – Temperature as a function of radial distance from the well after 180 days of injection of a hot fluid at a constant flow rate (300 m3/h) for different values of thickness H of the aquifer.

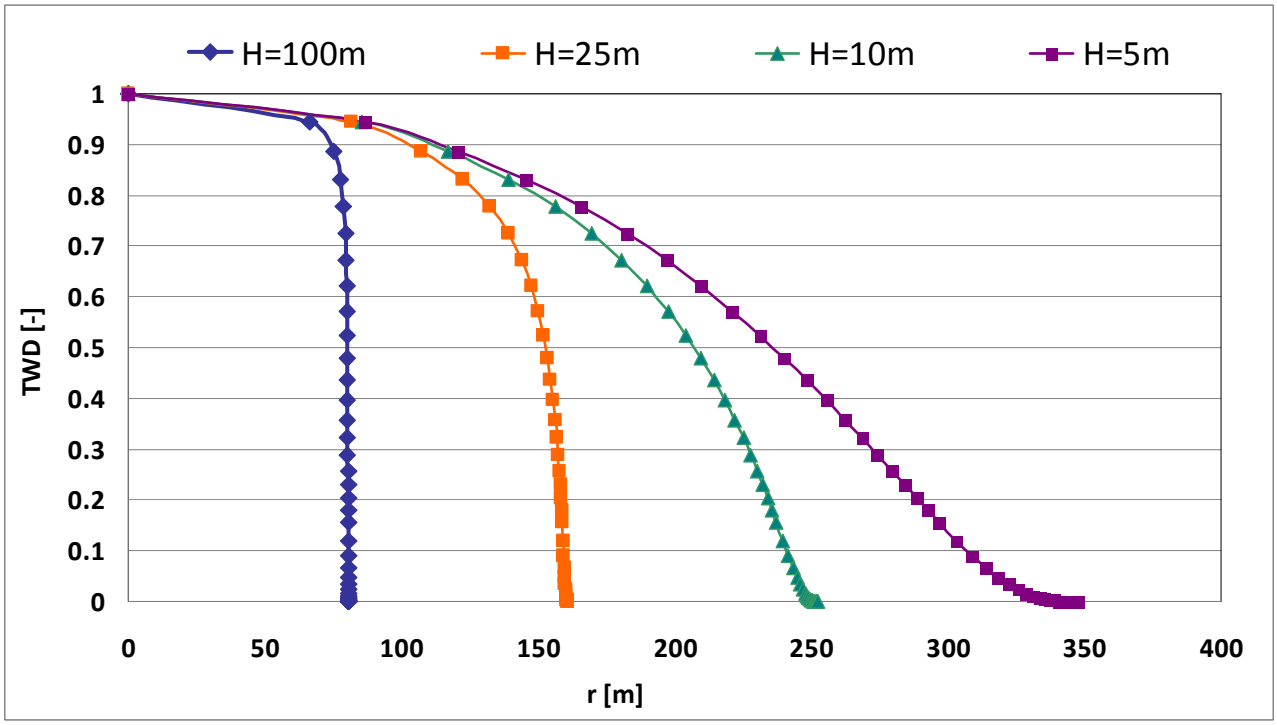

Figure 3.17 – Dimensionless Temperature as a function of radial distance from the well, the curves reflect the analytical solution of Lauwerier for different heights H of the aquifer.

It is noted that, to decrease the height H of the aquifer, injected at the same flow rate, the heat front travels ever at greater distances. This phenomenon is easily understood if one thinks that the injected water expands with a cylindrical shape, then with increasing distance from the well, the velocity of the water front decreases. However, the decrease of the height H the lateral area of the cylinder, directly proportional to the flow, decreases considerably, producing an inevitable increase of the radial velocity. This means that the thermal front travels faster, and propagates more distant from the well.

Moreover, the author Bourbiaux, offers interesting comments on these temperature profiles, which can help to define the heat losses due to conduction through the upper boundary and lower aquifer,, presenting the results in a table where ,for each thickness, he highlights the theoretical thermal aquifer radius R_{th} and the relative heat loss of the reservoir:

Table 3.2 . Heat loss from the tank through the upper and lower boundaries at the end of a storage period of 6 months with a flow rate of 300 m3/h.

Reservoir Thikness [m]	5	10	25	100
Heat loss (% of total stored heat)	57.5	37.3	20.0	7.1
Theoretical thermal radius R_{th} [m]	361	255	162	81

Finally, the author presents interesting considerations:

- For an aquifer thickness of 25 m, the losses conduction, are equal to 20% of heat stored after 180 days of injection;

- For a thickness groundwater which decreases from 100 m to 5 m, the losses by conduction increases from 7.1% to 57.5% of the accumulated heat. 10 m is considered the minimum thickness, as order of magnitude, for which the thermal losses by conduction through the boundaries become prohibitive. Opposite, an aquifer with thickness of the order of 100 m is an excellent reservoir for heat storage;

- For a given thickness groundwater, the losses by conduction show little sensitivity to the porosity of the rock, this is because the heat capacity of the rock saturated, is not very sensitive to the porosity of the rock. This means that the radius of the bubble does not change much heat to vary the porosity, contrary to the hydraulic radius;

- A reduction in the duration of storage, does not effectively compensate for the reduced characteristics of the vessel: for example, considering an aquifer thickness of 5 m, by reducing the period of charging and discharging at three months (instead of six) does reduce losses but not proportionally (thermal losses decreased from 57.5 to 48.5%, only 15% less in relative value).

Considerations and estimates carried out above, relate to the first cycle storage. At the end of this first injection, the quantity of heat lost through the boundaries is greater, the longer the time duration of the contact with the hot fluid is, that is the greater, the smaller the distance from the injection well is. During the subsequent period of discharge, a fraction of this lost heat can be recovered by conduction "inverse", but to a limited extent, because the cold fluid pumped from distant regions of the reservoir is heated by borders, but for a time much shorter than nearest the well.

The same phenomena are re-iterated during subsequent periods of loading / unloading but with a smaller amplitude, compared to the first cycle due to the decrease of the temperature gradient through the boundaries of the aquifer. Eventually, the succession of cycles contributes to create and maintain an environment heated for the accumulation of thermal energy, resulting in a higher recovery factor.

Numerical simulations of cycles of loading and unloading are required, to quantify the temperature distribution in the reservoir. Analytical solutions can only provide an estimate of the evolution of the thermal aquifer as a whole.

This study by Bourbiaux (2011), is useful to compare these results with a finite element model FEM, and verify the trend of the temperature in the aquifer within 180 days of injection.

3.6.3. FEM analysis and comparison of Studies conducted by Bourbiaux

For the realization of the model in the environment FEM,a system 2D asymmetric, was used; this is because the injected flow expands radially in all directions. Since, moreover, the system symmetric with respect to the centreline plane of the aquifer, is considered only half geometry in order to reduce the computational burden required to process the solution of the problem.

The geometry of the problem is therefore:

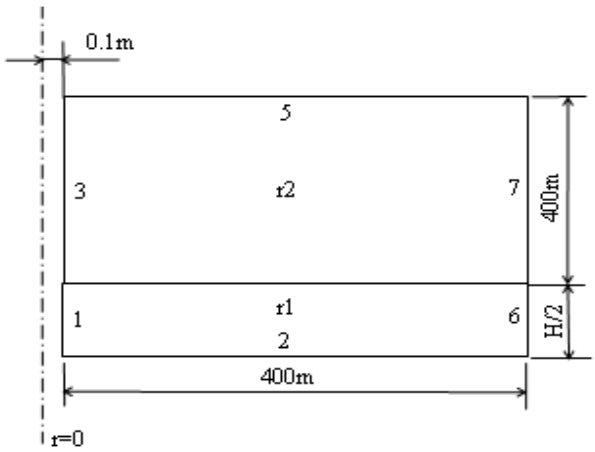

Figure 3.18 – Geometry for ATES system in COMSOL Multiphysics.

The conditions on the domains and boundaries are summarized in Table 3.3.

Table 3.3 . Conditions of domains and boundaries on the COMSOL model system ATES.

	DOMAIN		BOUNDARY					
	r1	r2	1	2	3	5	6	7
TEMPERATURE [°C]	60	60	90	-	-	-	-	-
VELOCITY [m/s]	vinx(rin/r)	-	-	-	-	-	-	-
FLOW OUTGOING	-	-	-	-	-	-	✓	-
INSULATION THERMAL	-	-	-	-	✓	✓	-	✓
SIMMETRY	-	-	-	✓	-	-	-	-

The block r_2 represents the layer of rock overlying the aquifer, while the block r_1 is the aquifer; they are respectively identified with the properties of Table 3.4. Note that the domain r_1 corresponds to a porous matrix having a porosity $\Phi = 0.2$, ie, 20% by volume of r_1 is formed by rock having the same properties of r_2; the remaining 80% is made up of water.

Table 3.4 . Parameter used in the solution of the problem.

Q [m^3/h]	300	Volumetric flow rate
ρ_w [kg/m^3]	1000	Density of water
c_w [J/(kgK)]	4180	Specific heat of water
ρ_r [kg/m^3]	2700	Rock density
c_r [J/(kgK)]	840	Specific heat of rock
λ_r [W/(mK)]	3	Conductivity of rock
T_{res} [°C]	60	Initial temperature
T_{w0} [°C]	90	Water inlet temperature
ϕ	0.2	Porosity aquifer
t [days]	180	Period of analysis

The flow velocity V_w, being variable as a function of the distance from the well, is defined in section variables of COMSOL Multiphysics It applies to:

$$V_w = v_{in}\left(\frac{r_{in}}{r}\right) \qquad v_{in} = \frac{Q}{2\pi r_{in} H}$$

Where: vin represents the radial velocity of the water at the edge of the well radius r_{in}. The flow rate Q is 300 m^3 / h, the radius of the well rin has been chosen equal to 0.1 m, while the thickness H takes the following values: 100, 25, 10, 5 m.

The analysis is purely thermal; in fact heat exchange by conduction and convection are considered. The equations used by the model are (3.33), (3.34).

The rate of temperature, along the centreline of the aquifer, results as follows:

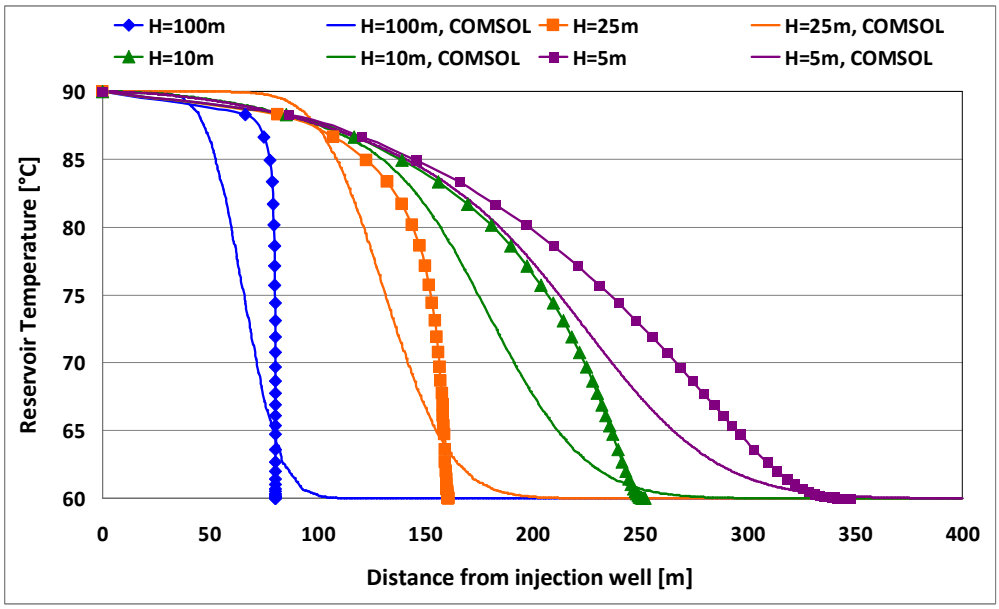

Figure 3.18 – Comparison of analytical results and FEM. Temperature as a function of radial distance from the injection well.

The following shows the comparison between the analytical results and the results obtained from the simulation in COMSOL Multiphysics.

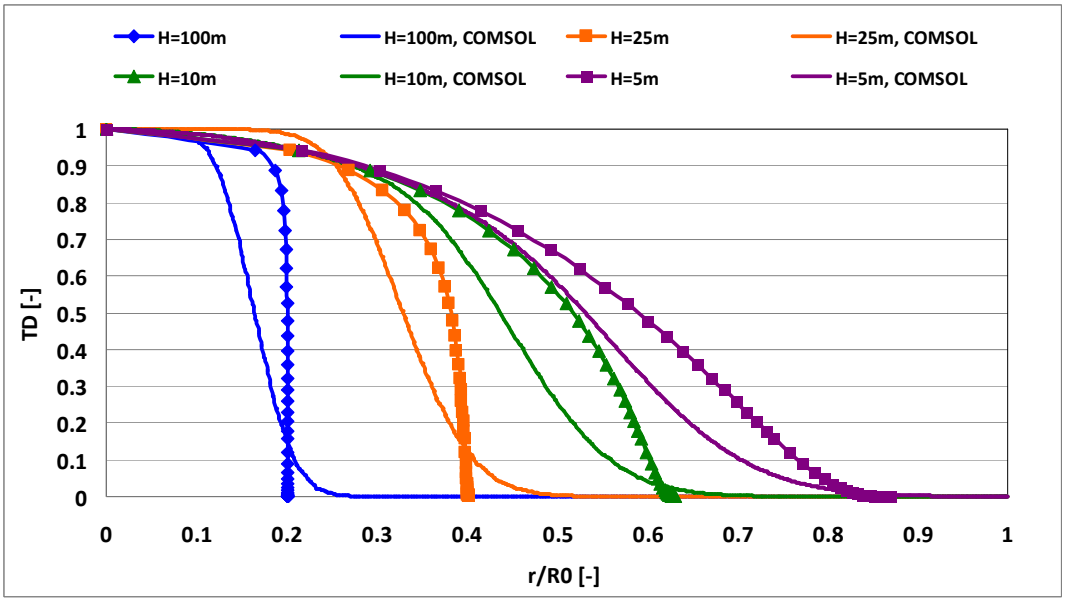

Figure 3.19 – Comparison of analytical results and FEM. Dimensionless temperature as a function of radial distance from the injection well also in dimensionless form.

Note, as the analytical curves tend to overestimate the temperature inside the reservoir approximately up to that $T_{WD} < 0.1$. For heights (H = 100m, H = 25m) the front thermal analytical curves, are very steep, almost vertical. From a physical point of view we would have a difference of a very high temperature in a few meters. The numerical curves, instead, show that the thermal front is not so steep, the temperature in the reservoir decreases more slowly.. In addition, the decrease of the thickness H of the analytical and numerical curves tend to get closer. To confirm this, the following proposes the comparison between numerical and analytical solution for height H = 1 m, see Figure 3.20, for small thicknesses of the aquifer curves are practically coincident. As a result, it was defined in the hypothesis of Lauwerier that the analytical solution can be used for small fractures, compared to the size of the aquifer or rock. This applies both in cylindrical and linear coordinates.

Increasing the thickness of the aquifer, the results obtained with finite elements tend not to coincide with analytical data. However, it must be said that, for systems ATES, the temperature profile has little relevance because we must be careful here, for a correct dimensioning, at the minimum distance from the well to the temperature undisturbed ground.

Now, it can be said that the solution of Lauwerier is not suitable to study the trend of temperature with thicknesses H high; for this reason, FEM simulations are important in programs. However, we can use the theory of Lauwerier to obtain quickly a preliminary value of the distance, to be able to position the second well. The procedure is divided into three steps:

known injection time t, and note the characteristics of the aquifer and the rock surrounding it is possible to calculate t_D and θ;

with the following formula to calculate the dimensionless parameter X_D:

$$X_D = -18\theta^2 + \sqrt{\left(18\theta^2\right)^2 + 36\theta^2 t_D} \tag{3.36}$$

the radial distance, r, is therefore:

$$r = \sqrt{\frac{H\rho_w c_w}{4\lambda_r \pi} X_D} \tag{3.37}$$

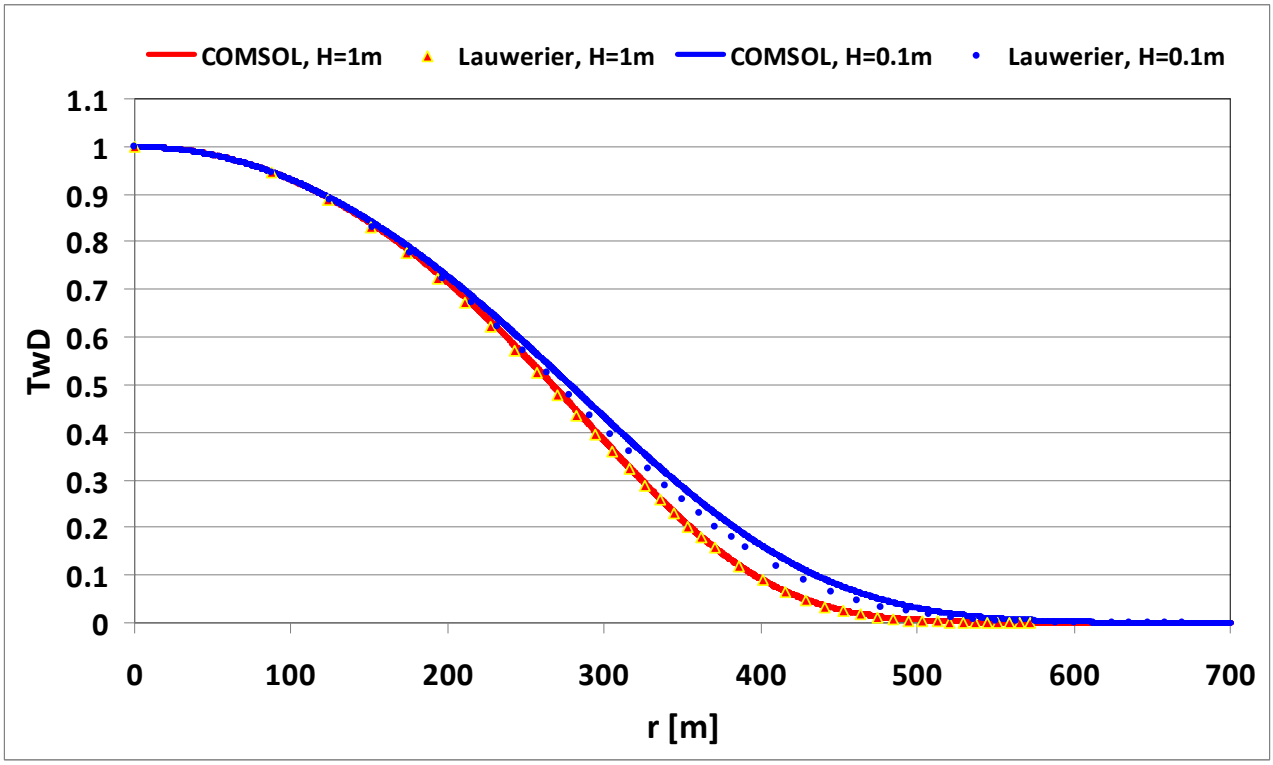

Figure 3.20 – Dimensionless temperature as a function of redial distance for the aquifer height equal to H = 0,1m and 1m. Comparison of the analytical method and FEM.

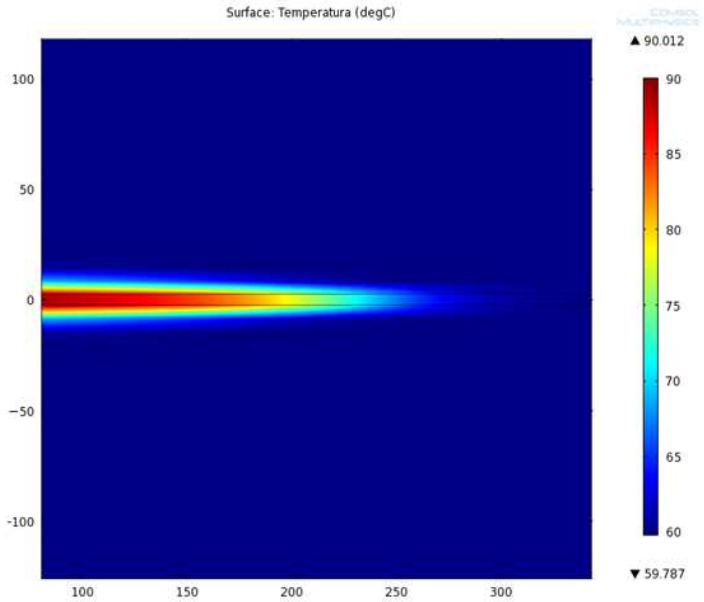

Figure 3.21 – Field of temperature in a system ATES with height H = 5m situation the 180th day of injection.

The same study was done comparing the FEM model, with the analytic theory of Lauwerier, and the analytic theory of Ghassemi; in this case the thermal parameters of the geothermal reservoir (see Table 3.5), have been changed:

Table 3.5. Parameter used in the solution of the problem.

Q [m^3/h]	1800	Volumetric flow rate
ρ_w [kg/m^3]	1000	Density of water
c_w [J/(kgK)]	4160	Specific heat of water
ρ_r [kg/m^3]	2600	Density rock
c_r [J/(kgK)]	1000	Specific heat of rock
λ_r [W/(mK)]	1.8	Conductivity rock
T_{res} [°C]	60	Initial temperature
T_{w0} [°C]	90	Water inlet temperature
ϕ	0.2	Porosity aquifer
t [days]	180	Period of analysis

In Figure 3.22, a comparison between the analytical solutions of Lauwerier, and Ghassemi with the FEM model is presented; also in this case the analytical solutions of both Lauwerier and Ghassemi are coincident with the solution obtained from the finite element model FEM, for very small thicknesses of aquifer (for example 0.1 m), in line with the assumptions made by the authors that pose small thickness to ensure the laminar regime of motion of the water,. while for greater thickness we begin to see differences in the solutions In fact, in the analytical solutions, the trend of the temperature decreases, along the radial distance, in a very quick steep, compared to the solutions of the finite element model FE. Also in this case, it is evident that the solution FEM model initially leans to the solution of Ghassemi, and then tend towards the solution of Lauwerie, It can be said that in the absence of a finite element model FEM, the solution of Lauwerier, easy to implement in a spreadsheet, gives interesting and safe results, to have an initial estimate of the minimum distance between the two wells: production and re - injection and then thermal evolution of the aquifer.

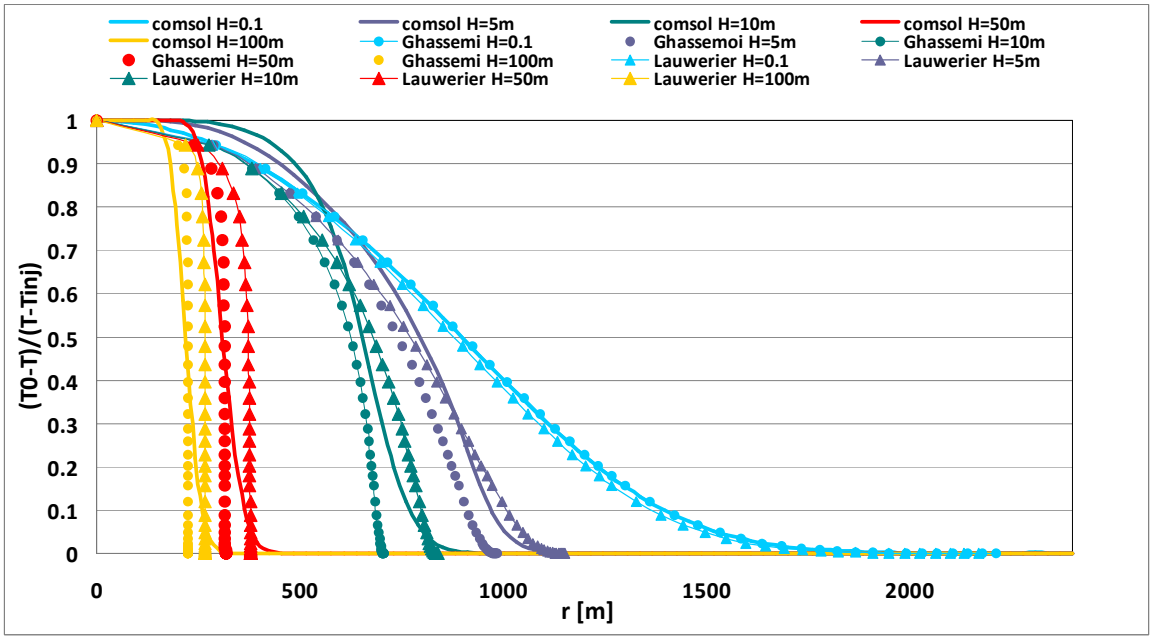

Figure 3.22 – Comparison of analytical results and FEM. Dimensionless temperature as a function of radial distance from the injection well.

In the graph of Figure 3.23, a comparison between dimensionless temperature and distance from the well, comparing the two analytical theories Lauwerier and Ghassemi, and the FEM model was presented. In this graph, it is confirmed that in small thicknesses, in this case 0.1 m, the three solutions coincide as it is respected the hypothesis of small thickness of the aquifer or the fracture of the rock.

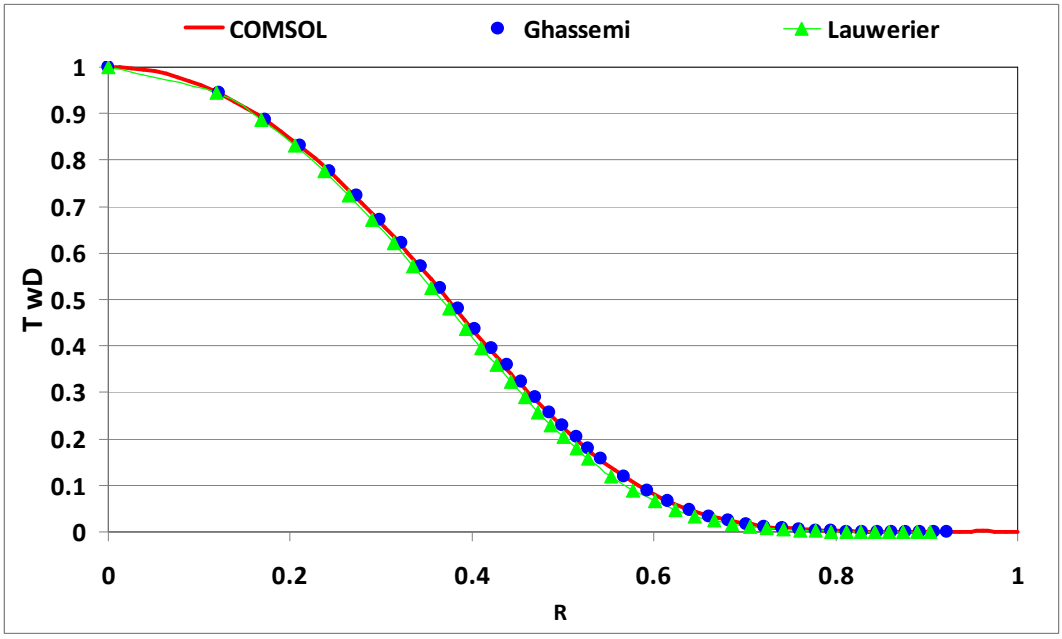

Figure 3.23 – Dimensionless temperature as a function of distance for dimensionless height of the aquifer equal to H = 0,1m, Comparison of analytical and FEM.

3.7 Conclusions

In this chapter,we have studied some aspects of the medium-temperature geothermal energy, mainly studying the thermal evolution of the aquifer in the case of ATES systems, analyzing, according to the theories of Lauwerier and Ghassemi, with regards to the results obtained using a finite element model FEM, the temperature trend, over time, of the aquifer once rejected hot water in the same, thus evaluating the size of the thermal bubble, then the heat stored in the geothermal reservoir, and evaluating the minimum distance to be kept between two production wells and injection.

The results have shown that for small thicknesses the trend is identical for both analytical theories and the FEM model, since the hypothesis of small thickness of the aquifer is placed in the analytic theories. Differences in the results are found when the thickness of the aquifer begins to be more of a meter, the FEM solution, in fact, tends to lean to the first solution for Ghassemi then approach, along the radial distance r, towards the solution of Lauwerier, also this latest theory tends to give higher results than Ghassemi and FEM, so to estimate the size of the thermal bubble theory. Lauwerier‘s theory is more precautionary than Ghassemi’s.

3.8 Reference

Axelsson, G., 2008a: Importance of geothermal reinjection. Proceedings of “Workshop for Decision Makers on the Direct Heating Use of Geothermal Resources in Asia”, organized by UNU-GTP, TBLRREM and TBGMED, Tianjin, China, 15 pp.

Axelsson, G., 2008b: Management of geothermal resources. Proceedings of “Workshop for Decision Makers on the Direct Heating Use of Geothermal Resources in Asia”, organized by UNU-GTP, TBLRREM and TBGMED, Tianjin, China, 15 pp.

Axelsson G., Role and management of geothermal reinjection, (2012), Presented at “Short Course on Geothermal Development and Geothermal Wells”, organized by UNU-GTP and LaGeo, in Santa Tecla, El Salvador, March 11-17, 2012.

Baietto A., Pochettino M., Salvatici E., (2010), Progettazione di impianti geotermici: sonde verticali e pozzi d’acqua, ISBN 978 – 88- 579 – 0058 – 2, Dario Flaccovio Editore s.r.l.

Banks D., 2009, Thermogeological assessment of open – loop well – doublet schemes: a review and synthesis of analytical approaches, Hydrogeology journal, 17, pp. 1149 – 1155.

Boubiaux B., ATES Contribution to the Housing Energy Balance: a Simple Assessment Methodology, Oil & Gas Science and Tecnology – Rev. IFP Energies nouvelles, Vol.66 (2011), No. 1. Pp. 21-36

Bulter R.M. (1991) Convective heating within reservoirs, in thermal recovery of oil e bitumen, Prentice – Hall, Englewwod Cliffs.

Carslaw H.S., Jaeger J.C., Conduction of Heat in Solids, 2nd ed. Clarendon Oxford, 1959, p. 396.

Cheng A.-D., Ghassemi A., Detournay E., 2001. A two-dimensional solution for heat extraction from a fracture in hot dry rock, Int. J. Numer. Analy. Meth. Geomech., 25, 1327-1338.

De Carli M., Roncato M., Zarrella A., Zecchin R., Energia dal terreno, (2007) Convegno AiCARR "Energie rinnovabili: tecniche e potenzialità", 21 Giugno 2007, Padova.

Deng Z., Modeling of standing column wells in ground source heat pump systems, Submitted to the Faculty of the Graduate College of the Oklahoma State University in partial fulfillment of the requirements for the degree of DOCTOR OF PHILOSOPHY December, 2004

Ghassemi A., Cheng A. H. D., Tarasovs S.. A Three-dimensional solution for heat extraction a fracture in hot dry rock using the boundary element method, Twenty-Seventh Workshop on Geothermal Reservoir Engineering Stanford University, Stanford, California, January 28-30, 2002 SGP-TR-171

Ghassemi A., S. Tarasovs S., Three-dimensional modeling of injection induced thermal stresses with an example from Coso, Twenty-Ninth Workshop on Geothermal Rservoir Engineering, Stanford University, Stanford, California, January 26-28, 2004

Lauwerier H.A., The transport of heat in an oil layer caused by the injection of hot fluid, Appl. Sci. Res., Sect. A Vol. 5, 1955, pp. 145 – 150.

Web site:

www.iii.to.cnr.it/laghi/maggiore.html

http://www.hvac.okstate.edu

4. HIGH TEMPERATURE GEOTHERMAL ENERGY

4.1 Introduction

The intense development of residential and industrial activities increased more in recent decades, using mainly the consumption of fossil fuels, resulting in climate change, greenhouse effect and environmental pollution.

World Climate Conferences and agreements signed by all the international countries, have lead to agree to reduce greenhouse gas emissions, improving the efficiency of systems and process, with the development of new technologies and diversifying as much as possible renewable energy sources.

Among the energy sources, geothermal energy is considered sustainable affordable, non-polluting, and renewable. It can be exploited for power generation, as well as for district heating.

The simple concept behind the Hot Dry Rock (HDR), is to exploit the thermal energy of the rock underground, heated over time by the presence of magma below.

The rock absorbs energy by conduction, by the latter, and yields water, which flows through the fractures of the rock, those formed by the hydraulic pressure of the water, injected artificially.

In the zones of thermal anomaly, where faults occur or in volcanic areas, the water temperature reaches high values of temperature, such as to provide hot water, steam, hot springs, fumaroles.

In HDR systems, two wells are installed below the ground, allowing the extraction of and the re - injection hot water (cooled by enthalpy exchange in a turbine and / or in a heat exchanger).

Many studies have been conducted by various authors, who presented the first simple theories of heat exchange between water and rock (single fracture), and then the generalized phenomenon of multi - fractures and randomly fractured rock, where it is necessary a parameter that identifies the density of fracture of the rock.

4.2 Principal theories on the extraction of heat from the rock through the heat exchange between the rock and water

A simplified solution of the problem was carried out by Carslaw and Jaeger (1959). Afterwards Lauwerier in 1955 modeled the heat transfer of a hot fluid injected into a fracture of thin, porous medium containing petroleum high density, in order to increase extractability of oil, reducing its viscosity. The mathematical study of Carslaw and Jaeger was taken up by Bodvarsson as well in its various studies (1969 - 1970 - 1972 - 1974), to quantify the extraction of heat from a hot dry rock, in the simple case of a single fracture. Similar Gringarten et al . (1975) be extended the problem from a single rock with a rock fracture to multiple vertical fractures, parallel and equidistant from each other. The model of Gringarten is much closer to reality, as in a geothermal reservoir rock multiple fractures, are present in order to achieve a high heat exchange surface, to assure the heat throughout the life cycle of the geothermal reservoir.

4.2.1 Carslaw and Jaeger (1948 – 1959)

The study of the extraction of heat in a single fracture, was conducted initially by Carslaw and Jaeger (1959) based on the following equations:

$$\dot{m} c \frac{\partial T}{\partial y} = 2\lambda \left(\frac{\partial T_r}{\partial x} \right)_0 \tag{4.1}$$

$$\lambda \frac{\partial^2 T}{\partial y^2} = (\rho c)_r \frac{\partial T_r}{\partial t} \Rightarrow a \frac{\partial^2 T}{\partial z^2} = \frac{\partial T}{\partial t} \tag{4.2}$$

$$\frac{T_r - T_{(y,t)}}{T_r - T_{W0}} = erfc \left[\frac{\lambda H}{\dot{m} c \sqrt{at}} \right] \tag{4.3}$$

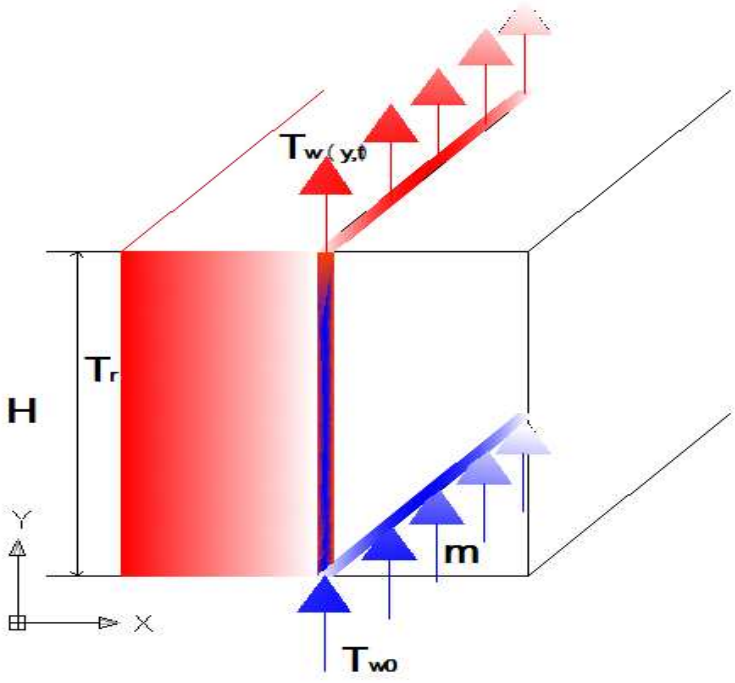

Figure 4.1 – Heat extraction in a single fracture

4.2.2 Lauwerier (1955)

Lauwerier proposed a mathematical model for the injection of hot water in a porous medium saturated with oil by studying the problem in partial differential equations. The hypotheses considered are: uniform thickness, permeability and porosity of the reservoir, constant flow, infinite conductivity in the direction normal to the flow of, absence of axial conduction, thermal equilibrium between water and rock. Energy balance equation:

$$b\rho_1 c_1 \frac{\partial T_w(x,t)}{\partial t} + b\rho_w c_w v \frac{\partial T_w(x,t)}{\partial x} - \lambda_r \left(\frac{\partial T_r}{\partial y} \right)_{y=b} = 0 \qquad (4.4)$$

General equation for the heat conduction of the rock in the HDR:

$$\lambda_r \frac{\partial^2 T_r}{\partial y^2} = \rho_r c_r \frac{\partial T_r}{\partial t} \qquad (4.5)$$

4.2.3 Bodvarsson (1969 – 1970 – 1972 – 1974)

The study conducted by Bodvarsson (1969) defines a simple theoretical model for the evolution of the temperature of water passing through a single fracture of impermeable rock. The assumptions made by the author are:

- Model fracture consisting of a flat open space of constant width h between two large blocks of homogeneous and isotropic, impermeable rock;
- The plane y = 0 coincides with one of the two edges of the fracture, with the y-axis oriented towards the adjacent rock;
- The x-axis follows the development of the fracture;
- Along the fracture, a constant mass flow per unit depth z of the fracture;
- Temperature of the rock T (x, y, t) does canot depend on z;
- The temperature range is symmetrical with respect to the fracture and the width h is small in order to consider constant the temperature of the fluid; one considers then the temperature of the fluid equal to that of the rock in y = 0;
- Transport of heat by conduction and convection in the rock along the x axis in the fracture;
- Absence of conduction along the x-axis.

The temperature field in the rock can be expressed by means of the heat equation:

$$\frac{\partial^2 T}{\partial z^2} + \frac{\partial^2 T}{\partial y^2} = \frac{1}{\alpha}\frac{\partial T}{\partial t} \qquad (4.6)$$

The effect of convective transport is considered as a boundary condition on the surfaces of the fracture:

$$\rho_w c_w b \frac{\partial T}{\partial t} + c_w q \frac{\partial T}{\partial z} = 2\lambda \frac{\partial T}{\partial y} \qquad at \quad y = 0 \qquad (4.7)$$

With:

ρ_w [kg/m3] = water density

c_w [J/kg K] = Specific heat of the water

b [m] = width fracture

q [kg/s m] = specific mass flow rate along the fracture

λ [W/m K] = thermal conductivity of the rock

An interesting case study is presented by Bodvarsson considering constant flow and sinusoidal temperature change, assuming the temperature $T = A\exp(i\omega t)$ in x =0, y = 0, where A is an arbitrary, real amplitude.

The solution of the dimensionless temperature, is equal to:

$$T_D = A\, erfc\left[\frac{(\alpha x + y)}{\sqrt{\alpha t}}\right] \qquad (4.8)$$

4.2.4 Gringarten, Witherspoon and Ohnishi (1975)

The authors have presented a more complete model on the extraction of heat from Hot Dry Rock, starting from the analytical solution of Carslaw and Jaeger and from Bodvarsson. They extend the problem of heat transfer from single fracture to multi - fracture, as , in general, a HDR geothermal reservoir presents multi – fracture. This allows, assuming the same flow rate, to increase the heat exchange surface, allowing to extract water at higher temperatures over the time, thus increasing the life of the reservoir. (see Figure 4.2).

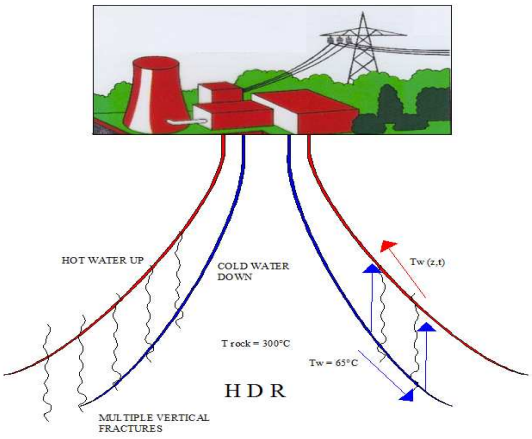

Figure 4.2 – Scheme of Hot Dry Rock.

The assumptions underlying the model are:

- Linear Model;
- Infinite vertical fractures parallel and equidistant;
- Width of fractures are uniform;
- Rock is homogeneous, isotropic and impermeable;
- Width of fracture are negligible compared to the distance between fractures.

Due to the symmetry of the model, it is possible to study the following simplified model. (Figure 4.3):

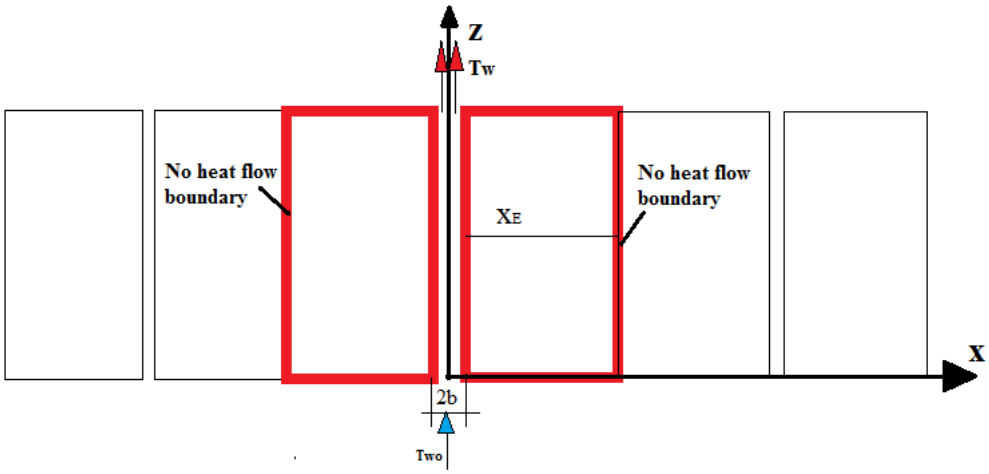

Figure 4.3 – Mathematical model for fractured Hot Dry Rock.

Simplifying assumptions:

- Density and specific heat of rock and fluid are constant;
- Constant thermal conductivity of the rock;
- Volume flow of the fluid is constant;
- The water temperature Tw (z, t) is uniform in each section of the fracture and equal for each height z to the temperature of the rock on the edge x = b;

- No conduction in the vertical direction of the fracture and in the rock. All the heat is transferred by conduction horizontal by into the rock and by forced convection in the fracture;

- Initially, both the water in the fracture and the rock are at the same temperature. This temperature is not uniform along the fracture but it depends on z. At a given height z, the initial value of the temperature is calculated is: T_{ro} '= T_{ro} - z * ω where T_{ro} is the temperature of the rock at the injection point and ω is the temperature gradient of the rock [K / m] ;

- No flow of heat is exchanged with the contour at a distance x = x_E + b.

The differential equation that governs the temperature of the water is obtained by writing the thermal balance of an element of fracture with a volume dV = dz * db * 1 m^3.

Gringarten studied a mathematical model first based on a single fracture and after on a multiple fracture, considering the vertical fractures to be parallel (Fig. 4.3).

The assumptions are based on: linear model, infinite parallel and equidistant vertical fractures, uniform fracture width, homogeneous isotropic impermeable rock, fracture width negligible. The heat equation in the rock is described as:

$$\frac{\partial^2 T_r(x,y,t)}{\partial x^2} = \frac{\rho_r c_r}{\lambda_r} \frac{\partial T_r(x,y,t)}{\partial t} \qquad (4.9)$$

The heat transfer from water to rock assumes pure convection of water and pure conduction in the rock:

$$b\rho_w c_w \left[\frac{\partial T_w(y,t)}{\partial t} + v \frac{\partial T_w(y,t)}{\partial y} \right] = 2\lambda_r \left. \frac{\partial T_r(x,y,t)}{\partial x} \right|_{x=b} \qquad (4.10)$$

Where:

ρ_w[kg/m^3] = water density

c_w [J/kgK] = water Specific heat

b [m] = fracture width

T_w [K] = water temperature

t [s] = time;

v [m/s] = water velocity

λ_R[W/mK] = rock thermal conductivity;

T_R [K] = rock temperature.

The equations of the model studied by Gringarten for the single fracture can be expressed as:

$$T_{wD}\left(t_D{}'\right)=1-2\beta\left(\frac{t_D{}'}{\pi}\right)^{0,5}\left[1-\exp\left(-\frac{1}{4t_D{}'}\right)\right]-(1-\beta)erf\left[\frac{1}{\sqrt{t_D}}\right] \quad (4.11)$$

Where β is dimensionless parameter of the geothermal gradient.

For multi – fracture and single fracture the equation for β = 0 can be written as:

$$\bar{T}_{wD}\left(y_D,s\right)=\frac{1}{s}\exp\left(-y_D s^{0,5}\tanh\frac{\rho_w c_w Q x_E}{2\lambda_r H}s^{0,5}\right) \quad (4.12)$$

These two equations can be solved by means of both Papoulis and Gaver – Stehfest.

4.3 Numerical methods for the solution of multi fracture: the algorithms of Gaver – Stehfest and Papoulis

The analytical solution of the equation of heat conduction in the rock desidered by the theory of Gringarten can be expressed in terms of the Laplace transform of the temperature (4.12). To derive the temperature as a function of time is necessary to apply to the temperature in the transformed space, the inverse transform, which is defined as:

$$f(t)=\frac{1}{2\pi j}\cdot\int_{c-j\infty}^{c+j\infty}F(p)\cdot e^{p\cdot t}\cdot dp \quad (4.13)$$

where c must be greater than the real part of each singularity of F (p). A singularity of the function F, is a value p, where F does not assume a single value or is not derivable in the complex plane.

4.3.1 Algorithms of Gaver - Stehfest

The principle of the method of Gaver (1966), later perfected by Stehfest in 1979, is based on the following property of the distribution of Dirac δ (t) which is valid for every function f (t):

$$f(t) = \int_0^\infty \delta(t-\lambda) \cdot f(\lambda) \cdot d\lambda \tag{4.14}$$

The function δ_N (t, λ) is an approximation of the Dirac distribution shifted in time δ (t-λ) and therefore satisfies the property:

$$\lim_{N\to\infty} \delta_N(t,\lambda) = \delta(t-\lambda) \tag{4.15}$$

The particular function choose by Stehfest is:

$$\delta_N(t,\lambda) = \sum_{j=1}^{N} u_j \frac{1}{t} e^{-\frac{a_j \lambda}{t}} \tag{4.20}$$

The coefficients u_j and a_j are chosen so as to optimize the relationship:

$$L[\delta_N(t,\lambda)] \cong L[\delta(t-\lambda)] = e^{-p\lambda} \tag{4.21}$$

Once optimized the coefficients a_j and u_j the function f (t) can be calculated as:

$$f(t) \cong \int_0^\infty \delta_N(t,\lambda) \cdot f(\lambda) \cdot d\lambda = \frac{1}{t} \sum_{j=1}^{N} u_j \int_0^\infty f(\lambda) e^{-\frac{a_j \lambda}{t}} d\lambda \tag{4.22}$$

Noting that the integral term is the calculated Laplace transform of f (t) we have:

$$f(t) \cong \frac{1}{t}\sum_{j=1}^{N} u_j F\left(\frac{a_j}{t}\right) \tag{4.23}$$

By placing $a_j = j \cdot \ln(2)$ and $u_j = V_j \cdot \ln(2)$, this equation becomes:

$$f(t) \cong \frac{\ln(2)}{t}\sum_{j=1}^{N} V_j \cdot F\left(\frac{j \cdot \ln(2)}{t}\right) \tag{4.24}$$

where V_j for a number N, equal is given by the expression:

$$V_j = (-1)^{\frac{j+N}{2}} \sum_{k=Int((j+1)/2)}^{Min(N/2,j)} \frac{k^{N/2}(2k)!}{(N/2-k)!\,k!\,(k-1)!\,(j-k)!\,(2k-j)!} \tag{4.25}$$

where Int is the integer part of a real number, and Min is the minimum of two numbers.

The Stehfest algorithm coefficients are constant, so it requires no parameters to be adapted to the specific problem. Moreover, the choice of the number N of coefficients to be used depends on the floating - point precision of the computer. For example, in single precision usually N = 10, while in the double precision N = 20.

4.3.2 Algorithms of Papoulis

Several methods represent f(t) by means of exponential functions, usually by introducing e^{-rt} as a new independent variable. Papoulis has proposed to seek an approximation to f(t) which has the form:

$$f(t) = \sum_{k=0}^{\infty} C_k \varphi_k(t) \tag{4.26}$$

where φ_k are known functions, and the constants C_k can readily be determined from the values of R(p) at the points a + kσ.

The φ_k can be chosen from several sets of complete orthogonal functions; Papoulis used the familiar trigonometric set, the Legendre set and the Laguerre polynomials.

In this work the interest is related to the use of the Legendre set polynomials:

$$f(x) = \sum_{k=0}^{\infty} C_k P_{2k}(x) \tag{4.27}$$

Using the time scale f(x) can be written in the form:

$$f(t) = \sum_{k=0}^{\infty} C_k P_{2k}\left(e^{-rt}\right) \tag{4.28}$$

To determine the coefficients C_k we observe that $P_{2k}(e^{-rt})$, is an even polynomial in e^{-rt} of degree 2k.

Taking the Laplace transformation of this formula, and substituting p = (2k + 1) r, k = 0, 1, 2, ……, N leads to the relations

$$rF[r] = C_0 \tag{4.29}$$

$$rF[3r] = \frac{C_0}{3} + \frac{2kC_1}{3 \cdot 5} \tag{4.30}$$

$$rF[(2k+1)r] = \frac{C_0}{2k+1} + \frac{2kC_1}{(2k+1)(2k+3)} + ... + \frac{2k(2k-2)...2C_k}{(2k+1)(2k+3)....(4k+1)} \tag{4.31}$$

In general:

$$rF[(2k+1)r] = \sum_{m=0}^{k} \frac{(k-m+1)_m}{2(k+1/2)_{m+1}} C_n \tag{4.32}$$

Again F(r) gives C_0, F(3r)C_1 and so on. The partial sum $r_N(x)$ is the average of r(x) whit the Legendre kernel as the weighting factor. The constant r is chosen with the same considerations as in I.

Equations may be solved recursively for the coefficients C_k; the Legendre polynomials are calculated from the relations:

$$\begin{aligned} &P_0(x) = 1; \\ &P_1(x) = x; \\ &\ldots\ldots\ldots\ldots\ldots; \\ &(n+1)P_{n+1}(x) = (2n+1)xP_n(x) - nP_{n-1}(x) \end{aligned} \qquad (4.33)$$

4.4 Approach to the study of the model built in FEM software

The approach is described by J. Willis-Richards and T. Wallroth (1995), who classifiy the various geothermal reservoirs they analyze the geothermal reserves and simulate it with mathematical and numerical theories. A geothermal reservoir can be descrived by a single fracture or by a more complex approach i.e. a multi – fracture. The problem can be complicated even more with a block of rock fractured randomly (such as to be compared to a porous medium). This approach makes possible to understand step by step the fundamental parameters that can affect the maximization of energy extracted from the geothermal reservoir, considering the life cycle of the system and allowing to properly design the geothermal power plant.

The finite element method (FEM), is a suitable numerical technique to find approximate solutions of boundary value problems, and the initial values described by partial differential equations, reducing them to a system of algebraic equations.

The problem domain is discretized to form a grid (mesh). On each element of the elemental form (triangles, quadrilaterals, tetrahedra, hexahedral), the solution is assumed to be linear combination of basic functions or shape functions.

Given a strong formulation in the edge of the domain, and assigned to the conditions, they may be of the type:

Neumann condition: the derivative of the function (flow) takes on values imposed on the edge of the domain;

Dirichlet condition: the solution (temperature) takes on values imposed on the edge of the domain;

Condition of Robin: it imposes a link between flow and temperature on the edge of the domain.

The model used here is COMSOL Multiphysics which consideres heat equation considers both conduction and convection in the fluid. Heat equation in the rock:

$$\rho_r c_r \frac{\partial T}{\partial t} = \nabla(\lambda_r \nabla T) \tag{4.34}$$

General equation of conduction and convection in the fluid:

$$\rho_w c_w \frac{\partial T}{\partial t} + \rho_w c_w v \nabla T = \nabla(\lambda_w \nabla T) \tag{4.35}$$

4.5 Results

The results section is composed of the research studies carried out during the PhD, including:

- Comparison of the results of single and multi fracture analytical and numerical solutions;
- Comparison between calculated values and measured data available from a site in the Philippines;

4.5.1 Comparison of theoretical results of single and multi fracture

The size of the rock and fracture are those considered by the example of Harlow and Pracht (1972) and Gringarten et al. (1975): rock size is 1000 m height and 1000 m depth; the other data are listed in table 4.1:

Table 4.1 – Project data by Harlow and Pracht (1972).

Q [m^3/s]	0.145	Volumetric flow rate
ρ_w [kg/m3]	1000	Density water
c_w [J/(kgK)]	4184	Specific heat water
ρ_r [kg/m3]	2650	Density rock
c_r [J/(kgK)]	1046	Specific heat rock
λ_r [W/(mK)]	2.6	Conductivity rock
T_r [°C]	300	Initial temperature of the rock
T_{w0} [°C]	65	Water inlet temperature

In the case of single fracture flow rate is equal to Q = 0,145 [m^3 / s]; in the case of multiple fracture N = 10 fractures were considered, where in each fracture Q_N = 0.0145 [m^3 / s], thus leading to the same averall flow rate.

In Figures 4.4 and 4.5, models of single fracture, and multi - fracture are presented, constructed in the FEM software, where the boundary conditions and the mesh used are shown.

As regards the mesh, in the fracture, where the water flows, the rectangular shape has been chosen, while in the rock the mesh was based on triangular finite elements. This choice ensures an accurate solution, and leads to time saving.

The results in the case of single fracture, are represented in Figure 4.6. In this graph the dimensionless temperature of the outlet water from the rock, as a function of dimensionless time is shown. The results show the analytic theory of Lauwerier the numerical solutions of Gringarten et al., resolved by both the methods of Papoulis and Gaver – Stehfest as well as FEM solution with COMSOL Multiphysics. All the solutions follow the same trend. The numerical solution of Gringarten et al. resolved by the method of Papoulis differs 3.5% compared to the other methods.

In Figure 4.7, instead, shows the dimensionless temperature of the outlet water from the rock as a function of dimensionless time, in the case of single fracture, considering the dimensionless geothermal gradient β, defined by Gringarten et al. Two values of gradient (β = 0 and β = 0.1) were considered. Also in this case the numerical solution resolved by the method of Papoulis differs by + 3.5% compared to FEM method. The presence of the geothermal gradient allows initially to extract water at a higher temperature and then tend to the case of β = 0 to higher extraction times; this depends on the value of the geothermal gradient and flow rate of extracted water from the production well.

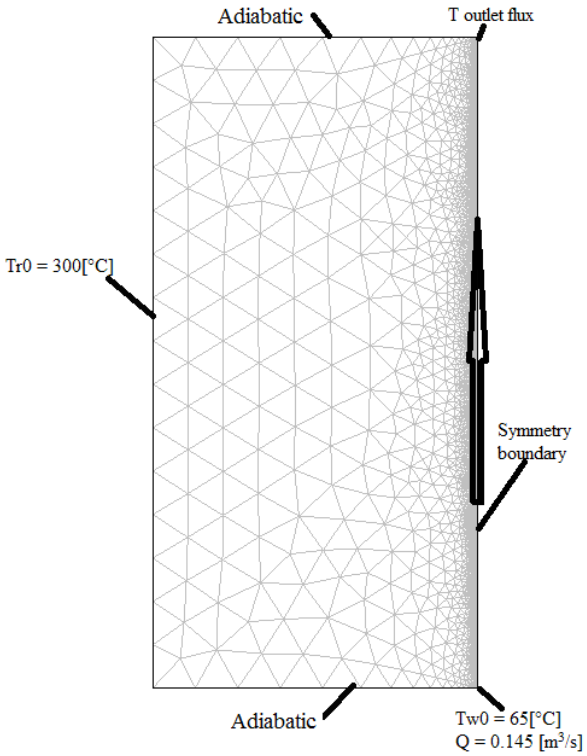

Figure 4.4 –FEM Model for the single fracture.

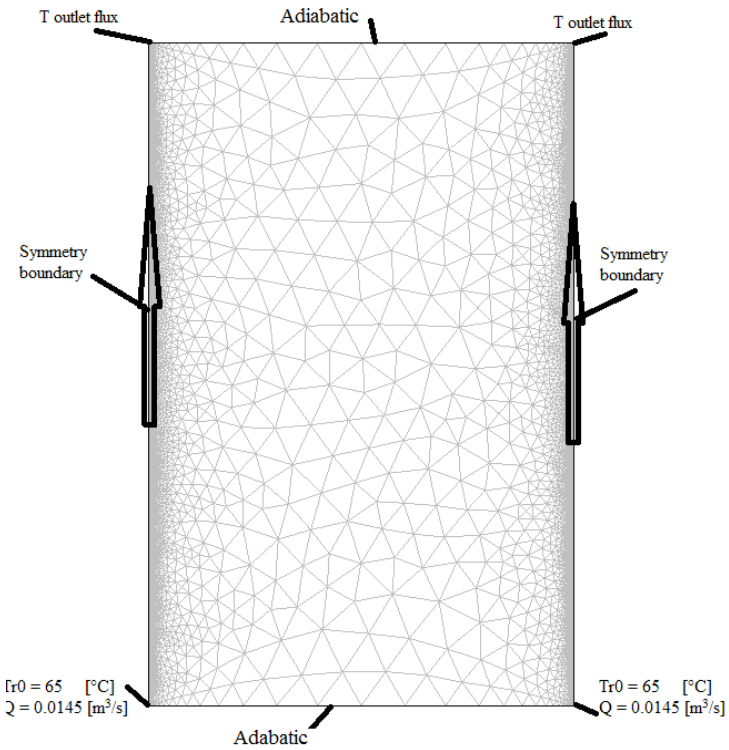

Figure 4.5 – FEM Model for the multy – fracture.

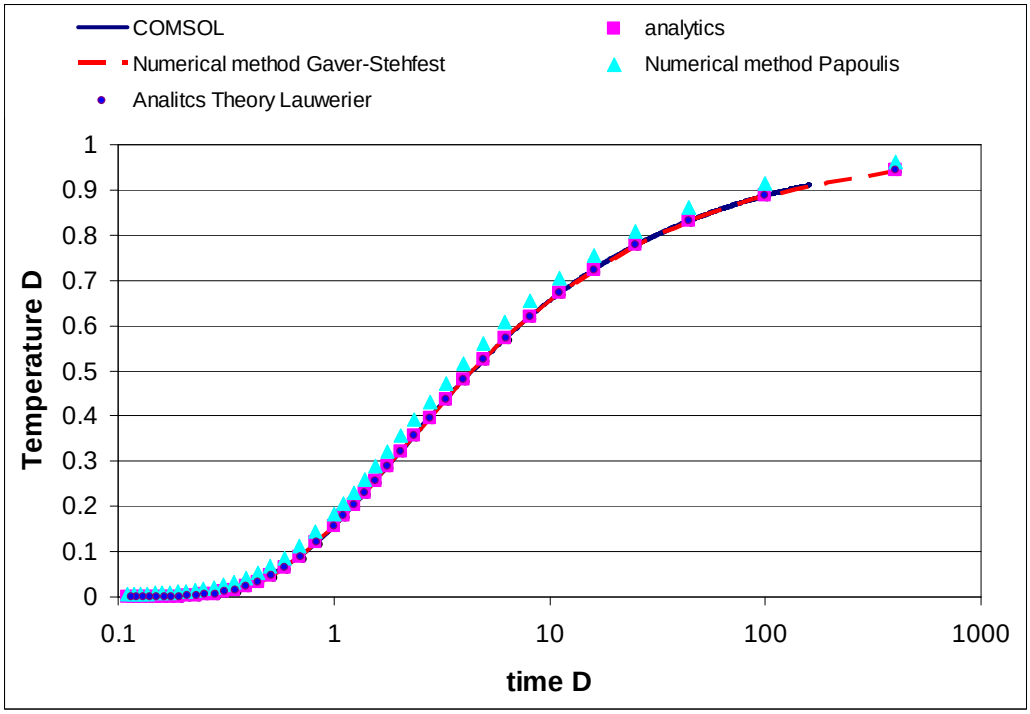

Figure 4.6 – Dimensionless water outlet temperature versus dimensionless time for the single fracture theory.

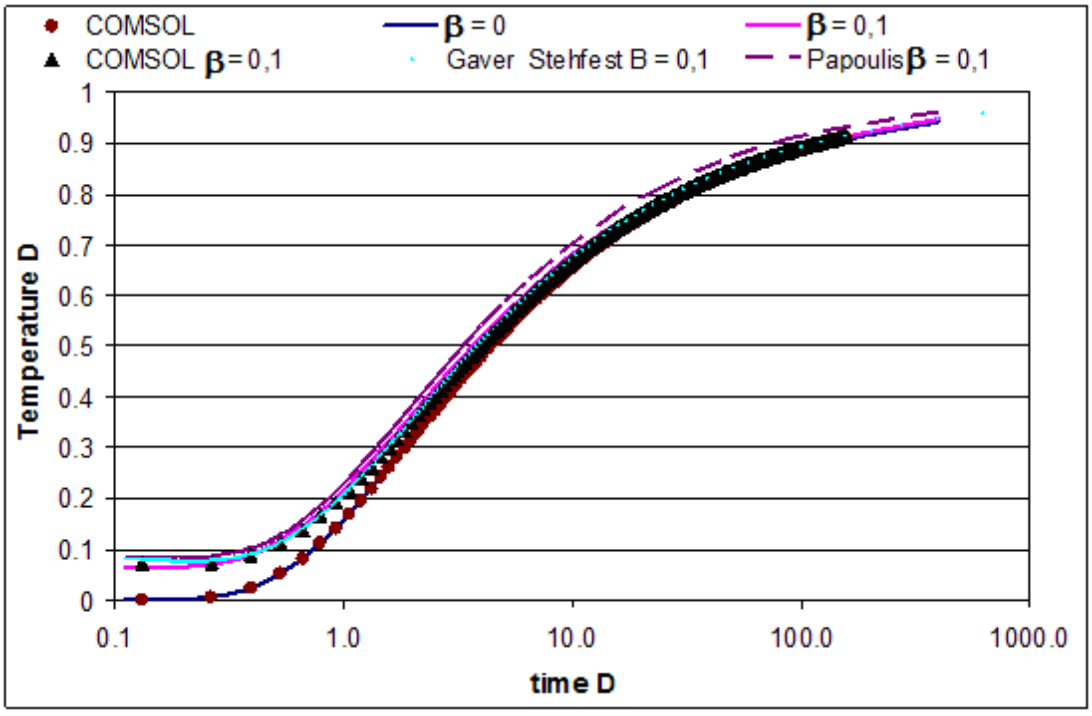

Figure 4.7 – Dimensionless water outlet temperature versus dimensionless time theory with geothermal gradient β for the single fracture theory.

Gringarten et al. define a simplified method for the preliminary design of a geothermal power plant, capable of producing electricity using the heat extracted from the rock to the water. For this purpose, a series of data are imposed, such as the thermal properties of the rock and the water present in situ, while another set of data must be fixed depending on the technical and economic considerations, which are realized as a function of the useful life of the geothermal reservoir, in this case the choice will be placed on the number of vertical fractures, the size of individual fractures, and the spacings between fractures. These parameters are chosen considering the graph of Figure 4.8 presented in the article of Gringarten et al (1975), which represents the dimensionless temperature of the outlet water from the rock as a function of the dimensionless time, by varying the spacing of the dimensionless fracture in the rock, this graph, in the article via obtained with the numerical solution resolved by the method of Papoulis.

For comparing the different methods the using different fracture spacing have been carried out.

In Figure 4.9, the results reported by Gringarten et al., is (1975), the numerical method of Gaver - Stehfest used in this work, FEM model in COMSOL Multiphysics are shown for temperature gradient β = 0 and as a function of multi - fracture spacing.

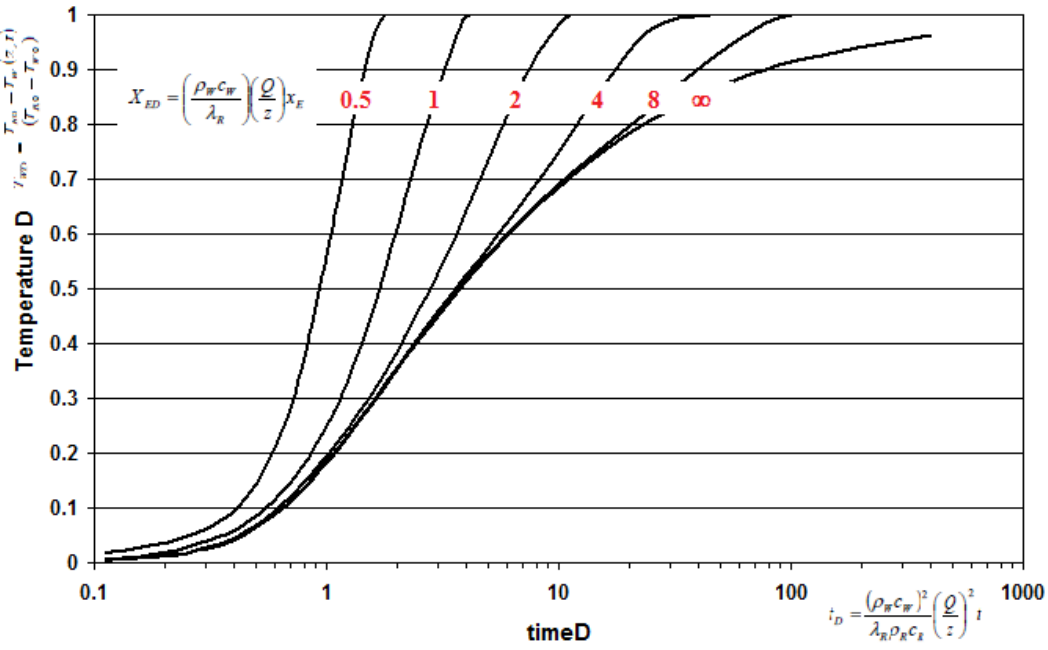

Figure 4.8 – Dimensionless water outlet temperature versus dimensionless time depending on the of fracture spacing (solved with Papoulis method).

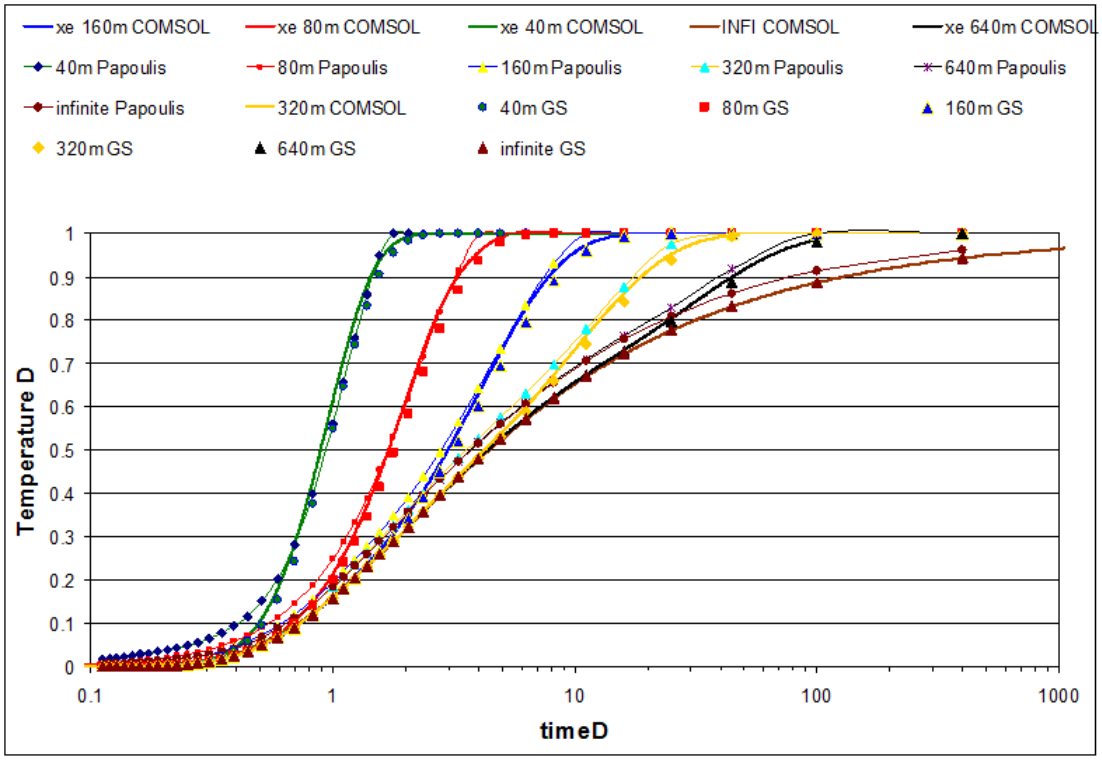

Figure 4.9 – Dimensionless water outlet temperature versus dimensionless time for Gringarten, Papoulis method and the FEM model.

For a clearer comparison, in Figure 4.10, the results of Gringarten et al. (1975) based on the numerical methods of Papoulis is compared to the Gaver – Stehfest method. In Figure 4.11 a comparison between the numerical solution of Papoulis and COMSOL Multiphysics, and in Figure 4.12 the comparison is done for the numerical solution of Gaver - Stehfest and COMSOL Multiphysics.

As shown in Figure 4.10 the two methods have the same trend of dimensionless temperature as a function of dimensionless time, as a function of the spacing between the dimensionless fracture. The small differences between the two solutions depend on the approximations made by the two methods, which lead to a maximum error of 7.5% in the case of a single fracture.

The method of Gaver - Stehfest is currently most used, in the field of hydrogeological problems and geothermal, as it is easier to implement compared to the method of Papoulis, which approximates the solutions with polynomials of n - degree.

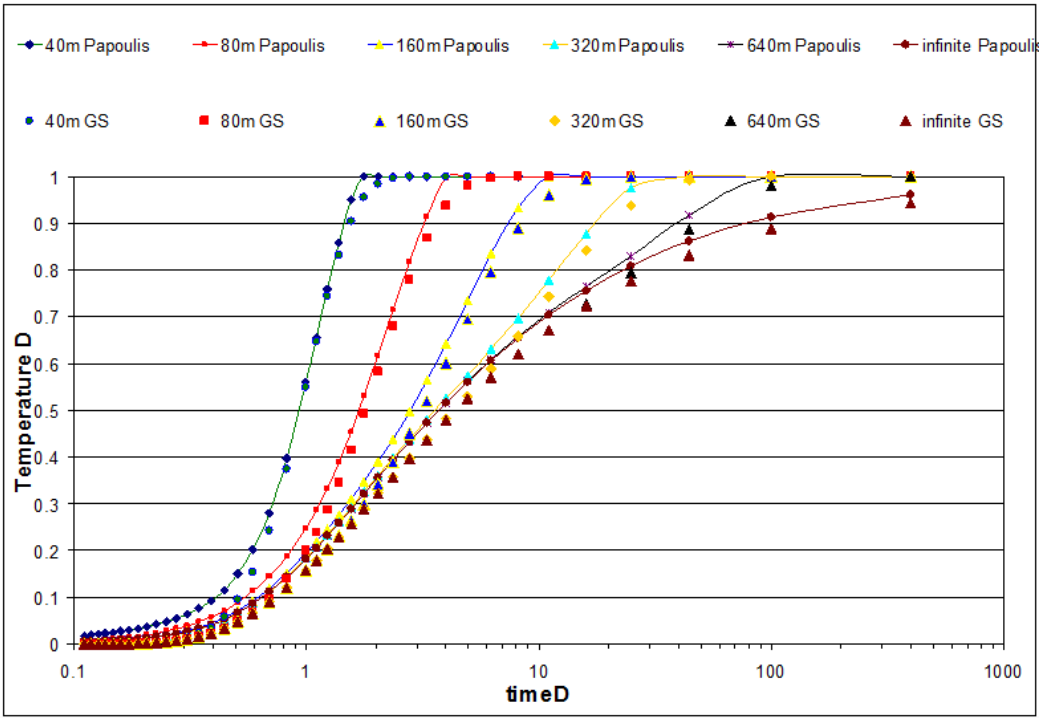

Figure 4.10 – Dimensionless water outlet temperature versus dimensionless time for Gringarten theory solved via Papoulis and Gaver – Stehfest methods.

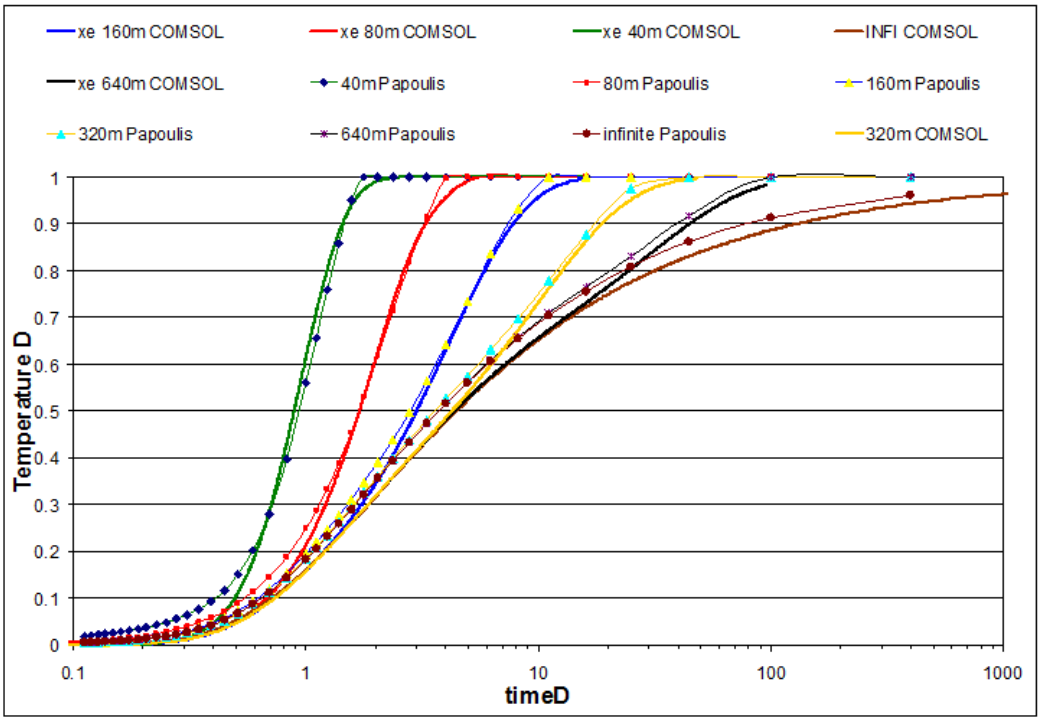

Figure 4.11 – Dimensionless water outlet temperature versus dimensionless time for Gringarten theory with the method of Papoulis and for the FEM model.

The solutions obtained by FEM models are very interesting, because the solution depends on the calculating step on the mesh used.

All the curves between Papoulis and COMSOL follow the same trend, with a maximum difference in the results in the case of single fracture of about 7%.

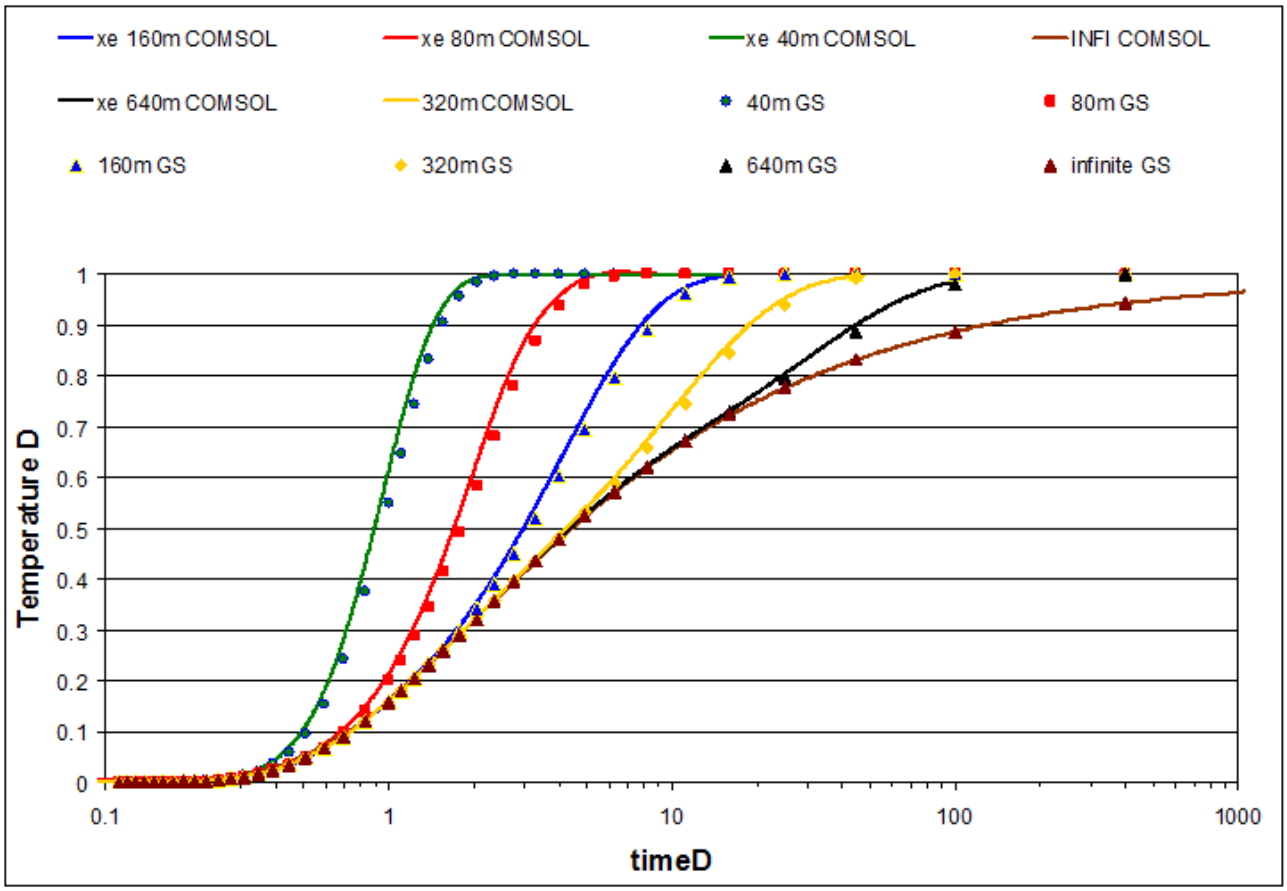

Figure 4.12 – Dimensionless water outlet temperature versus dimensionless time for the Gringarten theory solved by Gaver - Stehfest method and for FEM model.

The numerical solutions based on Gaver – Stehfest and the FEM model have a maximum difference of 3%. This allows to say that the solution of Gaver - Stehfest is preferable, compared to the method of Papoulis, used by Gringarten et al., since it is easier to implement, even in a spreadsheet, offering results closer to an accurate solution as the one of the FEM models.

The input data defined by Harlow and Pracht (1972), have been applied to the example of Gringarten et al. (1975). In this case temperature a function of time for various values of vertical fracture spacings have been calculated as shown in Figure 4.13:

$$T_w = T_r - T_{wD}\left(T_r - T_{w0}\right) \tag{4.36}$$

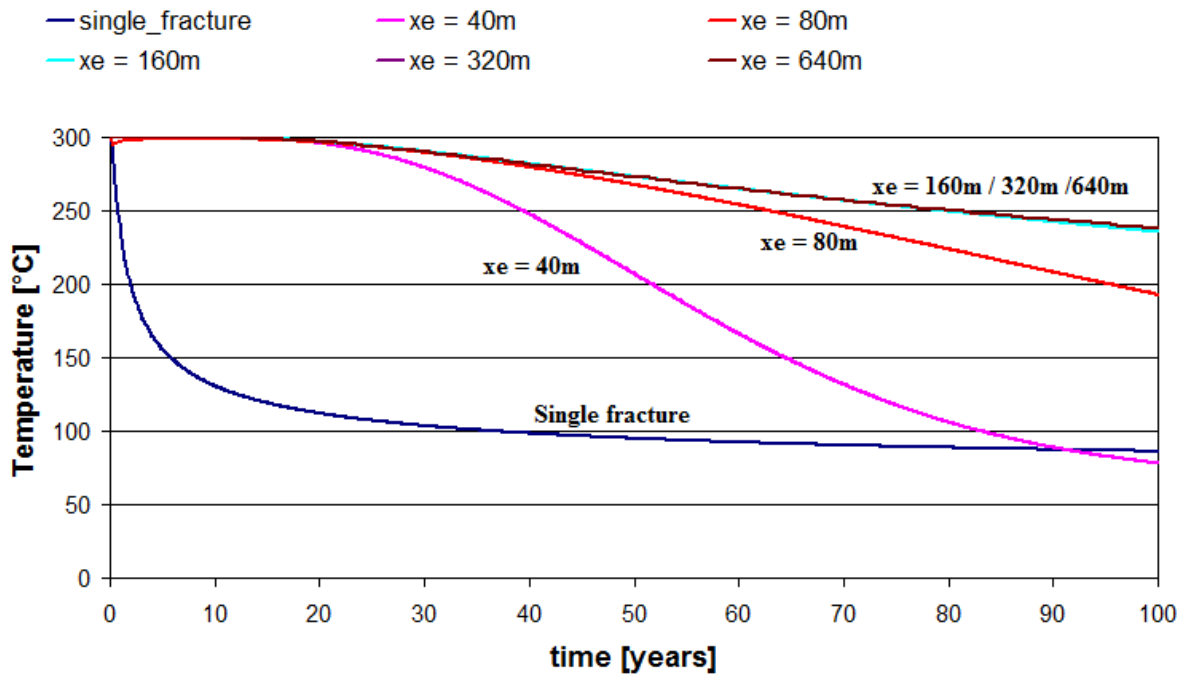

Figure 4.13 – Water outlet temperature versus time for different fracture spacings β.

Figure 4.13 reports results based on the same overall flow rate, i.e. the flow rate per fracture is devided by the number of considered fractures.

In the following figures the temperature of the rock in various steps of time are reported for: single fracture, a multi - fracture (X_E = 40m) and multi - fracture with X_E = 80m.

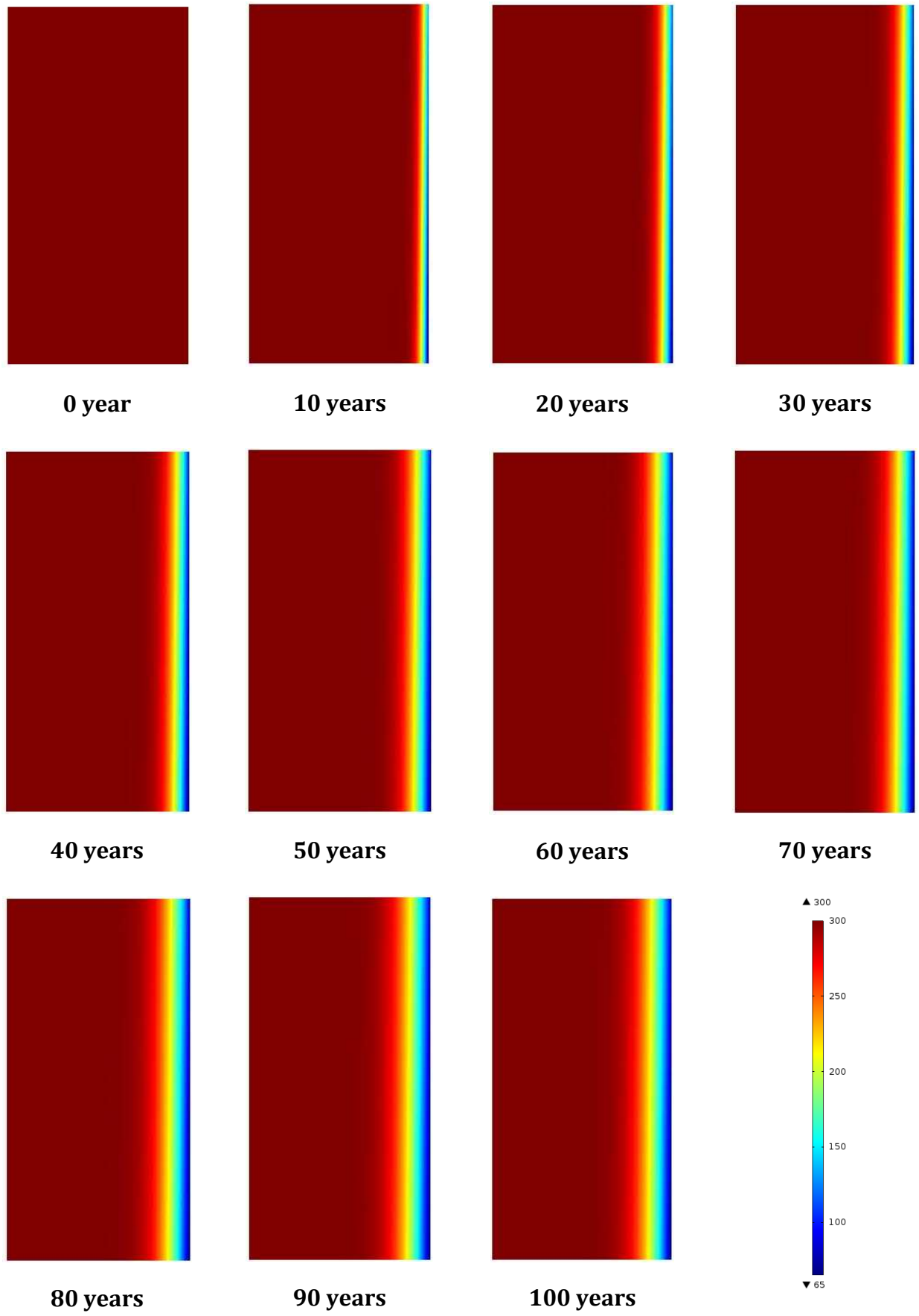

Figure 4.14 – geothermal maps: ***Single fracture***

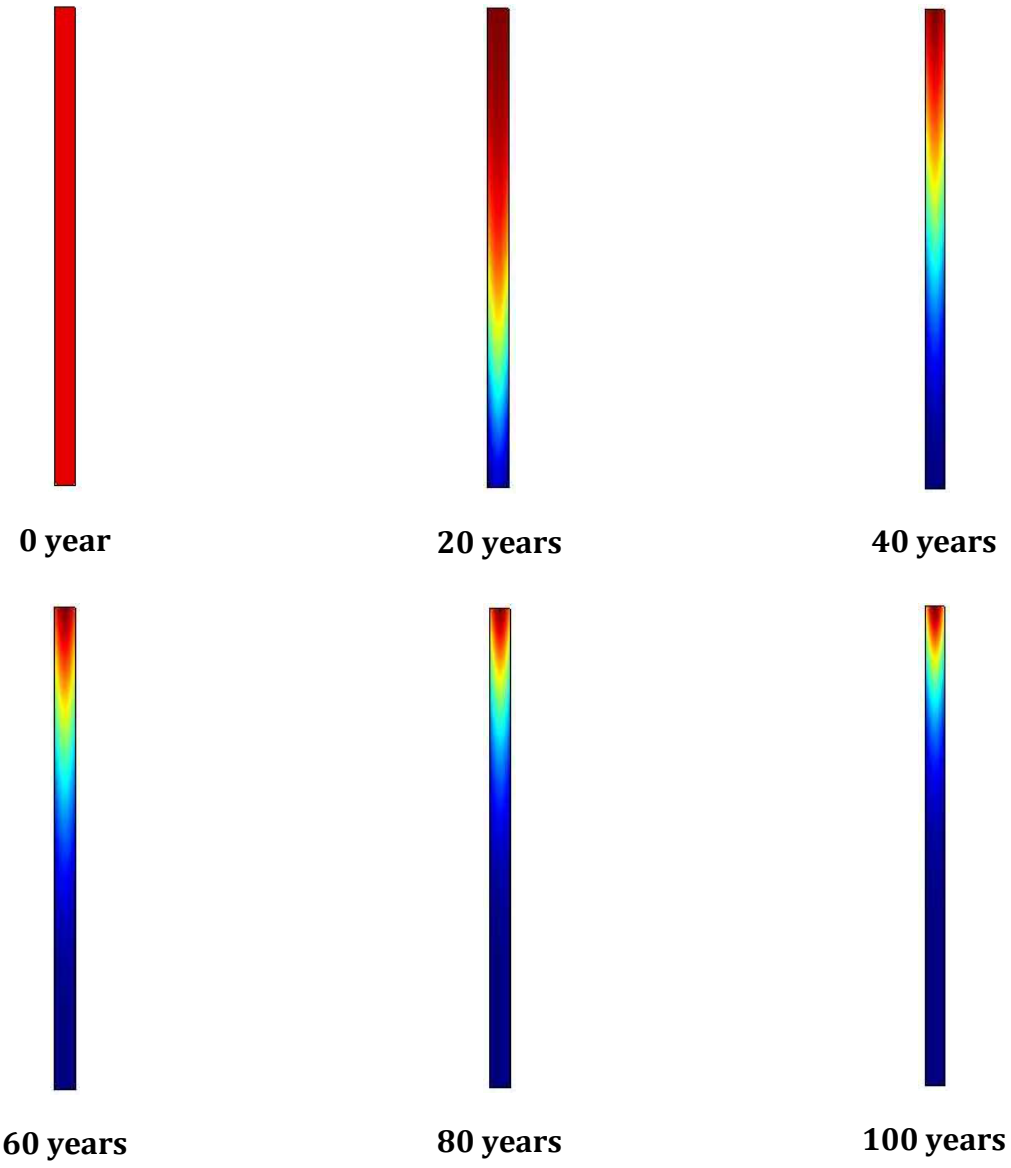

Figure 4.15 – geothermal maps: ***Multi – fractures X_E = 40m.***

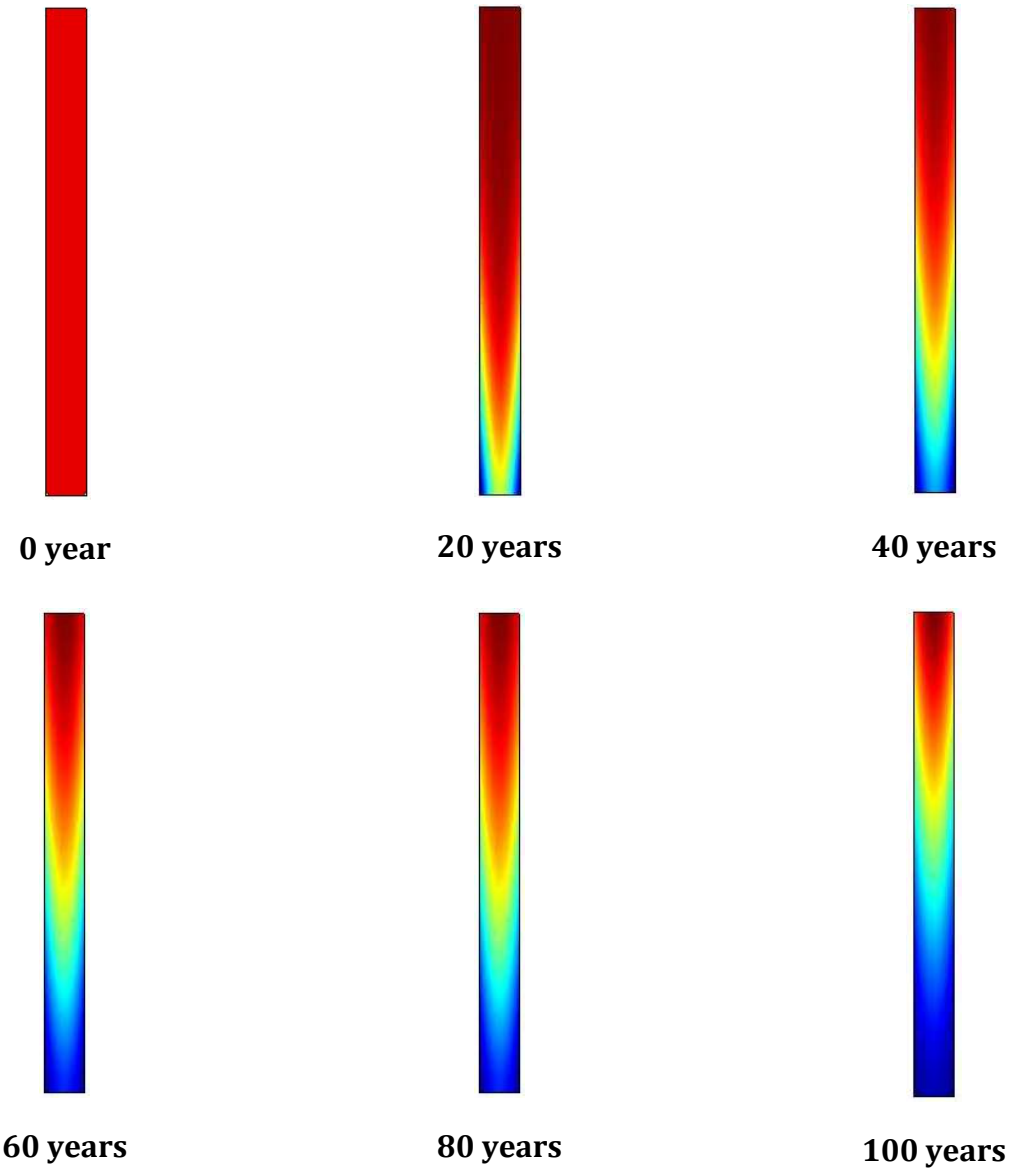

Figure 4.16 – geothermal maps: ***Multi – fractures X_E = 80m.***

4.5.2 The theory of single fracture applied to the porous medium of the site of the Philippines

In this part of the work the experimental results of RCM Malate and M.J. O'Sullivan (1991) in the Philippines. The authors have studied the variations of temperature of the production well over the time, by comparing the analytical theory of single fracture based on of Carslaw and Jaeger, adding the hypothesis of porous medium have been analysed.

Figure 4.17 shows the plan of the site, with the production and injection wells. In this case, the production and reinjection wells, and the single fracture are highlighted

The water is extracted from a group of production wells (21 wells), once extracted and used to transfer energy in the turbine, is rejected in injection wells, about 1000m away from the production wells.

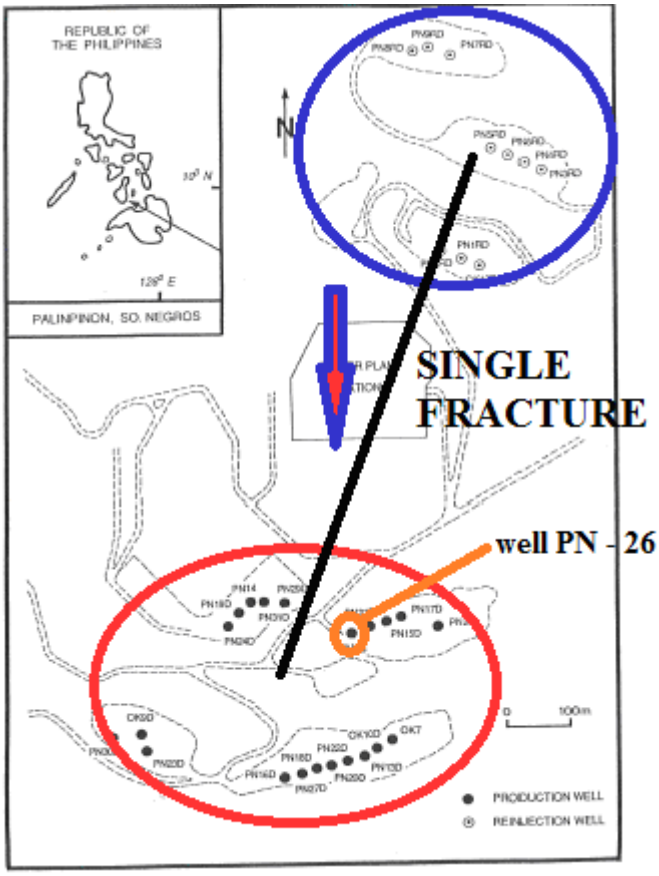

Figure 4.17 – Surface layout of Palinpinon production and reinjection wells (Malate and O'Sullivan 1991).

An experimental analysis of temperatures over time, has been conducted in the well PN – 26 which has a depth of 1600 m.

The experimental data show that after two years of production, the well PN - 26 has a gradual lowering of water temperatures. The temperatures drop after four years of operation by approximately a Δ t of about 38 ° C, i.e. from an initial temperature of 280 ° C it falls down to a temperature of about 242 ° C, as shown by RCM Malate and M.J. O'Sullivan (1991) in Figure 4.18.

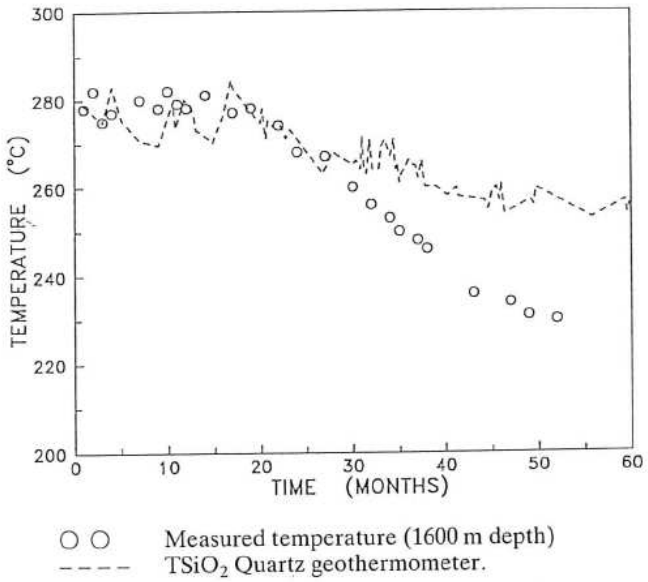

Figure 4.18 – Well PN _ 26 measured temperature versus time (R.C.M. Malate and M.J. O'Sullivan (1991)).

4.5.3 Simulation, for the temperature decrease in well PN - 26

The model used by R.C.M. Malate and M.J. O'Sullivan (1991) is based on the equation of energy balance:

$$V_p\left[(1-\phi)\rho_r c_r + \phi\rho_p c_p\right]\frac{dT}{dt} = -Pc_pT_p + RECc_{rec}T_{rec} + RETc_{ret}T_{ret}(t) \qquad (4.41)$$

where T_p, T_{rec}, T_{ret} are the temperatures of the production, recharge, and returning fluid respectively, V_p is the total volume of the production sector, ϕ is the porosity ρ_r and c_r are the density and specific heat of the rock matrix in the production sector, c_p, c_{rec}, and c_{ret} are the heat capacities of the production, recharge and returning fluids respectively. They are assumed to be identical in the model, i.e. $c_p = c_{rec} = c_{ret}$.; REC is the recharge flow of the production area [kg/s], and RET is flow of the reinjection fluid back to production [kg/s].

The recharge temperature is also assumed to be constant and equal to the initial reservoir temperature ($T_{rec} = T_0$). The temperature of the returning fluid T_{ret} is a function of time determined by the mathematical model of the fractured zone connecting the reinjection and production sectors. The given initial conditions are $T_p(0) = T_0$ and $T_{ret}(0) = T_0$, where T_0 is the initial reservoir temperature. It is convenient to use T_0 as a base temperature and define:

$$\theta_p = T_p - T_0 \tag{4.42}$$

$$\theta_{ret} = T_{ret} - T_0 \tag{4.43}$$

$$M_p(1+\beta)\frac{d\theta_p}{dt} = -P\theta_p + RET\theta_{ret}(t) \tag{4.44}$$

And the transformed initial condition is

$$\theta_p(0) = 0 \tag{4.45}$$

$$M_p = V_p\phi\rho_p \tag{4.46}$$

Once defined:

$$P = REC + RET \tag{4.47}$$

$$\beta = \frac{(1-\phi)\rho_r c_r}{\phi\rho_p c_p} \tag{4.48}$$

Rearranging the terms and simplifying the following equation can be written:

$$\frac{d\theta_p}{dt} + k\theta_p = \psi\theta_{ret}(t) \tag{4.49}$$

where

$$k = \frac{P}{\left[M_p(1+\beta)\right]} \tag{4.50}$$

and

$$\psi = \frac{RET}{\left[M_p(1+\beta)\right]} = Fk = fyk \tag{4.51}$$

The model by the authors assumes that, the trend of the temperature over the time in the production well, is a single fracture model based on porous medium.

Under these hypotheses the equation for conservation of Energy is:

$$\left[(1-\phi_f)\rho_r c_r + \phi_f \rho_l c_l\right]\frac{dT_f}{dt} + \rho_l c_l v \frac{\partial T_f}{\partial x} = \lambda \frac{\partial^2 T_f}{\partial x^2} \tag{4.52}$$

Where T_f is the temperature in the fractured zone, v is the Darcy velocity, ϕ_f is the porosity of the fractured zone and λ is the thermal conductivity of the rock matrix. Both ρ_l (the density), and c_l (the specific heat) of the fluid moving in the fracture, are assumed to be independent of temperature.

Assuming that the effect of heat conduction is negligible, as a simple advection model can be written in terms of $\theta_f = T_f - T_0$:

$$\frac{\partial \theta_f}{\partial t} + U\frac{\partial \theta_f}{\partial x} = 0 \tag{4.53}$$

The initial and boundary conditions are then:

$$\theta_f(x,0) = 0 \tag{4.54}$$

$$\theta_f(0,t) = \theta_1 = T_1 - T_0 \tag{4.55}$$

where T_1 is the injection temperature, and U is the thermal front velocity given by:

$$U = \frac{v\phi_f \rho_l c_l}{\left[(1-\phi_f)\rho_r c_r + \phi_f \rho_l c_l\right]} \tag{4.56}$$

The thermal front is the transition zone where the temperature changes from initial reservoir temperature T_0 to the injection temperature T_1.

With:

$$\theta_{ret}(t) = \theta_f(L,t) \tag{4.57}$$

where L is the distance between the production and reinjection areas. The solutions for the production and returning fluid temperatures can be derived using Laplace transforms.

In the Laplace transform domain, the temperature of the returning fluid can be expressed as:

$$\bar{\theta}_{ret} = \frac{\theta_1}{s} e^{-sL/U} \tag{4.58}$$

where s is the transform parameter. This gives a solution in the form of a step change in temperature so that the model can be defined as step function model:

$$s\bar{\theta}_p + k\bar{\theta}_p = \psi\bar{\theta}_{ret} \tag{4.59}$$

After substituting θ_{ret}:

$$\bar{\theta}_p = \frac{\psi\theta_1}{k}\left\{\frac{1}{s} - \frac{1}{s+k}\right\}\exp\left(\frac{-sL}{U}\right) \tag{4.60}$$

By inverting this equation, the solution becomes:

$$T_p = T_0 \text{ for } t \le t_T \tag{4.61}$$

$$T_p = T_0 + W\{1 - \exp[-k(t - t_T)]\} \quad \text{for } t > t_T \tag{4.62}$$

Where:

$$W = \frac{\psi}{k}(T_1 - T_0) \tag{4.63}$$

t_T is the time taken for the thermal front to cover the distance L and is defined by:

$$t_T = \frac{L}{U} \tag{4.64}$$

The distance between the production and reinjecton areas in the well PN – 26 is approximately 1 km, hence the thermal front velocity U can be easily evaluated as 56 m/month.

$$\frac{U}{v} = \frac{\phi_f \rho_l c_l}{\left[\phi_f \rho_l c_l + (1-\phi_f)\rho_r c_r\right]} \tag{4.65}$$

The data used in the model of the well PN - 26 Philippines, are summarized in Table 4.2.

Table 4.2 – Model data used to match the thermal decline in PN – 26.

P [kg/s]	50	Production rate
ρ_l [kg/m^3]	751	Density fluid
c_l [kJ/(kgK)]	5.26	Specific heat fluid
ρ_r [kg/m^3]	2500	Density rock
c_r [kJ/(kgK)]	1.00	Specific heat rock
λ_r [W/(mK)]	2.6	conducibilità roccia
T_0 [°C]	280	Reservoir temperature
T_1 [°C]	165	Injection temperature
U [m/month]	56	Thermal front velocity
$f = \frac{RET}{RI}$	0.90	f = fraction; RET = flow of the reinjection fluid back to production [kg/s]; RI = flow of reinjection fluid [kg/s];
β	7.0	

In Figure 4.19 the comparison between the experimental data and the theory of a single fracture in the porous medium is presented; as can be seen, the theory is similar to the experimental data.

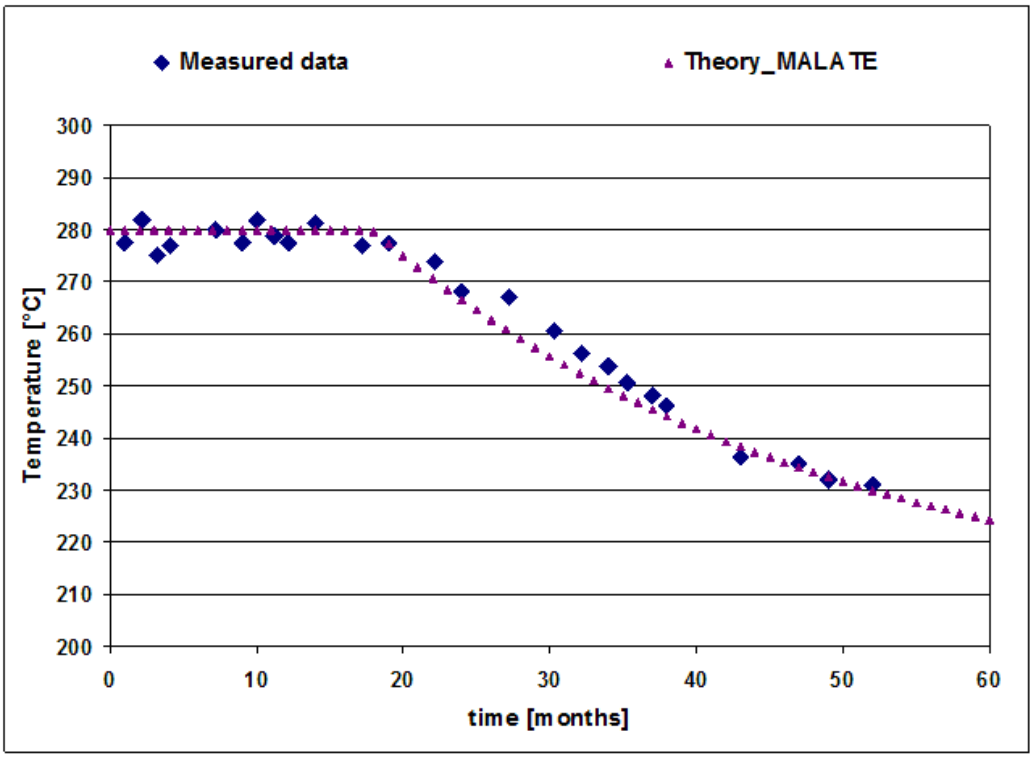

Figure 4.19 – Comparison experimental data Philippine with theory analytical – well PN – 26 measured temperature versus time.

As for FEM model a 3 – D model has been carried out, as shown in Figure 4.20. As shown in Figure 4.21 results of the FEM model are close to experimental data.

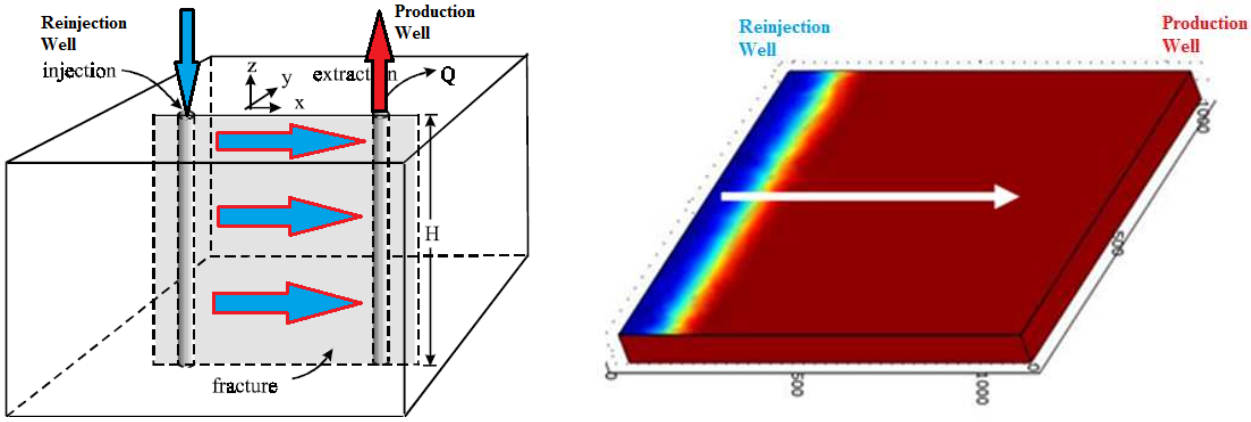

a **b**

Figure 4.20 – Example injection and extraction of water from the situ (Cheng et al 2001) ***a****, and Study of heat extraction in 3D at the site of the Philippines in FEM software* ***b****.*

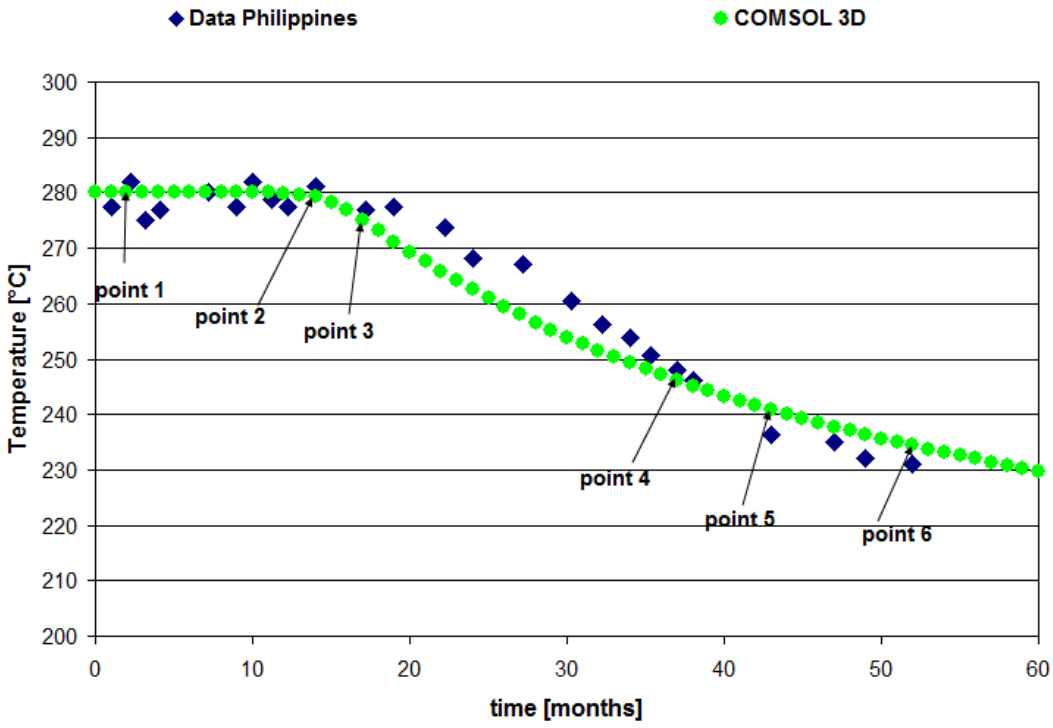

Figure 4.21 – Comparison between experimental data an results of the 3D FEM model

In Figure 4.22 various geothermal maps, rapresenting the temperature in the geothermal reservoir are shown in the different instants over the time.

The graph presented in Figure 4.23 compares the experimental data of well PN - 26, with the solutions obtained from the theory of a single fracture in a porous medium and the 3D model in FEM software.

As final comparison the data of the Philippines with the different calculation methods it can be seen that experimental data (green squares) fit with the different models (Figure 4.24).

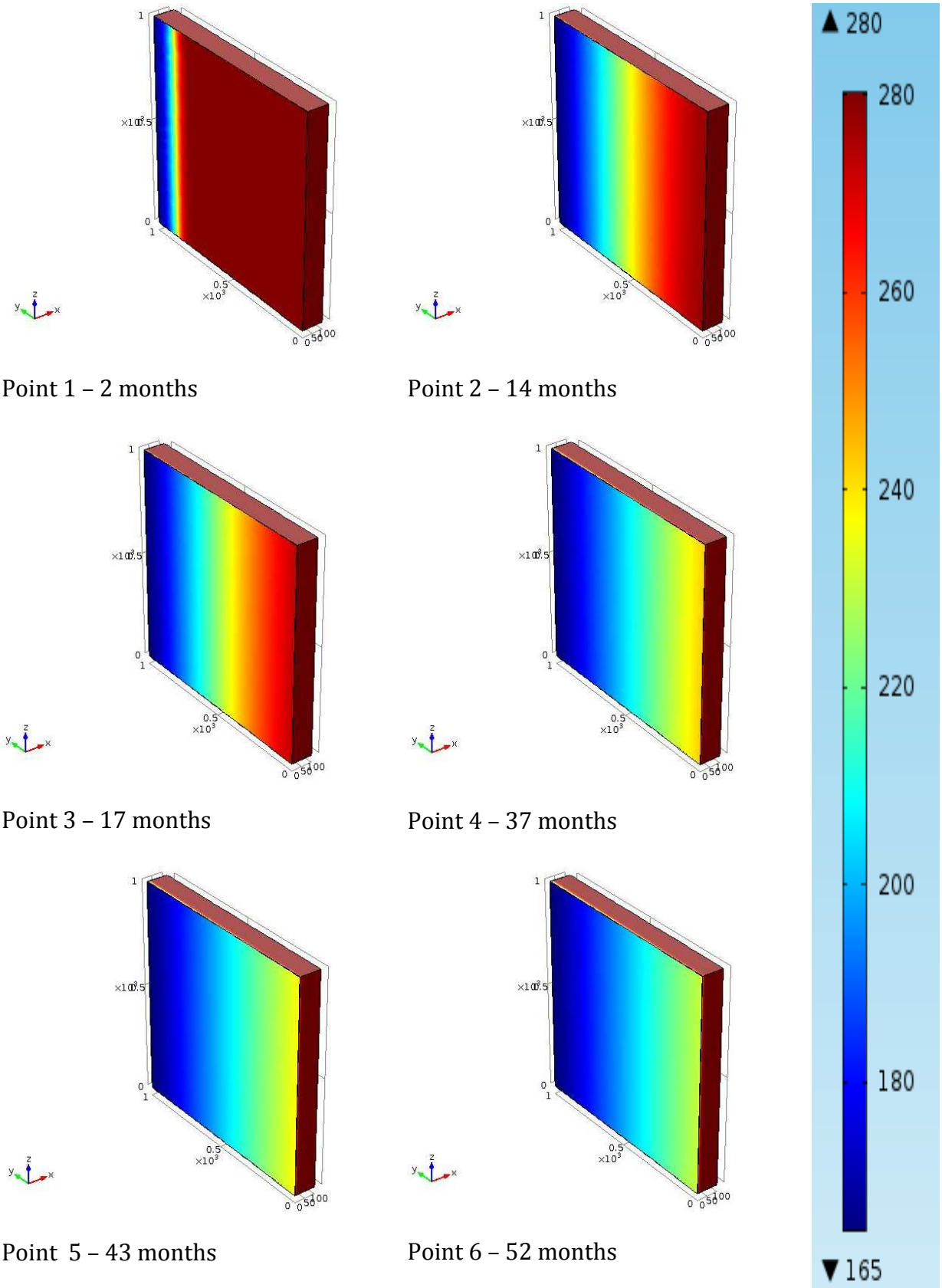

Point 1 – 2 months

Point 2 – 14 months

Point 3 – 17 months

Point 4 – 37 months

Point 5 – 43 months

Point 6 – 52 months

Figure 4.22 – geothermal maps in the Philippines.

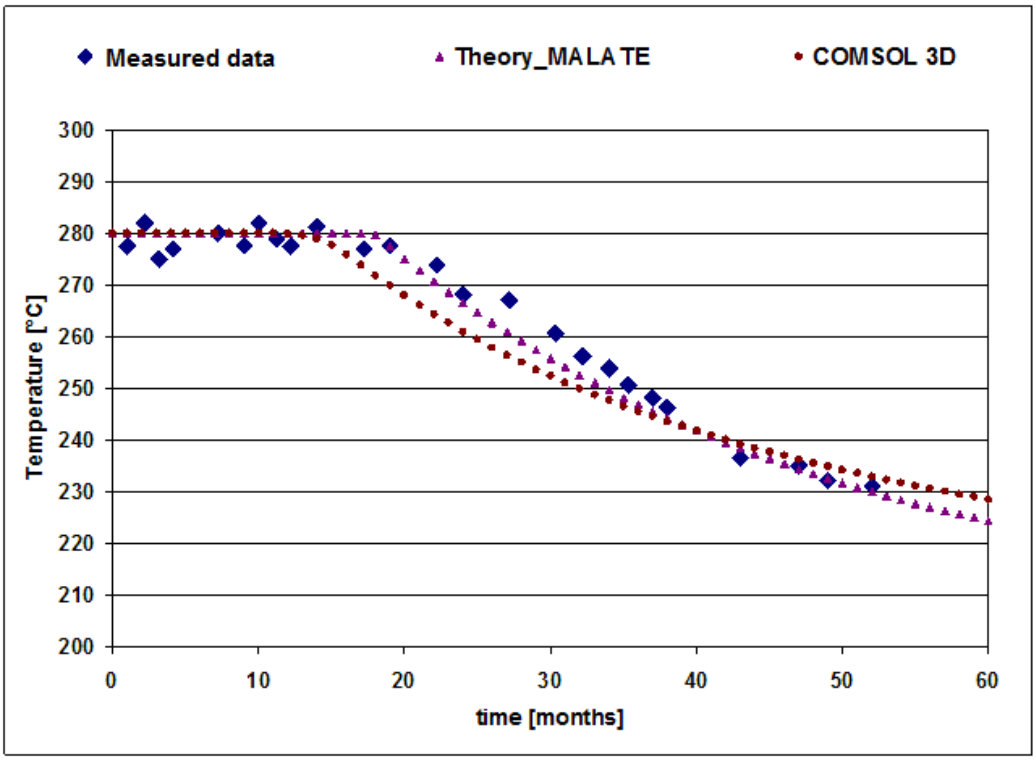

Figure 4.23 – Comparison of the experimental data with the analytical theory and the 3D FEM model.

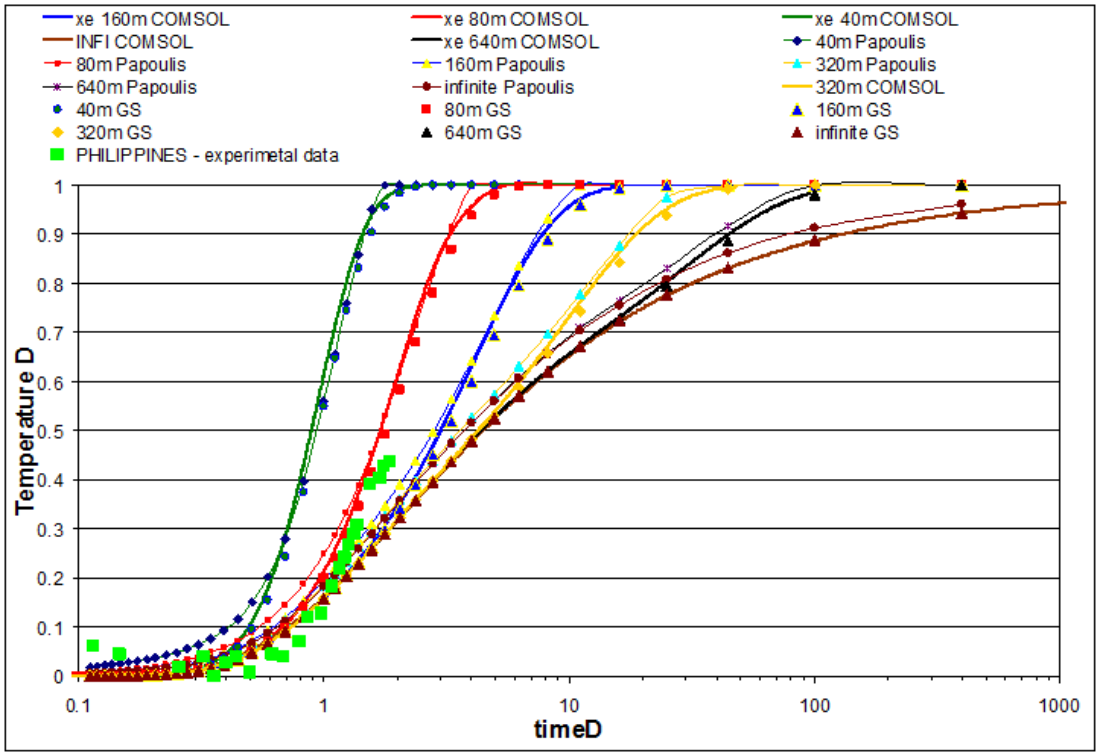

Figure 4.24 – Data Philippine . dimensionless parameters (green squares)

4.6 Reference

Bodvarsson G., On the temperature of water flowing trough fractures, Journal of geophysical research, Vol. 74, No. 8, 1969, pp. 1987 – 1992.

Bodvarsson G., An estimate of the natural heat resources in a thermal area in Iceland, Geothermics, Vol. 2, Part. 2, 1970, pp. 1289 – 1293.

Bodvarsson G., - "Thermal Problems in the Siting of Reinjection Wells" - Vol.1, Nr. 2,Geothermics (1972)

Bodvarsson G., Geothermal resource energetics, Geothermics, Vol. 3, No. 3, 1974, pp. 83

Carslaw H.S., Jaeger J.C., Conduction of Heat in Solids, 2nd ed. Clarendon Oxford, 1959, p. 396.

Cheng, A.-D., Ghassemi, A., Detournay, E., 2001. A two-dimensional solution for heat extraction from a fracture in hot dry rock. Int. J. Numer. Analy. Meth. Geomech., 25, 1327-1338.

Cheng, A.-D., Ghassemi, A., Detournay, E., 2001. Modeling heat extraction from a fracture in hot dry rock using an integral equation method.

COMSOL Multiphysics, Heat Transfer Module User's Guide COMSOL 4.1, 2010, pp. 222.

Gaver Jr. G.P., Observing stochastic processes and approximate transform inversions, Operat. Res. 1966, pp. 444 – 459.

Gringarten A.C., Witherspoon P.A., Ohnishi Y., Theory of heat extraction from fractured hot dry rock, Journal of geophysical research, vol. 80, no. 8, 1975, pp. 1120.

Harlow F.H., Pracht W.E., A theoretical study of geothermal energy extraction, Journal of geophysical research, vol. 77, no. 35, 1972, pp. 7038 – 7048.

Lauwerier H.A., The transport of heat in an oil layer caused by the injection of hot fluid, Appl. Sci. Res., Sect. A Vol. 5, 1955, pp. 145 – 150.

Lowell R.P., 1976. Comments on .Theory of heat extraction from fracture hot dry rock. by A.C. Gringarten, P.A. Witherspoon, and Y. Ohnishi. J. Geophys. Res., 81, 359-360.

Malate R.C.M., and O'Sullivan M.J. (1991): Modelling of chemical and thermal changes in well PN – 26 Palinpinon geothermal field, Philippines, Geothermics, 20, 291 - 318.

Murphy H. D., 1987. Hot dry rock reservoir engineering. PROCEEDINGS of NATO Adv. Study Institute on Geothermal Reservoir Engineering. July 1 - 10, 1987, Antalya, Turkey.

A. Papoulis, A new method of inversion of the Laplace transform, Quart, Applied Math., Vol. 14, 1957, pp. 405 – 414.

Stehfest H., Numerical inversion of Laplace transforms algorithm 368, Commun. ACM 13 Vol. 1, 1979, pp. 44 – 49.

Willis –Richards J., Wallroth T. 1995. Approaches to the modeling of HDR reservoirs: a review. Geothermics Vol. 24, No. 3, pp. 307-332, 1995

ANNEX

Comments by Lowell (1976)

Lowell in 1976, published a comment in reference to the article by Gringarten et al., Entitled "Comments on Theory of heat extraction from fractured hot dry rock by AC Gringarten, P.A. Witherspoon, and Y. Ohnishi ", where emphasizes the important study done by the authors, therefore, a greater efficiency of extraction of heat if the water passes through crosses multiple fractures, which not if it crosses one at constant flow rate Q.

The comment of Lowell, is to define the study authors is unnecessarily complicated, making escape, however, the most interesting results, in fact using the same equations, the solution of the water temperature is thus given:

$$T_W(z,t) = T_{W0} + (T_{R0} - T_{W0}) \cdot erf \frac{\lambda_r z}{c_W \rho_W Q \sqrt{\alpha_r t}} \tag{4.37}$$

Then:

$$\frac{T_W(z,t) - T_{W0}}{T_{R0} - T_{W0}} \propto \frac{1}{Q(t)^{1/2}} \tag{4.39}$$

That is, there is proportionality between the ratio of the temperatures, and the inverse of the flow rate for the time. this means that: a geothermal system ceases to operate effectively once the outlet temperature descends below a certain value. For which the ratio of the temperatures is fixed according to practical considerations, and shows that using a lower flow the geothermal system can operate effectively longer.

Lowell gives the example, that by adopting the same data part and using a time of 20 years, the result of Q = 0.146 [cm^3/s] per unit length of the fracture, which is practically equal to the result of Gringarten.

Furthermore, Lowell studies the model fractures as independent as it can give the same result of the model of Gringarten, considering the quantity of conductive cooling of the rock to any horizontal distance L from a fracture, then resting on the number of Fourier, given by:

$$N_F = \frac{\alpha_r t}{L^2} \tag{4.40}$$

For the amount of conductive cooling, must be $N_F < \frac{1}{9}$. Therefore, in order to consider the fractures thermally independent in a time t0, the condition must be satisfied $L \geq 3(\alpha_r t_0)^{1/2}$, where L is the separation between fractures. At this point, Lowell poses an example, if for t0 = 20 years then L > 70m, this result confirms what was seen in Figure 13. Furthermore, after 20 years shows little thermal interference, in case of separation between fractures greater than 40m (This is confirmed by the geothermal maps and graph of Figure 4.13). Lowell affirms that the results of Gringarten, can be adequately represented by a model based on terms of temperature determined for a single fracture, and then the geothermal system overall, is represented by the sum of the results for N independent fractures.

EVALUTATION THESIS: PhD Europeaus

DEBRECENI EGYETEM
MŰSZAKI KAR

UNIVERSITY OF DEBRECEN
FACULTY OF ENGINEERING

Ikt. ...

Ül: Dr. Lakatos Ákos/Tóth Nóra

Evaluation of Doctorate Thesis

„Mathematical models for the use of low and medium temperature geothermal energy"

written by Mirco Dona' PhD Student
Matriculation number: 967471 - DR

The Thesis was elaborated in the University of Padua. The Supervisor was Prof. Michele De Carli, Co-advisors were Prof. Guðni Jóhanesson and Prof. Guðrún Arnbjörg Saevarsdóttir from University of Reykjavik.

1. Importance and opportunity of the research work

The topic of the Doctorate research is very significant and up to date. In the last few decades the energy consumption of the world is significantly increasing, while the quantity of the available fossil materials is decreasing. The available energy resources are widely insufficient, thus the countries of the European Union are in strongly want importing them. Connecting to this, several scenarios has been planned. The European Parliament accepted a many Directives for increasing the energy efficiency, for decreasing the energy consumption, as well as for the use of the renewable energy sources. So that case the geothermal energy can be one of the problem solving possibilities for the continuous sustainability.

2. Content of the thesis

The main goal of the research work was to give a comprehensive report and to summarize the possibilities for the best application of the geothermal energy using simulations and problem-solving with mathematical models.

The Thesis being structured after a short introduction into 4 chapters, and has 307 pages. All of the chapters start with an introduction and close with a conclusion and with the list of references. The four chapters are the followings:

✉: H-4028 Debrecen, Ótemető u. 2-4. ☎: (52) 415-155 Fax: (52) 418-643 🖳: alakatos@eng.unideb.hu

- Chapter 1: *Geothermal Energy*

In this chapter the Candidate presents the structure and the geothermal possibilities of the Earth. Furthermore the basic definitions are presented as well. The past, present and the future of this energy "production" is also introduced. It contains and explores the relevant literature including several use of the geothermal energy. This chapter is closed with the list of used references as similar to the others.

- Chapter 2: *Low Temperature Geothermal Energy*

In this chapter the types of the geothermal heat pumps and heat exchangers are presented. After this bibliographic review the simulation of a GRT with a two-dimensional finite element analysis, using the software COMSOL, has been carried out. Besides the FEM model, thermal mode for summer and winter cases and mechanical models are presented. The results are represented in well-ordered tables. In this case economic analysis was carried out as well. After this chapter 3 annexes can be found where the thermodynamical, mathematical and theories and the computer simulations are presented.

- Chapter 3: *Medium Temperature Geothermal Energy*

At the beginning of this chapter the theoretical background of this topic can be read. Here first, the production wells and re – injection wells than the design and dimensioning is summarized. The ATES (Aquifer Thermal Energy Storage) is presented in some figures and introduced correctly. The literature review is well done. The Lauwerier theory and model is used for fitting the temperature distribution is in a porous medium. The results of the investigation have shown that for small thicknesses the trend is identical for both analytical theories and the FEM model, since the hypothesis of small thickness of the aquifer is placed in the analytic theories.

- Chapter 4: *High Temperature Geothermal Energy*

In this work, a bibliographic analysis of the most important theories in the literature, the study of the extraction of geothermal energy, was analysed. A simplified treatment of the problem was carried out the point of view mathematics, by Carslaw and Jaeger (1959), which was picked up by Lauwerier in 1955 to model the heat transfer of a hot fluid (already presented in the previous chapter), injected into a fracture of thin, in a porous medium containing petroleum high density, in order to increase extractability of oil, reducing its viscosity. The study conducted in this part of the thesis focused on geothermal energy at high temperatures.

The thermodynamical fittings and equation solving with modelling and simulations are very important for all the cases. The number of the references is grandiose and it bears witness to the diligence of the Candidate. The numerous figures are helping the reader to follow the thesis easily; they are in well order and quality.

✉: H-4028 Debrecen, Ótemető u. 2-4. ☎: (52) 415-155 Fax: (52) 418-643 🖷: alakatos@eng.unideb.hu

3. Contributions to the author

The Thesis is well structured, with lots of well ordered Figures; Tables are clear, the conclusions are well formulated, furthermore faults of spelling are can be found only in somewhere. The main contributions are (suggestions to the Candidate):

- SI units should be used:
  - e.g.: the density: somewhere g/cm^3, kg/m^3 etc.
  - The units of the thermal conductivity should be standardized.
  - use °C or K
- Somewhere the captions are Figure, somewhere Fig., please standardise them.
- Page 19, the Candidate said: "The enthalpy is a thermodynamic defined as..." please define it correctly. "H" is more used for the sign of enthalpy except "E".

4. Conclusions

The Doctorate Thesis written by Mirco Dona' is of high scientific level and at the same time has a high practical value taking into account the actuality of the analysed problems and utility of obtained results. The Thesis is built up logically; the conclusions are correctly drawn and well formulated.

Taking into account the indisputable scientific value of Doctorate Thesis entitled: "Mathematical models for the use of low and medium temperature geothermal energy" elaborated by Mirco Dona', I propose the public presentation of the mentioned Thesis in order to confer the PhD title ("Doctor Acuropeus") to Mirco Dona'.

Wish the best and good luck for the defending.

Sincerely yours,

Debrecen, 06.02.2013

Ákos Lakatos PhD
assistant professor
University of Debrecen, Faculty of Engineering
Department of Building Services and Building Engineering

KTH Architecture and the Built Environment

To
Universita' Degli Studi Di Padova
Servezio Relazioni Internazionali

Stockholm 16 February 2013,

My evaluation of the preliminary thesis „MATHEMATICAL MODELS FOR THE USE OF LOW AND MEDIUM TEMPERATURE GEOTHERMAL ENERGY" submitted for the Ph.D degree at Universita' Degli Studi Di Padova by the PhD Student: Mirco Dorà with Matriculation number: 967471 - D/R, in January 2013.

The possibility to expand the energy system of a building or a district with the energy state in the ground opens a lot of possibilities for improving the energy efficiency of the society. In his thesis Mirco Dorà has collected and applied basic and up to date knowledge in this field.

In Part 2 of the thesis there is a thorough investigation of different possibilities and technical options in energy piles and ground source heat pumps.

In Part 3 different approaches are applied for description of medium temperature geothermal energy in aquifer cases where thermal storage is done in a thermal bubble.

Part 4 includes comparison between different models applicable for geothermal energy of high temperature.

This is an extensive undertaking that gathers and applies the essential knowledge base needed to take advantage of geothermal energy in an effective way. The thesis has a clear structure and the readability is high.

By his thesis the candidate has convincingly shown that he has a thorough understanding of this complex subject and knows how to use the methods and standards of a good scholar.

Overall, I can say that this work, as presented in the submitted document, is of sufficient extent and height to award the candidate a Ph.D. degree.

Folke Björk
Professor
Head of division of Building Technology

Kungliga Tekniska högskolan, *Div of Building Technology*
Dept of Civil and Architectural Engineering

KTH Brinellvägen 34, – SE-100 44 Stockholm, Sweden, Tel: +46 8 790 86 63, Email: folke.bjork@byv.kth.se , www.kth.se